ELECTRICAL PROPERTIES OF BISMUTH TELLURIDE.

A Thesis submitted for the Degree of Ph.D. in

the University of London by M. Wendy Williams.

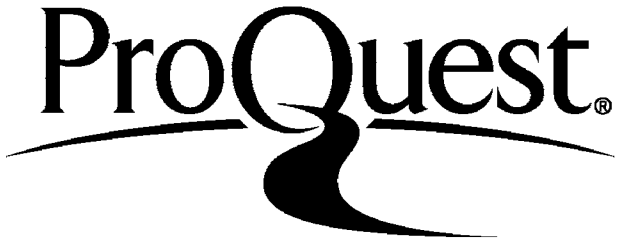

Abstract.

Measurements have been made of the electrical conductivity, thermoelectric power and quasi-adiabatic Hall and Nernst coefficients over the temperature range 100°K to 600°K on n- and p-type specimens of Bi_2Te_3 with a wide variation of impurity content. Zone-refined material and single crystals were used with the current flow parallel and magnetic field either perpendicular or parallel to the cleavage planes. For one n- and one p-type specimen the isothermal coefficients were measured from 100°K to 450°K. An original method has been developed for measuring the isothermal galvanomagnetic effects accurately which is simpler than A.C. methods. Values of the isothermal Nernst coefficient were used to calculate the Ettingshausen coefficient. The Righi-Leduc effect, however, does not appear to obey simple semiconductor theory. The measured coefficients exhibit the anisotropy expected from the crystal structure and their temperature variation the general behaviour expected for a semiconductor, although the Hall coefficient is anomalous in the extrinsic region. Possible scattering mechanisms have been examined, taking into account the partial degeneracy of the specimens. Over the temperature range studied acoustical mode lattice scattering is the predominant mechanism, while at lower temperatures ionized impurity scattering becomes important. Conductivity measurements yield

the temperature variations of mobility, $T^{-1.63}$ for electrons and $T^{-1.94}$ for holes, and an energy gap of (0.21 ± 0.02) ev at $0^{o}K$. Optical and thermal values for the gap differ and possible reasons are discussed. The Nernst coefficient agrees qualitatively with theory. The experimental results are in general agreement with previously published data on Bi_2Te_3. In many cases the interpretation differs from that in previous work and the differences are discussed. It is thought that the activation energy for impurities is zero, and that even in the extrinsic range a two (or more) band model must be used. Lack of knowledge about the basic parameters in Bi_2Te_3 makes the interpretation of the results, even in the extrinsic region, uncertain.

INDEX

Chapter VI. Discussion of Results

Papers (a) Mansfield and Williams, 1958.

(b) Williams, 1959.

I. Introduction.

§1·1 Introductory remarks; interest in Bi_2Te_3; references to experimental work; interpretation of results; anomalies; chemical bonding; outline of accepted properties; aim of present investigation.

Interest in the properties of semiconductors over the past thirty years has been greatly stimulated by commercial application in various semiconductor devices. The starting point was the discovery that such substances as copper oxide and selenium have rectifying properties. Later interest shifted to germanium and silicon and their application to such devices as radar wave detectors and transistors. More recently there has been an increasing interest in certain compound semiconductors and their use in thermoelectric elements. At the same time, since the advent of quantum mechanics some thirty years ago, understanding of the electrical and magnetic properties of solids has progressed enormously (Bardeen, 1959; Busch, 1958; Fan, 1955, 1958; Joffé, 1959; Pincherle and Radcliffe, 1956; Welker and Weiss, 1956; Wright, 1958).

Bismuth telluride (Bi_2Te_3) is a semiconductor with a large thermoelectric power. The possibility of using semiconductors having a large thermoelectric power and low thermal conductivity in thermoelectric elements dates from 1954 (Goldsmid and Douglas, 1954). Since then a considerable amount

of research has been directed towards this problem (Goldsmid, Sheard and Wright, 1958; Shilliday, 1957; Joffé, 1957). The electrical and optical properties of Bi_2Te_3 and of alloys of Bi_2Te_3 with other substances have thus been extensively studied, both for their theoretical and practical interest (e.g. Fuschillo et al, 1959; Rosi et al, 1959; Benel, 1958; Gordiakova, Kokosh and Sinani, 1958; Gordiakova and Sinani, 1958; Wright, 1958, 1959; Austin and Sheard, 1957).

Comprehensive studies of the electrical and magnetic properties of single crystals of Bi_2Te_3 or zone refined material (§ 3·2) are not so numerous. Bi_2Te_3 belongs to the $R\bar{3}m$ class of crystals (§ 3·1) with a layer-like structure and electrical and magnetic properties which are markedly anisotropic. Thus the results obtained in many of the investigations cited above, and also in the first systematic investigation of Bi_2Te_3 (Vlasova and Stil'bans, 1955) on polycrystalline material, are very difficult to interpret.

The first measurements of the electrical conductivity, thermoelectric power and Hall coefficient on single crystals were made by Konorov (1956) over the temperature range $300^\circ \longrightarrow 600^\circ K$ and Shigetomi and Mori (1956) over the range $100^\circ \longrightarrow 750^\circ K$. The first measurements of thermal conductivity were made by Goldsmid (1956 (a) and (b)) over the range $150^\circ \longrightarrow 300^\circ K$.

More recent studies of these properties are reported by Lagrenaudie (1957), Black et al (1957) (both including some

optical measurements), Harman et al (1957), Satterthwaite and Ure (1957), Goldsmid (1958 (a) and (b)), Parrott and Penn (1958), Nii (1958), Kanai and Nii (1959), Macdonald et al (1959), Walker (1959) (thermal conductivity and thermoelectric power from 6 to 200°K) and Yates (1959) (electrical conductivity and Hall coefficient from 1·3 to 660°K). Magneto-resistance measurements (Drabble et al, 1958; Drabble, 1958) and magneto-thermoelectric effects (Bowley et al, 1958) have also been published. The only extensive study of the optical properties has been made by Austin (1958).

The only observations on the Nernst effect, except those presented in this thesis, are given by Bashirov (1958), but he used cast and pressed specimens. Measurements of Hall and Nernst coefficients, electrical conductivity and thermo-electric power on both n- and p-type specimens (single crystal and zone refined) of widely differing purity over the temperature range 100° $\longrightarrow$ 600°K are presented by Mansfield and Williams (1958). These measurements (§ 5·2) form the basis of part of the present thesis. However they were made under approximately adiabatic conditions, whereas formulae used in the interpretation of results are usually in terms of the isothermal coefficients. Therefore measurements of the isothermal Hall and Nernst coefficients were made over the temperature range 100° $\longrightarrow$ 450°K, and used to calculate the Ettingshausen coefficient (Williams, 1959). These results are also presented in this thesis (§ 5·3).

Magnetic susceptibilities have been measured on polycrystalline Bi_2Te_3 (Matyáš, 1958) and on zone refined material (Mansfield, 1959). Measurements of the structure cell parameters and expansion coefficients have also been published (Francombe, 1958).

Interpretation of the electrical properties of semiconductors is mainly in terms of band theory (see, for example, Ehrenberg, 1958; Shockley, 1950; Wilson, 1953). Although there are known to be certain limitations to its application (Slater, 1959), the basic ideas are those originally put forward about thirty years ago.

On the simple band theory a plot of log R or log σT^s against $\frac{1}{T}$, where R is the Hall coefficient, σ the electrical conductivity, T the temperature and s a constant depending on the type of scattering, in the region where conduction is by intrinsic carriers (intrinsic region) yields the energy gap E_o at 0^oK, provided that the variation of energy gap with temperature is linear. In the extrinsic region the temperature variation of the Hall mobility $\mu_H = R\sigma$ indicates the predominant scattering mechanism, while the Hall coefficient yields the number of impurity carriers and their sign. An extension of the analysis to include the thermoelectric power yields other basic parameters, such as the effective mass m* of carriers (Pearson and Bardeen, 1949). It should be emphasized that in order to be able to correlate the various electrical properties they should all be observed on the same specimen (§ 3·5; § 5·2)

(see, for example, Middleton and Scanlon, 1953) and that where possible single crystals should be used (§ 3·2) (Shockley, 1950, page 338). It is now possible to make very good large single crystals of germanium and silicon. Results on these substances are relatively easy to interpret as it is found that close agreement is obtained between theory and experimental results. In other semiconductors, however, the agreement between experimental and simple theory is not so good. Smith (1954) gives an assessment of the validity of basic methods of interpretation when applied to certain compound semiconductors (§ 6·2).

Although Bi_2Te_3 exhibits the general behaviour associated with semiconductors, there are many details which can only be explained by making assumptions additional to those of the basic theory. Except for some of the early work, the experimental results obtained in the papers quoted above are in fairly good agreement. However, the interpretation of these results is not always satisfactory. Bi_2Te_3 shows certain anomalies, as far as basic semiconductor theory is concerned, which makes it impossible to interpret the results as simply as is done for germanium and silicon (Mansfield and Williams, 1958). Far too simple an interpretation has been used by many workers (Black et al, 1957; Harman et al, 1957; Lagrenaudie, 1957; Satterthwaite and Ure, 1957; Shigetomi and Mori, 1956). Various workers note anomalies and these will be discussed in this thesis. In particular, attempts have been made to explain anomalies in the Hall coefficient (Harman et al, 1958; Williams,

1959; Yates, 1959) and thermoelectric power (Black et al, 1958; Goldsmid, 1958 (a)).

Almost all the electrical and magnetic properties of Bi_2Te_3 are anisotropic (§ 6·6). Drabble and Wolfe (1956) proposed a 'many-valley' model in order to account for the observed anisotropy in the extrinsic region in terms of a one-band model. This model has since been applied to Bi_2Te_3 (Drabble, 1958, 1959; Drabble et al, 1958).

Material obtained from a melt of stoichiometric composition, however pure the constituent materials (§ 3·2), is always p-type with a high concentration of carriers ($\sim 10^{18}$ cm^{-3}) and a reduction in the number of carriers can only be obtained by compensation. Harman et al (1958) explain this in terms of a "wrong-atom defect" theory (§ 6·8). Mooser and Pearson (1958) explain both this and a supposed double reversal in the Hall coefficient of n-type Bi_2Te_3 (attributed incorrectly to Satterthwaite and Ure, 1957) by a three-band model. However, this model is inconsistent with other observations (§ 6·8).

The nature of the chemical bonding in Bi_2Te_3 and its relation to the semiconducting properties of the compound were first discussed by Lagrenaudie (1957) and Mooser and Pearson (1956). These papers are later criticised by Drabble and Goodman (1958) who have proposed a bonding scheme which explains the band gap anomaly in the $Bi_2Te_{3-x}Se_x$ system (Austin and Sheard, 1957) (§ 3·1).

It is generally agreed that Bi_2Te_3 is a semiconductor with anisotropic properties consistent with its crystal structure. For the reasons explained above it is necessarily a heavily doped semiconductor, with a small energy gap, which at sufficiently high temperatures shows intrinsic behaviour (§ 6·3). The impurity levels are thought to form impurity bands overlapping the conduction and valence bands (§ 6·3; § 6·8). The type of scattering is uncertain but it is generally assumed that acoustical mode lattice scattering predominates except at very low temperatures (§ 6·2; § 6·4). Previous workers have been unable to apply the theory of impurity scattering to observations on Bi_2Te_3 and have concluded that impurity scattering is insignificant in most specimens above about 100°K. It is shown (§ 6·4), however, that if allowance is made for the degeneracy of the charge carriers when calculating the mobility due to impurity scattering, the results obtained can be interpreted in terms of impurity scattering.

Without further knowledge of the parameters of the band structure the Hall coefficient of Bi_2Te_3 cannot be accurately related to the carrier concentration. Thus quantities such as the mobilities, concentrations and effective masses of electrons and holes are uncertain. In addition, because of the high impurity concentration and small temperature range over which Bi_2Te_3 samples are intrinsic, the energy gap, which is small and varies with temperature, is not well known. The value of E_o obtained from electrical measurements does not agree with the optical value (§ 6·3).

The work presented in this thesis is an attempt to clarify the position on the fundamental semiconductor parameters associated with Bi_2Te_3. It is for this reason that comprehensive measurements of electrical conductivity, thermoelectric power and quasi-adiabatic Hall and Nernst coefficients, including some anisotropic effects, were made over as wide a temperature range and impurity content as could be obtained. Isothermal Hall and Nernst coefficients were also measured, but over more restricted temperature and impurity content ranges. Interpretation of these results enables a better understanding of the mechanisms of conduction in Bi_2Te_3 to be obtained.

It would be interesting, if suitable facilities were available, to extend measurements on the same specimens down to liquid helium temperatures (cf. Yates, 1959). In particular measurements of the Nernst coefficient and thermoelectric power might reveal the existence of the phenomenon of phonon drag (§6·9) in Bi_2Te_3 at temperatures lower than those obtainable in the present investigation, although Walker (1959) finds no appreciable contribution to the thermoelectric power due to the phonon-drag effect.

II. Definitions and Units.

§2·1 Definitions; sign convention; calculation of coefficients in terms of measured quantities; units.

The quantities which have been measured in the present investigation are the electrical conductivity, thermoelectric power and Hall and Nernst coefficients. The Ettingshausen coefficient has been calculated and an attempt was made to obtain the Righi-Leduc coefficient. The definition of thermal conductivity is also required as values of the thermal conductivity are used in the calculations of the Ettingshausen coefficient.

The definitions used for these quantities are given in Table 2·1 with respect to a right-handed system of Cartesian coordinates. With the primary electric current density J, or primary thermal current density ω through the specimen in the x-direction and a magnetic field H applied in the z-direction, the transverse galvanomagnetic and thermomagnetic effects are measured in the y-direction (Figure 1). For the Hall and Nernst coefficients it is necessary to state the conditions in the y-direction. For isothermal conditions $\frac{\partial T}{\partial y} = 0$, where T is temperature, and for adiabatic conditions $\omega_y = 0$. The conditions under which the Ettingshausen and Righi-Leduc coefficients are defined are necessarily adiabatic. Electrical

* This definition is often given in the literature, although it is incorrect since $\frac{dE}{dT}$ should be defined in terms of the electrochemical potential, Σ^*, instead of E_x, ie. $\frac{dE}{dT} = \frac{1}{e} \cdot \frac{\Delta \Sigma^*}{\Delta T}$

conductivity, thermoelectric power and thermal conductivity are normally defined for isothermal conditions, and in zero magnetic field. All definitions refer to steady state conditions. E is electric field intensity, except in the symbol used for thermoelectric power ($\frac{dE}{dT}$).

Table 2·1.

Name of coefficient	Symbol	Definition	Conditions
Electrical conductivity	σ	$\frac{J_x}{E_x}$	$J_y = 0 \quad \frac{\partial T}{\partial x} = \frac{\partial T}{\partial y} = 0 \quad H_z = 0$
Thermoelectric power	$\frac{dE}{dT}$	$\frac{E_x}{\partial T/\partial x}$ *	$J_x = J_y = 0 \quad \frac{\partial T}{\partial y} = 0 \quad H_z = 0$
Thermal conductivity	K	$-\frac{\omega_x}{\partial T/\partial x}$	$J_x = J_y = 0 \quad \frac{\partial T}{\partial y} = 0 \quad H_z = 0$
Isothermal Hall coefficient	R_i	$+\frac{E_y}{H_z \cdot J_x}$	$J_y = 0 \quad \frac{\partial T}{\partial x} = \frac{\partial T}{\partial y} = 0$
Adiabatic Hall coefficient	R_a	$+\frac{E_y}{H_z \cdot J_x}$	$J_y = 0 \quad \frac{\partial T}{\partial x} = 0 \quad \omega_y = 0$
Isothermal Nernst coefficient	Q_i	$-\frac{E_y}{H_z \cdot \frac{\partial T}{\partial x}}$	$J_x = J_y = 0 \quad \frac{\partial T}{\partial y} = 0$
Adiabatic Nernst coefficient	Q_a	$-\frac{E_y}{H_z \cdot \frac{\partial T}{\partial x}}$	$J_x = J_y = 0 \quad \omega_y = 0$
Ettingshausen coefficient	P	$-\frac{\partial T/\partial y}{H_z \cdot J_x}$	$J_y = 0 \quad \frac{\partial T}{\partial x} = 0 \quad \omega_y = 0$
Righi-Leduc coefficient	S	$+\frac{\partial T/\partial y}{H_z \cdot \frac{\partial T}{\partial x}}$	$J_x = J_y = 0 \quad \omega_y = 0$

Obviously many other coefficients could be defined. For a comprehensive account of the definitions of all the possible effects and the relations between them reference is made to Jan (1957).

The definitions stated in Table 2·1 make the sign convention used the same as that stated by Gerlach (1928). An equivalent definition for the sign of the thermoelectric power is that it is positive when conventional current flows from metal to semiconductor at the hot junction. The sign of the thermoelectric power is then the same in the extrinsic region as that of the charge carriers.

In practice the coefficients are measured in terms of the current I_x through the specimen and the potential differences developed between various points on the specimen, rather than current density and electric field intensity.

Referring to Figure 2, the galvanomagnetic and thermomagnetic effects are measured in terms of the potential difference $V_y(= aE_y)$ developed between the probes A and B. In the absence of a magnetic field H_z, but with a current I_x flowing, A and B both make contact with the specimen on the same equipotential surface. The current $I_x = abJ_x$. The temperatures at points C and D are measured by thermocouples in electrical contact with the specimen. Thus the temperature gradient down the specimen $\frac{\partial T}{\partial x} = \frac{T_C - T_D}{\ell}$, and the potential gradient down the specimen E_x is measured in terms of the potential difference $V_x(= \ell E_x)$ existing between the two T_1 leads of the thermocouples at C and D.

In Table 2·2 the definitions of the four coefficients, which were determined by direct measurement in this investigation,

are given in terms of the measured quantities. These have been derived directly from the definitions given in Table 2·1, in which all quantities are in absolute c.g.s.m.units. The modified formulae which must be used to obtain the coefficients in practical units when I is in ampères, v in microvolts, H in oersteds, $\frac{\partial T}{\partial x}$ or $\frac{\partial T}{\partial y}$ in $^{o}K\ cm^{-1}$ and all distances in cms, are thus also given.

Thermal conductivity and the Ettingshausen and Righi-Leduc coefficients are not included in this table as they were not measured directly but are deduced from measurements of the other coefficients.

The practical units for these coefficients are:-

K: watt cm^{-1} deg^{-1}

P: cm^3 deg $Joule^{-1}$

S: cm^2 sec^{-1} $volt^{-1}$

Table 2·2.

Coefficient	c.g.s.	Practical	Units	Comments
σ	$\frac{I_x \ell}{ab.V_x}$	$\frac{I_x \ell.10^6}{ab.V_x}$	$ohm^{-1}cm^{-1}$	
$\frac{dE}{dT}$	$\frac{V_x}{T_C-T_D}$	$\frac{V_x}{T_C-T_D}$	$\mu V\ deg^{-1}$	
R_i, R_a	$+\frac{V_y b}{H_z.I_x}$	$+\frac{V_y b.10^2}{H_z.I_x}$	$cm^3 coul^{-1}$	b is always the dimension in the direction of H_z.
Q_i, Q_a	$-\frac{V_y \ell}{aH_z(T_C-T_D)}$	$-\frac{V_y \ell.10^2}{aH_z(T_C-T_D)}$	$cm^2 sec^{-1} deg^{-1}$	a is always the dimension in the direction of V_y.

III. Bismuth Telluride.

§3·1 Crystal structure; §3·2 Methods of making Bi_2Te_3;
§3·3 Type of specimens used; § 3·4 Preparation of specimens;
§3·5 Diffusion of copper into Bi_2Te_3.

3·1. Crystal Structure.

Bismuth telluride, Bi_2Te_3, is a semiconductor formed between elements from Groups VB (Bi) and VIB (Te) of the periodic table. It crystallizes in a rhombohedral lattice and belongs to the crystal class $R\bar{3}m$ or C33 (Lange, 1939; Wyckoff; 1951; Mooser and Pearson, 1956, 1958), being isomorphous with the naturally occurring mineral tetradymite (Bi_2Te_2S). It thus has a "layer" structure consisting of multiple layers which are perpendicular to the axis of three-fold symmetry or 'c' axis (see Figure 3(a)). Each layer is formed of five monatomic layers in the sequence Te-Bi-Te-Bi-Te. The sequence in three multiple layers is thus:

$$Te^{(1)}\text{-}Bi\text{-}Te^{(2)}\text{-}Bi\text{-}Te^{(1)}\text{-}Te^{(1)}\text{-}Bi\text{-}Te^{(2)}\text{-}Bi\text{-}Te^{(1)}\text{-}Te^{(1)}\text{-}Bi\text{-}Te^{(2)}\text{-}Bi\text{-}Te^{(1)}$$

where the superscripts are used to distinguish between tellurium atoms bonded in two different ways. $Te^{(2)}$ atoms have six Bi nearest neighbours. Bi atoms are bonded to three $Te^{(2)}$ atoms on one side and three $Te^{(1)}$ atoms on the other - the bond lengths to $Te^{(2)}$ and $Te^{(1)}$ atoms being slightly different. Each $Te^{(1)}$ atom has three Bi neighbours in the same multiple layer, while the next

nearest atoms are three $Te^{(1)}$ atoms in the adjacent multiple layer. Drabble and Goodman (1958) work out the bond lengths from the crystal structure data given by Lange (1939). A more recent determination of structure cell parameters than those quoted above is given by Francombe (1958).

Mooser and Pearson (1956) explain the structure in Bi_2Te_3 in terms of "resonating bonds" which involves the promotion of electrons into higher orbitals. This theory suggests that Bi_2Te_3 should show metallic behaviour. Mooser and Pearson claim that Bi_2Te_3 shows a metallic temperature dependence of electrical conductivity, but all other measurements (§ 1·1) show conclusively that Bi_2Te_3 is a semiconductor. Lagrenaudie (1957) also suggests a bonding scheme, but this does not account for all the available valence electrons.

Drabble and Goodman (1958) put forward a bonding scheme which removes these difficulties. The bonding existing between $Te^{(1)}$ atoms in adjacent multiple layers is assumed to be of the van der Waals type. This explains the easy cleavage of the single crystal and zone refined Bi_2Te_3 between the weakly bonded $Te^{(1)}$-$Te^{(1)}$ planes (0001 planes). Within multiple layers the bonding is predominantly homopolar - with an ionic component along the Bi-$Te^{(1)}$ bonds. Similar conclusions were stated by Konorov (1956) and by Black et al (1957) who investigated a number of $M_2^{VB}N_3^{VIB}$ semiconductors and pointed out that the relatively large variation of energy gap between different members of the series is characteristic of covalent bonding. Goldsmid et al (1958) suggest that

the best materials for thermoelectric elements may have bonding intermediate between covalent and ionic. Drabble and Goodman draw support for their theory from the observations of Austin and Sheard (1957) on $Bi_2Te_{3-x}Se_x$ alloys. Measurements on the optical energy gap support the theory that the $Te^{(1)}$ and $Te^{(2)}$ atoms are differently bonded, and that the Bi-$Te^{(1)}$ bond is partially ionic. Additional support is given by the results of Fuschillo et al (1959). Other interesting comments on the bonding in Bi_2Te_3 occur in the paper by Joffé (1959) and the discussion which follows by **Shockley.**

3·2. Methods of Making Bi_2Te_3.

The preparation of Bi_2Te_3 crystals is discussed by Ainsworth (1956), Harman et al (1957) and Satterthwaite and Ure (1957). The preparation of single **crystals** as described by Ainsworth is criticised by Satterthwaite and Ure.

Four of the five specimens used in the present investigation (§3·3) were obtained from G.E.C., Wembley. The single crystal specimens were prepared as reported by **Drabble et al** (1958). The rest were of zone-refined material (e.g. Goldsmid et al, 1958). Goldsmid (1958 (a)) has reported that zone-refined ingots of Bi_2Te_3 are generally polycrystalline, but that the c axes (§3·1) of the individual crystals are always perpendicular to the direction of the zone refining. Since all directions in the cleavage plane are equivalent as far as electrical properties are concerned (Drabble and Wolfe, 1956),

such ingots are suitable for measurements where electrical current or heat flow are parallel to the cleavage planes. Goldsmid also reports that no difference between the properties of single crystals and of the zone-refined material has been found.

When Bi_2Te_3 is prepared from a melt consisting of the pure elements in the correct proportions for a stoichiometric composition, it is always p-type with about $10^{18} \longrightarrow 10^{19}$ holes per unit volume at room temperature. The number of atoms per unit volume in Bi_2Te_3 is about 3×10^{22} so that the number of carriers, calculated from the Hall coefficient, is far greater than would be expected from the impurity content (less than 1 in 10^6) of the starting materials. Repeated zone-melting does not result in purer specimens as it does in materials such as InSb, where carrier concentrations as low as 10^{14} cm^{-3} can be obtained (Offergeld and van Cakenberghe, 1959). The production of p-type material with fewer carriers or of n-type material can only be obtained by compensation. This can be done by adding excess tellurium, any of the halogens, copper oxide or certain metals such as lithium or aluminium. Excess bismuth, lead or cadmium produces additional p-type carriers (Goldsmid, 1958 (a); Rosi et al, 1959). In the experimental methods referred to it is possible to control quite accurately the added impurity content of specimens.

Some attempts have been made to explain the high concentration of p-type carriers in stoichiometric Bi_2Te_3. These theories will be discussed in section 6·8.

3·3. Type of specimens used.

The specimens used are listed in Table 3·1, together with the sign of the extrinsic carriers and the value of the room temperature Hall coefficient measured with current flow along, and magnetic field perpendicular to, the cleavage planes (§ 5·1). Also listed are the sources from which the specimens were obtained, the element used for doping, whether zone refined or single crystal, the specimen designation used by G.E.C. and A.E.I. for the specimens and references to any published results on specimens from the same ingot.

Table 3·1.

Specimen	Sign	R (cm^3 $coul^{-1}$)	Source	Doping material	Type of specimen	Specimen designation	References*
R3·1	n	—	G.E.C.	iodine?	zone refined	SRT L/2 ?	
R3·21		0·56					
R5	p	0·32	G.E.C.	none	zone refined		(3)
R7	n	0·057	A.E.I.	?	zone refined	/BT 1/17/B	
R8	p	0·87	G.E.C.	iodine	single crystal	SBTC/19 J	(1) (2) (3) (4) (5)
R9	n	0·84	G.E.C.	iodine	single crystal	SBTC/16	(1) (3) (4) (5)

*References: (1) Austin (1958); (2) Drabble (1958);
(3) Mansfield (1959); (4) Walker (1959);
(5) Yates (1959).

3·4. Preparation of specimens.

Specimens were obtained in the desired shape by cutting and cleaving. The ratio of the length to either of the transverse dimensions 'a' or 'b' (Figure 2) was always made greater than 4 : 1 (Isenberg et al, 1948). An exception was specimen R3·1 (Table 3·2) which was only used for measurement of electrical conductivity. Owing to the ease with which Bi_2Te_3 cleaves, care had to be taken to see that the specimens used were free from cracks.

Specimens were etched and then washed in distilled water followed by alcohol. After trying various etches a solution of HCl, HNO_3 and distilled water in the proportions of 3 : 1 : 4 respectively was used. The variation of 'a' and 'b' down the length of a specimen was measured using either a travelling microscope or vernier screw gauge. For all the specimens listed in Table 3·1, 'a' and 'b' were each constant to better than 1 in 100 over the region used for measurement.

Since the method of mounting (§ 4·2), which must be used in order to obtain uniformity of the current flow pattern throughout the part of the specimen used for measurements, depends on the dimensions of the specimen, these are given in Table 3·2.

Table 3·2.

Specimen	Length, cms	'a' cms	'b' cms
R3·1	0·52	0·352 ± 0·004	0·309 ± 0·003
R3·21	1·3	0·308 ± 0·003	0·206 ± 0·002
R5	7·0	0·603 ± 0·006	0·243 ± 0·002
R7	1·7	0·429 ± 0·004	0·248 ± 0·002
R8	2·5	0·487 ± 0·005	0·298 ± 0·003
R9	5·7	0·285 ± 0·003	0·182 ± 0·002

3·5. Diffusion of Copper into Bi_2Te_3.

During preliminary observations on Bi_2Te_3 it was found that soldering a specimen into a copper holder could change the specimen from p- to n-type. Subsequent heating to the melting point of lead solder produced further irreversible effects, the concentration of donors increasing each time. Heating to 350°C resulted in a return to the original p-type behaviour. Attempts were made to introduce a known concentration of copper into a specimen by means of heat treatment following the deposit of a known quantity of copper on the surface by electrolysis or evaporation. If the type and concentration of carriers could be controlled in this way, then observations of the electrical

properties of Bi_2Te_3 for various impurity concentrations could be made on the same specimen. Thus the variations with carrier concentration of the various properties could be more accurately determined than by using several specimens, since any errors incurred in the measurement of the dimensions of the specimen (§ 3·4), or due to defects in the specimen, would affect each set of results in the same way. No reproducible results were obtained, so the results obtained on these specimens were discarded. All the results presented in this thesis were obtained on specimens which have at no time been in contact with copper. Completely reproducible results were then obtained.

Similar effects due to copper are reported by Goldsmid (1958 (a)) who suggests that copper is a donor impurity with an exceptionally high rate of diffusion in Bi_2Te_3. On the other hand, Gordiakova and Sinani (1958) find that adding metallic copper to the melt has very little effect on the electrical conductivity of Bi_2Te_3. They explain this as probably due to its very low solubility.

There is a certain similarity between some results observed by Matukura (1957) on Si and the results obtained with Bi_2Te_3 when in contact with copper. A specimen of silicon could be made n-type and p-type alternately by suitable heat treatment. These results are interpreted at low temperatures in terms of surface impurities and at higher temperatures as due to lattice defects. However, the investigation of these phenomena in Bi_2Te_3 was not sufficiently extensive to enable any conclusions to be reached.

IV. Experimental Procedure.

§4·1 Apparatus; §4·2 Mounting of specimens; §4·3 Measurement of temperature; §4·4 Experimental technique and calculations; §4·5 Preliminary measurements on Bi_2Te_3.

4·1. Apparatus.

The type of specimen holder employed is indicated in Figure 4. Specimens were mounted in a vertical position on an insulating board of syndanyo which just fitted into the non-magnetic stainless steel tube. Temperatures above room temperature could be obtained by means of the insulated heating coil, wound non-inductively on the outside of the stainless steel tube. Temperatures below room temperature could be obtained by immersing the tube in liquid air contained in a dewar flask as shown. The whole was placed between the pole pieces of an electromagnet, with the centre of the specimen at the centre of the gap. The orientation of the specimen with respect to the magnetic field could be adjusted by turning the syndanyo board. All readings were taken at atmospheric pressure, using conventional D.C. methods.

An air-cooled electromagnet (Clarendon Laboratory, type A, Newport Instruments Ltd.) was used with shaped pole pieces as shown in Figure 4. The magnetic field at the centre of the gap between the pole pieces was determined using the room temperature Hall coefficient of a mounted specimen of Indium

Antimonide which had previously been calibrated over a range of magnetic fields using a proton resonance method. The maximum variation of magnetic field with position over the whole of the central region of the gap was 1 in 300. Subsequently, when the size of the gap was altered and it was necessary to recalibrate the field, this was done using the known room temperature Hall coefficient of one of the Bi_2Te_3 specimens, assuming this to be independent of magnetic field (§ 4·5).

The magnetic properties of the specimen holder were tested using the room temperature Hall coefficient of the InSb specimen. Observations made when this specimen was supported between the pole pieces, without the specimen holder present and when inserted in the holder, agreed to better than 1%.

With a gap of about 6·5 cm, required to accommodate the dewar flask for low temperature readings, and a magnetising current of 4 amps the value of the magnetic field was about 4500 oersted. For readings above room temperature the gap could be reduced to about 3·5 cm, giving, for 4 amps, about 6500 oersted.

All potential differences were measured using a vernier potentiometer (Cambridge Instrument Co. Ltd.) with a short period, low resistance galvanometer. The resistance of the potential leads was of the order of 50 $\longrightarrow$ 150 ohms for the thermocouples and 10 ohms or less for the Hall probes. All contact resistances were effectively zero (§ 4·2). Thus potential differences could be obtained to the nearest 10μV and 1μV on the 0 $\longrightarrow$ 1·9 volt and 0 $\longrightarrow$ 0·19 volt ranges respectively.

4·2. Mounting of specimens.

Owing to the high coefficient of diffusion of copper into Bi_2Te_3 (§ 3·5) it is essential, in order to obtain reproducible results, that specimens are mounted without any contact with copper or materials containing copper. Some workers nickel-plate, or, for use in a magnetic field, rhodium-plate, the ends of the specimen and then solder current leads (e.g. Goldsmid, 1957, 1958 (a)). In the present case, since observations were made up to 350°C, this method was unsuitable.

It is also essential that over the part of the specimen used for electrical conductivity readings the current density through the specimen should be uniform. In preliminary observations it was found that the use of unsuitable current contacts could lead to values of σ in error by a factor of two or more. For short specimens (1·3 $\longrightarrow$ 2·5 cm), where a large percentage of the specimen must be used, pressure contacts had to be employed. The surfaces actually in contact with the ends of the specimen were of silver or platinum. The ends of the specimens were filed flat and then pressure applied along the axis of the specimen by means of a spring, as shown in Figure 5(a). For longer specimens (6 $\longrightarrow$ 7 cm), where it was possible to keep the measuring probes well away from the ends of the specimen, it was found satisfactory to make current contacts by means of platinum wires over the ends of the specimen (Figure 5(b)). These methods were found satisfactory over the whole temperature range (100° $\longrightarrow$ 625°K) investigated.

When current contacts had been made, the uniformity of current density and electrical conductivity along the specimen was tested by a potential probe method. A steady direct current was passed through the specimen. Then, by means of two chromel probes, one fixed near one end and the other moveable, the variation of potential along the specimen was determined using a potentiometer. Distances were measured with a travelling microscope. A plot of potential difference between the two probes against the position of the moveable probe should be a straight line. Any specimens not showing a linear variation, except very near the ends of the specimen, were assumed to be inhomogeneous and were rejected. Figure 6 shows a representative potential difference versus distance plot for one of the specimens used in the present investigation.

In order to establish a temperature gradient along the specimen (in the x-direction: Figure 1), an insulated heater was placed just above the specimen. The direct current through this could be controlled by a variable resistance.

The thermocouples used were of T_1 and T_2 alloys, similar in their properties to 'Chromel' and 'Alumel' respectively (Putley, 1955). The pair of thermocouples used for a given specimen were "matched" in order to avoid errors due to non-uniformity between the two couples. Initially this was done by the method described by Middleton and Scanlon (1953). The two junctions to be placed in contact with the specimen were

formed from as nearly identical material as possible by taking a long, homogeneous piece of each kind of thermocouple wire to be used, cutting them, and silver soldering these freshly cut ends to form the junctions making contact with the specimen. The free ends of the T_2 alloy wires were then silver soldered to additional pieces of T_1 alloy wire to form the ice junctions. This is illustrated in Figure 7(a). The junctions formed by cutting the T_1 alloy wire at a-b and the T_2 alloy wire at a'-b', and then joining a to a' and b to b', are matched. Junctions c-c' and d-d' are unmatched. Thus, although the specimen junctions are matched by this method, the equally important ice junctions are not. For thermocouples employed in later measurements a method was devised of matching both specimen and ice junctions. This is illustrated in Figure 7(b) and it is seen that all unmatched connections occur at room temperature. Wires of 40 S.W.G. were used and the junctions cut so that they were as small as possible. These thermocouples were each compared with a calibrated $T_1 - T_2$ thermocouple (§ 4·3). The maximum difference in e.m.f. between any of the thermocouples employed in the present investigation and the calibrated thermocouple was 1 in 200 at the temperature of liquid air. The difference in e.m.f. of a pair of "matched" thermocouples recording liquid air temperature was of the order of 1 in 5000.

Thermocouple wires were insulated with enamel paint, except near the junctions. The wires near the specimen junction

were insulated with fine glass tubing for high temperature observations. Thermocouples were spot-welded to one side of the specimen, as shown in Figures 5 (a) and (b), care being taken not to place them too near the ends. The junctions were pressed against the specimen and then an 80μF condenser, charged to about 12 volts, discharged through the pressure contact (Mitchell, 1954). Satisfactory contacts, with effectively zero contact resistance, were obtained by this method over the whole temperature range investigated. Spot-welded contacts are mechanically weak and all wires were secured by screws to the syndanyo board before spot-welding. The distance between the thermocouple junctions was measured with a travelling microscope. Thus, with the thermocouples connected via a selecting key into the potentiometer, as shown in Figure 7(c), temperature and potential gradients down the specimen and the mean temperature of the specimen could be determined. The Hall probes, of T_1 alloy or Bi_2Te_3 (§ 5·3), were also spot-welded to the specimen. The current flowing through the specimen was determined from the potential difference across a standard 0·1 ohm resistance (H.W. Sullivan Ltd.) in series with the specimen, as shown in Figure 7(c).

Thus observations of the electrical conductivity, thermoelectric power and Hall and Nernst coefficients at a given temperature could be taken very rapidly. This is essential, especially for observations below room temperature where only limited temperature control was possible. Observations were

first obtained at the lowest temperature attainable with the dewar kept full of liquid air (Figure 4). Observations between this temperature and room temperature were made as the apparatus warmed up. The rate of increase of mean temperature of the specimen was sufficiently slow, and the method of taking readings sufficiently rapid, for satisfactory results to be obtained. Temperature control above room temperature was far easier. This was done by controlling the alternating current through the main heating coil by means of a Variac transformer. Below room temperature it was impossible to prevent a temperature gradient existing along the specimen. This was shown (§ 4·4; § 4·5) to have no effect on the values obtained for the Hall coefficient and the electrical conductivity.

Rapidity in taking readings above room temperature was not so essential, but did keep to a minimum the slight oxidation of the surfaces which occurred with some specimens when trying to obtain readings above 350°C. The melting point of bismuth telluride is 580°C (Shigetomi and Mori, 1956), but the range over which readings could be taken at atmospheric pressure was limited by this oxidation (§ 4·5).

4·3. Measurement of Temperature.

A saturated vapour pressure thermometer was used below 0°C to calibrate a thermocouple of T_1 - T_2 alloys, constructed as described previously (§ 4·2). Above 0°C the standard

calibration for chromel-alumel couples (American Institute of Physics Handbook, 1957) was checked and found satisfactory.

The gases used in the S.V.P. thermometer were sulphur dioxide (SO_2), carbon dioxide (CO_2) and ethylene (C_2H_4) over the temperature ranges $(-10 \longrightarrow -50)^{\circ}C$, $(-75 \longrightarrow -100)^{\circ}C$ and $(-105 \longrightarrow -150)^{\circ}C$ respectively. The type of S.V.P. thermometer employed is described by Farkas and Melville (1939), who also give tables of S.V.P. versus temperature for the three gases used. Care was taken in each case to ensure that only the pure gas required for the thermometer was present in the apparatus.

One junction of the thermocouple was inserted in a mixture of ice and water, while the other, the wires insulated except at the junction, was attached to the bulb of the S.V.P. thermometer. This was inserted in a tube containing mercury which was then placed in alcohol in a dewar flask. When the alcohol was cooled with liquid air any desired temperature could be obtained. The e.m.f. of the couple for various temperatures, as recorded by the S.V.P. thermometer, is given in Figure 8. The thermoelectric power of T_1 relative to T_2 alloy against temperature over the whole temperature range studied is given in Figure 9.

In order to obtain the correct mean temperature of, and temperature gradient down, the specimen the position of the thermocouples is of great importance. In particular, when small temperature gradients are employed, a small error in one or both

of the measured temperatures can result in a large error in values of the thermoelectric power, Nernst and Righi-Leduc coefficients. This problem has been extensively studied in connection with the measurement of the thermoelectric power of semiconductors (e.g. Joffé, 1957; Skanavi and Kashtanova, 1956).

In the measurement of the thermoelectric power of a specimen relative to the measuring probes, the temperature difference giving rise to the measured thermal e.m.f. must be accurately found. In the two experimental arrangements commonly employed the specimen is clamped (Joffé, 1957, page 132) or soldered between metal blocks. In one arrangement the temperature difference between the ends of the specimen is measured by means of thermocouples inserted in the metal blocks as near to the ends of the specimen as possible (e.g. Goldsmid, 1956 (a)). This method is simple but would be unsatisfactory in the present investigation. Pressure contacts have to be used (§ 4·2), and hence there would be temperature drops across the specimen-to-metal contacts at each end of the specimen. The measured temperature difference across the specimen would thus be higher than the one giving rise to the measured thermal e.m.f. and the calculated thermoelectric power would be lower than the true value. In the second arrangement, used here (§ 4·2), the thermocouples are placed at one side of the main heat flux. This method has been discussed by Middleton and Scanlon (1953) and Skanavi and Kashtanova (1956). Experimentally this is not as simple as the first arrangement as it is often difficult to make satisfactory contact between

the specimen and thermocouple junctions. In some cases contact may be made by soldering, but the area of contact must be kept to a minimum (Dunlap, 1950), while inserting the thermocouple junctions in small holes in the side of the specimen disturbs the heat flow.

It is considered that the present arrangement satisfies the requirements for accurate temperature measurement (§ 4·5; § 5·4). The thermocouple wires are thin (40 S.W.G.), the junctions are small and pairs of couples have been matched, while the technique of spot-welding produces a contact of small area and negligible resistance. Consideration of the accuracy is particularly important since the experimental values obtained for the thermoelectric power are higher than those obtained by other workers using specimens of a similar carrier concentration (§ 6·9).

Joffé (1957, page 132) describes a third, and better, method for the measurement of thermoelectric power which, however, would not allow the simultaneous measurement of electrical conductivity when dealing with short specimens.

4·4. Experimental technique and calculations.

Hall coefficient and electrical conductivity measurements were made using direct current. When making observations the conditions assumed in § 2·1 are not realised and the usual precautions of reversing current and magnetic field were observed. In this way all the voltages which are superimposed

on the Hall voltage can be eliminated with the exception of the voltage resulting from the Ettingshausen temperature difference (§ 5·3). The thermoelectric power of Bi_2Te_3 with respect to the material of the measuring probes (T_1 alloy) is large and varies quite rapidly with temperature. Since readings are taken under varying temperature conditions (§ 4·2) they had to be taken as rapidly as possible. In making observations of the Hall voltage, the magnetic field H_z had to be reversed several times for each direction of the current through the specimen and the average value of the Hall voltage calculated corresponding to the mean temperature of the specimen over the time taken to make the observations. Calculations based on the measured values of the Nernst coefficient showed that the value obtained for the Hall coefficient, using this experimental technique, is independent of the value of the temperature gradient down the specimen.

The effect of Peltier heating and cooling at the junctions is large in Bi_2Te_3 and could cause errors in the measured values of electrical conductivity. The influence of the Peltier effect on the conductivity can be reduced by making measurements on the centre portion of a long specimen, which was possible for R5, R8 and R9, and by a suitable technique of making observations. With steady conditions the potential difference down the specimen was recorded, and then the current was reversed and the new potential difference immediately found

(Satterthwaite and Ure, 1957). It was found that this method gave reliable values of the electrical conductivity for small currents (§ 4·5). Several workers use A.C. methods (e.g. Goldsmid, 1958 (a)), while Drabble et al (1958) use a compensating arrangement to eliminate the effects due to the temperature gradient associated with the passage of current through the specimen.

In the measurement of the thermoelectric power and Nernst coefficient measurement of the temperature difference $|T_C - T_D|$ (§ 2·1; § 4·3) requires care. The quantities actually measured were the e.m.f.s E_C and E_D of the $T_1 - T_2$ thermocouples corresponding to the temperatures T_C and T_D (Tables 5·2 and 5·4). The mean temperature of the specimen $\frac{T_C + T_D}{2}$ may be obtained from Figure 8, but the individual values of T_C and T_D cannot be obtained with sufficient accuracy (§ 5·4) to give $|T_C - T_D|$. The temperature difference was thus obtained by use of Figure 9 and the relation (Middleton and Scanlon, 1953)

$$\left(\frac{dE}{dT}\right)_{(T_1 - T_2)} = \frac{E_C - E_D}{T_C - T_D}.$$

Electrical conductivity, thermoelectric power and Hall and Nernst coefficients were calculated in practical units using the equations in Table 2·2. Since the measuring probes were of T_1 alloy (≡ Chromel) the thermoelectric power of Bi_2Te_3 was measured relative to T_1 alloy. A correction was then

applied to give the thermoelectric power of Bi_2Te_3 relative to lead. The e.m.f. of a T_1-Pb thermocouple was plotted against the temperature as recorded by a calibrated $T_1 - T_2$ thermocouple (Figure 10). This was used to plot the thermoelectric power of T_1 relative to lead against temperature (Figure 11) (Lemon and Ference, 1946, p. 338). Thus the correction to be applied to the measured e.m.f. at any temperature could be obtained from Figure 11.

4·5. Preliminary measurements on Bi_2Te_3 .

(i) Electrical conductivity.

The effect on the electrical conductivity of altering the current through the specimen was tested at about 100 and 300° K. It was found that the effects of Peltier heating resulted in deviations from Ohm's law if the current was made too large. The limit to the current which could be used depended on the size of the specimen but was of the order of 0·3 amperes for R3·21.

Specimen R5 is a long specimen, so that it was possible to attach extra conductivity probes of Bi_2Te_3 cut from material originally adjacent to the specimen (§ 5·3). Conductivity readings made using Bi_2Te_3 probes are not expected to be influenced by Peltier heating effects and thus serve as an additional check on the validity of the experimental method used for the conductivity (§ 4·4). Measurements were taken

simultaneously of the conductivity using both T_1 alloy and Bi_2Te_3 probes. Since R5 is a long specimen, for very small currents both quantities should be the same. Readings were taken for different values of the current through the specimen at room temperature and at 110°K. Over the range of currents normally used no evidence could be found of an error in the conductivity due to the Peltier effect. However, such an error would depend on the size of the specimen and is much more likely to be appreciable for small specimens.

It was shown for each specimen that the electrical conductivity was independent of the position of the thermocouples over the central regions of the specimen (§ 4·2).

Magnetoresistance measurements were made on specimen R5 at room temperature over the range of magnetic induction 1,600 to 14,000 gauss with current flow parallel to and magnetic field perpendicular to the cleavage planes (§ 5·1). At 14,000 gauss the fractional change in conductivity, $\frac{\sigma_0 - \sigma_H}{\sigma_0}$, was about 1 in 285. It was found that conditions were not sufficiently stable to measure such a small effect accurately (Drabble et al, 1958), a large scatter being obtained on the results.

It was found that as long as there was no contact with copper (§ 3·5) the conductivity and the Hall and Nernst coefficients were reproducible over the whole temperature range 100° to 620°K.

(ii) Hall Effect.

The Hall coefficient was measured with the current parallel to and the magnetic field either parallel or perpendicular to the cleavage planes (§ 5·1). For either of these experimental arrangements it was found that the value obtained for the Hall coefficient was not very sensitive to the exact orientation of the specimen with respect to the magnetic field. Deviations of as much as 5° from the correct orientation produced less than 1% change in the measured value of the Hall coefficient.

The dependence of the Hall coefficient on the magnetic field was tested for magnetic inductions up to 14,000 gauss. Figure 12 shows values of the Hall coefficient measured with the magnetic field perpendicular to the cleavage planes for specimen R5 at room temperature. It is seen that up to 9,000 gauss, within the experimental scatter, the Hall coefficient is independent of the magnetic field, while at 14,000 gauss the change is only 2·5%. Similar results are reported by other workers (e.g. Drabble, 1958). In all the measurements described in § 5·2 and § 5·3 the maximum magnetic field was of the order of 6,500 oersteds (§ 4·1).

(iii) Thermoelectric power.

Both the thermoelectric power and Nernst coefficient appeared independent of the temperature gradient down the specimen over the range 5° to 40°C per centimetre.

A check was also made to show that the value obtained for the thermoelectric power was independent of the intermediate metal used in its measurement. Some observations were made above 300°K of the thermoelectric power of Bi_2Te_3 relative to T_2 instead of T_1 alloy. A correction (Lemon and Ference, 1946) was applied in the same way as in § 4·4 to give the thermoelectric power relative to lead, and it was found that the values obtained were independent of the intermediate metal used in their measurement.

Any variation of the thermoelectric power with magnetic induction was small (less than 0·1% for 4,570 gauss) and masked by thermal fluctuations.

The value obtained for the thermoelectric power was found to be dependent on surface conditions. The temperature gradient was always parallel to the cleavage planes, but the positions of the thermocouples and the state of the surface could be altered. The values of the thermoelectric power shown in Figures 15 and 24 were obtained in each case for a clean surface and with the thermocouples making contact with a surface of the specimen which was perpendicular to the cleavage planes. For specimen R8 the room temperature value of the thermoelectric power was found to be reduced by 10% after heating the specimen to 620°K. After cleaning the surface the original value and variation of thermoelectric power with temperature could be obtained. However, values of the thermoelectric power at room

temperature differing by 20% were obtained when the thermocouples were in contact with different parts of the specimen. When the thermocouples were spot-welded to the surface of a cleavage plane - even when the specimen was freshly cleaved - lower readings were always obtained.

For given positions of the thermocouples the difference in the thermoelectric power readings before and after heating the specimen to 620°K may be due to oxidation of the surface. Horne (1959) shows that bismuth-tellurium alloys show the greatest sensitivity to oxide impurities when their composition is in the range corresponding to Bi_2Te_3. The addition of oxide impurities to the melt of specimens having a stoichiometry corresponding to Bi_2Te_3 causes a significant decrease in the thermoelectric power.

It was thought that spot welding contacts to the specimen might influence the readings. This was checked and, with the values of the capacity and voltage given in §4·2, there appeared to be no effects due to spot-welding.

V. Experimental Results.

§ 5·1 Experimental arrangements appropriate to Bi_2Te_3; § 5·2 Electrical properties of Bi_2Te_3; § 5·3 Adiabatic and isothermal effects; § 5·4 Errors.

5·1. Experimental arrangements appropriate to Bi_2Te_3.

As far as the measurements of electrical conductivity and Hall coefficient of Bi_2Te_3 are concerned, all directions in the cleavage planes are equivalent (Drabble and Wolfe, 1956). Thus from symmetry considerations there must be two independent values of the Hall coefficient and electrical conductivity (Drabble, 1958) and also of the Nernst, Ettingshausen and Righi-Leduc coefficients and of the thermal conductivity. In principle all these quantities can be measured using the three experimental arrangements shown in Figure 13. In (a) and (b) I_x is parallel to the cleavage planes. In (a) H_z is perpendicular and in (b) H_z is parallel to the cleavage planes. In (c) I_x is perpendicular and H_z is parallel to the cleavage planes.

5·2. Electrical properties of Bi_2Te_3.

In all specimens (§ 3·4), except R3·1, the current I_x was parallel to the cleavage planes. Measurements of electrical conductivity, thermoelectric power and Hall and Nernst

coefficients were made on specimens R3·21, R5, R7 and R8 over the temperature range $100^{\circ} \longrightarrow 600^{\circ}K$. The Hall and Nernst coefficients of R8 were measured for both the experimental arrangements (a) and (b) in Figure 13, i.e. with the magnetic field both perpendicular and parallel to the cleavage planes. For the other specimens these effects were only measured with the magnetic field perpendicular to the cleavage planes. The results obtained are illustrated in Figures 14 to 17.

The experimental techniques used for measuring the various coefficients are described in §4·4. R3·21, R7 and R8 were "short" specimens (§ 4·2) for which current contacts were made as shown in Figure 5 (a). R3·21 and R7 had only one pair of Hall probes, $H_1 - H_2$, attached; this made it possible to measure only the Hall coefficient with H_z perpendicular to the cleavage planes since these were in the plane of the diagram. R8 had both $H_1 - H_2$ and $H_1' - H_2'$ attached. Both Hall coefficients (or Nernst coefficients when $I_x = 0$, $\frac{\partial T}{\partial x} \neq 0$) were taken in the same temperature run - the specimen holder being turned through 90° between readings (§ 4·5). R5 was a "long" specimen and current contacts were made as shown in Figure 5 (b) and only one set of Hall probes $H_1 - H_2$ were attached. In each case the Hall probes were of T_1 alloy, so that quasi-adiabatic Hall and Nernst coefficients were obtained (§ 5·3).

Room temperature readings are given in Tables 5·1 $\longrightarrow$ 5·4. These illustrate the method of taking readings and also the order of magnitude of the measured quantities.

Table 5.1. Electrical conductivity measurements at room temperature.

Specimen	I_x (amps)	V_x (μV)	Average I_x	$2V_x$	$\frac{I_x}{2V_x}$	ℓ (cm)	$\frac{2\ell \times 10^6}{a.b}$	σ ($ohm^{-1}.cm^{-1}$)
R3.21	+0.1808 -0.1804	+4180 -4792	0.1806	8972	2.013×10^{-5}	0.857	2.703×10^7	545
R5	+0.1970 -0.1970	+1946 -1906	0.1970	3852	5.114×10^{-5}	1.360	1.857×10^7	950
R7	+1.0245 -1.0242	+1885 -1841	1.0244	3726	2.749×10^{-4}	0.874	1.643×10^7	4,517
R8	+0.1593 -0.1520	+3280 -2790	0.1557	6070	2.565×10^{-5}	0.885	1.220×10^7	313

I_x is the current through the specimen, V_x the potential difference measured across the two T_1 - alloy wires of the thermocouple junctions at points C and D on the specimen (Figure 2), ℓ the distance between C and D and $\frac{2\ell \times 10^6}{a.b}$ the constant term, for a given specimen, involved in the calculation of the conductivity σ (Table 2.2.)

Table 5.2. Thermoelectric power measurements at approximately room temperature.

Specimen	Type	dE (μV)	E_C (μV)	E_D (μV)	T °K	dT °K	$(\frac{dE}{dT})_{T_1}$	$(\frac{dE}{dT})_{Pb}$
R3.21	n	-4618, -4618 = -4618	1714, 1715 = 1715	1131	308	14.35	-322	-300
R5	p	+1655, +1659 = +1657	1055, 1065 = 1060	685	295	9.282	+179	+200
R7	n	- 981, - 981 = -981	1517, 1521 = 1519	1103	305	10.10	- 97	- 75
R8	p	+2782, +2782 = +2782	1184, 1189 = 1187	846	298	8.417	+331	+353

dE is the thermal e.m.f. measured across the two T_1-alloy wires of the thermocouple junctions at points C and D on the specimen (figure 2), E_C and E_D are the e.m.f.'s of the thermocouples at C and D respectively, T is the mean of the temperatures at C and D, and dT is the temperature difference between C and D, and $(\frac{dE}{dT})_{T_1}$ and $(\frac{dE}{dT})_{Pb}$ are the thermoelectric power of $Bi_2 Te_3$ relative to T_1-alloy and lead respectively.

Table 5.3 Hall coefficient measurements at room temperature.

Specimen	Type	I_x (amps)	V_y (μV)		Average I_x	$2V_y$	$\frac{2V_y}{I_x}$	$\frac{b \times 10^2}{2 H_z}$	H_z	R (cm^3 $coul^{-1}$)
			For (+H_z)	For (-H_z)						
R3.21	n	+0.1860	- 55 - 59	- 11	0.1853	-45.5	- 245.5	2.264 x 10^{-3}	4550	- 0.556
		-0.1846	+ 173 + 175	+ 129						
R5	p	+0.9461	- 207 - 209	- 292 - 291	0.9463	+82.75	+ 87.4	3.650 x 10^{-3}	3359	+ 0.319
		-0.9465	+ 180 + 180	+ 263						
R7	n	+1.0215	- 108 - 108	- 76	1.0212	-32.0	- 31.35	1.834 x 10^{-3}	6762	- 0.0574
		-1.0208	+ 118 + 118	+ 86						
R8	p	+0.1590	+ 118 + 118	+ 78	0.1550	+40.0	+ 258.1	3.363 x 10^{-3}	4431	+ 0.868
		-0.1510	- 114 - 114	- 74						

I_x is the current through the specimen, V_y the potential difference between the Hall probes at A and B (Figure 2) for positive and negative directions of the magnetic field H_z, and $\frac{b \times 10^2}{2H_z}$ the constant term, for a given specimen, involved in the calculation of the Hall coefficient R (Table 2.2).

Table 5.4. Nernst Coefficient measurements at approximately room temperature.

Specimen	$E_C(\mu V)$	$E_D(\mu V)$	T^oK	dT^oK	$V_y(\mu V)$ For $(+H_z)$	$V_y(\mu V)$ For $(-H_z)$	$2V_y$	$\frac{2V_y}{dT}$	l (cms)	H_z	$\frac{l \times 10^2}{2a\ H_z}$	Q ($cm^2.sec^{-1}\ deg^{-1}$)
R3.21	1715) 1716) = 1716	1133	308	+1434	+138.5	+139	-0.5	-0.0349	0.857	4550	3.047×10^{-2}	+0.001
	1720) 1720) = 1720	1136			+138.5							
R5	1075) 1089) = 1082	710	296	+9.258	-59	-66	+7.0	+0.756	1.360	4550	2.479×10^{-2}	-0.019
	1120) 1128) = 1124	748			-59							
R7	1525) 1529) = 1527	1111	306	+10.25	-32	-41	+9.0	+0.878	0.893	4550	2.288×10^{-2}	-0.020
	1541) 1545) = 1543	1127			-32							
R8	637) 639) = 638	202	284	+10.87	-35	-29	-6.5	0.598	0.885	4431	2.051×10^{-2}	+0.012
	676) 686) = 681	245			-36							

For notation see captions to Tables 5.1, 5.2 and 5.3.

The importance of measuring as many coefficients as possible on the same specimen cannot be over emphasized (§ 1·1; § 3·5). This fact was recognised in 1916 by Wold who measured the electrical properties of tellurium. Studies of all the coefficients given in Table 2·1 are however rare. Notable is the work by Putley (1955) on PbSe and PbTe.

Specimens R3·1 and R3·21 were cut from the same ingot (Table 3·1). In R3·1 current flow was perpendicular and in R3·21 parallel to the cleavage planes. Measurements at room temperature of the electrical conductivity in these two specimens gave the result, for n-type material with $2{\cdot}2 \times 10^{18}$ excess donors per unit volume (Table 6·2), of:-

$$\sigma_{\parallel \ell} : \sigma_{\perp r} = 3{\cdot}9 : 1$$

5·3. Adiabatic and Isothermal Effects.

The measurements presented in § 5·2 were made under approximately adiabatic rather than isothermal conditions (§2·1). However, formulae used in the interpretation of the results are usually in terms of the isothermal coefficients. In Bi_2Te_3, because of the large value of the thermoelectric power, this could lead to misinterpretation - if the Hall coefficient is in error due to an Ettingshausen effect and the Nernst coefficient due to a Righi-Leduc effect.

The results presented in Figure 16 show that the Hall coefficient of Bi_2Te_3 is anomalous in the extrinsic region. The value of the coefficient for p-type material decreases by

as much as 50% on decreasing the temperature from 300°K to 90°K, whereas electrical conductivity measurements indicate that the material is extrinsic, with a constant concentration of carriers, over this temperature range (§ 6·2). This variation of Hall coefficient is inexplicable in terms of the usual theory of impurity semiconductors. Measurements of the isothermal coefficient might help to explain these results while, in general, use of the isothermal coefficients should make the results on Bi_2Te_3 easier to interpret.

Under adiabatic conditions any transverse Ettingshausen temperature gradient would, in conjunction with the thermoelectric power, produce a voltage which would be combined with the Hall voltage. This Ettingshausen voltage cannot be separated from the Hall voltage by the D.C. method of making Hall coefficient measurements (§ 4·4). It is thus necessary to use other techniques in order to measure the isothermal Hall and Nernst coefficients.

The method most commonly used to measure the isothermal Hall coefficient is to use an alternating current through the specimen of sufficiently high frequency for the Ettingshausen transverse temperature gradient not to have time to develop (e.g. Fukuroi et al, 1950). However, the use of a similar method for measuring the Nernst coefficient would be difficult since a large alternating magnetic field would be required. A far simpler arrangement, which can be used for both the Hall and Nernst

coefficients, is to use probes of the same material as the specimen (Jan, 1957) so that any transverse temperature gradient does not give rise to a potential difference. This method is particularly suitable since Bi_2Te_3 readily cleaves into thin slices from which it is easy to cut probes.

If in addition to the isothermal coefficients the adiabatic Hall and Nernst coefficients can be measured, then, assuming simple theory applies, the Ettingshausen and Righi-Leduc coefficients can be calculated (§ 6·7). For adiabatic conditions the transverse heat flow is zero (§ 2·1). As much as possible of the central part of the syndanyo board on which the specimen was mounted was cut away and mica was inserted between the specimen and remaining board in order to reduce the transverse heat flow (Figure 18). Probes of Bi_2Te_3, cut from material originally adjacent to the specimen, and T_1 probes were spot-welded to the specimen for the measurement of the isothermal (R_i, Q_i) and adiabatic (R_a, Q_a) coefficients respectively. Specimens R5 and R9 (§ 3·4) were used since they are sufficiently long for all the probes to be attached away from the ends of the specimen, and spare material which had originally been adjacent to the specimen in the parent ingot was available in each case.

Observations were made of the Hall and Nernst coefficients obtained with the Bi_2Te_3 and T_1 probes over the temperature range 100°K to about 450°K. The current flow was parallel to the cleavage planes and measurements were made with

the magnetic field both parallel and perpendicular to the cleavage planes. Since perfect adiabatic conditions were not obtained, so that the transverse heat flow was not zero, the quantities measured with the T_1 probes were quasi-adiabatic Hall (R_a^*) and Nernst (Q_a^*) coefficients (§ 6·7). The results obtained are shown in Figures 19 to 22. The electrical conductivity (Figure 23) and thermoelectric power (Figure 24) were also measured for R9 over the temperature range 100° to 600°K.

The transverse heat flow must be zero in order to obtain the true adiabatic coefficients. This would necessitate mounting the specimen in vacuum and without the support of the 'syndanyo board (e.g. Putley, 1955) which forms a transverse heat path. A correction would have to be applied for the small heat losses along the Hall probes. Although the adiabatic coefficients are not actually obtained, measurement of the isothermal Nernst coefficient does provide a simple method of obtaining the Ettingshausen coefficient (§ 6·7). The Ettingshausen coefficient is difficult to measure by direct methods (e.g. Wold, 1916; Putley, 1955; Mette et al, 1959) because of the small transverse temperature differences involved.

5·4. Errors.

It is difficult to assess the accuracy of the measurements. As is usual when measuring the bulk electrical properties of solids, the accuracy with which one can measure the change of the electrical properties with temperature appears

much greater than that for the measurement of the absolute quantities, which depend on the determination of the dimensions of the specimen, the probe separations and the magnetic field. The absolute quantities are also subject to error, which is difficult to estimate, due to the crystalline state of the specimen (§3·5) and, in the case of Bi_2Te_3, the use of a D.C. method introduces the possibility of yet additional errors (§4·4; §5·3).

Using the notation of Chapter II, the estimated errors (§3·4; §4·1; §4·2; §4·3; §5·2) in the measured coefficients and in the temperature variation of the coefficients are given in Tables 5·5 and 5·6 respectively.

Table 5·5 - Estimated errors in coefficients.

Coefficient	Estimated errors	Total error
σ	1% in l; 2% in (a.b); 0·1% in V_x; 0·5% in T; 0·1% in I_x.	3·7%
$\frac{dE}{dT}$	0·2% in V_x; 0·2% in $(T_C - T_D)$; 0·5% in T.	0·9%
R	1% in b; 1% in H_z; 1% in V_y; 0·1% in I_x; 0·5% in T.	3·6%
Q	1% in l; 1% in a; 1% in H_z; 1% in V_y; 0·2% in $(T_C - T_D)$; 0·5% in T.	4·7%

Table 5·6 - Estimated errors in temperature variation of coefficients.

Coefficient	Estimated errors	Total error
σ	0·1% in I_x; 0·1% in V_x; 0·5% in T.	0·7%
$\frac{dE}{dT}$	0·2% in V_x; 0·2% in $(T_C - T_D)$; 0·5% in T.	0·9%
R	1% in V_y; 0·1% in I_x; 0·5% in T.	1·6%
Q	1% in V_y; 0·2% in $(T_C - T_D)$; 0·5% in T.	1·7%

The estimated errors in the values of V_x, V_y and $(T_C - T_D)$ vary with the mean temperature of the specimen and the values given are average values over the whole temperature range. Taking into account the possibility of other errors, it is concluded that the maximum error in the absolute values of the coefficients is probably of the order of 6%. Similarly, the maximum error in the temperature variation of σ and $\frac{dE}{dT}$ is about 1·0% and in R and Q about 2·0%.

The error in the ratio of the Hall or Nernst coefficients for the two orientations of the magnetic field with respect to the specimen (§ 6·6) was estimated from the mean of the average error and the probable error in the ratios over the whole temperature range. If 'v' is the deviation of a given

ratio from the arithmetic mean and 'n' is the number of observations, then the

$$\text{average error} = \frac{\Sigma |v|}{n}$$

$$\text{and probable error} = 0{\cdot}67\sqrt{\frac{\Sigma v^2}{n(n-1)}} \ .$$

VI. Discussion of Results.

§6·1 Introduction; §6·2 Scattering mechanisms in Bi_2Te_3; §6·3 Calculation of energy gap; §6·4 Impurity scattering; §6·5 Interaction of charge carriers at high temperatures; §6·6 Anisotropic effects; §6·7 Isothermal and adiabatic effects; §6·8 Anomalous effects in Bi_2Te_3; §6·9 Thermoelectric power; §6·10 Nernst effect.

6·1. Introduction.

For any medium it is possible to set up the Boltzmann equation for the electron distribution function f. Assuming a time of relaxation τ exists, the equation then takes the form (Wilson, 1953, equation 8.11.2)

$$-\frac{2\pi e}{h}\left(\bar{E}+\frac{\bar{v}\wedge\bar{H}}{c}\right).\mathrm{grad}_{\bar{k}}f+\bar{v}.\mathrm{grad}_{\bar{r}'}f=-\frac{f-f_o}{\tau} \qquad (1\cdot1)$$

where E and H are electric and magnetic field intensities respectively, and v is the velocity of electrons. These are described by one electron wave functions with a wave vector $\bar{k}$. The charge on an electron is (-e), the constants 'π', 'h' and 'c' have their usual meanings and $\bar{r}'$ is the radius vector. The energy surfaces $\mathcal{E}(k)$ must have the same symmetry as the crystal.

Bismuth telluride is anisotropic (§3·1) and consequently an exact solution would be extremely complicated. The procedure adopted is to use the solutions of equation (1·1) for isotropic media, modified where necessary to account for

anisotropic effects. Assuming a two band model with spherical energy surfaces $\varepsilon \propto \bar{k}^2$, $\bar{E} = (E_x, E_y, 0)$, $\bar{H} = (0, 0, H_z)$ and $\frac{\partial T}{\partial r} = (\frac{\partial T}{\partial x}, \frac{\partial T}{\partial y}, 0)$, then for isotropic media the solution of equation (1·1) gives (Wilson, 1953, equations 8.53.1 $\longrightarrow$ 8.53.5):

$$J_x = \frac{e}{3\pi^2\hbar^4}\left[i_1^{(1)}W + i_1^{(2)}X + (i_2^{(1)} - i_2^{(2)})\frac{1}{T}\cdot\frac{\partial T}{\partial x} - i_4^{(1)}Y + i_4^{(2)}Z - (i_5^{(1)} + i_5^{(2)})\frac{1}{T}\cdot\frac{\partial T}{\partial y}\right] \quad (1\cdot2)$$

$$J_y = \frac{e}{3\pi^2\hbar^4}\left[i_4^{(1)}W - i_4^{(2)}X + (i_5^{(1)} + i_5^{(2)})\frac{1}{T}\cdot\frac{\partial T}{\partial x} + i_1^{(1)}Y + i_1^{(2)}Z + (i_2^{(1)} - i_2^{(2)})\frac{1}{T}\cdot\frac{\partial T}{\partial y}\right] \quad (1\cdot3)$$

$$\omega_x = -\frac{1}{e}(\varepsilon_1^* + \varepsilon_2^*)J_x^{(2)}$$

$$-\frac{1}{3\pi^2\hbar^4}\left[i_2^{(1)}W - i_2^{(2)}X + (i_3^{(1)} + i_3^{(2)})\frac{1}{T}\cdot\frac{\partial T}{\partial x} - i_5^{(1)}Y - i_5^{(2)}Z - (i_6^{(1)} - i_6^{(2)})\frac{1}{T}\cdot\frac{\partial T}{\partial y}\right] \quad (1\cdot4)$$

$$\omega_y = -\frac{1}{e}(\varepsilon_1^* + \varepsilon_2^*)J_y^{(2)}$$

$$-\frac{1}{3\pi^2\hbar^4}\left[i_5^{(1)}W + i_5^{(2)}X + (i_6^{(1)} - i_6^{(2)})\frac{1}{T}\cdot\frac{\partial T}{\partial x} + i_2^{(1)}Y - i_2^{(2)}Z + (i_3^{(1)} + i_3^{(2)})\frac{1}{T}\left(\frac{\partial T}{\partial y}\right)\right] \quad (1\cdot5)$$

with $W = (eE_x + T\frac{\partial}{\partial x}\cdot\varepsilon^*_{1/T})$

$X = (eE_x - T\frac{\partial}{\partial x}\cdot\varepsilon^*_{2/T})$

$Y = (eE_y + T\frac{\partial}{\partial y}\cdot\varepsilon^*_{1/T})$

$Z = (eE_y - T\frac{\partial}{\partial y}\cdot\varepsilon^*_{2/T})$

In equations (6·2) $\longrightarrow$ (6·5), $\mathcal{E}_1^*$ and $\mathcal{E}_2^*$ are the Fermi energies for electrons and holes respectively and:

$$i_n^{(s)} = -(2m_s^*)^{3/2}\frac{m_s^*}{\hbar}\int_0^\infty \frac{\mathcal{E}^{n+1/2}}{\tau_s\left[\left(\frac{e\bar{H}}{\hbar c}\right)^2+\left(\frac{m_s^*}{\hbar\tau_s}\right)^2\right]}\cdot\frac{\partial f_o}{\partial\mathcal{E}}\cdot d\mathcal{E}. \qquad (n=1,2,3.) \qquad (1\cdot6)$$

$$i_n^{(s)} = -(2m_s^*)^{3/2}\frac{e\bar{H}}{\hbar c}\int_0^\infty \frac{\mathcal{E}^{n-5/2}}{\left(\frac{e\bar{H}}{\hbar c}\right)^2+\left(\frac{m_s^*}{\hbar\tau_s}\right)^2}\cdot\frac{\partial f_o}{\partial\mathcal{E}}\cdot d\mathcal{E}. \qquad (n=4,5,6.) \qquad (1\cdot7)$$

s = 1 (2) for band 1 (2) with conduction by electrons (holes), while m_s^* is the effective mass of carriers in the appropriate band. $J_x^{(2)}$ and $J_y^{(2)}$ are the contributions to the electric current density components from band (2).

For small values of $\bar{H}$, equations (1·6) and (1·7) reduce to

$$i_n^{(s)} = -2(2m_s^*)^{1/2}\hbar\int_0^\infty \tau_s\,\mathcal{E}^{n+1/2}\frac{\partial f_o}{\partial\mathcal{E}}\cdot d\mathcal{E}. \qquad (n=1,2,3.) \qquad (1\cdot6a)$$

$$i_n^{(s)} = -2\left(\frac{2}{m_s^*}\right)^{1/2}\hbar\frac{e\bar{H}}{c}\int_0^\infty \tau_s^2\,\mathcal{E}^{n-5/2}\frac{\partial f_o}{\partial\mathcal{E}}\cdot d\mathcal{E}. \qquad (n=4,5,6.) \qquad (1\cdot7a)$$

It is assumed that $\tau = a\,\eta^r$ (1·8)

where $\eta = \mathcal{E}/kT$, r is a constant depending on the type of scattering of the charge carriers and a is a constant independent of $\mathcal{E}$, but generally dependent on T. Then if 'f_o' is the Fermi-

Dirac function, in the simplified case of a one band model for small (or zero) $\bar{H}$ equations (1·2) $\longrightarrow$ (1·5), when combined with the definitions given in Table 2·1, yield the following expressions:

$$\left.\begin{aligned}
&\sigma = \frac{16e^2(2m^*)^{\frac{1}{2}}\pi(kT)^{3/2}a}{3h^3} \times A. \\
&\frac{dE}{dT} = \pm \frac{k}{e} \times B. \\
&K = K_L + \sigma\left(\frac{k^2}{e^2}\right).T.C. \\
&R_i = \pm \frac{1}{nec} \times D. \\
&Q_i = - \frac{3h^3\sigma}{8(2m^*)^{3/2}e^2\pi cT(kT)^{\frac{1}{2}}} \times E. \\
&P = + \frac{Q_i T}{K}
\end{aligned}\right\} \quad (1\cdot9)$$

where $A = (r + \frac{3}{2})F_{r+\frac{1}{2}}$

$$B = \frac{(r + \frac{5}{2})}{(r + \frac{3}{2})} \cdot \frac{F_{r+3/2}}{F_{r+\frac{1}{2}}} - \eta^*$$

$$C = \frac{(r + \frac{7}{2})(r + \frac{3}{2})F_{r+5/2}F_{r+\frac{1}{2}} - (r + \frac{5}{2})^2(F_{r+3/2})^2}{(r + \frac{3}{2})^2(F_{r+\frac{1}{2}})^2}$$

$$D = \frac{3}{2} \cdot \frac{(2r + \frac{3}{2})}{(r + \frac{3}{2})} \cdot \frac{F_{\frac{1}{2}} \cdot F_{2r+\frac{1}{2}}}{(F_{r+\frac{1}{2}})^2}$$

$$E = \frac{(r + \frac{5}{2})(2r + \frac{3}{2})F_{r+3/2} \cdot F_{2r+\frac{1}{2}} - (2r + \frac{5}{2})(r + \frac{3}{2})F_{2r+3/2} \cdot F_{r+\frac{1}{2}}}{(r + \frac{3}{2})^3 \cdot (F_{r+\frac{1}{2}})^3}$$

where F_m is written for

$$F_m(\eta^*) = \int_0^\infty \frac{\eta^m}{e^{\eta-\eta^*}+1}\,.\,d\eta. \qquad (1\cdot10)$$

The reduced chemical potential $\eta^* = \varepsilon^*/kT$, is defined in terms of the number of free carriers 'n' per unit volume, where

$$n = 4\pi\frac{(2m^*kT)^{3/2}}{h^3}\,.\,F_{\frac{1}{2}}(\eta^*). \qquad (1\cdot11)$$

For n-type specimens η^* is obtained relative to $\varepsilon = 0$ at the bottom of the conduction band, while for p-type specimens the energy zero is at the top of the valence band.

These equations should apply for arbitrary degeneracy and scattering as long as τ can be represented by $\tau = a\eta^r$. Gaussian c.g.s. units have been used throughout. In the expressions for $\frac{dE}{dT}$ and R, the lower sign refers to the case in which there are n free electrons in band (1) and the upper to the case where there are n vacant levels in band (2).

The value of r depends on the type of scattering. It can be shown that for acoustical mode lattice scattering $r = -\frac{1}{2}$, for "high temperature" optical mode scattering $r = +\frac{1}{2}$ and for scattering by ionized impurity atoms $r = +\frac{3}{2}$ (§ 6·2) (Ehrenberg, 1958; Joffé, 1957; Wilson, 1953; Wright, 1951). Wright (1951) plots A,B,D, $\left[E \times (r+\frac{3}{2}) \times F_{r+\frac{1}{2}}\right]$ and $\left[P \times (\frac{K}{K_e}) \times \frac{2nkc}{3}\right]$ for both acoustical and optical mode lattice scattering and for all values of η^*. (Wright assumes $l = l_o\eta^r$ and in the derivation of P that the total thermal conductivity K equals the electronic thermal conductivity K_e.)

If more than one type of scattering is present, the reciprocals of the relaxation times τ_i associated with each type of scattering are additive

$$\frac{1}{\tau} = \sum \frac{1}{\tau_i} \qquad (1\cdot12)$$

In this case the dependence of τ on η cannot be represented by an equation of the form of (1·8) and the analysis of the scattering mechanisms present is very complicated unless one type of scattering greatly predominates over the others.

For non-degenerate statistics $f_o = e^{\eta^* - \eta}$ and equation (1·11) reduces to:

$$n = \frac{2(2\pi m^* kT)^{3/2}}{h^3} e^{\eta^*} \qquad (1\cdot13)$$

Thus for non-degenerate statistics and small values of the magnetic field equations (1·6) and (1·7) reduce to:

$$i_n = \frac{nh^4 (kT)^{n-1}}{(2\pi)^2 \sqrt{\pi}\, m_s^*} \int_o^\infty \tau\, \eta^{n+\frac{1}{2}}\, e^{-\eta}\, d\eta. \quad (n = 1,2,3,) \qquad (1\cdot14)$$

$$i_n = \frac{nh^4}{(2\pi)^2 \sqrt{\pi}\, m_s^*} (kT)^{n-4} \frac{e\bar{H}}{m_s^* c} \int_o^\infty \tau^2\, \eta^{n-\frac{5}{2}} (e^{-\eta})\, d\eta$$

$$(n = 4,5,6,) \qquad (1\cdot15)$$

Equations (1·9) which, apply for arbitrary degeneracy and scattering in the extrinsic region, reduce in the case of non-degenerate statistics, small fields and acoustical mode lattice scattering to (cf. Putley, 1955):

$$\sigma = \frac{4e^2 na}{3m\sqrt{\pi}} = ne\mu$$

$$\frac{dE}{dT} = \pm \frac{k}{e}(2 - \eta^*)$$

$$K = K_L + 2\sigma\left(\frac{k}{e}\right)^2 T$$

$$R_i = \pm \frac{3\pi}{8} \cdot \frac{1}{nec}$$

$$Q_i = -\frac{3}{16} \cdot \frac{\pi k}{ne^2 c} \cdot \sigma = \frac{3\pi}{16} \cdot \frac{k}{e} \cdot \mu$$

$$P = + \frac{Q_i T}{K}$$

(1·16)

6·2. Scattering Mechanisms in Bi_2Te_3.

Assuming that τ can be defined by $\tau = a\eta^r$ (equation 1·8) it is normal to obtain the value of r from the temperature variation of mobility in the extrinsic region. Various definitions have been used for the mobility of charge carriers in solids (e.g. Blatt, 1957; Kontorova, 1956; Shockley, 1950) and in the present work it is the conductivity mobility which will be employed. The mobilities of electrons (μ_n) and holes (μ_p) are then defined from the conductivity in the extrinsic range by:

$$\sigma = ne\mu_n \qquad (2·1)$$

and $$\sigma = pe\mu_p$$

Many workers define a Hall mobility μ_H by:

$$\mu_H = R\sigma \qquad (2\cdot2)$$

Even for substances which are described by simple semiconductor theory μ_H is only equal to the conductivity mobility under the limiting condition (equations 1·9) of degenerate statistics.

The analysis of the experimental results on Bi_2Te_3 is complicated by three factors:-

(i) Bi_2Te_3 is anisotropic (§ 3·1).

(ii) The concentration of carriers is high (§ 3·2) so that there is a transition from non-degenerate to degenerate statistics over the extrinsic range (§ 6·2).

(iii) The Hall coefficient is anomalous (§ 6·8).

This means that experimental results on Bi_2Te_3 cannot be interpreted in terms of simple theory.

It is found that in order to relate the measured value of the extrinsic Hall coefficient (R), for a given orientation of the magnetic field with respect to the axis of three-fold symmetry (§ 3·1), and the concentration of carriers (n) a factor (B'), depending on the anisotropy of the crystal, must be included in equation (1·9).

$$R = \pm \frac{D}{nec} \times B' \qquad (2\cdot3)$$

(Drabble et al, 1958; Drabble, 1958). In addition the variation of the Hall coefficient with temperature in the extrinsic region is inexplicable in terms of the usual theory of impurity semiconductors (§ 6·8). It cannot be explained in

terms of a change of degeneracy of the charge carriers as the temperature changes (see later this section). However, in terms of the many valley model of the band structure in Bi_2Te_3 (Drabble and Wolfe, 1956), the anomalous variation of the Hall coefficient in the extrinsic region could appear as a temperature dependence of B' (Goldsmid, 1958 (a)). Unfortunately values of B' have only been found experimentally at 77°K (Drabble et al, 1958; Drabble, 1958).

Since the temperature dependence of the Hall coefficient is anomalous there is no point in using the Hall mobility μ_H in order to find the dependence of mobility on temperature. It is better to consider the conductivity mobility, making the assumption that the concentration of carriers must be constant in the extrinsic region (Drabble, 1958). Most of the early results (§ 1·1) on Bi_2Te_3 have been interpreted in terms of the Hall mobility, and the relationship between Hall coefficient and carrier concentration given by simple theory. It is considered that use of the Hall coefficient in this way, without a knowledge of the band structure parameters and their variation with temperature, gives completely unreliable results.

In Figures 14 and 23 the variation of σ with T has been plotted on a double logarithmic scale. The shape of the curves indicates that below 300°K the specimens are extrinsic, and if it is assumed that the concentration of charge carriers is constant in this region[1], the slopes give c in

$$\mu \propto T^c. \qquad (2\cdot4)$$

(1) This assumption does not conflict too badly with the variation of η^* with T given in Figure 26 as it can be shown that the concentration of charge carriers, assumed proportional to $T^{3/2}F_{1/2}(\eta^*)$ (See page 66) does not vary by more than about 30%.

Table 6.1

	1	2	3	4	5	6
Specimen	Type	n_s or p_s	c in $\mu \propto T^c$	c_o in $\mu_o \propto T^{c_o}$	Temperature dependence of mobility	E_o
R3.21	n	2.2×10^{18}	-1.6	-1.63	$\mu_n \propto T^{-1.63}$ $\mu_p \propto T^{-1.94}$	0.21 ev
R5	p	1.7×10^{19}	-1.9	-2.12	$\mu_n \propto T^{-1.7}$ $\mu_p \propto T^{-2.1}$	0.23 ev
R7	n	4.1×10^{19}	-1.0	-1.63	-	-
R8	p	3.3×10^{18}	-1.9	-1.94	$\mu_n \propto T^{-1.63}$ $\mu_p \propto T^{-1.94}$	0.21 ev
R9	n	1.2×10^{18}	-1.9	-1.91	$\mu_n = \mu_p \propto T^{-1.93}$	0.19 ev

The following data are given for the various specimens:-

Column 1. Type of conductivity in the extrinsic region.

2. Concentration of extrinsic carriers per unit volume (§6.4) - assumed constant.

3. The value of c in $\mu \propto T^c$ obtained from a plot of $\log\sigma$ against $\log T$ over the extrinsic region.

4. The value of c_o in $\mu_o \propto T^{c_o}$ obtained from a plot of $\log \sigma_o$ against $\log T$ over the extrinsic region where σ_o is the calculated value of the electrical conductivity in the absence of degeneracy.

5. Values of the temperature dependence of mobility assumed for electrons (μ_n) and for holes (μ_p) in the mixed conduction region.

6. Energy gap at absolute zero obtained from a plot of $\log\left(\frac{np}{T^3}\right)$ against $\frac{1}{T}$ in the mixed conduction region.

The values of c for the various specimens are given in Table 6·1. The information obtained from a log - log plot can be unreliable. The variation of $\log\sigma$ against log T must be linear over a large temperature range to yield an accurate value of c and the values quoted are only approximate. However, the variation of c with impurity content does suggest that there is a transition from degenerate to non-degenerate statistics over the extrinsic region.

In order to discuss the effect of degeneracy it is necessary to know η^*. This can be calculated directly from the thermoelectric power (equation 1·9) provided that it is possible to express τ by $\tau = a\eta^r$ and r is known. This means that the predominant scattering mechanism must be known.

The chemical bonding within the multiple layers of Bi_2Te_3 crystals is predominantly co-valent with some ionic bonding (§ 3·1). There are two types of lattice vibrations, acoustical and optical (see, for example, Mott and Gurney, 1948). In co-valent type crystals the former type is responsible for scattering the charge carriers, while in crystals with ionic bonds the latter type is usually the most important. For acoustical mode scattering r is $-\frac{1}{2}$ and the theoretical temperature dependence for degenerate samples $\mu_{ac} \propto T^{-1}$ (Wilson, 1953) and non-degenerate samples $\mu_{ac} \propto T^{-3/2}$ (Seitz, 1948). For optical modes a distinction must be made between low temperatures ($kT \leqslant h\nu_0$) and high temperatures ($kT \geqslant h\nu_0$) (Rodot, 1958).

Howarth and Sondheimer (1953) show that at low temperatures a unique time of relaxation cannot be defined. The variation of μ_{op} with T is thus complicated and cannot be written in the form $\mu_{op} \propto T^{c}$. However, the "high temperature" variation of mobility μ_{op} obtained for optical mode lattice scattering applies down to temperatures of the order of $\frac{1}{2}\,\Theta$ where Θ is the Debye temperature (Howarth and Sondheimer, 1953). From specific heat measurements $\Theta = \frac{h\nu_o}{k} \simeq 145^{o}K$ in Bi_2Te_3 (Wright, 1959) and thus the low temperature approximation need not be considered for temperatures above about $75^{o}K$. At high temperatures r is $+\frac{1}{2}$ and theoretically for degenerate samples $\mu_{op} \propto T^{-1}$ and for non-degenerate samples $\mu_{op} \propto T^{-\frac{1}{2}}$. For scattering by ionized impurities r is $+\frac{3}{2}$. This would give theoretically, for non-degenerate samples, $\mu_I \propto T^{3/2}$ (or a temperature dependence of mobility of less than $T^{3/2}$ - Blatt, 1957; Debye and Conwell, 1954), while for degenerate samples μ_I would be independent of temperature (Mansfield, 1956 (a)). For partially degenerate samples the temperature dependence would be expected to lie in between the extremes indicated for the completely degenerate and non-degenerate cases. These are the mechanisms normally considered as limiting the mobility of charge carriers in semi-conductors. Lattice scattering increases in importance as the temperature increases, while impurity scattering is most important at low temperatures.

Bi_2Te_3 is a compound semiconductor and thus it might be expected that optical modes should be important. However, the bonding in Bi_2Te_3 is predominantly covalent, suggesting acoustical mode scattering should be the most important. In fact, in homopolar crystals the effect of optical modes is difficult to estimate and its importance is uncertain (Fan, 1958). Since only the "high temperature" approximation, applicable above $\frac{1}{2}\Theta$, need be considered, optical mode scattering would lead to a temperature dependence of mobility of between $T^{-\frac{1}{2}}$ and T^{-1}; i.e. the variation would be much less rapid than is observed experimentally for most specimens. Thus the present results for Bi_2Te_3 appear to be most consistent with acoustical mode scattering. The n-type specimens R3·21, R7 and R9 have widely differing impurity content. R7 with the highest concentration of carriers behaves like a metal with $\mu \propto T^{-1}$, while R3·21 behaves very like a non-degenerate semiconductor where, assuming acoustical mode scattering, $\mu \propto T^{-3/2}$. The n-type specimen with the smallest concentration of carriers (R9) and the two p-type specimens have more rapid variations of mobility with temperature.

Scattering by charged impurities would reduce the variation of mobility with temperature, and at very low temperatures in a non-degenerate semiconductor lead to a positive value of c. Although Bi_2Te_3 always has a large concentration of charge carriers in the extrinsic region, the experimental values obtained for c in the extrinsic region

would suggest that impurity scattering is not generally very important (§ 6·4).

Other types of scattering mechanisms (Blatt, 1957; Fan, 1955, 1958; Sodha, 1958) include scattering of charge carriers by neutral impurities or by dislocations and the scattering of electrons by electrons or electrons by holes. Impurities in Bi_2Te_3 are always found to be ionized (§ 6·8) so that there is no neutral impurity scattering (§ 6·4). In the extrinsic range, with relatively few carriers present, electron-electron scattering is expected to be small (§ 6·5). Since the energy gap is small in Bi_2Te_3 (§ 6·3) the number of intrinsic carriers increases rapidly with increasing temperature and electron-hole scattering (§ 6·5) could be important in the intrinsic region.

At any given temperature the time of relaxation τ for carriers is given by equation (1·12). The rigorous use of this equation is extremely complicated. It is even difficult to combine the effects of only two scattering mechanisms if the τ_i have different energy dependences (e.g. Mansfield, 1956 (a) and (b); Debye and Conwell, 1954).

It is usual practice to add the reciprocals of the mobilities μ_i obtained assuming the various relaxation times τ_i to give the net mobility μ:

$$\frac{1}{\mu} = \sum \frac{1}{\mu_i} \qquad (2·5)$$

This expression is only strictly true when the τ_i for different types of scattering have the same dependence on energy. If the

τ_i have different energy dependences, equation (2·5) can lead to serious errors. (Lark-Horovitz, 1954).

Owing to the complexity of the problem in Bi_2Te_3, in order to interpret the results it is necessary to assume that the predominant scattering mechanism is that due to acoustical mode lattice vibrations. An indication of the importance of other types of scattering is given later (§ 6·4; § 6·5) justifying this assumption.

Assuming acoustical mode scattering, then in equation (1·8) 'a' = $\frac{\text{const.}}{T^{3/2}}$ (Wright, 1951) and $r = -\frac{1}{2}$. Substitution of these quantities in equation (1·9) gives:

$$\frac{dE}{dT} = \pm \frac{k}{e} \left(2 \cdot \frac{F_1}{F_o} - \eta^*\right) \qquad (2·6)$$

and that $\frac{\sigma}{F_o}$ should be a constant independent of temperature. The absolute thermoelectric power $\frac{dE}{dT}$ is determined principally by the value of η^*, which is independent of lattice structure. Thus the thermoelectric power is the quantity which will be affected least by the anisotropy of the crystal and should give the best value for η^*.

Using values of F_m given by Rhodes (1950), the relation between $\frac{dE}{dT}$ and η^* given by equation (2·6) was obtained (Figure 25). Using this graph and the experimental values of $\frac{dE}{dT}$ (Figures 15 and 24), the dependence of η^* on temperature between 100° and 300°K was then obtained (Figure 26). These graphs confirm the transition from degenerate to non-degenerate

statistics over the extrinsic region. The constancy of $\frac{\sigma}{F_o}$ over this temperature range was then tested and found to be satisfactory. As a check on the predominant scattering mechanism, for optical mode scattering in the high temperature approximation, $r = +\frac{1}{2}$, $a \propto \frac{1}{T^{\frac{3}{2}}}$ (Wright, 1951), and from equations (1·9)

$$\frac{dE}{dT} = \pm \frac{k}{e} \left(\frac{3}{2} \cdot \frac{F_2}{F_1} - \eta^*\right) \qquad (2·7)$$

and $\frac{\sigma}{TF_1}$ should be constant. The variation of $\frac{\sigma}{TF_1}$ with temperature, derived using values of η^* given by equation (2·7) (Figures 25 and 26), was found to be far greater than the variation of $\frac{\sigma}{F_o}$ on the assumption of acoustical mode lattice scattering.

From equations (1·9) and (1·11):

$$R = \pm \frac{\text{constant}}{T^{3/2} F_{\frac{1}{2}}} \times D. \qquad (2·8)$$

Over the ranges of η^* between 100° and 300°K (Figure 26) the variation of D is very small (Wright, 1951). Thus $\frac{1}{T^{3/2} F_{\frac{1}{2}}}$ should have the same variation with temperature as the Hall coefficient R. Values of $\frac{1}{T^{3/2} F_{\frac{1}{2}}}$ were calculated using η^* obtained from both equations (2·6) and (2·7). The Hall coefficient is anomalous and the results were inconclusive. It should be noted that the possible variation of D in equation (2·8), even over the complete range of degeneracy, could not account for the observed anomalous variation of Hall coefficient in the extrinsic region.

Assuming therefore acoustical mode lattice scattering with $r = -\frac{1}{2}$ and the values of η^* deduced from equation (2·6),

the conductivity σ_o which would be obtained if there were no degeneracy was calculated from the measured σ, using the expression (Appendix I):

$$\sigma_o = \sigma . \frac{2F_{\frac{1}{2}}}{\sqrt{\pi} . F_o} \qquad (2\cdot9)$$

The derived curves, showing the variation of σ_o with temperature, are also plotted in Figures 14 and 23. The values of c_o in the expression

$$\mu_o \propto T^{c_o} \qquad (2\cdot10)$$

(where μ_o is the mobility in the absence of degeneracy) were obtained from these curves, assuming a constant concentration of charge carriers. These values are given in Table 6·1. It is seen that, for all specimens, the variation of mobility with temperature is more rapid than the theoretical $T^{-3/2}$ law. The variation for p-type is more rapid for n-type specimens.

Similar results have been obtained with other semiconductors and many suggestions have been put forward for their justification. Some of these are presented below.

The theory given in § 6·1 and used in this section to interpret the experimental results is greatly over simplified. It is assumed that the medium is isotropic and the energy surfaces spherical. The electrical and magnetic properties of Bi_2Te_3 cannot be explained on such a simple model. It has been shown (Drabble and Wolfe, 1956) that a 'many-valley' model should be used (Sodha, 1958). In addition the valence and conduction bands may be degenerate.

Blatt (1957) reviews the work on the scattering mechanisms in germanium and silicon, which also have 'many-valley' energy band structures.

In germanium $\mu_n \propto T^{-1.66}$; $\mu_p \propto T^{-2.3}$

and in silicon $\mu_n \propto T^{-2.5}$; $\mu_p \propto T^{-2.3}$.

Scattering by optical modes can be important for both electrons and holes, and over a limited part of the temperature range below the Debye temperature can lead to a more rapid temperature variation of mobility than is given by the $T^{-3/2}$ law. For n-type germanium and silicon intervalley scattering by both acoustical and optical modes may be important. Observations of the ratio of Hall to drift mobilities with temperature variation indicates that this type of scattering is important in silicon but not in germanium. Intervalley scattering cannot occur in p-type germanium and silicon. Here the departure from the $T^{-3/2}$ law may be associated with the degeneracy at the top of the valence band, with the resultant presence of holes of two different effective masses and the possibility of interband scattering. Enz (1954) suggests multi-phonon processes may be responsible, since the usual theory only takes one-phonon processes into account and two- or three-phonon processes increase the temperature dependence of mobility. Stilbans (1959) reports that at high temperatures in strongly degenerate samples of Bi_2Te_3, the mean free path $l \propto 1/T^2$, which can only be explained by the inclusion of two-phonon processes at a high concentration of phonons.

Radcliffe (1955) showed that the experimentally observed results for germanium and silicon could be explained on the assumption of acoustical mode lattice scattering and non-degeneracy if the band edges were assumed to deviate from the simple parabolic shape. Ehrenreich (1957) also used a non-parabolic band structure in the analysis of results on InSb, where $\mu_n \propto T^{-1.68}$ and $\mu_p \propto T^{-2.1}$ (e.g. Rodot, 1958). It seems likely that since the impurities in Bi_2Te_3 occupy bands overlapping the bottom of the conduction band and the top of the valence band (§ 6·3; § 6·8) that the band edges must deviate from the simple parabolic shape.

In PbS, PbSe and PbTe, for both n- and p-type specimens, $\mu \propto T^{-5/2}$ in the extrinsic region (Smith, 1954). Smith tentatively suggests that a combination of 'low temperature' optical mode and acoustical mode scattering might explain these results. However, Stilbans et al (1956) explain the observed temperature dependence of mobility in these substances in terms of multi-phonon collisions. The probability of these increases as the temperature increases. With certain assumptions the temperature dependence of mobility can be changed as the temperature increases, becoming steeper as the probability of double or triple collisions increases with increasing temperature.

In conclusion, acoustical mode scattering is probably the predominant mechanism in Bi_2Te_3. This is in agreement with the conclusions of other workers. (For references see § 1·1.

Goldsmid (1958 (a)) gives a summary of previously published results.)

Yates (1959) states that the conductivity cannot be explained in terms of optical mode scattering and that measurements of $\sigma_{\parallel}$ and $\sigma_{\perp}$ (§ 5·2) indicate that scattering of carriers is isotropic. Thus the determination of r in $\tau = a\eta^r$ and the assumptions concerning the predominant scattering mechanism should be uninfluenced by the anisotropy of the crystal.

Goldsmid (1958 (a) and (b)) uses values of r = -0·72 for n-type and r = -0·94 for p-type material and evaluates the integrals F_m by extrapolation. It is, however, difficult to justify this method or to see the physical interpretation to be put on the results. The same procedure is adopted by Bowley et al (1958) who obtain r from magnetothermoelectric and magnetothermal resistance effects. The values of r obtained for p-type material by these methods show reasonable agreement with acoustical mode scattering. The results for n-type material show a wide variation. It is suggested that a scattering law as simple as $\tau = a\eta^r$ may not be justified. Drabble (1958) suggests that the assumption that τ is a function of energy only is open to question since it leads to the thermoelectric power being isotropic, whereas experimentally Goldsmid (1957) finds the thermoelectric power of n-type Bi_2Te_3 to be slightly anisotropic. However, it is hard to see theoretically how the thermoelectric power can be anisotropic and it is possible that

the observed anisotropy arises due to the experimental techniques employed.

6·3. Calculation of Energy Gap.

The thermal energy gap between valence and conduction bands can in principle be calculated from the high temperature conductivity measurements, provided that conduction is essentially intrinsic and the conductivity due to extrinsic carriers can be neglected in this range. For a non-degenerate semiconductor

$$\sigma = \text{constant.}\ T^{3/2}\ (\mu_n + \mu_p)\ e^{-\frac{E_g}{2kT}} \qquad (3\cdot1)$$

If the mobilities of electrons and holes, μ_n and μ_p, vary as $T^{-3/2}$, and there is a linear variation of energy gap E_g with temperature so that $E_g = E_o + \beta T$, a plot of $\log\sigma$ against $1/T$ yields E_o, the energy gap at 0^oK, from the slope. In general, not all these conditions are satisfied and this method only gives reliable results when the energy gap is large ($E_g > 0\cdot5$ ev) (Pincherle and Radcliffe, 1956; Smith, 1954).

Black et al (1957) obtained a value of $E_o = 0\cdot16$ ev from the slope of $\log\sigma$ against $1/T$. Goldsmid (1958 (a)), taking into account the departure of mobility from the expected $T^{-3/2}$ dependence, also obtained a value of 0·16 ev. Black et al obtained an optical energy gap at 300^oK of 0·15 ev and a temperature coefficient of the gap of -9×10^{-5} ev deg^{-1}. This gives $E_o = 0\cdot18$ ev. Austin (1958) obtained an optical gap of

0·13 ev at 300°K, a temperature coefficient of $-9{\cdot}5 \times 10^{-5}$ ev deg^{-1} and hence E_o = 0·16 ev. However, Satterthwaite and Ure (1957) and Shigetomi and Mori (1956) obtained a value of E_o = 0·2 ev by calculating np/T^3 from conductivity and Hall coefficient measurements.

For spherical energy surfaces and non-degenerate statistics (Shockley, 1950)

$$np = N_c N_v \, e^{-E_g/kT} \qquad (3{\cdot}2)$$

where N_c and N_v are the effective density of states in the conduction and valence bands. $(N_c N_v)$ is proportional to T^3, so that

$$\frac{np}{T^3} = \text{constant} \cdot e^{-E_g/kT} \qquad (3{\cdot}3)$$

When considering Bi_2Te_3 this method must be criticized if the calculation of np involves use of the Hall coefficient. As in equation (2·3), which applies in the extrinsic region, the general expression for the Hall coefficient must include an anisotropy factor and it is impossible to take into account the possible variations with temperature and degeneracy of this factor.

However, it is possible to obtain the temperature dependence of np/T^3 from the conductivity measurements without using the Hall coefficient (Appendix II). For material which is p-type in the extrinsic range:

$$\frac{np}{T^3} = \frac{1}{e^2(\mu_n + \mu_p)^2 T^3} \cdot (\sigma - \sigma_s)(\sigma + b\sigma_s) = \text{constant} \cdot e^{-E_g/kT} \qquad (3{\cdot}4)$$

while for material which is n-type in the extrinsic range:

$$\frac{np}{T^3} = \frac{1}{e^2(\mu_n + \mu_p)^2 T^3} \cdot (\sigma - \sigma_s)(\sigma + \frac{\sigma_s}{b}) = \text{constant} \cdot e^{-E_g/kT} \qquad (3\cdot5)$$

where the extrapolated extrinsic conductivity σ_s in equation (3·4) equals $p_s e\mu_p$, and in equation (3·5) equals $n_s e\mu_n$. 'b' is the ratio of mobilities, μ_n/μ_p.

The p-type specimens R5 and R8 were analysed using equation (3·4) and the n-type specimens R3·21 and R9 using equation (3·5). The temperature dependences assumed for μ_n and μ_p in each case are those obtained from the extrinsic regions in the non-degenerate limit and are shown in Table 6·1 (page 60). It was assumed for the variation of μ_p that the results obtained on R8, a single crystal, were probably more reliable than those obtained on R5, of zone refined material. However, in choosing the variation of μ_n, the same importance was not attached to the results on the single crystal R9, since other observations made on this specimen appear anomalous (§ 6·6; § 6·7; § 6·10). The value of 'b' was considered to be close to unity and was determined by assuming b = 1 at 380°K. The reason for this assumption is that a sign reversal of the Hall effect is observed for the p-type specimens shown in Figure 16, and has also been observed by Shigetomi and Mori (1956), indicating that $b > 1$ above 430°K, whereas Satterthwaite and Ure (1957), using n-type specimens with low impurity content, find a reversal in the Hall coefficient, indicating that $b < 1$ below 320°K (§ 6·4; § 6·5). It is seen from equations (3·4) and (3·5) that the

values of E_o determined by this method are not very dependent on the value chosen for 'b'. The variation of np/T^3 is essentially given by $(\sigma - \sigma_s)$ which varies very rapidly with temperature, whereas $(\sigma + b\sigma_s)$ and $(\sigma + \frac{\sigma_s}{b})$ both vary slowly with temperature over the range of temperatures for which measurements have been made. Thus the choice of the exact value of 'b' is unimportant and could be considerably in error without affecting E_o appreciably. The value chosen for 'b' is in reasonable agreement with the values used by previous workers (Goldsmid, 1958 (a)). It should be noted, however, that calculation of the individual mobilities μ_n and μ_p at 100°K from electrical conductivity and Hall coefficient measurements does not confirm this choice since the value $b \simeq 2$ is obtained. The discrepancy could possibly be due to an error in Satterthwaite and Ure's results, since in no other published data on Bi_2Te_3 is the Hall coefficient of n-type material observed to change sign. Another possible source of error is in the values used for the anisotropy factors in the expressions for the Hall coefficient (§ 6·4).

The values of $(\frac{np}{T^3}.\text{constant})$, calculated from equations (3·4) and (3·5), are plotted against 1/T in Figure 27. The calculated values of E_o are shown in Table 6·1.

It is seen that there is a 20% difference between the extreme values obtained for E_o which is far greater than the experimental error associated with the variation of σ with T for each specimen (§ 5·4). In Table 6·2 the specimens are

arranged in order of increasing amount of doping material (iodine) added to the stoichiometric melt. The extrinsic carrier concentrations are calculated as described in §6·4.

Table 6·2.

	1	2	3	4
Specimen	n_s or p_s cm^{-3}	Type	Added iodine	E_o ev
R5	$1·65 \times 10^{19}$	p	?	0·23
R8	$3·31 \times 10^{18}$	p	0·055%	0·21
R9	$1·24 \times 10^{18}$	n	0·07%	0·19
R3·21	$2·24 \times 10^{18}$	n	?	0·21

Table showing specimens in order of increasing amount of iodine added to the stoichiometric melt.

Column 1. Extrinsic concentration of carriers (§6·4).

2. Type of conductivity in extrinsic region.

3. Percentage of iodine added, where known (Walker, 1959).

4. Energy gap at $0^{\circ}K$ (Table 6·1).

It appears that in making n-type material the p-type impurities present in Bi_2Te_3 prepared from a stoichiometric melt (§3·2) are compensated by the added iodine impurities. Stern

and Dixon (1959) suggest that the energy gap, E_g, can be decreased by the addition of large and equal numbers of both donor and acceptor impurity atoms. Their effect is to lower the bottom of the conduction band and raise the top of the valence band, thus narrowing the energy gap while maintaining a low carrier concentration. The concentration of impurities must be sufficiently large that impurity levels are no longer well separated from the band edge. This means that (Stern and Dixon)

$$\text{Impurity concentration} \gtrsim 3 \times 10^{23} \left(\frac{m^*}{m\epsilon}\right)^3 \text{ cm}^{-3} \qquad (3\cdot6)$$

Using $m_n^* = 0\cdot46m$, $\epsilon = 85$ (§ 6·4), equation (3·6) gives a minimum impurity concentration of the order of 5×10^{16} cm^{-3} required to make some of the impurity levels overlap the bottom of the conduction band in n-type material. The impurity concentrations observed in Bi_2Te_3 (Table 6·2 and references in § 1·1) are always greater than 5×10^{16} cm^{-3} and, in fact, the temperature variation of the Hall coefficient at low temperatures (Yates, 1959) shows that the impurity levels form an impurity band overlapping the bottom of the conduction band (§ 6·8). Under these conditions the difference in the egergy gap, ΔE, between an "impure" and a "pure" specimen has been calculated by Stern and Talley (1955) assuming a periodic arrangement of impurities. They obtain the relation

$$\Delta E = \left(1 + \frac{m_n^*}{m_p^*}\right) (\eta_o^* - \gamma) \, kT \qquad (3\cdot7)$$

where $\gamma \simeq 4$ and η_o^* is the reduced Fermi level at 0°K.

Although from equation (3·7) it is seen that the resultant variation of E_g with temperature is linear at low temperatures and thus should not affect the value of E_o calculated from a graph of $\log\left(\frac{np}{T^3}\right)$ against $\frac{1}{T}$, there is the possibility of the expression for ΔE changing at high temperatures.

Probably the largest factor contributing to a non-linear variation of E_g with temperature is the variation with temperature of the coefficient of expansion of the medium, since it is known that this must become zero at $0^\circ K$. For germanium, for example, it has been found from optical measurements (Macfarlane and Roberts, 1955) that the variation of E_g at low temperatures is quadratic - the temperature coefficient vanaishing at absolute zero. Francombe (1958) gives some measurements of the expansion coefficients of Bi_2Te_3 over the temperature range $(-200 \longrightarrow +400)^\circ C$.

Another effect which can decrease the value of E_g is the electrostatic interaction of charge carriers at high temperatures (§ 6·5). The change in E_g due to electrostatic interaction, $\Delta E'$, is given by

$$\Delta E' = -\left(\frac{2}{\epsilon}\right)^{3/2} e^3 \left(\frac{\pi}{kT}\right)^{\frac{1}{2}} (np)^{1/4} \qquad (3\cdot9)$$

resulting in a non-linear variation of E_g with temperature. However, even at $630^\circ K$, the greatest effect on E_g, due to electrostatic interaction of the carriers, is of the order of 0·005 ev, which is too small to lead to the observed differences in E_o.

Thus the 20% variation obtained in the calculated values of E_o for the different specimens remains unexplained. The value of E_o is assumed to be 0·21 ev, although the true value is probably lower since E_g cannot be linear down to 0^oK owing to the vanaishing of the expansion coefficient.

One difficulty which is inherent in the calculation of the temperature dependence of (np) in the intrinsic region is the need to extrapolate the temperature dependence of mobility observed in the extrinsic region to higher temperatures. The probability of double or triple phonon collisions increases as the temperature increases and thus the temperature dependence of mobility can change as the temperature changes (§ 6·2). However, with the present state of knowledge of the scattering mechanisms which are effective in Bi_2Te_3, it would be pure speculation to postulate any such variation in the extrapolated extrinsic mobility. Another difficulty in the method used is the extrapolation of the extrinsic conductivity σ_s. This had to be done with great care as the calculated values of (np) are chiefly dependent upon $(\sigma - \sigma_s)$.

It is probable that the lower value of E_o obtained by authors using the ($\log \sigma$, 1/T) plot was found because the condition $\sigma \gg \sigma_s$ was not satisfied. For specimen R8, Figure 28 shows the measured conductivity σ at high temperatures. Also shown are the extrapolated extrinsic conductivity σ_s obtained from Figure 14 and the calculated intrinsic conductivity

σ_i obtained from the equation $\sigma_i = (\sigma - \sigma_s)$.
It is seen that the graph of the measured conductivity appears linear at the highest temperatures and this linear portion gives $E_o = 0{\cdot}16$ ev. When $\log \sigma T^{0{\cdot}33}$ is plotted against $1/T$, $E_o = 0{\cdot}19$ ev. These results for E_o are in agreement with other authors who used this method. However, in the case of specimen R8, the condition $\sigma \gg \sigma_s$, which is required to estimate the energy from conductivity measurements directly, was not satisfied. It is also obvious that $\sigma \gg \sigma_s$ will not be satisfied in any other specimens of comparable or greater extrinsic carrier concentration.

It is seen that in Bi_2Te_3 the value obtained for E_o by optical means is smaller than the value obtained from the intrinsic conductivity measurements. It has already been shown that a non-linear expansion coefficient could result in the value determined by thermal means being too large, but other possible reasons for the discrepancy between the values obtained by the two methods must now be considered.

Because of the small band gap in Bi_2Te_3 (of the same order as in InSb - Ehrenreich, 1957) and therefore the large concentrations of intrinsic carriers, it might be expected that electron - hole scattering would be important at high temperatures. If electron - hole scattering becomes important μ_n and μ_p will decrease more rapidly with increasing temperature than is obtained by extrapolation of the extrinsic mobility.

Thus in the high temperature region the measured conductivity will be lower than would be observed in the absence of electron-hole scattering, and the value of E_o, calculated from equation (3·4) or (3·5), lower than the true value. Thus, if electron-hole scattering is important, the resultant correction to the value of the thermal energy gap(*) would increase the discrepancy between the thermal and optical energy gaps at 0^oK. Ehrenreich (1957) discusses the difference between the thermal and optical energy gaps in InSb. In InSb, however, the optical gap is larger than the thermal gap, which can be explained if the maximum of the valence band is displaced from k = 0. Initially in InSb the thermal gap, determined from conductivity measurements, was thought to be considerably higher than the optical gap. Allowances for the fact that conduction was not intrinsic and for degeneracy at high temperatures produced agreement between the values of E_o by the two methods (Austin and McClymont, 1954). However, in the present determination of E_o for Bi_2Te_3, allowance has been made for the fact that $\epsilon >> \epsilon_s$ is not satisfied and any degeneracy effects at high temperatures would have very little effect on the calculated value of E_o. Scanlon (1953) points out that in some compound semiconductors, where the concentration of extrinsic carriers is governed by deviations from stoichiometric proportions of the constituent elements, excessive heating leads to irreversible effects. He shows that for PbS irreversible changes due to heat treatment can result in the value obtained for the energy gap, from the measured values

* (The energy gap determined in the usual way from thermal experiments, e.g. Hall or conductivity observations at different temperatures is referred to merely as the "thermal gap")

of the Hall coefficient or electrical conductivity in the intrinsic region, being too large. However, all the measurements on Bi_2Te_3 presented in this thesis were shown to be reproducible. Smith (1954) examines the validity of the interpretation of both electrical and optical measurements in PbS, PbSe and PbTe. It is concluded that the best determinations of E_g are from optical measurements (Smith, 1954; Pincherle and Radcliffe, 1956).

6·4. Impurity Scattering.

The calculation of the effect of impurity scattering in Bi_2Te_3 is complicated by a lack of knowledge of the values to be associated with the basic parameters (§ 1·1; § 6·2) involved in the expression for the mobility due to impurity scattering. Previous workers have been unable to interpret experimental results in Bi_2Te_3 in terms of impurity scattering. The calculations in this section show that, by making certain assumptions, the experimental results in the extrinsic region can be interpreted in terms of a combination of impurity and lattice scattering. However, owing to the number of uncertainties in the parameters involved, the calculations on impurity scattering are regarded as only being approximate - although they give some indication of the importance of this quantity.

The temperature variation of the electrical conductivity in the extrinsic region indicates that, over the

temperature range investigated, impurity scattering is not very important (§6·2). The deviation at low temperatures of the calculated conductivity in the non-degenerate limit (σ_0) from the relationship $\sigma_0 \propto T^{c_0}$, found to hold at higher temperatures, is small (Figures 14 and 23). For R7, the most impure specimen, there is no indication of impurity scattering above 175°K from the shape of the log σ_0 against log T plot. Black et al (1957), from consideration of the variation of conductivity with temperature, conclude that impurity scattering is unimportant in Bi_2Te_3 and Goldsmid (1958 (a)) states that there appears to be no effect of impurity scattering down to 150°K.

The galvanomagnetic coefficients are sensitive to even a small amount of impurity scattering (Drabble, 1958) and thus, since the effects of impurity scattering are highly anisotropic (Fan, 1958), any variation of the ratios $\frac{R_{H\parallel\ell}}{R_{H\perp r}}$, $\frac{Q_{H\parallel\ell}}{Q_{H\perp r}}$ or $\frac{\sigma_{\parallel\ell}}{\sigma_{\perp r}}$ (§6·6) could indicate impurity scattering. Except for the low temperature values of $\frac{Q_{H\parallel\ell}}{Q_{H\perp r}}$ for R9, the values of $\frac{R_{H\parallel\ell}}{R_{H\perp r}}$ and $\frac{Q_{H\parallel\ell}}{Q_{H\perp r}}$ are independent of temperature (§6·6). Yates (1959) also reports that $\frac{\sigma_{\parallel\ell}}{\sigma_{\perp r}}$ for p-type specimens is independent of temperature from 77°K to 300°K. Thus from these observations it is not expected that impurity scattering should be important over the temperature range investigated. In fact, the observations of Bowley et al (1958) on the magnetothermoelectric effect of n-type specimens with varying degrees of doping at 77°K show a variation in 'r' (equation 1·8) contrary to that which

would be expected if impurity scattering occurred. Austin (1958) notes the connection to be expected between a large dielectric constant ($\sim$85) and the reported absence of ionized impurity scattering in samples containing relatively high impurity concentrations.

On the other hand, Bashirov (1958) calculates the mobility from $\mu_H = R\sigma$ and from the Nernst coefficient and then attributes the deviation of the mobility from an experimental relation $\mu \propto T^{-2\cdot3}$ to impurity scattering. Walker (1959) finds that at very low temperatures ($T \ll 100^{\circ}K$) impurities cause appreciable scattering of the charge carriers. Thus an attempt has been made to interpret the results obtained at low temperatures in terms of a combination of impurity and lattice scattering.

A more sensitive test for impurity scattering than the temperature variation of conductivity or mobility is a plot of mobility against the concentration of ionized impurities at a given temperature. Yates (1959) reports that the Hall mobility $R\sigma$ of n-type Bi_2Te_3 does not vary in a simple manner with doping. Parrott and Penn (1958) plot the Hall mobility against carrier concentration at room temperature. No account was taken of the anisotropy constant B' (equation 2·3) and efforts to analyse these results in terms of the theory of impurity scattering (Mansfield, 1956 (a)) proved unsuccessful.

The concentration of ionized inpurities is unknown. Since the impurities form impurity bands overlapping the bottom of the conduction band and the top of the valence band they are always ionized, and thus the concentration of ionized impurities equals the sum of the donor and acceptor concentrations. Since Bi_2Te_3 is always p-type when prepared from a melt of stoichiometric composition (§ 3·2), n-type material must always contain a higher concentration than p-type material of ionized impurities. However, although the concentrations of impurities are large ($\sim 10^{18} \longrightarrow 10^{19}$ cm^{-3}), owing to the large dielectric constant, it will be shown that the effects of ionized impurity scattering are small. Owing to the large number of uncertainties in the calculations only an indication of the importance of impurity scattering is obtained, the error involved in equating the concentration of extrinsic carriers to the concentration of ionized impurities being neglected.

The relationship between the measured Hall coefficients and the concentration of carriers in Bi_2Te_3 is uncertain (§ 6·2). An estimation of the concentration of impurity carriers in each specimen was made using equation (2·3). The anisotropy factors B' have only been found for 77°K (Drabble et al, 1958; Drabble, 1958), whereas the lowest experimental results in the present investigation were obtained at about 100°K. Difficulty was experienced in attempting to extrapolate the Hall coefficient curves to 77°K since the variation of the Hall coefficient with

temperature is anomalous and the form of the curves could change between 77°K and 100°K (Yates, 1959). Thus the experimental results at 100°K were used together with the values of B' determined for n- and p-type material at 77°K, the assumption being made that B' does not vary very rapidly with temperature. The variation of D with degeneracy is small (Wright, 1951) and the degenerate limit D = 1 was used (Figure 26). For specimens R5 and R9 the isothermal Hall coefficient was used. If the Hall coefficient is measured with the magnetic field perpendicular to the cleavage planes, for n-type material B' = 0·326 (Drabble et al, 1958):

$$n_s e = \frac{0\cdot326}{R_{H_{\perp r}}} \qquad (4\cdot1)$$

and

$$\mu_n = \frac{R_{H_{\perp r}}}{0\cdot326} \times \sigma \qquad (4\cdot2)$$

while for p-type material B' = 0·476 (Drabble, 1958), so that

$$p_s e = \frac{0\cdot476}{R_{H_{\perp r}}} \qquad (4\cdot3)$$

and

$$\mu_p = \frac{R_{H_{\perp r}}}{0\cdot476} \times \sigma \qquad (4\cdot4)$$

In quoting B' = 0·476 for p-type material it is assumed that "r = 1·08" has been omitted from equation 6 (a) of Drabble's paper (1958). The values obtained for the concentrations of electrons (n_s) and holes (p_s) at 100°K are given in Table 6·2. These values are then assumed to apply throughout the extrinsic region (§ 6·2). Using the calculated values of $n_s(p_s)$ and σ_o (§ 6·2), and the relation $\sigma_o = \begin{cases} n_s e\mu_o \\ p_s e\mu_o \end{cases}$, the calculated mobility

in the non-degenerate limit, has been plotted as a function of $n_s(p_s)$ for 100, 150, 200 and 250°K (Figures 29a and 29b). The values of σ_o are obtained from the measured conductivity on the assumption that acoustical mode lattice scattering predominates and, since the effect of degeneracy has been taken into account, the decrease in μ_o as $n_s(p_s)$ increases indicates the presence of impurity scattering. It is concluded that above 200°K the effects of impurity scattering are unimportant in all specimens, while impurity scattering is important in R5 and R7 below 200°K. Since in most specimens the charge carriers cannot be considered as being either completely degenerate or completely non-degenerate (Figure 26), the theory for impurity scattering in the general case of arbitrary degeneracy must be used (Mansfield, 1956 (a)).

The general equation for the conductivity due to impurity scattering (σ_I), derived assuming scattering by impurity centres having a screened Coulomb field and a density of ionized impurities equal to the density of conduction electrons or holes, is:

$$\sigma_I = \frac{32\,\epsilon^2 m^*(kT)^3 F_2(\eta^*)}{n_s e^2 h^3 f(x)} \qquad (4.5)$$

where $f(x) = \log_e(1 + x) - \frac{x}{1 + x}$

$$x = \frac{\bar{\eta}\,(kT)^{\frac{1}{2}}\epsilon h}{e^2(2m^*)^{\frac{1}{2}}F_{\frac{1}{2}}'(\eta^*)}$$

n_s = density of ionized impurities

ϵ = permittivity of medium

m^* = effective mass of either electrons or holes,

and $F_2(\eta^*)$ and $F_{\frac{1}{2}}'(\eta^*)$ are tabulated Fermi integrals (Beer et al, 1955; Johnson and Shipley, 1953).

The total conductivity σ due to the combined effects of impurity and lattice scattering must be calculated using equation (1·12)

$$\text{i.e.} \quad \frac{1}{\tau} = \frac{1}{\tau_I} + \frac{1}{\tau_L}$$

and the value of η in the resulting expression for σ which makes this a maximum used for $\bar{\eta}$ in the expression for x.

In the degenerate limit, $\eta^* \gg 0$.

$$\sigma_I = \frac{3h^3 \epsilon^2 n_s}{16\pi^2 e^2 (m^*)^2 f(x)} \qquad (4\cdot6)$$

where $$x = \left(\frac{h}{e}\right)^2 \frac{\epsilon}{m^*} \cdot \left(\frac{3n_s}{8\pi}\right)^{1/3}$$

while in the non-degenerate limit, $\eta^* \ll 0$

$$\sigma_I = \frac{2^{7/2} \epsilon^2 (kT)^{3/2}}{\pi^{3/2} (m^*)^{\frac{1}{2}} e^2 f(x)} \qquad (4\cdot7)$$

$$x = \frac{6\epsilon m^* (kT)^2}{\pi n_s \hbar^2 e^2}$$

The conductivity mobility due to impurity scattering (μ_I) is given by $\sigma_I = n_s e \mu_I$ and equation (4·7) is then seen to be the expression for impurity scattering derived by Herring (Debye and Conwell, 1954).

Table 6·3 - Test for ionized impurity scattering at 100°K.

		1	2	3	4		5	
Specimen	Type	μ_{obs}	μ_{ex}	μ_L	μ_I		μ	
					(a) $r = -\frac{1}{2}$	(b) $r = +\frac{3}{2}$	(a)	(b)
R3·21	n	7,003	8,984	7,394	10,120	133,400	3,370	6,813
R5	p	2,045	4,607	3,170	806	12,030	591	2,384
R7	n	1,950	8,984	3,360	2,110	2,110	1,260	1,280
R8	p	3,550	4,607	4,040	2,589	34,620	1,223	3,329
R9	n	7,100	8,984	7,726	22,760	280,600	4,613	7,370

Column 1. Observed mobility, μ_{obs}, given by σ/en_s or σ/ep_s where σ is the observed electrical conductivity and n_s or p_s are the extrinsic concentrations of carriers (Table 6·1).

2. Mobility, μ_{ex}, assuming only lattice scattering in the non-degenerate limit obtained from linear variation of σ_o, the conductivity in the absence of degeneracy, extrapolated to 100°K.

3. Mobility, μ_L, assuming only lattice scattering for actual degeneracy in specimen and obtained from μ_{ex} (Appendix I). η^* obtained from $\frac{dE}{dT}$ assuming lattice scattering.

4. Mobility, μ_I, assuming only ionized impurity scattering:
   (a) using η^* obtained from $\frac{dE}{dT}$ assuming lattice scattering;
   (b) using η^* obtained from $\frac{dE}{dT}$ assuming impurity scattering.

Column 5. Final calculated mobility due to combination of lattice and impurity scattering:

(a) due to μ_L and μ_I as obtained in 4(a);

(b) due to μ_L and μ_I as obtained in 4(b) where the value of η^* used in calculating the final mobility was taken as the average η^* for lattice and impurity scattering.

Note. All mobilities are in $cm^2V^{-1}\ sec^{-1}$.

The effects of impurity scattering at 100°K were calculated for R3·21, R5, R7, R8 and R9 making various assumptions and the results are summarised in Table 6·3. In each case it is assumed that the mobility μ_j is related to the corresponding conductivity σ_j by the expression $\sigma_j = n_s e\mu_j$ for n-type and $\sigma_j = p_s e\mu_j$ for p-type material.

The values of μ_{ex} at 100°K, the mobility assuming only lattice scattering in the non-degenerate limit, were obtained from the calculated values of σ_o at higher temperatures (§ 6·2) extrapolated to 100°K. The value of μ_{ex} assumed for p-type material was obtained from results on R8 and for n-type material from R3·21 (Figure 14).

The values of μ_L, the mobilities due to lattice scattering only for the actual values of the degeneracy, were then calculated from the values of μ_{ex} using the expression derived in Appendix I. The values assumed for η^* were those obtained from the thermoelectric power assuming acoustical mode scattering ($r = -\frac{1}{2}$) (Figure 26) (§ 6·2).

The mobility due to impurity scattering, μ_I, was then calculated for R3·21, R5, R8 and R9 using equation (4·5). It was assumed that the dielectric constant $\epsilon = 85$ (Austin, 1958), $m_p^* = 0{\cdot}51\ m_o$ and $m_n^* = 0{\cdot}46\ m_o$ (Drabble, 1959; Goldsmid, 1958 (a)). The values used for m_p^* and m_n^* are density of states effective masses and may differ appreciably from the values which should be used to calculate μ_I.

Values of μ_I were calculated using two different values of η^* (Figure 26).

(a) η^* obtained from $\frac{dE}{dT}$ assuming acoustical mode scattering $(r = -\frac{1}{2})$.

(b) η^* obtained from $\frac{dE}{dT}$ assuming impurity scattering $(r = +\frac{3}{2})$.

The procedure adopted was to guess at the importance of impurity scattering and hence the order of magnitude of the quantity $\frac{\sigma_L}{\sigma_I}$ for each specimen. Values of $\overline{\eta}$ were then obtained from Mansfield (1956 (a)), Figure 2, and used to calculate a value of σ_I. The ratio $\frac{\sigma_L}{\sigma_I}$ was then redetermined and a new value of σ_I calculated. Hence μ_I, in Gaussian units, was obtained and converted to practical units by dividing by 300.

A mobility, μ_{calc}, due to a combination of impurity and lattice scattering was then calculated from the approximate equation (2·5)

$$\frac{1}{\mu_{calc}} = \frac{1}{\mu_I} + \frac{1}{\mu_L}$$

A correction factor

$$F = \frac{\frac{1}{\mu_I} + \frac{1}{\mu_L}}{\frac{1}{\mu}}$$

was then applied to μ_{calc} in order to obtain the total mobility μ. This factor F was obtained from Mansfield (1956 (a)), Figure 1, assuming in case:

(a) η^* obtained for $r = -\frac{1}{2}$,

(b) an average value of η^* from the values for $r = -\frac{1}{2}$ and $r = +\frac{3}{2}$.

The value of μ obtained was then compared with the observed mobility, μ_{obs}, obtained from the measured conductivity at 100°K.

It is seen that if it is assumed that impurity scattering is small and that lattice scattering predominates, and then the values of η^* obtained on this assumption from the measured thermoelectric power are used in calculating μ_I, the values obtained are always smaller than the observed mobility μ_{obs}. If, on the other hand, the values of η^* obtained from the thermoelectric power on the assumption that only impurity scattering occurs are used in the calculation of μ_I, it is seen that the values of μ agree well with the values of μ_{obs}.

Obviously η^* must have a unique value in a given specimen and at a given temperature, and thus there are inconsistencies in the second set of calculations where μ_L is calculated assuming that $r = -\frac{1}{2}$ and μ_I that $r = +\frac{3}{2}$. Thus it is difficult to attach any physical significance to the agreement obtained.

The values of η^* are usually calculated from equation (1·11) since this is independent of the scattering mechanism. The uncertainties in calculating the values of n_s in Bi_2Te_3 (§ 6·4) make this method unreliable. The values of η^* calculated from equation (1·11) are given in Table (6·4) and it is seen that they are more consistent with the values of η^* from the thermoelectric power assuming $r = -\frac{1}{2}$ than with those assuming $r = +\frac{3}{2}$. For a discussion of the assumptions made in calculating η^*, see § 6·9.

Table 6·4.

Specimen	Type	η^*		
		$r = -\frac{1}{2}$	$r = +\frac{3}{2}$	equation (1·11)
R3·21	n	+ 1·12	+ 4·95	+ 0·9
R5	p	+ 2·88	+ 9·00	+ 5·2
R7	n	$\sim$ 13	$\gg$ 10	+ 10·7
R8	p	+ 0·41	+ 3·65	+ 1·25
R9	n	+ 0·67	+ 4·10	+ 0·12

Reduced Fermi level, η^*, relative to the bottom of the conduction band (n-type) or the top of the valence band (p-type) at 100°K. The values were calculated from the thermoelectric power assuming lattice scattering ($r = -\frac{1}{2}$) and ionized impurity scattering ($r = +\frac{3}{2}$) and from the concentration of carriers (equation (1·11).

R7 is the specimen with the highest concentration of impurities and in this case μ_I was calculated using equation (4·6). The results at 100°K are given in Table (6·3).

If μ_I, for the specimens studied here, is calculated using equation (4·7), i.e. the expression for μ_I in the non-degenerate limit, the values obtained are always much less than the observed mobilities. Since equation (4·7) is the expression most commonly employed to calculate the mobility due to impurity scattering in semiconductors, this does not explain why some workers conclude that impurity scattering is unimportant in Bi_2Te_3.

Extension of the analysis of ionized impurity scattering in Bi_2Te_3 to lower temperatures would be interesting. Yates (1959) gives Hall coefficient and electrical conductivity measurements taken on a number of n- and p-type specimens down to 1·3°K, and from these results it is deduced that ionized impurity scattering is the only important scattering mechanism below about 20°K. Walker (1959) gives the thermoelectric power down to 6°K taken on a number of specimens, some of which came from the same ingots as those used by Yates. However, electrical and chemical measurements reveal the existence of large inhomogeneities within the ingots and slices taken from the ingots (Wright, private communication). Thus it does not seem to be very meaningful to use results obtained on two different specimens, even when these are from the same ingot, in order to calculate μ_I.

A very rough calculation was made of the impurity scattering in specimens from ingot SBTC 16 (Specimen R9 was from this ingot). At $10^{o}K$ Walker gives the thermoelectric power as about 30 $\mu V\ deg^{-1}$, which means that $\eta^{*} > 6$ (Figure 25) and the specimen can be treated as degenerate (Mansfield, 1956 (a)). A value for n_s was calculated from the low temperature Hall coefficient (Yates, 1959, Figure 2) using equation (4·1) and hence μ_I from equation (4·6) and the relation $\sigma_I = n_s e \mu_I$. This value of μ_I was found to be lower, by a factor of about ten, than the experimental value of the mobility determined by use of equation (4·2). The low value obtained for μ_I could be due to a lack of knowledge of the degeneracy in the specimen, but, in view of the large number of other uncertainties in the calculation, it was not thought worthwhile to extend calculations to include possible values of η^{*} less than infinity.

It should be stressed that in the calculation of μ_I formulae applying to isotropic media have been assumed to apply to Bi_2Te_3, whereas the effects of impurity scattering are anisotropic. Density of state values have been used for the effective masses m_n^{*} and m_p^{*}, carrier concentrations in place of ionized impurity concentrations and the value used for the permittivity of the medium (ϵ), obtained from infra-red measurements, is uncertain. A variation of m_n^{*} or m_p^{*} over reasonable limits (0·1 m_o to m_o) does not generally have much effect on the calculated value of μ_I, but an error in ϵ could have far more effect.

Since the impurity levels in Bi_2Te_3 occupy an impurity band overlapping either the bottom of the conduction band in n-type material or the top of the valence band in p-type material (§ 6·3), the impurity atoms are always ionized and therefore cannot contribute to neutral impurity scattering (Erginsoy, 1950).

6·5. Interaction of Charge Carriers at High Temperatures.

The position of the Fermi level, and hence the value of η^*, is not known even approximately in specimens of Bi_2Te_3 showing mixed conduction. Thus the mobility due to electron-hole scattering, μ_{np}, can only be calculated in the limits of degeneracy. The theory for ionized impurity scattering can easily be modified to apply to electron-hole scattering. In the intrinsic region, where $n \simeq p$, $(np)^{\frac{1}{2}}$ replaces n and $\left(\frac{m_n^* \cdot m_p^*}{m_n^* + m_p^*}\right)$ replaces m^* in the expressions for ionized impurity scattering. In the non-degenerate limit the expression for μ_{np}, obtained from equation (4·7), and the relation $\sigma_j = n e \mu_j$ is given by:

$$\mu_{np} = \frac{2^{7/2} \epsilon^2 (kT)^{3/2}}{(np)^{\frac{1}{2}} \pi^{3/2} \left(\frac{m_n^* \cdot m_p^*}{m_n^* + m_p^*}\right)^{\frac{1}{2}} e^3 f(x)} \qquad (5·1)$$

$$f(x) = \log(1 + x) - \frac{x}{1 + x}$$

$$x = \frac{6\left(\frac{m_n^* \cdot m_p^*}{m_n^* + m_p^*}\right) \epsilon (kT)^2}{\hbar^2 \pi (np)^{\frac{1}{2}} e^2}$$

This expression is the same as that used by Morin and Maita (1954) except for the factor π occurring in x.

Values of μ_{np} were calculated over the temperature range 315° to 630°K for specimen R9 using equation (5·1). The same values were used for ϵ, m_p^* and m_n^* as in the calculations of the ionized impurity mobility (§ 6·4). The product (np) was calculated from equation (3·5) using the values of $(\sigma - \sigma_s) \times (\sigma + \frac{\sigma_s}{b})$ calculated in the determination of E_o (§ 6·3). For specimen R9, b = 1 and $\mu_n = AT^{-1\cdot93}$ (Table 6·1). The constant, A, was determined from the non-degenerate lattice mobility, μ_{ex}, for R9 at 100°K (§ 6·4).

The calculated values of the mobility due to electron-hole scattering, μ_{np}, are plotted in Figure 30 together with the variation of the lattice mobility for both electrons and holes given by $\mu_L = AT^{-1\cdot93}$. From this electron-hole scattering is seen to be unimportant in specimen R9 compared with lattice scattering, assuming that the specimen is non-degenerate and that the values used for ϵ, m_n^* and m_p^* are correct. As with ionized impurity scattering at low temperatures (§ 6·4) a reasonable variation of m_n^* or m_p^* does not have much effect on μ_{np}, but if the value of the dielectric constant, ϵ, is decreased sufficiently the value of μ_{np} becomes of the same order of magnitude as μ_L. A further uncertainty arises from the calculation of (np). The values of μ_{ex} for n- and p-type material (Table 6·3) indicate that $b = \frac{\mu_n}{\mu_p} \simeq 2$ at 100°K and there is a discrepancy between the values of μ_{ex} calculated by this method and those assumed when calculating E_o (§ 6·3). However, the value of (np) is determined principally by the

value of $(\sigma - \sigma_s)$ in equation (3·5) and, as in the determination of E_o, the value of b can be considerably in error without affecting (np) appreciably.

Values of the mobility, μ_{np}, were not calculated for any other specimens owing to the insignificance of electron-hole scattering in specimen R9 and the fact that the values of (np) at a given temperature in the intrinsic region were found to be the same for all four specimens, R3·21, R5, R8 and R9, within the limits of the possible errors in the calculations. Although electron-hole scattering is presumed to be unimportant, there is a definite possibility of intervalley scattering and multi-phonon processes occurring at high temperatures (§ 6·3). Sufficient data are not available to test these possibilities.

Since electron-hole scattering is small in the mixed conduction range it is assumed that at lower temperatures, with fewer carriers present, electron-electron scattering is unimportant.

A further possible effect in the intrinsic region, where the concentration of charge carriers is large, is a decrease in the forbidden energy gap, E_g, due to electrostatic interaction of the carriers (Morin and Maita, 1954).

The decrease, $\Delta E'$, of the energy gap is given by the sum of two quantities:

$$\Delta E' = \Delta\bar{\mu}(\text{for electrons}) + \Delta\bar{\mu}(\text{for holes}) \qquad (5·2)$$

where $$\Delta\bar{\mu} = -\frac{e^2}{2\epsilon}\left[4\pi \cdot e^2\left(\frac{n+p}{\epsilon kT}\right)\right]^{\frac{1}{2}}$$

Assuming that $n \simeq p$, then $(n + p) = 2n = 2(np)^{\frac{1}{2}}$ and equation (5·2) becomes:

$$\Delta E' = -\left(\frac{2}{\epsilon}\right)^{\frac{3}{2}} e^3 \left(\frac{\pi}{kT}\right)^{\frac{1}{2}} (np)^{\frac{1}{4}} \qquad (5·3)$$

Values of $\Delta E'$ have been calculated for specimen R9 over the temperature range 315° to 630° K and for specimens R3·21, R5 and R8 at the highest temperature for which experimental results are available. The calculated values of $-\Delta E'$, in electron volts, are given in Table 6·5.

Table 6·5. Values of the decrease in the energy gap due to electrostatic interaction of carriers given in electron-volts.

T°K / Spec.	R3·21	R5	R8	R9
316				0·0019
355				0·0023
398				0·0028
447				0·0034
501				0·0040
562	0·0034			0·0047
631		0·0045	0·0038	0·0053

It is seen that over the whole of the intrinsic region the variation in E_g due to electrostatic interaction of carriers is small ($\sim$ 0·003 ev) and that this effect cannot cause the observed differences in E_o calculated for different specimens (§ 6·3).

6·6. Anisotropic Effects.

Values of the Hall and Nernst coefficients with the magnetic field both (i) perpendicular and (ii) parallel to the cleavage planes (§ 5·2; § 5·3) have been obtained for specimens R5, R8 and R9 over a range of temperatures.

Drabble et al (1958) analyse Hall coefficient and low field magnetoresistance measurements on n-type specimens at 77°K in terms of a 'many-valley' model (Drabble and Wolfe, 1956) for Bi_2Te_3. With the magnetic field H perpendicular, and current flow parallel, to the cleavage planes, they calculate that the anisotropy factor B' in equation (2·3) has the value 0·326 at 77°K. Thus

$$R_{H\perp r} = -\frac{D}{nec} \times 0{\cdot}326 \qquad (6{\cdot}1(a))$$

When the magnetic field is parallel to the cleavage planes, B' = 0·670 and

$$R_{H\parallel \ell} = -\frac{D}{nec} \times 0{\cdot}670 \qquad (6{\cdot}1(b))$$

Thus the theoretical ratio of the measured Hall coefficients at 77°K is

$$\frac{R_{H\parallel \ell}}{R_{H\perp r}} = \frac{0{\cdot}670}{0{\cdot}326} = 2{\cdot}06 \qquad (6{\cdot}1(c))$$

For p-type material at 77°K Drabble (1958) gives (see also § 6·4)

$$\left.\begin{aligned} R_{H\perp r} &= \frac{D}{nec} \times 0{\cdot}476 \\ R_{H\parallel \ell} &= \frac{D}{nec} \times 0{\cdot}981 \\ \frac{R_{H\parallel \ell}}{R_{H\perp r}} &= 2{\cdot}06 \end{aligned}\right\} \qquad (6{\cdot}2)$$

Specimens R5 and R8 are both p-type. Specimen R8 came from the same ingot as the specimens labelled (SBTC/19) in work reported by Drabble (1958), Walker (1959) and Yates (1959). The values obtained for the ratio $R_{H\|\ell}/R_{H\perp r}$ are (2·2 ± 0·1) for R5 from Figure 19 and (2·0 ± 0·1) for R8 from Figure 16. For R5 the isothermal Hall coefficients (§ 5·3) were used. The ratios for both specimens are independent of temperature over the whole of the temperature range studied. Drabble also reports that there is no significant variation in the ratio of the Hall coefficients with temperature for the p-type specimens studied. It is thus seen that within the experimental error the values of $R_{H\|\ell}/R_{H\perp r}$ for R5 and R8 are in agreement with both the theory (equations 6·2) and the experimental results obtained by other workers.

Specimen R9 is n-type and is from the same ingot as specimen SBTC/16 studied by Walker (1959) and Yates (1959). From Figure 20 the ratio of the isothermal Hall coefficients is (2·3 ± 0·2) and is independent of temperature. Thus agreement is obtained with equation (6·1(c)) within the experimental error.

For R5 the ratio of the Nernst coefficients $Q_{H\|\ell}/Q_{H\perp r}$ is (2·3 ± 0·1) and for R8 (2·4 ± 0·1) (Figures 21 and 17). Both these quantities are independent of temperature and, within the experimental error, agree with each other. For R9 the ratio of the isothermal Nernst coefficients (Figure 22) is approximately unity at 100°K. The ratio increases with

increasing temperature for negative values of the Nernst coefficient, becoming independent of temperature for positive values of the coefficient with a value of $(1{\cdot}7 \pm 0{\cdot}1)$. The values obtained for the ratio $Q_{H\|\rho}/Q_{H\perp r}$ for R9 are unexpected. It is also found that other quantities calculated for R9 in the extrinsic range do not seem to conform with those of the other specimens (§ 6·10).

The ratio of the electrical conductivities with current flow parallel and perpendicular to the cleavage planes was determined at room temperature for specimens R3·1 and R3·21 (§ 5·2). The result, for n-type material, is

$$\frac{\sigma_{\|\rho}}{\sigma_{\perp r}} = 3{\cdot}9$$

Drabble et al (1958) predict a value of 4·1 at 77°K for this quantity and quote an experimental value, due to Goldsmid, of 3·8 at 77°K, while Goldsmid (1957) also gives values of 4·0 at 150°K and 4·75 at 300°K. Since it is not expected that the value of the ratio should vary with temperature, the experimental result of 3·9 is in good agreement with theory.

6·7. Isothermal and Adiabatic Effects.

Since the Hall coefficient of Bi_2Te_3 is found to be anomalous in the extrinsic region, measurements were made of the isothermal Hall coefficient for one p-type specimen (R5) and one n-type specimen (R9) over the temperature range 100°K to 450°K

(§ 5·3). Although it is seen (Figure 19) that the anomaly in the Hall coefficient of R5 is decreased by measuring the isothermal coefficient, it is not removed. However, in any theories to try to explain the anomalous behaviour of the Hall coefficient in Bi_2Te_3 the variation of the isothermal coefficient with temperature should be considered (§ 6·8). In addition it is shown in this section that measurement of the isothermal Nernst coefficient provides a simple method of obtaining the Ettingshausen coefficient.

The definitions of the various coefficients, the conditions under which they are measured and the sign convention employed are stated in Chapter II. The relations between isothermal and adiabatic coefficients (Heurlinger relations) follow directly from the definitions of the various coefficients. The relation between the isothermal and adiabatic Hall coefficients is (cf. Chambers, 1952):

$$R_a = R_i - \frac{dE}{dT} \cdot P \qquad (7\cdot1)$$

where $\frac{dE}{dT}$ is the absolute thermoelectric power of Bi_2Te_3 relevant to heat flow in the y-direction and P is the Ettingshausen coefficient.

Taking into account the lattice thermal conductivity when deriving the Bridgman relation (Appendix III), then:

$$P = \frac{Q_i T}{K_y} \qquad (7\cdot2)$$

where Q_i is the isothermal Nernst coefficient and K_y is the

isothermal thermal conductivity relevant to heat flow in the y-direction and in a transverse magnetic field.

This relation should hold for an isotropic medium over the whole temperature range investigated. Bi_2Te_3 is anisotropic, but when the magnetic field is perpendicular to the cleavage planes, the cleavage planes are in the x-y plane and thus the x- and y-directions in the crystal are equivalent (Drabble and Wolfe, 1956). With primary currents in the x-direction and the transverse effects measured in the y-direction, the Bridgman relation should apply.

The sign of P is thus always the same as that for Q_i, and R_a should equal R_i at the temperature where $Q_i = 0$. Then from equation (7·1) $|R_a| > |R_i|$ below, and $|R_a| < |R_i|$ above this temperature for both n- and p-type specimens. It is seen that the general behaviour is as predicted, not only for the case considered, with the magnetic field perpendicular to the cleavage planes, but also when the magnetic field is applied parallel to the cleavage planes (Figures 19 and 20).

Under adiabatic conditions, with $\omega_y = 0$, the adiabatic Hall coefficient R_a is not directly measurable (Jan, 1957). The measured Hall coefficient R_m is given by the relation

$$R_m = R_i - \left(\frac{dE}{dT}\right)_{T_i} P \qquad (7·3)$$

where $\left(\frac{dE}{dT}\right)_{T_i}$ is the thermoelectric power of Bi_2Te_3 relative to T_1 alloy, the material of the measuring probes. However, the

thermoelectric power of Bi_2Te_3 is large compared with that of the metal of the measuring probes, so that the value of R_m is approximately equal to R_a.

The measurements of thermoelectric power were made with the heat flow parallel to the cleavage planes (Figure 24). The variation of K_y with temperature (Figure 31) was calculated for each specimen from the measured electrical conductivity (Figures 14 and 23) and data given by Goldsmid (1958 (b)) from measurements made on Bi_2Te_3 with the heat flow parallel to the cleavage planes. Thus, for the case when the magnetic field is perpendicular to the cleavage planes, values of P have been calculated from the measured values of Q_i using equation (7·2). These have been used to calculate $|R_m - R_i|$ from equation (7·3). Then, using the measured values of R_i, the variation of R_m with temperature has been calculated. This is plotted for both specimens on Figures 19 and 20. It is seen that this theory always predicts a larger value for $|R_m - R_i|$ than is, in fact, found experimentally.

In equations (7·2) and (7·3) K_y and $(\frac{dE}{dT})_{T_1}$ are respectively the thermal conductivity and thermoelectric power in a transverse magnetic field. In the calculations values of these quantities were used which had been obtained for zero magnetic field. However, it is known that these quantities are almost independent of magnetic field (Goldsmid, 1958 (b); Bowley et al, 1958), and this factor would not lead to the observed differences between the measured and calculated values

of R_m. There are also other second order effects which can contribute to the measured voltage in the adiabatic case (Fieschi, 1955; Jan, 1957). Probably the main factor contributing to this difference is the fact that ω_y is not zero and true adiabatic conditions are not obtained. It is, in fact, difficult to know the exact experimental conditions in the y-direction. In preliminary experiments no effort was made to reduce the transverse heat flow, and an even smaller value of $|R_m - R_i|$ was observed (see results for R5, Figure 16). While taking the readings shown in Figures 19 and 20 an effort was made to reduce this heat flow to a minimum (§ 5·3). However, if $\omega_y \neq 0$, the quantity measured would be a quasi-adiabatic Hall coefficient R_a^*, where $|R_a^* - R_i| < |R_m - R_i|$.

Thus, assuming equation (7·2) to be obeyed in Bi_2Te_3 for this direction of the magnetic field with respect to the cleavage planes, the variation of the Ettingshausen coefficient with temperature, obtained using this relation, is plotted in Figure 32.

Sufficient data are not available for interpreting the corresponding results obtained with the magnetic field parallel to the cleavage planes. In the derivation of the Bridgman relation (Appendix III) it is seen that when the magnetic field is parallel to the cleavage planes, the simple relation $P = \frac{Q_i T}{K_y}$ does not necessarily hold. In addition, in order to calculate the Ettingshausen coefficient for the magnetic field parallel to

the cleavage planes, the thermal conductivity K_y for heat flow perpendicular to the cleavage planes would be required. These values of the thermal conductivity are not known. The only published data are by Goldsmid (1956 (a) and (b)) who states that the lattice component of the thermal conductivity with heat flow perpendicular to the cleavage planes appears to be about half the value obtained from measurements parallel to the cleavage planes. Thus the calculation of the Ettingshausen coefficient with the magnetic field parallel to the cleavage planes was not attempted.

Examination of equations (1·9) shows that the variation of the Ettingshausen coefficient with temperature obtained for specimens R5 and R9 cannot be compared with the expected variation on the assumption of lattice scattering and the values of η^* deduced from equation (2·6). The total thermal conductivity K occurs in the expression for the Ettingshausen coefficient P, whereas only the electronic part K_e can be calculated in terms of η^*. However, it is obvious, since the two quantities are related by the Bridgman relation (equation 7·2), that even if the thermal conductivity obeys the simple theory presented in § 6·1, agreement between theory and experiment cannot be better for the Ettingshausen coefficient than is obtained for the Nernst coefficient (§ 6·10).

For non-degenerate semiconductors in the extrinsic region, assuming acoustical mode scattering,

$$P = -\frac{3\pi}{16} \cdot \frac{kT}{e} \cdot \frac{\mu}{K} \qquad (7·4)$$

where $\mu = \mu_n$ for n-type and $\mu = \mu_p$ for p-type semiconductors (equations 1·16). This relation has been used as a check on the order of magnitude of the values of P calculated from equation (7·2). Values of μ_n and μ_p were calculated as described in § 6·4 and values of K were obtained from Figure 31.

For R9, at 200°K, $\eta^* = -1{\cdot}3$ (Figure 26) and P = -720 cm^3 deg $Joule^{-1}$ from equation (7·2), and -925 cm^3 deg $Joule^{-1}$ from equation (7·4), using R_a, and -993 cm^3 deg $Joule^{-1}$ using R_i at 100°K in the determination of μ_n.

For R5, at 300°K, $\eta^* = +0{\cdot}05$ (Figure 26) and P = -270 cm^3 deg $Joule^{-1}$ from equation (7·2) and -271 cm^3 deg $Joule^{-1}$ from equation (7·4).

Considering the theoretical limitations of the equations used, the agreement between these results is considered to be satisfactory.

An interpretation of the adiabatic and isothermal Nernst coefficients is more complicated. The relation between the two quantities is (cf. Chambers, 1952):

$$Q_a = Q_i - \frac{dE}{dT} \cdot S \qquad (7{\cdot}5)$$

where S is the Righi-Leduc coefficient.

Now there is no simple relation giving the sign of S from some experimentally-determined quantity over the whole temperature range. However, according to simple semiconductor theory, S is positive for p-type specimens and negative for n-

type specimens in the extrinsic range, only changing sign in p-type specimens ($b > 1$) after Hall and thermoelectric power readings have indicated that the specimens have become intrinsic (Putley, 1955). At low temperatures b may be less than unity (§ 6·3) but this fact would not change the signs of S in the extrinsic region. Thus, over the complete temperature range studied, S should be negative for R9 and positive for R5, and, from equation (7·5), below the temperature where $Q_i = 0$, it is predicted that $|Q_a| > |Q_i|$, while above this temperature $|Q_a| < |Q_i|$. As with the adiabatic Hall coefficient, the quantity Q_a is not directly measurable (Jan, 1957).

The measured Nernst coefficient Q_m is given by

$$Q_m = Q_i - \left(\frac{dE}{dT}\right)_{T_1} . S \qquad (7·6)$$

where $Q_m \simeq Q_a$. Following the same reasoning as for the Hall coefficient, a quasi-adiabatic Nernst coefficient Q_a^* should be obtained such that $|Q_a^* - Q_i|$ is smaller than predicted. No definite results could be obtained for R5 (Figure 21). For R9 (Figure 22) it is found that $|Q_a^*| < |Q_i|$, over the whole of the temperature range investigated. Thus the results are not as predicted, and S does not appear to behave according to the simple theory.

In the extrinsic region for a non-degenerate n-type semiconductor with acoustical mode lattice scattering

$$S = -\frac{21\pi}{32} . \frac{k^2 T}{eK} . n\mu_n^2 \qquad (7·7)$$

where K is the total thermal conductivity, and (equation 1·16)

$$Q_i = -\frac{3\pi}{16} \cdot \frac{k}{e} \cdot \mu_n \qquad (7\cdot8)$$

These formulae assume an isotropic medium (Putley, 1955).

From equations (7·7) and (7·8) and making the substitution $\sigma = ne\mu_n$ (equation 2·1), the following expression is obtained for the Righi-Leduc coefficient:

$$S = +3\cdot5\left(\frac{k}{e}\right) \cdot \frac{T\sigma Q_i}{K} \qquad (7\cdot9)$$

For p-type material, making the same assumptions,

$$S = +\frac{21\pi}{32} \cdot \frac{k^2 T}{eK} p \cdot \mu_p^2$$

$$Q_i = -\frac{3\pi}{16} \cdot \frac{k}{e} \cdot \mu_p \qquad \text{and} \qquad \sigma = pe\mu_p,$$

giving

$$S = -3\cdot5\left(\frac{k}{e}\right) \cdot \frac{T\sigma Q_i}{K} \qquad (7\cdot10)$$

Considering only the temperature ranges for which the measured isothermal Nernst coefficients are negative, values of the Righi-Leduc coefficient were estimated for specimen R5 using equation (7·10) and for specimen R9 using equation (7·9). The measured values of electrical conductivity and isothermal Nernst coefficient (H_z perpendicular to the cleavage planes) were used (Figures 14, 21, 22 and 23) and the values of the thermal conductivity (Figure 31) were obtained in the same way as in the calculation of the Ettingshausen coefficient. The values obtained for S should be those with the magnetic field perpendicular to the cleavage planes. Values of Q_m were then

calculated using the measured values of Q_i ($H_{\perp r}$ to the cleavage planes) and $(\frac{dE}{dT})_{T_1}$ (Figure 24) in equation (7·6). The calculated values of Q_m are plotted in Figures 33 and 34. It is seen that in the extrinsic region a measurable $|Q_a^* - Q_i|$ is predicted, but not found, for R5, while the sign of $(Q_a^* - Q_i)$ predicted for R9 is the opposite to that observed.

Equations (7·9) and (7·10) are only expected to apply to isotropic non-degenerate semiconductors when the conduction is extrinsic and limited by acoustical mode scattering. Although it is known (§ 6·2; § 6·4; § 6·10) that all these conditions do not apply to Bi_2Te_3, it is expected that equation (7·9) should give the correct order and sign of the effect at low temperatures in the purer specimen R9. For temperatures in the region where the sign of Q_i changes from negative to positive, mixed conduction sets in and equation (7·9) is not valid (§ 6·10). Thus the Righi-Leduc coefficient in Bi_2Te_3 does not appear to follow the simple theory of semiconductors and the reason for this is not known.

6·8. Anomalous effects in Bi_2Te_3.

Attempts have been made by various workers to try and explain why:

(1) Samples of Bi_2Te_3 grown from a melt of stoichiometric composition are always p-type with approximately the same concentration of free charge carriers.

(2) The number of free carriers is always far greater than would be expected from the impurity content of the starting materials (Bi, Te) and repeated zone melting does not produce any appreciable effect on this concentration of free carriers.

(3) The temperature variation of the Hall coefficient is anomalous (Harman et al, 1957; Mooser and Pearson, 1958; Williams, 1959; Yates, 1959).

These experimental facts for Bi_2Te_3 can only be explained within the framework of simple semiconductor theory if additional and somewhat arbitrary assumptions are made. In addition, the thermoelectric power and Nernst coefficients show small anomalous effects which are discussed in § 6·9 and § 6·10 respectively.

It has been shown that the value of the Hall coefficient is independent of the magnetic field strength (§ 4·5) and of the value of the temperature gradient down the specimen (§ 4·4). All the normal precautions concerning specimen dimensions (§ 3·4) and experimental technique (§ 4·4) were observed, while measurements of the isothermal, as opposed to the adiabatic, Hall coefficient only slightly reduces the anomaly (§ 5·3). It has been shown theoretically (§ 6·2) that the anomaly is not due to the effects of degeneracy.

It is known that CdS, when prepared from a melt of stoichiometric composition, is always n-type and that the

properties of all specimens depend markedly on the atmosphere in which they are prepared, on small deviations from stoichiometric composition and on the type of impurities introduced. It has been shown that the results obtained for CdS can be explained by consideration of the conditions necessary for electro-neutrality (Kröger and Vink, 1954; Kröger et al, 1954). Scanlon and Brebrick (1954) have also shown that the electrical properties of PbS, in the absence of appreciable concentrations of impurity atoms, depend markedly on deviations from stoichiometry. Excess lead makes PbS n-type while excess sulphur leads to p-type conductivity.

Harman et al (1957) show that, even by using very high purity elements and special preparation techniques, a low concentration of charge carriers and hence a "high purity" Bi_2Te_3 cannot be obtained. They suggest that the lowest obtainable purity concentration is the "wrong atom defect level". Even if the separate elements are present in exactly stoichiometric proportions, a bismuth atom may occupy a tellurium lattice site and vice versa, and these atoms would act as impurities. They state that for each semiconducting compound there is an intrinsic number of atoms of each constituent which act as impurities and then define this concentration level as the wrong atom defect level. If a bismuth atom occupies a tellurium lattice site it is expected that the atom would contribute a hole to the conduction, while if a tellurium atom occupies a bismuth lattice

site it is expected that it would contribute an electron. Thus they conclude that the high concentration of carriers in Bi_2Te_3 could be due to bismuth and/or tellurium atoms in the wrong lattice sites, and for this reason Bi_2Te_3 is necessarily a heavily doped semiconductor.

This theory is consistent with the idea, which has already been put forward (§ 6·3), of impurity band conduction in which the impurity levels form a band overlapping, for p-type impurities, the top of the valence band and, for n-type impurities, the bottom of the conduction band. This means that the measured coefficients must be interpreted, even in the extrinsic region, in terms of a model with at least two bands. Some of the multi-band models which have been suggested for Bi_2Te_3 are thus discussed later in this section.

Mooser and Pearson (1958) try to explain both the large concentration of p-type impurities in Bi_2Te_3 obtained from a melt of stoichiometric composition and an anomalous behaviour of the Hall coefficient of n-type material. Their model leads to a double reversal of the Hall coefficient for n-type specimens - a phenomenon which has not, in fact, been observed in Bi_2Te_3, but which they erroneously quote as having been observed by Satterthwaite and Ure (1957).

The temperature variations of the isothermal Hall coefficients for p- and n-type material obtained in the present investigation are shown in Figures 19 and 20. Although it is

immediately obvious (§ 5·3; § 6·7) that the results for p-type material are anomalous, it is not so obvious for n-type material. Now the electrical conductivity exhibits no anomalous effects over the extrinsic region. Figure 35 shows the variation of σ deduced from equation (1·9), assuming acoustical mode scattering ($r = -\frac{1}{2}$) and where the magnitudes of the calculated and experimental quantities have been made to agree at 200°K. The theoretical value of the Hall coefficient of specimen R9 ($b = 1$) has thus been calculated from the electrical conductivity using the relation (Appendix IV)

$$R_{th} = R_s\left(\frac{\sigma_s}{\sigma}\right)^2 \qquad (8\cdot1)$$

where R_s is the value of the isothermal Hall coefficient in the extrinsic region and σ_s is the extrapolated saturation conductivity. Assuming that $R_i = R_s$ at 100°K, the calculated values of R_{th} are plotted together with the experimental values of R_i in Figure 36.

Harman et al (1957) find a similar experimental variation of the Hall coefficient of n-type material with temperature and suggest that impurity band conduction is the reason. Yates (1959), who makes measurements down to lower temperatures (1·3°K), finds anomalies in the Hall coefficients of both n- and p-type material which he attempts to interpret in terms of an impurity band model.

Figure 37 shows the three band model used by Mooser and Pearson (1958) to calculate the charge carrier concentrations

in Bi_2Te_3. They assume the density of states in both the valence and conduction bands to be that of free electrons, while in the third overlapping band it is taken to be forty times smaller. Taking the energies of the band edges (Figure 37) as $E_{n_1} = -0{\cdot}125$ ev, $E_p = -0{\cdot}1$ ev and $E_{n_2} = +0{\cdot}1$ ev, Mooser and Pearson find the charge carrier concentrations n_1, n_2 and p given in Figures 38 and 39 for what they call "intrinsic" Bi_2Te_3 and for Bi_2Te_3 containing 2×10^{18} cm^{-3} donors (excess tellurium atoms).

These results were used by Mooser and Pearson to calculate the variation of the Hall coefficient with temperature for the two types of specimens. The Hall coefficient is given by:

$$R = \frac{-n_1\mu_{n_1}^2 - n_2\mu_{n_2}^2 + p\mu_p^2}{e.(n_1\mu_{n_1} + n_2\mu_{n_2} + p\mu_p)^2} \qquad (8{\cdot}2)$$

where μ_{n_2}, μ_p and μ_{n_1} are the mobilities of the carriers in the conduction, valence and third overlapping bands respectively. It was assumed that $\mu_{n_2} \propto \mu_p \propto T^{-3/2}$; $\mu_{n_1} \propto T^{-1}$ and, at 300°K,

$$\mu_{n_1} : \mu_{n_2} : \mu_p = 0{\cdot}6 : 1{\cdot}1 : 1$$

leading, for the specimen containing excess donors, to a double reversal of the Hall coefficient.

Using the results of Mooser and Pearson for n_1, n_2 and p (Figures 38 and 39), the present author has calculated the variation of Hall coefficient from $150^\circ \longrightarrow 600^\circ$K for the two types of specimen, making various assumptions. The results

of these calculations are presented in Figures 40 and 41.

The variations of Hall coefficient in Figure 40 were calculated assuming the concentrations of carriers given by Figure 38 and

(1) $\mu_{n_2} \propto \mu_p \propto T^{-3/2}$; $\mu_{n_1} \propto T^{-1}$

and at 300°K $\mu_{n_1} : \mu_{n_2} : \mu_p$ is (a) 0·6 : 1·1 : 1

(b) 0·45 : 1·1 : 1

(2) $\mu_{n_2} \propto T^{-1\cdot63}$; $\mu_p \propto T^{-1\cdot94}$ (Table 6.1); $\mu_{n_1} \propto T^{-1}$

and at 300°K $\mu_{n_1} : \mu_{n_2} : \mu_p$ is (a) 0·6 : 1·1 : 1

(b) 0·45 : 1·1 : 1

(c) 0·1 : 1·1 : 1

The results in Figure 41 were obtained from Figure 39, making the same assumptions as in 1 (a) and (b) and in 2 (a).

The results presented in Figures 40 and 41 can be compared with the experimental variation of the Hall coefficient obtained for p-type material in the extrinsic region (Figures 16 and 19). If the concentrations of carriers for "intrinsic" Bi_2Te_3 (Figure 38) are used, the calculated Hall coefficient always increases with decreasing temperature. If the concentrations for Bi_2Te_3 containing excess donors (Figure 39) are used, the calculated Hall coefficient can be made to be positive and to have a positive temperature coefficient over the temperature range 300° $\longrightarrow$ 100°K by a suitable choice of mobility ratios and variations. However, if the experimentally-

observed decrease in the Hall coefficient as the temperature is lowered is to be explained in terms of this model, the Hall coefficient becomes negative at sufficiently low temperatures because of the presence of excess donors. Measurements made by Yates (1959) down to 1·3°K on specimens which are p-type at 300°K do not show a reversal of sign to electron conduction at any temperature below 300°K. Thus the model proposed by Mooser and Pearson does not explain the observed Hall coefficient readings over the whole temperature range. In addition, whatever the assumptions made in the calculation of the Hall coefficient, the resulting temperature variation of the electrical conductivity is completely inconsistent with experiment. Instead of the conductivity changing by a factor of about 10 over the temperature range 100° $\longrightarrow$ 300°K (Figure 14) the calculated conductivity is approximately constant, only varying by a factor of about 1·1.

There are a large number of unsatisfactory assumptions associated with this model for Bi_2Te_3 including the values taken for the densities of states of carriers in the various bands, the constancy of the energy gap (taken at 0·2 ev) with temperature and the values taken for the ratios of mobilities. However, it is seen that the temperature variation of both the Hall coefficient and conductivity over the whole temperature range cannot be explained by this model on a single set of assumptions, and thus it is not worth considering this model in any more detail.

Yates (1959) attempts to explain the observed Hall coefficient anomalies in terms of impurity band conduction (Hung and Gliessman, 1954). When the concentration of impurities is sufficiently large, interaction of the impurity states causes broadening into impurity bands leading to impurity band conduction. Figure 42 shows the simple energy band model used by Hung and Gliessman and Figure 43 the variation with temperature of the Hall coefficient which is to be expected for an n-type specimen. On this theory, although there will always be some acceptors in an n-type specimen, the acceptor band is filled by electrons from the donor band and therefore does not contribute to conduction in the extrinsic region. At very low temperatures conduction is in the donor band only and the Hall coefficient is constant. At higher temperatures, with the conduction still in the extrinsic region, the conduction is completely in the conduction band and the Hall coefficient is again constant with the same value as at very low temperatures. This is the normal exhaustion region for an impurity semiconductor. The experimental indication of impurity band conduction is a maximum in the Hall coefficient curve between these two regions. At still higher temperatures the exhaustion region passes over into intrinsic conduction. Normally the excitation energy ΔE_D is very small compared with the main energy gap E_g and the maximum in the Hall coefficient curve appears at a low temperature (less than $40^{\circ}K$).

The mobility of carriers in an impurity band is usually very small compared with the mobility of electrons in the conduction band or holes in the valence band, but as the impurity concentration increases the mobility of carriers in the impurity band increases and the Hall coefficient maximum shifts to slightly higher temperatures. When the concentration of impurity centres is very large the mobility of electrons becomes the same in the donor band as in the conduction band, or the bands actually overlap and become one band, so that the Hall coefficient maximum should disappear and the energy band diagram of Figure 42 would no longer apply. In Bi_2Te_3 the maxima observed in the Hall coefficient curves are not followed by an exhaustion range as the temperature is increased but pass straight into the mixed conduction and then intrinsic regions. This is impossible on the simple impurity band model of Hung and Gliessman if the ionization energy for donors is much less than the energy gap ($E_o \simeq 0{\cdot}2$ ev). The situation of the impurity bands near the centre of the energy gap, resulting in a shorter exhaustion region before the beginning of mixed conduction, conflicts with existing optical data (Austin, 1958) which give no indication of impurity levels in such a position. In fact, a maximum in the Hall coefficient curve which is not followed at higher temperatures by an exhaustion range cannot be due to impurity band conduction, as proposed by Hung and Gliessman. In addition, there are no minima in the conduction curves corresponding to the Hall coefficient maxima.

The interpretation which the author puts on the results obtained by Yates is that the ionization energy of impurities is zero. This seems to be the only explanation of the constancy of the measured Hall coefficient from about 100°K right down to 1·3°K in each case. The maxima occurring in the Hall coefficient curves between about 100° and 300°K cannot then be interpreted in terms of the equations for impurity band conduction, as proposed by Hung and Gliessman, and this would explain the inconclusive nature of Yates's analysis of his results. Black et al (1957) and Goldsmid (1958 (a)) have previously suggested the possibility of the impurity levels merging with the band edges in Bi_2Te_3, and Wright (1959) does, in fact, suggest that Yates's results could be interpreted as due to impurity bands overlapping the conduction and valence bands.

Other substances show similar variations of Hall coefficient in the extrinsic region when the concentrations of impurities are greater than about 10^{17} cm^{-3} (see, for example, work on silicon by Longo et al (1959) and Carlson (1955), and on germanium by Fritzsche and Lark-Horovitz (1954) and Fritzsche (1955)). In discussion these authors suggest impurity band conduction, although for large concentrations of impurities the theory is uncertain (Conwell, 1956). For impurity concentrations above about 10^{16} cm^{-3} the observed effects are very complicated and the theory of impurity band conduction

(Hung and Gliessman, 1954) has to be considerably refined. Since the theory of impurity band conduction in this region is so uncertain, very little attention has been paid to the observations on high impurity content samples of silicon and germanium in the papers quoted.

The theories presented so far which have attempted to explain the anomalous behaviour of the low temperature Hall coefficient in Bi_2Te_3 assume spherical energy surfaces for conduction and valence bands centred on the origin of k space. This means that the densities of states near the band edges are assumed to be proportional to the square root of the energy. However, since the concentration of impurities is known to be high and impurity bands are thought to overlap the conduction and valence bands, the effects of impurities may cause the density of states to depart from this simple law. In addition, the maximum of the valence band and/or the minimum of the conduction band may not be at $k = 0$ and one or both of the bands may be degenerate.

Information on energy band structure can be obtained from optical measurements. For substances such as InSb and InAs, where the minimum of the conduction band is at $k = 0$ (from cyclotron resonance measurements), the effect of a linear term in the valence band can be calculated (Kane, 1957) and compared with experiment. It is found that at low temperatures the presence of a linear term in the valence band affects the

electrical properties of a p-type semiconductor (Stern, 1959). Stern quotes a p-type sample of InAs as having a Hall coefficient of +26 $coul^{-1}$ cm^3 at room temperature, +2·6 $coul^{-1}$ cm^3 at 4·2°K and an intermediate maximum value of +50 $coul^{-1}$ cm^3. He suggests that the large reduction in the Hall coefficient at low temperatures for this sample may be associated with the linear term in the valence band.

The main cause of a linear term in the expression for the band edge is spin - orbit interactions (Elliott, 1954; Herman, 1955) and, since the atomic numbers of bismuth and tellurium are large, it is expected that spin - orbit coupling will be large in Bi_2Te_3.

Drabble and Wolfe (1956) propose a many-valley type energy band model for Bi_2Te_3. The crystal symmetry of Bi_2Te_3 indicates (Wright, 1959) that the number of valleys is likely to be 1, 3, 6 or 12. Measurements by Drabble et al (1958) and Drabble (1958) indicate that the number of valleys for both n- and p-type material is six, taking the most general interpretation This implies valleys with their minima centred on the reflection planes. If, however, the valleys are in the most extreme positions at the edge of the Brillouin zone (Figure 3b), their number would be three for the same scheme of interpretation. Preliminary measurements on the Faraday rotation effect in Bi_2Te_3 (Austin, 1959) indicates that the number of valleys is three in p-type crystals and six for n-type.

Available optical data (Black et al, 1957; Austin, 1958) would be inadequate to allow a detailed analysis of band structure in Bi_2Te_3, even if the parameters required in the calculations were known sufficiently accurately. The effects of a small linear term in the valence band energy are probably too small to be detected from the shape of the main absorption edge connected with transitions between the valence and conduction bands. The shape of the intrinsic absorption edge obtained by Austin (1958) is very similar to results obtained for InSb. However, an analysis of the InSb results has not led to any definite conclusions (Blount et al, 1956; Potter, 1956). Blount et al explain the observed results in terms of two phonons to conserve energy, implying two maxima in the valence band and the existence of two types of holes, whereas Potter suggests an equally good fit to the results can be made by using four phonons. In Bi_2Te_3 it is to be expected that indirect transitions from each valley in the valence band will take place to the three or six conduction band minima. The absorption edge shows a structure which Austin interprets in terms of indirect transitions, assisted by phonon interaction. He concludes that it is impossible to give a simple interpretation and that the resolution obtained is inadequate to offer a sensitive test for the transitions occurring.

Wright (1959) suggests an alternative explanation of the shape of the absorption edge - namely that both the valence band and conduction band are double with two maxima and two

minima respectively, separated slightly in energy. The type of chemical bonding (§ 3·1) in Bi_2Te_3 leads to a band structure of this type. The value of the energy gap in a semiconductor is usually determined by the weakest bond (Bi - $Te^{(2)}$), but since there is only a 3% difference in the Bi-$Te^{(1)}$ and Bi-$Te^{(2)}$ bond lengths it is to be expected that there will be a second pair of bands having a slightly greater energy gap.

A more sensitive test for the existence of a linear term in the valence band energy arises from the study of the absorption connected with transitions between light and heavy hole bands (Matossi and Stern, 1958). The absorption peak associated with transitions between light- and heavy-hole bands occurs away from the intrinsic absorption edge at much lower energies, in a region for which there are no experimental results for Bi_2Te_3. Matossi and Stern compare the observed optical absorption for InAs with curves calculated using Kane's theory. This theory (Kane, 1957) involves a large number of parameters which are not known for Bi_2Te_3, so that it is not even possible to estimate the possible effect due to a linear term in the valence band on the Hall coefficient at low temperatures.

It is known (Wright, 1959) that compensated samples of Bi_2Te_3 frequently show inhomogeneities which could lead to anomalous values of the Hall coefficient. However, the variation with temperature of the Hall coefficient seems to show systematic trends with impurity content, both for n- and p-type material (Yates, 1959), and this would appear to be too easy a dismissal of the problem.

In conclusion, it would appear that a two (or more) band model must be used in the extrinsic region for Bi_2Te_3 - where, from the crystal symmetry, it is to be expected that the energy surfaces are warped. It is obvious that a model of this sort could very well lead to an explanation of the observed temperature variation of the Hall coefficient if the correct parameters could be determined.

6·9. Thermoelectric Power.

In previous sections it has been assumed that the thermoelectric power of Bi_2Te_3 in the extrinsic region could be interpreted in terms of a single band model in which the density of states for carriers is proportional to the square root of the energy. By use of equation (1·9) the values of η^* were calculated over the extrinsic region for various scattering mechanisms (Figure 26) and then used to estimate the relative importance of the various types of scattering at different temperatures in this range (§ 6·2; § 6·4). However, it was found, when calculating the effect of ionized impurity scattering at 100°K, that the best fit to the experimental results was obtained if different values of η^* were used in the calculation of the ionized impurity and lattice mobilities. In addition, the value of η^* calculated from the concentration of carriers (equation 1·11) does not conform with the values obtained for η^* from the thermoelectric power (Table 6·4). With increasing impurity content (§ 6·3, Table 6·2) the value of η^* obtained

from equation (1·11) agrees more closely with the value of η^* obtained from the thermoelectric power, assuming acoustical mode lattice scattering ($r = -\frac{1}{2}$), than when assuming ionized impurity scattering ($r = +\frac{3}{2}$). By its definition η^* must have a unique value in a given specimen and at a given temperature. For a semiconductor with spherical energy surfaces, when conduction takes place in one band only, η^* is defined by equation (1·11) which is independent of the type of scattering of the carriers. It is known that the energy surfaces in Bi_2Te_3 are not spherical, which introduces an uncertainty into the determination of the density of carriers (§ 6·4). In addition, if conduction takes place in more than one band, the simple relationship (equation 1·11) between the carrier concentration and η^* can no longer apply.

The absolute thermoelectric power of a semiconductor is determined primarily by the value of η^* and the type of scattering of the carriers. For spherical energy surfaces or for a 'many-valley' model such as that proposed by Drabble and Wolfe (1956), theory shows that the thermoelectric power is isotropic. Goldsmid (1957) finds the thermoelectric power of Bi_2Te_3 to be slightly anisotropic, so that some of the assumptions in the simple theory (§ 6·1) must be invalid or possibly Goldsmid's results are incorrect (§ 6·2). Konorov (1956) finds a considerably greater degree of anisotropy. However, owing to the large differences between the values of

various electrical properties obtained by Konorov and those obtained by other workers, it is not thought that these results for the anisotropy of the thermoelectric power are very reliable.

Even when all the conditions assumed in § 6·1 are valid, the value of η^* obtained from the thermoelectric power assuming ionized impurity scattering is suspect. The expression for the relaxation time contains a term of the form

$$f(x) = \log_e(1 + x) - \frac{x}{1 + x}$$

where x is a function of η (see equation 4·5). As an approximation f(x) is treated as a constant (Mansfield, 1956 (a) and (b)) when deriving equation (1·9).

The factor which would probably have most influence on the measured thermoelectric power in the extrinsic region is conduction occurring in more than one band. If more than one band is necessary to explain the temperature variation of the Hall coefficient in the extrinsic region (§ 6·8), the simple relation for the thermoelectric power, given by equation (1·9), would no longer apply. (See, for example, Johnson (1956) who reviews the theory of the thermoelectric power in semiconductors.) Thus it is concluded that the determination of the reduced Fermi energy, η^*, in Bi_2Te_3 is uncertain.

Previous workers (Black et al, 1957; Harman et al, 1957) in analysing the extrinsic thermoelectric power have calculated η^* from the Hall coefficient and then the expected

variation of $\frac{dE}{dT}$ using equation (1·9). They always found that the theoretical variation of $\frac{dE}{dT}$ with temperature was less rapid than that observed experimentally. This method is unreliable and nothing can be deduced from their results.

Goldsmid (1958 (a)), assuming a non-degenerate semiconductor with a constant carrier concentration, plots $\frac{dE}{dT}$ against $\log_e T$. For these conditions,

$$\frac{dE}{dT} = \frac{3}{2}\frac{k}{e}\log_e T + \text{constant},$$

and the slope should equal 129 $\mu V\ deg^{-1}$. In Figure 44 $\frac{dE}{dT}$ is plotted against $\log_e T$ for specimens R3·21 and R5. For R3·21 (n-type) the slope is 165 $\mu V\ deg^{-1}$ and for R5 (p-type) 124 $\mu V\ deg^{-1}$. Goldsmid obtains 167 $\mu V\ deg^{-1}$ for n-type and 150 $\mu V\ deg^{-1}$ for p-type material. He discusses the departure of these values from the theoretical slope but, however, comes to no definite conclusion as to the reason for the discrepancies.

Welker (1954) gives the approximate relation

$$\left|\frac{dE}{dT}\right|_{max} = \frac{E_g}{eT} \qquad (9·1)$$

connecting the maximum value of the thermoelectric power and the value of the energy gap at the temperature when the thermoelectric power is a maximum. The values of E_g calculated from equation (9·1) are given in Table 6·6 and for all specimens it is seen that E_g is smaller than obtained by other methods.

Table 6·6. Energy gap from maximum of thermoelectric power.

Specimen	T_{max} (°K)	$\left\|\frac{dE}{dT}\right\|_{max}$ ($\mu V\ deg^{-1}$)	E_g (e-V)
R3·21	306	306	0·09
R5	350	212	0·07
R8	276	407	0·11
R9	238	310	0·07

The values of $\left|\frac{dE}{dT}\right|$ obtained by the author and shown in Figures 15 and 24 are larger than are obtained by other workers using specimens of similar impurity content. For example, Walker (1959) obtains $\frac{dE}{dT} = +252\ \mu V\ deg^{-1}$ for specimen SBTC.19 at 200°K, whereas for R8 the value obtained is $+335\ \mu V\ deg^{-1}$. For SBTC.16, at 200°K, $\frac{dE}{dT} = -238\ \mu V\ deg^{-1}$ and for R9 $-295\ \mu V\ deg^{-1}$. The differences in the thermoelectric power of specimens obtained from the same ingot (Table 3·1) is thus about 25 to 30%. The maximum estimated error in the readings of $\frac{dE}{dT}$ is of the order of 6% (§ 4·3; § 4·5; § 5·4), which does not cover the observed differences. The values of the Hall coefficient also differ slightly and thus the specimens are probably not identical, although from the same ingot. The discrepancy between the author's results and those obtained by Walker is still larger than would be expected and it is thought that the experimental techniques employed by Walker might be at fault. Walker soldered his specimens to copper discs and for his

temperature measurements used thermocouples composed of copper and copper alloys, both of which could alter the properties of the specimens (§ 3·5). Care was taken in the present work not to have any copper in contact with the specimens (§ 5·2). In addition, Walker's thermocouples were not in direct contact with the specimen, but were attached to the side of the specimen via two short lengths of 20 S.W.G. copper wire, which were then soldered to the specimen, and this is not considered as satisfactory as spot welding. If the values of the thermoelectric power are actually smaller than observed, this would make the values of E_g calculated from equation (9·1) even lower.

In the extrinsic region, with only one type of carrier present, the simple theory presented in § 6·1 predicts that in the limiting case of complete degeneracy the thermoelectric power should be proportional to the absolute temperature. It is assumed that the lattice is not significantly perturbed by the existence of a thermal gradient. However, at low temperatures phonons can diffuse far more freely than at higher temperatures, giving rise to an additional mechanism affecting the thermoelectric power. The phonon-drag contribution to the thermoelectric power is caused by a build-up of charge carriers in the cold end of the sample due to preferential scattering of the charge carriers from hot to cold by the asymmetric distribution of phonons existing in the thermal gradient (Herring, 1954; Geballe et al, 1959). The direction of the

thermoelectric field caused by the drag the phonons exert on the carriers always increases the magnitude of the thermoelectric power at low temperatures.

It is seen (Figures 15 and 24) that there is no indication of a contribution to the thermoelectric power due to the phonon-drag effect in Bi_2Te_3 down to 100°K. Goldsmid (1958 (a)) comes to the same conclusion for the temperature range 150° to 300°K. Walker (1959), who measures the thermoelectric power down to 6°K, finds that the phonon-drag effect makes no appreciable contribution over the whole temperature range. He attributes the slight increase in the thermoelectric power at very low temperatures to the effects of ionized impurity scattering, and the absence of a phonon-drag effect in Bi_2Te_3 to its low thermal conductivity and high impurity content. These results for Bi_2Te_3 are very different from the results obtained for high purity germanium in the extrinsic region where phonon-drag is the dominant mechanism controlling the value of the thermoelectric power.

When both electrons and holes are present in a temperature gradient, ambipolar diffusion of electrons and holes (Price, 1955, 1956) arises from the difference in their diffusion coefficients. The equilibrium concentration of electrons and holes increases with increasing temperature and thus there is a concentration gradient of both electrons and holes in the direction of the temperature gradient. In the absence of an applied electric field diffusion causes fluxes of electrons and holes

down the temperature gradient with a resultant transfer of ionization energy. Transport of ionization energy by ambipolar diffusion of electrons and holes can have a large effect on the thermoelectric power, Nernst coefficient and thermal conductivity (Fröhlich and Kittel, 1954; Price, 1955, 1956 (a) and (b)). Each electron - hole pair transports annihilation energy, E_g, as well as band energy of the order of (kT). Observations of the thermal conductivity of Bi_2Te_3 in the intrinsic region have been explained in terms of this transport of ionization energy (Satterthwaite and Ure, 1957; Goldsmid, 1956 (a) and (b), 1958 (b); Nii, 1958; Kanai and Nii, 1959).

Ambipolar diffusion of electrons and holes cannot occur in the extrinsic region in Bi_2Te_3 since the impurity bands overlap the conduction and valence bands and the concentrations of carriers are thus independent of temperature.

A further possibility is the transport of energy by excitons or electron - hole pairs (Joffé, 1956, 1959). The concentration of excitons, n_{exc}, is given by (cf. Pikus, 1956)

$$n_{exc} = \left(\frac{2 \times 2\pi m_{exc} kT}{h^2}\right)^{3/2} e^{-\frac{E_{exc}}{kT}} \qquad (9\cdot2)$$

where m_{exc} = effective mass of exciton

and E_{exc} = energy of excitation.

A temperature gradient results in an exciton concentration gradient, diffusion of excitons from hot to cold and thus transport of exciton activation energy. It is difficult to estimate

the importance of exciton diffusion in the presence of ambipolar diffusion, as there appears to be no direct experimental method of separating the two effects. Measurements of the intrinsic thermal conductivity can be explained in terms of ambipolar diffusion, from which it is concluded that any exciton contribution in this temperature range is small. Since the contribution due to excitons increases with increasing temperature (equation 9·2), it is concluded that any contribution due to excitons in Bi_2Te_3 is negligible in the extrinsic region. In any case, owing to the large carrier concentrations in Bi_2Te_3, the life time for excitons would be exceedingly small.

6·10. Nernst Effect.

An analysis of the Nernst effect should yield additional information about the scattering mechanisms occurring in the extrinsic region and about the temperature dependence of the hole and electron mobilities in the intrinsic region.

Obraztsov (1955) derives expressions for the electrical conductivity and the isothermal Hall and Nernst coefficients when both electrons and holes are present and scattering is by acoustical mode lattice vibrations and ionized impurities. When conduction is by one type of carrier only, the simultaneous observation of the isothermal Hall and Nernst effects and of the electrical conductivity can be used to calculate the relative contributions of ionized impurity and of lattice scattering at a given temperature. Obraztsov considers the case of isotropic

media in the non-degenerate limit and, for one type of scattering only, his formulae reduce to the normal expressions under such conditions (e.g. Putley, 1955; Mansfield, 1957). He also explains the signs obtained experimentally for the Nernst coefficient at various temperatures. If $r > 0$ in the expression for the relaxation time $\tau = a\eta^r$ (equation 1·8) and conduction is by one type of carrier only, then the isothermal Nernst coefficient $Q_i > 0$, while if $r < 0$ then $Q_i < 0$. In the intrinsic region Q_i is always positive as long as $b < 8$. Thus over the complete temperature range Q_i changes sign once, twice or not at all, with the increasing importance of ionized impurity scattering.

Examination of figures 17, 21 and 22 indicates that the effect of ionized impurity scattering is unimportant in specimens R3·21, R8 and R9 over the whole of the temperature range studied, while impurity scattering may be important in specimen R5 below about 200°K and in R7 below about 400°K. A similar conclusion was reached from the variation of mobility with carrier concentration in the extrinsic region (§ 6·4). In order to make any quantitative estimation of the relative importance of the different types of scattering from the Nernst effect, it would be necessary to take degeneracy and anisotropy effects into account. Because of the uncertainty in basic parameters such as effective masses and dielectric constant and in the values of the reduced Fermi energy, η^*, in any given specimen at a given temperature (§ 6·4; §6·9) such calculations were not attempted.

In the mixed conduction regions measurement of the Hall coefficient and electrical conductivity at a given temperature is insufficient to enable the calculation of n, p, μ_n and μ_p (§ 6·2). In certain cases the measurement of the temperature dependence of the isothermal Nernst coefficient in the intrinsic temperature range can give the temperature dependence of the mobility for one type of carrier (Bashirov and Tsidil'kovskiĭ, 1956). A simultaneous determination of the isothermal Nernst and Hall coefficients and the electrical conductivity at a given temperature yields all four quantities n, p, μ_n and μ_p at that temperature, provided that the value of the energy gap E_g is known and the conditions under which the equations are derived are applicable.

For an isotropic, non-degenerate semiconductor in the intrinsic region, putting n = p and $b = \frac{\mu_n}{\mu_p}$ and assuming acoustical mode lattice scattering (cf. Putley, 1955):

$$R_i = - \frac{3\pi}{8en} \frac{(b - 1)}{(b + 1)} \qquad (10·1)$$

$$\sigma = ne\mu_p(b + 1) \qquad (10·2)$$

$$Q_i = - \frac{3\pi}{16} \cdot \frac{k}{e} \mu_p \left[\frac{1 + b^2 - b(8 + \frac{2E_g}{kT})}{1 + b} \right] \qquad (10·3)$$

The conditions in Bi_2Te_3 are not so simple. Bi_2Te_3 is anisotropic, so that anisotropy factors (§ 6·2) must be included in equations (10·1) and (10·3). These factors, which are unknown

for both the Hall and Nernst coefficients in the intrinsic region, could vary with temperature. The value of E_g is small and is known to vary with temperature. Extrapolation of the values of the energy gap, determined below about 300°K, into the intrinsic region has been found to be impossible. Thus the value of E_g in the intrinsic region is unknown. A large difference was observed between the isothermal and quasi-adiabatic Nernst coefficients for positive values of the coefficients (Figures 21 and 22). As it was found impossible to obtain measurements of the isothermal coefficient in the intrinsic region, the hole (or electron) mobility could not be obtained by this method.

The Nernst effect is rarely studied in systematic investigations of semiconducting materials, although it is seen that it should yield interesting, and sometimes new, information. In Bi_2Te_3 it cannot be used to deduce new information without a far more accurate knowledge of the basic parameters than is possessed at the moment.

The only previous observations of the Nernst coefficient in Bi_2Te_3 were made by Bashirov (1958). Cast and pressed specimens were used so that the observed coefficients do not correspond to any particular orientation of the temperature gradient, $\frac{dT}{dx}$, and magnetic field H_z with respect to the cleavage planes (§ 5.1). In addition, quasi-adiabatic coefficients, rather than isothermal coefficients, were probably

observed. Bashirov considers the non-dimensional Nernst field given by the relation (cf. Table 2·1)

$$\mathcal{E}_y = + \frac{E_y}{\frac{k}{e} \cdot \frac{\partial T}{\partial x}} = - \frac{Q_i H_z}{\frac{k}{e}} \qquad (10\cdot4)$$

The variations with temperature of the Nernst coefficient for the various specimens (Figures 17, 21 and 22) are very similar to the results obtained by Bashirov for $(-\mathcal{E}_y)$ against temperature.

Bashirov, assuming non-degeneracy of the carriers, finds that over the temperature range $100^{\circ} \longrightarrow 600^{\circ}K$ acoustical mode lattice scattering is the predominate scattering mechanism. For some specimens, at low temperatures, there is indication of ionized impurity scattering. These results are in agreement with the conclusions already reached in this section. From the temperature dependence of $\mathcal{E}_y$ in the n-type specimens Bashirov found $\mu_n \propto T^{-2\cdot3}$ and his results indicate that μ_p varies less rapidly with temperature.

If the degeneracy is taken into account, for a single type of carrier and acoustical mode lattice scattering (Appendix V):

$$\log \left[\frac{Q_i \cdot F_o^2}{F_1 F_{-\frac{1}{2}} - \frac{3}{2} F_{\frac{1}{2}} F_o} \right] = c_o \log T + \text{const.} \qquad (10\cdot5)$$

where the mobility in the absence of degeneracy μ_o is proportional to T^{c_o}. Using values of η^* deduced from the thermo-

electric power assuming $r = -\frac{1}{2}$ (§ 6·2) and the experimental values of Q obtained with the magnetic field perpendicular to the cleavage planes (the isothermal coefficient was used for R9), values of $\frac{Q F_o^2}{F_1 F_{-\frac{1}{2}} - \frac{3}{2} F_{\frac{1}{2}} F_o}$ were calculated over the temperature range for which Q is negative for specimens R3·21, R5, R8 and R9. These are shown on log - log plots in Figure 45, the slopes giving values of c_o. For the n-type specimens R3·21 and R9, in R3·21 $c_o = -2·29$ and in R9 $c_o = -2·08$, giving $\mu_n \propto T^{-2·2}$, while for the p-type specimens R5 and R8, in R5 $c_o = -1·15$ and in R8 $c_o = -1·23$, giving $\mu_p \propto T^{-1·2}$. These results are in fair agreement with those obtained by Bashirov in spite of the different type of specimens and the different assumptions made in the analysis.

The calculations were repeated for specimens R5, R8 and R9 using values of the Nernst coefficient obtained with the magnetic field parallel to the cleavage planes. The variations of $\log \left[\frac{Q F_o^2}{F_1 F_{-\frac{1}{2}} - \frac{3}{2} F_{\frac{1}{2}} F_o} \right]$ with log T are shown in Figure 46, and for all three specimens $\mu \propto T^{-1·6}$.

The temperature variation of mobility obtained from Q_i with the magnetic field perpendicular to the cleavage planes should correspond to the temperature variation of mobility obtained from conductivity measurements with current flow parallel to the cleavage planes (Appendix III). Reference to Table 6·1 shows that from conductivity measurements a more rapid

variation with temperature was obtained for the hole mobility than for the electron mobility. A knowledge of the anisotropy factors associated with the Nernst effect might explain the differences found in the temperature variations of the electron and hole mobilities from electrical conductivity and from Nernst effect measurements.

As with the thermoelectric power (§ 6·9), phonon-drag may affect the value of the low temperature Nernst coefficient. However, since there is no indication of phonon-drag effects in the thermoelectric power, it is unlikely that phonon-drag has any appreciable effect on the Nernst coefficient of Bi_2Te_3 over the temperature range studied.

The value of the minority carrier concentration as a percentage of the total number of carriers per unit volume was calculated for each specimen at the temperature for which the Nernst coefficient is zero. At this temperature (cf. Putley, 1955):

$$n^2\mu_n^3 + p^2\mu_p^3 = np\mu_n\mu_p(\mu_n + \mu_p)(7 + \frac{2E_g}{kT}) \qquad (10·6)$$

Putting $x = \frac{n}{p}$ and $b = \frac{\mu_n}{\mu_p} = 1$ in equation (10·6)

$$x^2 - 2(7 + \frac{2E_g}{kT})x + 1 = 0 \qquad (10·7)$$

Values of the energy gap, E_g, given by Austin (1958) (§ 6·3) were assumed and equation (10·7) solved for x. Then for n-type specimens a value of $(\frac{p}{n + p})$ and for p-type specimens a value of $(\frac{n}{n + p})$ was calculated. These values are shown in Table 6·7.

Also shown are the same quantities calculated from electrical conductivity measurements at the temperature when Q = 0. Writing the electrical conductivity as $\sigma = \sigma_i + \sigma_s$ where σ_i and σ_s are the contributions due to intrinsic and extrinsic carriers respectively, the ratio of the number of minority carriers to the total number of carriers is given by the expression $\frac{\sigma_i}{2\sigma}$, assuming that $b = \frac{\mu_n}{\mu_p} = 1$.

Table 6·7. Concentration of minority carriers at temperature that Q = 0.

Specimen	$T^{o}K$ (Q = 0)	E_g (e.v)	$(\frac{n}{n+p})$ or $(\frac{p}{n+p})$%	$(\frac{\sigma_i}{2\sigma})$%
R3·21	306	0·1294	2·9	1·5
R5	344	0·1258	3·4	0·7
R8	274	0·1324	2·9	0·6
R9	266	0·1332	2·6	13·3

By use of equation (10·7) it appears that the Nernst coefficient changes from negative to positive when the concentration of minority carriers is about 3% of the total concentration of carriers. From his results Bashirov obtains a figure of 5% for n-type specimens. From the electrical conductivity measurements the percentage of minority carriers corresponding to the zero of the Nernst coefficient appears to be less than 1·5%, except for specimen R9.

Measurements on specimen R9 show other features which do not appear to agree with measurements on the other specimens. The value of c_o in $\mu_n \propto T^{c_o}$ does not agree with the value for the other two n-type specimens and the value of E_o for this specimen is lower than for the other specimens (Table 6·1). The variation of $Q_{H\perp r}/Q_{H\parallel e}$ with temperature is not the same for R9 as for the other specimens. The reason for the differences between measurements on specimen R9 and on the other specimens is not known.

Comparison of the temperature variations of the thermoelectric power and Nernst coefficient for a given specimen is of interest. It is found that the temperature at which the thermoelectric power is a maximum (Table 6·6) is approximately the same as that for which the Nernst coefficient is zero (Table 6·7). In addition, the temperature for which the Nernst coefficient is a maximum coincides approximately with the point of inflexion of the thermoelectric power. This would suggest a simple relation between Q and $\frac{d^2E}{dT^2}$. Moreau proposed a relation between the Nernst coefficient Q, the Thomson coefficient σ_T, the Hall coefficient R and the electrical conductivity σ as follows:

$$Q = -\sigma_T R \sigma = -T\frac{d^2E}{dT^2} R\sigma \qquad (10·8)$$

since $\sigma_T = T\frac{d^2E}{dT^2}$ (cf. Bridgman, 1924).

In Table 6·8 are compared the values of the Nernst coefficient Q_o, calculated from equation (10·8), with the experimental, quasi-adiabatic values Q_E for the magnetic field perpendicular to the cleavage planes. It is seen that over a wide variation of Q_E the ratio $\frac{Q_E}{Q_o}$ is constant. The actual value of the constand depends on the measurements of the absolute values of the various properties and the cumulative error will be large. However, there is an indication that the constant increases with increasing iodine content (cf. Table 6·2). The relation is not obeyed in the intrinsic region and it is seen (Table 6·9) that, for specimen R9, no improvement is obtained by use of the isothermal coefficients. The reason for this may be the contribution which the transport of ionization energy, due to ambipolar diffusion of electrons and holes, makes to the intrinsic Nernst coefficient (§ 6·9).

Table 6.8 Test for validity of Moreau relation - using experimental quasi-adiabatic values of the Nernst coefficient.

Specimen	R3.21			R5			R7			R8			R9		
T (°K)	Q_o	Q_E	Q_E/Q_o	Q_o	Q_E	Q_E/Q_o	Q_o	Q_E	Q_E/Q_o	Q_o	Q_E	Q_E/Q_o	Q_o	Q_E	Q_E/Q_o
120	-0.281	-0.169	0.60	-0.096	-0.056	0.58	-0.016	-0.014	0.88	-0.228	-0.090	0.39	-0.324	-0.133	0.41
160	-0.189	-0.110	0.58	-0.070	-0.049	0.70	-0.016	-0.015	0.94	-0.202	-0.071	0.35	-0.154	-0.088	0.57
240	-0.073	-0.040	0.55	-0.052	-0.033	0.63	-0.017	-0.017	1.00	-0.124	-0.029	0.23	≃ 0	-0.021	-
320				-0.017	-0.010	0.59	-0.017	-0.020	1.17	+0.166	+0.055	0.33	+0.090	+0.048	0.53
400	+0.038	+0.040	1.05	+0.030	+0.021	0.70	-0.016	-0.022	1.37	+0.036	+0.065	1.80	+0.019	+0.047	2.42
480	+0.015	+0.033	2.2	+0.016	+0.028	1.7	-0.003	-0.010	3.3	0	+0.038	-	-	-	-

Table 6.9. Test for validity of Moreau relation - using isothermal Nernst coefficient.

T	Q_o	Q_i	Q_i/Q_o
120	-0.324	- 0.174	0.54
160	-0.154	- 0.119	0.77
200	-0.078	- 0.077	0.98
240	~ 0	- 0.035	-
280	+0.054	+ 0.020	0.37
320	+0.090	+ 0.070	0.78
360	+0.043	+ 0.089	2.06
400	+0.019	+ 0.090	4.61
440	+0.009	+ 0.077	8.06

Conclusion.

Observations of the electrical conductivity, thermoelectric power, Hall and Nernst coefficients of Bi_2Te_3 are in general agreement with existing semiconductor theory. However, lack of knowledge about the basic parameters in Bi_2Te_3 makes the interpretation of the results, even in the extrinsic region, uncertain. Anisotropy, a transition from degenerate to non-degenerate statistics and an anomalous temperature variation of the Hall coefficient must be taken into account in the extrinsic region.

It is shown that over the temperature range $100^{\circ} \rightarrow 600^{\circ}K$ the results are most consistent with the predominant scattering of carriers being due to acoustical mode lattice vibrations. Optical mode scattering is considered but is thought to be unimportant. At low temperatures ionized impurity scattering becomes important in some specimens. It is thought that the impurity levels form impurity bands overlapping the top of the valence band and the bottom of the conduction band, which would mean that impurity atoms are always ionized and there is no neutral impurity scattering. It is shown that electron-hole scattering in the mixed conduction region can be neglected, if the many assumptions made are valid. The numerous uncertainties in the calculations of electron-hole and ionized impurity mobilities are emphasized.

From analysis of the thermoelectric power and electrical conductivity in the extrinsic region, assuming a constant concentration of carriers and taking partial degeneracy into account, the temperature dependence of mobility is found to be $T^{-1.63}$ for electrons and $T^{-1.94}$ for holes. Possible reasons for the deviations from the theoretical $T^{-1.5}$ law for a non-degenerate semiconductor and acoustical mode lattice scattering are discussed. Lack of data prevents any conclusions being reached, although overlapping of the impurity bands with the conduction and valence bands could produce warping of the band edges consistent with the observed temperature variations of mobility for electrons and holes.

In the high temperature range the conductivity measurements yield a value of the energy gap at $0^{\circ}K$ of (0.21 ± 0.02) ev. An attempt is made to relate the 20% scatter obtained between values of the energy gap at $0^{\circ}K$ for different specimens with the impurity content. The most probable reason for the discrepancies between the results obtained from electrical conductivity measurements and the values obtained by other authors from optical measurements is a temperature variation of the expansion coefficient of Bi_2Te_3. It is shown that the observed differences do not arise from electrostatic interaction of charge carriers in the mixed conduction region.

The measured Hall and Nernst coefficients and the electrical conductivity exhibit the anisotropy expected from the crystal structure. Measured values of the ratios of

coefficients for different orientations of the current and magnetic field relative to the axis of three-fold symmetry in a specimen were compared with those predicted by Drabble and Wolfe's 'many-valley' model for Bi_2Te_3, and the agreement obtained was satisfactory.

Most of the Hall and Nernst coefficients were obtained under quasi-adiabatic conditions – the extrinsic Hall coefficient showing an anomalous temperature variation. A simple method has been used to obtain the isothermal Hall and Nernst coefficients for Bi_2Te_3 specimens, using probes of the same material as the specimen. It is found that the isothermal coefficient can vary appreciably from the quasi-adiabatic coefficient, but although the Hall coefficient anomaly is decreased by measuring the isothermal coefficients, it is not removed. Measurement of the isothermal Nernst coefficient provides a simple method of obtaining the Ettingshausen coefficient, but an attempt to estimate the Righi-Leduc coefficient shows that this effect does not appear to obey simple semiconductor theory.

Attempts by other workers to explain the anomalous Hall coefficient, the high concentration of extrinsic carriers and the fact that Bi_2Te_3 obtained from a melt of stoichiometric proportions is always p-type have been examined. It is shown that the models of Mooser and Pearson and of Yates are inconsistent with the experimental results. The observed

temperature variation of the Hall coefficient could arise from a linear term, due to spin - orbit coupling, in the expression for either the conduction or valence band edge, but lack of optical data prevents the derivation of the necessary band structure parameters to check this possibility.

The thermoelectric power and Nernst coefficients are shown to be in general agreement with semiconductor theory. The values obtained for the thermoelectric power by the author are higher than those obtained by other workers on specimens of comparable impurity content. The experimental accuracy is discussed and concluded to be satisfactory. It is found that there is no evidence of phonon-drag or exciton effects — and ambipolar diffusion, which is important in the mixed conduction ranges, does not occur in the extrinsic region. Analysis of the Nernst coefficient in the extrinsic region confirms the conclusions already reached on the nature of the scattering mechanisms which are important in Bi_2Te_3. The Nernst coefficient is in general agreement with the other electrical properties and it is shown that, except in the intrinsic region, it obeys a relation which can be derived from Moreau's relation,

$$Q \propto TR\sigma \frac{d^2E}{dT^2}$$

However, without a better knowledge of the basic parameters in Bi_2Te_3, analysis of the Nernst coefficient is extremely uncertain.

Acknowledgements.

The author wishes to record her gratitude to Dr. R. Mansfield who, in his capacity of supervisor of the work for this thesis, has given constant advice and encouragement. In addition she wishes to thank other members of the Physics Department, Bedford College - Dr. L. Pincherle, Dr. B. Donovan and Dr. Nora Hill - for very useful discussions and criticisms of this work. She also wishes to thank Dr. I.R. Williams of the Atomic Energy Authority Isotope School, Wantage, for encouragement in completing the thesis.

The help of the technical staff of the Physics Department, Bedford College is gratefully acknowledged. Very grateful thanks are also given to Mrs. J. Dunn for typing this thesis and for advice in its presentation.

The author is grateful to the General Electrical Company and Associated Electrical Companies for supplying the specimens of Bi_2Te_3 used in this investigation. In addition she wishes to thank members of the Solid State Group of the G.E.C. Research Laboratories, Wembley - Dr. D.A. Wright, Dr. J.R. Drabble and Dr. H.J. Goldsmid - for useful discussions, and in particular Dr. J.R. Drabble for permission to reproduce his diagrams of the Brillouin Zone of Bi_2Te_3 which are presented in Figure 3 (b). Acknowledgement is also made to the G.E.C. Research Laboratories for permission to reproduce the photographs

of the structural model of Bi_2Te_3 presented in Figure 3 (a). These have previously been published in a paper by Dr. D.A. Wright entitled 'Some Physical Properties of Bismuth Telluride' (Proceedings of 1956 Garmisch Conference, Halbleiter und Phosphoren, p. 477, Braunschweig: Vieweg and Sohn, 1958).

This work was aided by a grant from the Research Fund of the University of London, used in the purchase of the electromagnet.

APPENDIX I

Expression for conductivity in the absence of degeneracy

The conductivity σ in the extrinsic region is given for arbitrary degeneracy by equation (1.9). For acoustical mode lattice scattering $r = -\frac{1}{2}$ and $a \propto 1/T^{3/2}$, so that:

$$\sigma = A'F_o \tag{1}$$

where A' is a constant independent of temperature and energy.

In the non-degenerate limit $\eta^* \to -\infty$

$$\sigma_o = ne\mu_o = A'e^{\eta^*} \tag{2}$$

and from equation (1.11)

$$n = \frac{4\pi(2m^*kT)^{3/2}}{h^3} \cdot \frac{\sqrt{\pi}\, e^{\eta^*}}{2} \tag{3}$$

Substituting e^{η^*} from (3) into equation (2)

$$A' = \frac{2(2m^*\pi kT)^{3/2}}{h^3} \cdot e\mu_o$$

and from equation (1)

$$\sigma = \frac{2(2m^*\pi kT)^{3/2}}{h^3} \cdot e\mu_o F_o = ne\mu \tag{4}$$

But substituting for n from equation (1.11)

$$\frac{2(2m^*\pi kT)^{3/2}}{h^3} \cdot e\mu_o F_o = \frac{4\pi(2m^*kT)^{3/2}}{h^3} \cdot F_{\frac{1}{2}} \cdot e\mu$$

$$\mu_o = \mu \cdot \frac{2}{\sqrt{\pi}} \frac{F_{\frac{1}{2}}}{F_o}$$

or for constant carrier concentration in the extrinsic region

$$\sigma_o = \sigma \frac{2F_{\frac{1}{2}}}{\sqrt{\pi}F_o}.$$

APPENDIX II

Calculation of np/T^3 in terms of conductivity

The electrical conductivity is given by the expression

$$\sigma = ne\mu_n + pe\mu_p \qquad (1)$$

where n, p, μ_n and μ_p are the concentrations and mobilities of electrons and holes respectively.

For material which is p-type in the extrinsic range

$$n = p - p_s \qquad (2)$$

so that $\sigma = pe(\mu_n + \mu_p) - p_s e\mu_n$

or $$p = \frac{1}{e(\mu_n + \mu_p)} \cdot (\sigma + p_s e\mu_n). \qquad (3)$$

From (2) and (3)

$$np = p.(p - p_s)$$

$$= \frac{1}{e^2(\mu_n + \mu_p)^2} \cdot (\sigma + p_s e\mu_n)\,(\sigma - p_s e\mu_p). \qquad (4)$$

Writing $\sigma_s = p_s e\mu_p$ = the extrapolated extrinsic conductivity

and $$b = \frac{\mu_n}{\mu_p}$$

$$\frac{np}{T^3} = \frac{1}{e^2(\mu_n + \mu_p)^2} \cdot \frac{(\sigma + b\sigma_s)(\sigma - \sigma_s)}{T^3}$$

For material which is n-type in the extrinsic range

$$p = n - n_s$$

must be substituted in equation (1).

Thus $np = n(n - n_s)$

$$= \frac{1}{e^2(\mu_n + \mu_p)^2} \cdot (\sigma + n_s e\mu_p)(\sigma - ne\mu_n).$$

Writing $\sigma_s = n_s e\mu_n, \qquad b = \frac{\mu_n}{\mu_p}$

$$\frac{np}{T^3} = \frac{1}{e^2(\mu_n + \mu_p)^2} \cdot \frac{(\sigma + \frac{\sigma_s}{b})(\sigma - \sigma_s)}{T^3}$$

APPENDIX III

Expression for Ettingshausen Coefficient

Ettingshausen coefficient $P = -\frac{\partial T/\partial y}{H_z J_x}$; $J_y = 0$, $\frac{\partial T}{\partial x} = 0$, $\omega_y = 0$

(Table 2.1)

For a single band model and small magnetic fields, equations (1.2), (1.3) and (1.5) reduce to

$$\frac{3\pi^2\hbar^4}{e} \cdot J_x = i_1' W - i_4' Y - \frac{i_5'}{T} \cdot \frac{\partial T}{\partial y} \qquad (1)$$

$$0 = i_4 W + i_1 Y + \frac{i_2}{T} \cdot \frac{\partial T}{\partial y} \qquad (2)$$

$$0 = i_5 W + i_2 Y + \frac{i_3}{T} \cdot \frac{\partial T}{\partial y} + 3\pi^2\hbar^4 K_L \cdot \frac{\partial T}{\partial y} \qquad (3)$$

where, on substituting for i_n, i_n' refers to the expressions given by (1.6a) and (1.7a) with m^* relevant to the x-direction and i_n to those relevant to the y-direction. This is not a rigorous treatment. For an anisotropic medium the integrals i_n and i_n' in equations (1) $\longrightarrow$ (3) should be given by more complicated expressions than equations (1.6a) and (1.7a). However, the exact forms of i_n and i_n' do not affect the final expression for the Ettingshausen Coefficient (equation 11).

In equation (3) heat flow in the y-direction, due to the thermal conductivity of the lattice (K_L), is included.

From (2) and (3)

$$0 = \left(\frac{i_1}{i_4} - \frac{i_2}{i_5}\right) Y + \left(\frac{i_2}{i_4} - \frac{i_3}{i_5} - \frac{3\pi^2\hbar^4 K_L T}{i_5}\right) \frac{1}{T} \cdot \frac{\partial T}{\partial y}$$

$$\text{and} \quad 0 = \left(\frac{i_4}{i_1} - \frac{i_5}{i_2}\right) W + \left(\frac{i_2}{i_1} - \frac{i_3}{i_2} - \frac{3\pi^2\hbar^4 K_L T}{i_2}\right) \frac{1}{T} \cdot \frac{\partial T}{\partial y}$$

Substituting for W and Y in (1)

$$\frac{3\pi^2\hbar^4}{e}.J_x = -\frac{i_1' i_1 i_2}{(i_4 i_2 - i_5 i_1)}.\left(\frac{i_2}{i_1} - \frac{i_3}{i_2} - \frac{3\pi^2\hbar^4 K_L T}{i_2}\right)\frac{1}{T}.\frac{\partial T}{\partial y}$$

$$+\frac{i_4' i_4 i_5}{(i_1 i_5 - i_2 i_4)}.\left(\frac{i_2}{i_4} - \frac{i_3}{i_5} - \frac{3\pi^2\hbar^4 K_L T}{i_5}\right)\frac{1}{T}.\frac{\partial T}{\partial y} - \frac{i_5'}{T}.\frac{\partial T}{\partial y} \quad (4)$$

Neglecting H^2 and higher powers of H, equation (4) reduces to

$$\frac{3\pi^2\hbar^4}{e}.J_x = \frac{1}{(i_5 i_1 - i_4 i_2)}.\left(i_1' i_2^2 - i_1 i_1' i_3 - 3\pi^2\hbar^4 K_L T i_1 i_1'\right)\frac{1}{T}.\frac{\partial T}{\partial y}$$

$$= -\frac{i_1 i_1'}{(i_5 i_1 - i_4 i_2)}\left[\frac{(i_1 i_3 - i_2^2)}{i_1} + 3\pi^2\hbar^4 K_L T\right]\frac{1}{T}.\frac{\partial T}{\partial y} \quad (5)$$

Thermal conductivity $K_y = -\frac{\omega_y}{\partial T/\partial y}$; $J_x = J_y = 0$, $\frac{\partial T}{\partial x} = 0$, $H_z = 0$.

(cf. Table 2.1)

From equations (1.3) and (1.5) the electronic component K_e of the thermal conductivity for heat flow in the y-direction is given by

$$K_e = \frac{1}{3\pi^2\hbar^4}.\frac{1}{T}.\left(\frac{i_3 i_1 - i_2^2}{i_1}\right)$$

Substitution in equation (5) gives

$$\frac{J_x}{e} = -\frac{i_1 i_1'}{(i_5 i_1 - i_4 i_2)}.(K_e + K_L)\frac{\partial T}{\partial y}$$

Both K_e and K_L refer to heat flow in the y-direction.

Total thermal conductivity $K_y = K_e + K_L$.

So
$$P = -\frac{\partial T/\partial y}{H_z J_x} = \frac{(i_5 i_1 - i_4 i_2)}{i_1 i_1'}.\frac{1}{eK_y H_z} \quad (6)$$

Nernst coefficient $Q = -\frac{E_y}{H_z \frac{\partial T}{\partial x}}$; $J_x = J_y = 0$, $\frac{\partial T}{\partial y} = 0$, (Table 2.1)

Substituting in equations (1.2) and (1.3)

$$0 = i_1' W + \frac{i_2'}{T}\frac{\partial T}{\partial x} - i_4' eE_y \tag{7}$$

$$0 = i_4 W + \frac{i_5}{T}\frac{\partial T}{\partial x} + i_1 eE_y \tag{8}$$

and from equations (7) and (8), for small magnetic fields

$$eE_y = \frac{i_2' i_4 - i_1' i_5}{i_1 i_1'} \cdot \frac{1}{T} \cdot \frac{\partial T}{\partial x}$$

$$Q = -\frac{E_y}{H_z \frac{\partial T}{\partial x}} = \frac{i_1' i_5 - i_2' i_4}{i_1 i_1'} \cdot \frac{1}{eH_z . T} \tag{9}$$

From equations (6) and (9)

$$P = \frac{Q_i T}{K_y}\left(\frac{i_5 i_1 - i_4 i_2}{i_5 i_1' - i_4 i_2'}\right) \tag{10}$$

If the x- and y-directions are equivalent, equation (10) reduces to

$$P = \frac{Q_i T}{K_y} \tag{11}$$

APPENDIX IV

Determination of the Hall Coefficient from conductivity data

The expression for the Hall coefficient, for mixed conduction, assuming a two band model, is given by:

$$R = -\frac{D}{e}\cdot\frac{(n\mu_n^2 - p\mu_p^2)}{(n\mu_n + p\mu_p)^2} \qquad (1)$$

where D is given by equation (1.9) and all the quantities are in practical units.

For material which is n-type in the extrinsic region

$$p = n - n_s \qquad (2)$$

where n_s, the concentration of carriers in the extrinsic region, is assumed constant.

Electrical conductivity, $\sigma = e(n\mu_n + p\mu_p)$ (3)

Substitution from equations (2) and (3) in (1) gives

$$R = -\frac{De}{\sigma^2}(n(\mu_n^2 - \mu_p^2) + n_s\mu_p^2)$$

$$= -\frac{De}{\sigma^2}\left[(\mu_n - \mu_p)(n\mu_n + p\mu_p + n_s\mu_p) + n_s\mu_p^2\right]$$

and by substituting $b = \mu_n/\mu_p$; and $\sigma_s = n_s e\mu_n$

$$R = -\frac{D}{n_s e\,\sigma^2 b^2}\left[\sigma_s(b-1)(b\sigma + \sigma_s) + \sigma_s^2\right]$$

Since the Hall coefficient in the extrinsic region R_s is given by

$$R_s = -\frac{D}{n_s e}$$

APPENDIX V

Variation of the Nernst coefficient assuming conduction by the theoretical value of the Hall coefficient R_{th}, derived from conductivity data, is given by

$$R_{th} = \frac{R_s}{\sigma^2 b^2}\left[\sigma_s(b-1)(b\sigma+\sigma_s)+\sigma_s^2\right]$$

and, when b = 1,

$$R_{th} = R_s.\left(\frac{\sigma_s}{\sigma}\right)^2.$$

APPENDIX V

Variation of the Nernst coefficient assuming conduction by one type of carrier only

For acoustical mode lattice scattering ($r = -\frac{1}{2}$) the expression for the isothermal Nernst coefficient given by equation (1.9) reduces to

$$Q_i = - \frac{3h^3 \sigma}{8(2m^*)^{3/2} e^2 \pi c T (kT)^{\frac{1}{2}}} \cdot \frac{(F_1 F_{-\frac{1}{2}} - (3/2) F_{\frac{1}{2}} F_0)}{F_0^3} \qquad (1)$$

where F_m is defined in equation (1.10).

But for one type of carrier only

$$\sigma = ne\mu \qquad (2)$$

where the number of free carriers, n, per unit volume is defined by equation (1.11) and μ is the mobility.

From Appendix I, the mobility in the absence of degeneracy μ_o is given by

$$\mu = \mu_o \frac{\sqrt{\pi}}{2} \cdot \frac{F_0}{F_{\frac{1}{2}}} \qquad (3)$$

Substitution in equation (1) for σ, given by equation (2), and then the values of 'n' and μ, given by equations (1.11) and (3) respectively, yields

$$Q_i = - \frac{3\sqrt{\pi}}{4c} \cdot \frac{k}{e} \mu_o \cdot \frac{(F_1 F_{-\frac{1}{2}} - (3/2) F_{\frac{1}{2}} F_0)}{F_0^2} \qquad (4)$$

But $\mu_o \propto T^{+C_o}$ (equation 2.10)

which gives $\log \left[\frac{Q F_0^2}{F_1 F_{-\frac{1}{2}} - (3/2) F_{\frac{1}{2}} F_0} \right] = C_o \log T + \text{const.}$

References.

Ainsworth, L. (1956) Proc. Phys. Soc. 69B, 606.

American Institute of Physics Handbook (1957) McGraw Hill.

Austin, I.G. (1958) Proc. Phys. Soc. 72, 545.

(1959) J. Electronics and Control 6, 271.

Austin, I.G. and McClymont, D.R. (1954) Physica 20, 1077.

Austin, I.G. and Sheard, A.R. (1957) J. Electronics and Control 3, 236.

Bardeen, J. (1959) J. Phys. Chem. Solids 8, 2.

Bashirov, R.I. (1958) Sov. Phys. Tech. Phys. 3, 917.

Bashirov, R.I. and Tsidil'kovskiĭ, I.M. (1956) Zh. tekh. Fiz. 26, 2195.

Beer, A.C., Chase, M.N. and Choquard, P.F. (1955) Hel. Phys. Act. 28, 529.

Benel, M.H. (1958) C.R. Acad. Sci. (Paris) 247, 584.

Black, J., Conwell, E.M., Seigle, L. and Spencer, C.W. (1957) J. Phys. Chem. Solids 2, 240.

Blatt, F.J. (1957) Solid State Physics, Vol. 4 (Academic Press, New York) p. 199.

Blount, E., Callaway, J., Cohen, M., Dumke, W. and Phillips, J. (1956) Phys. Rev. 101, 563.

Bowley, A.E., Delves, R. and Goldsmid, H.J. (1958) Proc. Phys. Soc. 72, 401.

Bridgman, P.W. (1924) Phys. Rev. 24, 644.

Busch, G.A. (1958) Nuovo Cimento, Suppl. 7, 696.

Carlson, R.O. (1955) Phys. Rev. 100, 1075.

Chambers, R.G. (1952) Proc. Phys. Soc. A 65, 903.

Conwell, E.M. (1956) Phys. Rev. 103, 51.

Debye, P.P. and Conwell, E.M. (1954) Phys. Rev. 93, 693.

Drabble, J.R. (1958) Proc. Phys. Soc. 72, 380.

(1959) J. Phys. Chem. Solids 8, 428.

Drabble, J.R. and Goodman, C.H.L. (1958) J. Phys. Chem. Solids 5, 142.

Drabble, J.R., Groves, R.D. and Wolfe, R. (1958) Proc. Phys. Soc. 71, 430.

Drabble, J.R. and Wolfe, R. (1956) Proc. Phys. Soc. 69, 1101.

Dunlap, W.C. (1950) Phys. Rev. 79, 286.

Ehrenberg, W. (1958) Electron conduction in semiconductors and metals (Oxford University Press).

Ehrenreich, H. (1957) J. Phys. Chem. Solids 2, 131.

Elliott, R.J. (1954) Phys. Rev. 96, 266.

Enz, Ch. (1954) Physica 20, 983.

Erginsoy, C. (1950) Phys. Rev. 79, 1013.

Fan, H.Y. (1955) Solid State Physics, Vol. 1 (Academic Press, New York) p. 283.

(1958) Nuovo Cimento, Suppl. 7, 661.

Farkas, A. and Melville, H.W. (1939) Experimental methods in gas reactions (Macmillan, London).

Fieschi, R. (1955) Nuovo Cimento, Suppl. (Ser. 10) 1, 1.

Francombe, M.H. (1958) Brit. J. Appl. Phys. 9, 415.

Fritzsche, H. (1955) Phys. Rev. 99, 406.

Fritzsche, H. and Lark-Horovitz, K. (1954) Physica 20, 834.

Fröhlich, H. and Kittel, C. (1954) Physica 20, 1086.

Fukuroi, T., Tanuma, S. and Tobisawa, S. (1950) Sci. Rep. RITU 2, 239.

Fuschillo, N., Bierly, J.N. and Donahoe, F.J. (1959) J. Phys. Chem. Solids 8, 430.

Geballe, T.H., Herring, C. and Kunzler, J.E. (1959) J. Phys. Chem. Solids 8, 347.

Gerlach, W. (1928) Handb. d. Phys. 13, 228 (Berlin: Springer).

Goldsmid, H.J. (1956a) Proc. Phys. Soc. B 69, 203.

(1956b) Report of Rugby Conference on Semiconductors (London Physical Society) p.127.

(1957) Ph.D. Thesis. University of London.

(1958a) Proc. Phys. Soc. 71, 633.

(1958b) Proc. Phys. Soc. 72, 17.

Goldsmid, H.J. and Douglas, R.W. (1954) Brit. J. Appl. Phys. 5, 386.

Goldsmid, H.J., Sheard, A.R. and Wright, D.A. (1958) Brit. J. Appl. Phys. 9, 365.

Gordiakova, G.N., Kokosh, G.V. and Sinani, S.S. (1958) Sov. Phys.-Tech. Phys. 3, 1.

Gordiakova, G.N. and Sinani, S.S. (1958) Sov. Phys.-Tech. Phys. 3, 908.

Harman, T.C., Paris, B., Miller, S.E. and Goering, H.L. (1957) J. Phys. Chem. Solids 2, 181.

Herman, F. (1955) Proc. I.R.E. 43, 1703.

Herring, C. (1954) Phys. Rev. 96, 1163.

Horne, R.A. (1959) J. Appl. Phys. 30, 393.

Howarth, D.J. and Sondheimer, E.H. (1953) Proc. Roy. Soc. A 219, 53.

Hung, C.S. and Gliessman, J.R. (1954) Phys. Rev. 96, 1226.

Isenberg, I., Russell, B.R. and Greene, R.F. (1948) Phys. Rev. 74, 1255 (A).

Jan, J.P. (1957) Solid State Physics, Vol. 5 (Academic Press, New York) p. 1.

Joffé, A.F. (1956) Can. J. Phys. 34, 1342.

(1957) Semiconductor thermoelements and thermoelectric cooling (Infosearch, London).

(1959) J. Phys. Chem. Solids 8, 6.

Johnson, V.A. (1956) Progress in semiconductors (Heywood, London) Vol. 1, p. 63.

Johnson, V.A. and Shipley, F.M. (1953) Phys. Rev. 90, 523.

Kanai, Y. and Nii, R. (1959) J. Phys. Chem. Solids 8, 338.

Kane, E.O. (1957) J. Phys. Chem. Solids 1, 249.

Konorov, P.P. (1956) Sov. Phys.-Tech. Phys. 1, 1371.

Kontorova, T.A. (1956) Sov. Phys.-Tech. Phys. 1, 646.

Kröger, F.A. and Vink, H.J. (1954) Physica 20, 950.

Kröger, F.A., Vink, H.J. and van den Boomgaard, J. (1954) Z. Phys. Chem. (B) 203, 1.

Lagrenaudie, J. (1957) J. Phys. Radium 18, 39 (suppl.).

Lange, P.W. (1939) Naturwiss 27, 133.
Lark-Horovitz, K. (1954) The New Electronics. The present state of physics. A.A.A.S. New York
Lemon, H.B. and Ference, M. (1946) Analytical experimental Physics (University of Chicago Press) p. 338.
Longo, T.A., Ray, R.K. and Lark-Horovitz, K. (1959) J. Phys. Chem. Solids 8 259.
Macdonald, D.K.C., Mooser, E. Pearson, W.B., Templeton, I.M. and Woods, S.B. (1959) Phil. Mag. 4, 433.
Macfarlane, G.G. and Roberts, V. (1955) Phys. Rev. 97, 1714.
Mansfield, R. (1956a) Proc. Phys. Soc. 69, 76.
(1956b) Proc. Phys. Soc. 69, 862.
(1957) Proc. Phys. Soc. 70, 240.
(1959) Proc. Phys. Soc. 74, 599.
Mansfield, R. and Williams, W. (1958) Proc. Phys. Soc. 72, 733.
Matossi, F. and Stern F. (1958) Phys. Rev. 111, 472
Matukura, Y. (1957) J. Phys. Soc. Jap. 12, 103.
Matyáš, M. (1958) Czech. Journ. of Physics 8, 309.
Mette, H., Gärtner, W.W. and Loscoe, C. (1959) Phys. Rev. 115, 537.
Middleton, A.E. and Scanlon, W.W. (1953) Phys. Rev. 92, 219.
Mitchell, W.H. (1954) J. Sci. Instrum. 31, 147.
Mooser, E. and Pearson, W.B. (1956) Can. J. Phys. 34, 1369.
(1958) J. Phys. Chem. Solids 7, 65.
Morin, F.J. and Maita, J.P. (1954) Phys. Rev. 94, 1525.
Mott, N.F. and Gurney, R.W. (1948) Electronic processes in ionic crystals (Oxford University Press).
Nii, R. (1958) J. Phys. Soc. Japan 13, 769.

Obraztsov, Y.N. (1955) Zh. tekh. Fiz. 25, 995.

Offergeld, G. and van Cakenberghe, J. (1959) Nature, Suppl. No. 4, 184, 185.

Parrott, J.E. and Penn, A.W. (1958) Associated Electrical Industries Report No. A 773.

Pearson, G.L. and Bardeen, J. (1949) Phys. Rev. 75, 865.

Pikus, G.E. (1956) Zh. tekh. Fiz. 26, 36.

Pincherle, L. and Radcliffe, J.M. (1956) Advances in Physics 5, 271.

Potter, R. (1956) Phys. Rev. 103, 861.

Price, P.J. (1955) Phil. Mag. 46, 1252.

(1956a) Phys. Rev. 102, 1245.

(1956b) Phys. Rev. 104, 1223.

Putley, E.H. (1955) Proc. Phys. Soc. B 68, 35.

Radcliffe, J.M. (1955) Proc. Phys. Soc. 68, 675.

Rhodes, P. (1950) Proc. Roy. Soc. A 204, 396.

Rodot, M. (1958) Journ. Phys. Radium 19, 140.

Rosi, F.D., Abeles, B. and Jensen, R.V. (1959) J. Phys. Chem. Solids 10, 191.

Satterthwaite, C.B. and Ure, R.W. (1957) Phys. Rev. 108, 1164.

Scanlon, W.W. (1953) Phys. Rev. 92, 1573.

Scanlon, W.W. and Brebrick, R.F. (1954) Physica 20, 1090.

Seitz, F. (1948) Phys. Rev. 73, 549.

Shigetomi, S. and Mori, S. (1956) J. Phys. Soc. Jap. 11, 915.

Shilliday, T.S. (1957) J. Appl. Phys. 28, 1035.

Shockley, W. (1950) Electrons and holes in semiconductors (New York).

Skanavi, G.I. and Kashtanova, A.M. (1956) Sov. Phys.-Tech. Phys. 1, 882.

Slater, J.C. (1959) J. Phys. Chem. Solids 8, 21.

Smith, R.A. (1954) Physica 20, 910.

Sodha, M.S. (1958) Progress in Semiconductors (Heywood, London) Vol. 3, p. 153.

Stern, F. (1959) J. Phys. Chem. Solids 8, 277.

Stern, F. and Dixon, J. (1959) J. Appl. Phys. 30, 268.

Stern, F. and Talley, R.M. (1955) Phys. Rev. 100, 1638.

Stil'bans, L. (1959) J. Phys. Chem. Solids 8, 123.

Stil'bans, L.S., Bok, B.I. and Lifshits, E.L. (1956) Dokl. Akad. Nauk. S.S.S.R. 111, 1011.

Vlasova, R.M. and Stil'bans, L.S. (1955) Zh. Tekh, Fiz. 25, 569.

Walker, P.A. (1959) G.E.C. Report No. 904 - submitted for publication.

Welker, H. (1954) Physica 20, 893.

Welker, H. and Weiss, H. (1956) Solid State Physics, Vol. 3 (Academic Press, New York) p. 1.

Williams, W. (1959) Proc. Phys. Soc. 73, 739.

Wilson, A.H. (1953) The theory of metals (Cambridge University Press).

Wold, P.I. (1916) Phys. Rev. 7, 169.

Wright, D.A. (1958) Nature 181, 834.

(1959) Research 12, 300.

Wright, R.W. (1951) Proc. Phys. Soc. A 64, 984.

Wyckoff, R.W.G. (1951) Crystal Structures (Interscience, New York).

Yates, B. (1959) J. Electronics and Control 6, 26.

Figure 1. Specimen orientation referred to a right-handed system of cartesian co-ordinates.

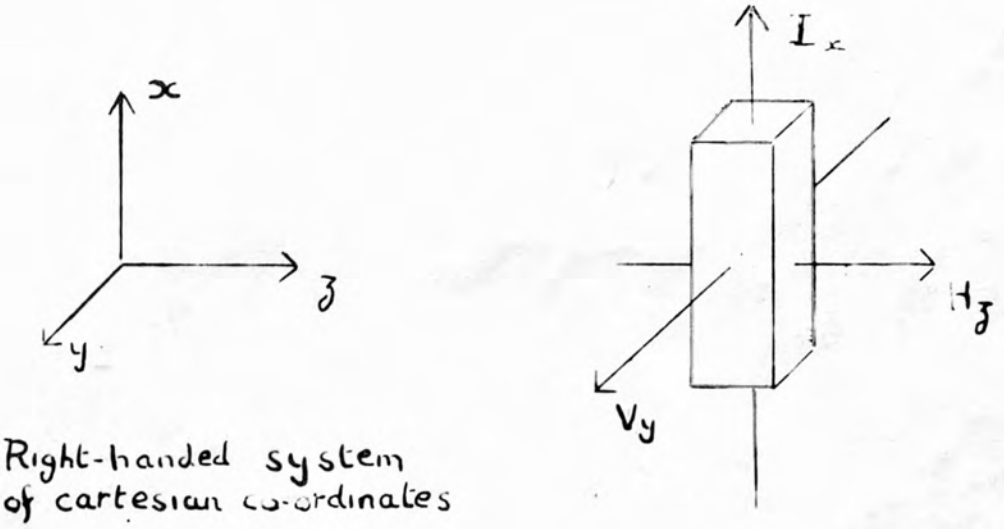

Right-handed system of cartesian co-ordinates

Figure 2. Dimensions of specimen.

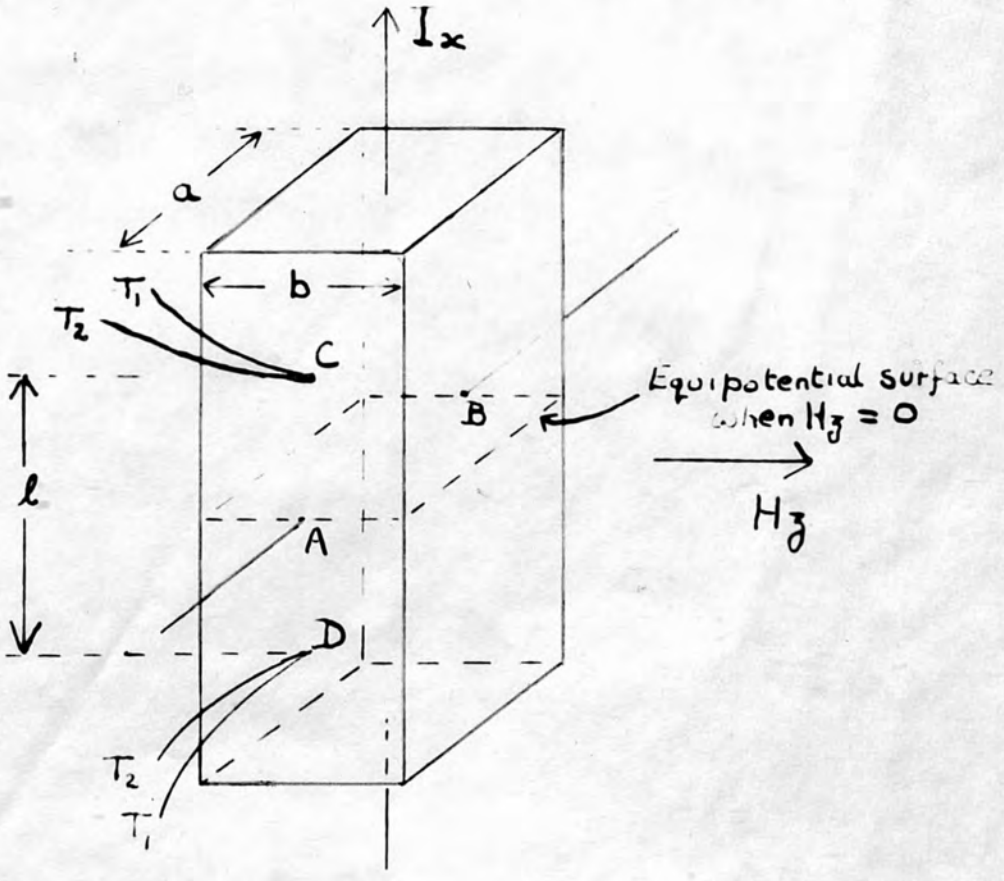

Figure 3(a). Crystal structure of Bi_2Te_3.

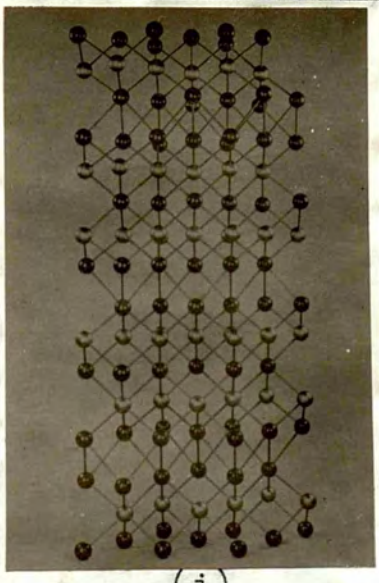

(i)

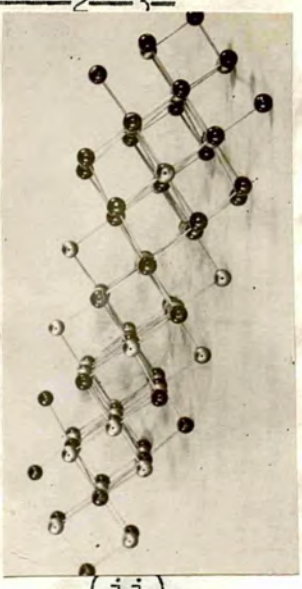

(ii)

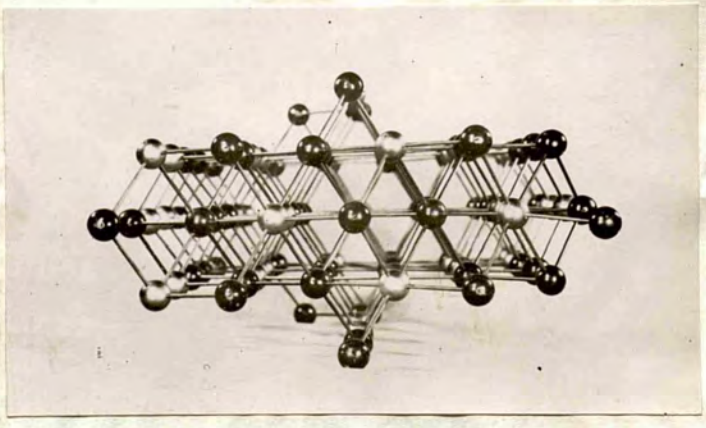

(iii)

The figures show

(i) the layer structure

(ii) the quasi-cubic structure

and (iii) the hexagonal structure around the 'c' axis.

The dark spheres represent tellurium atoms, and the light bismuth.

These photographs were obtained from the Research Laboratories of The General Electric Company Limited, Wembley.

Brillouin Zone. Figure 3(b)

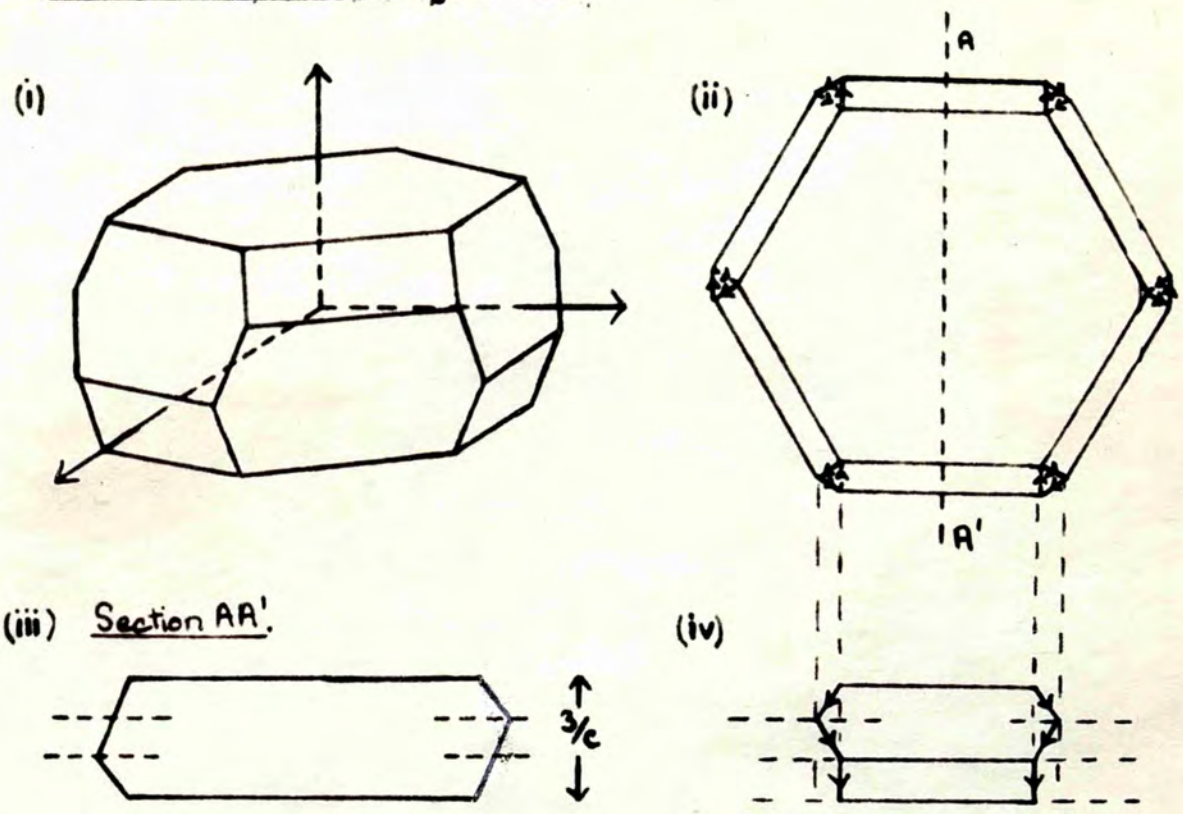

The Brillouin Zone for Bi_2Te_3 is the same as the unit cell of a trigonal lattice.

(i) Symmetrical unit cell for the trigonal lattice (Koster, Solid State Physics Volume 5, page 209). This is not drawn to the correct scale for Bi_2Te_3.

(ii)→(iv) Brillouin Zone of Bi_2Te_3 drawn to scale (Drabble, private communication).

There is six fold inversion symmetry for the system, so that on taking the situation at 60° to AA' the side elevation (iv) and the section (iii) are both inverted.

The height of the zone is 3/c and the hexagonal sides are $\frac{b}{2}\left[\frac{2}{3b^2} - \frac{1}{c^2}\right]$, where $b=a.\sin\frac{\alpha}{2}$, and $c = 3.a.(1 + 2\cos\alpha)^{\frac{1}{2}}$

Rhombohedral parameters; $a=10.48$ Å, $\alpha = 24^\circ 8'$

Hexagonal parameters; $b=4.384$ Å, $c = 30.47$ Å

Figure 4. Specimen holder.

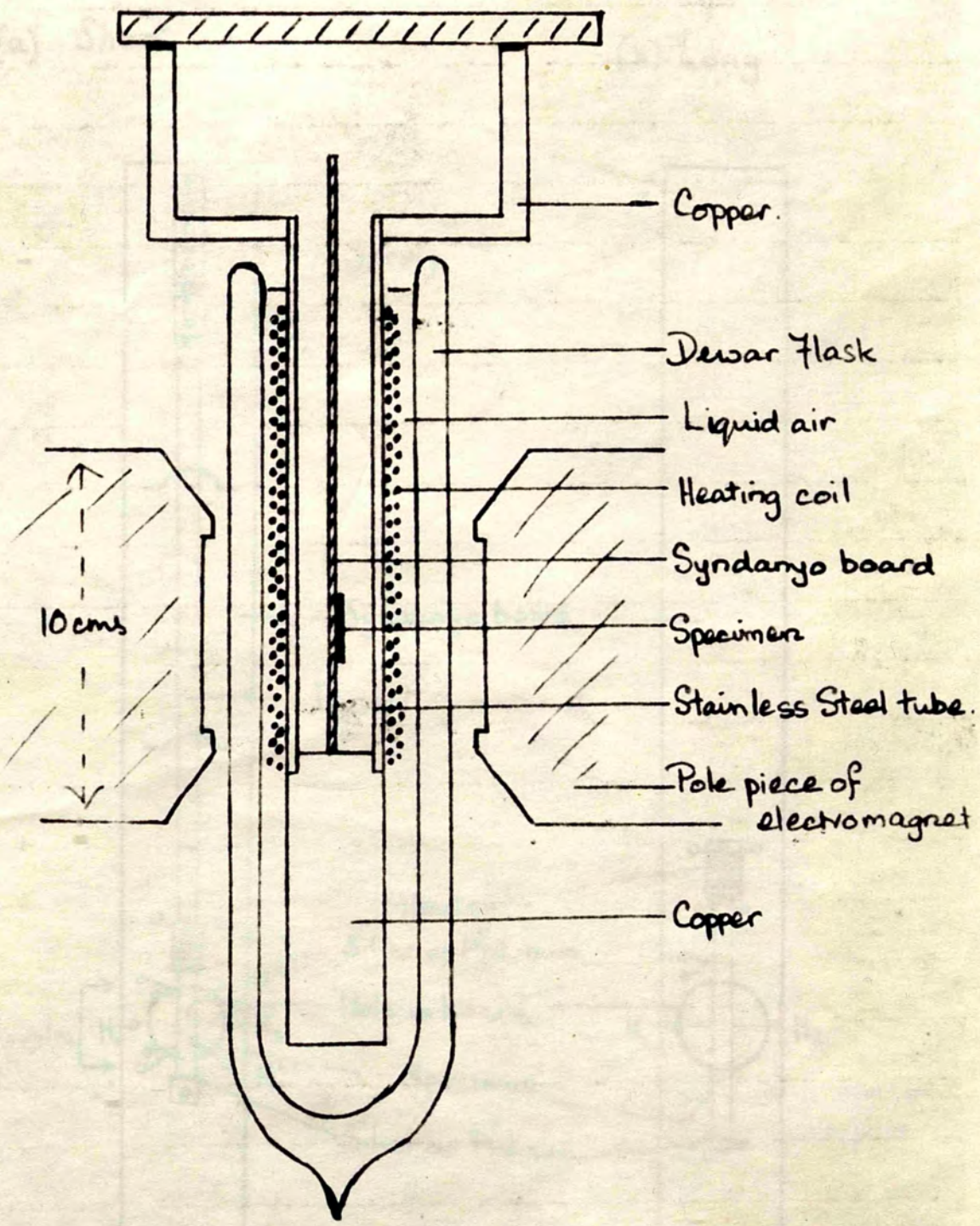

Figure 5. Mounting of Specimens

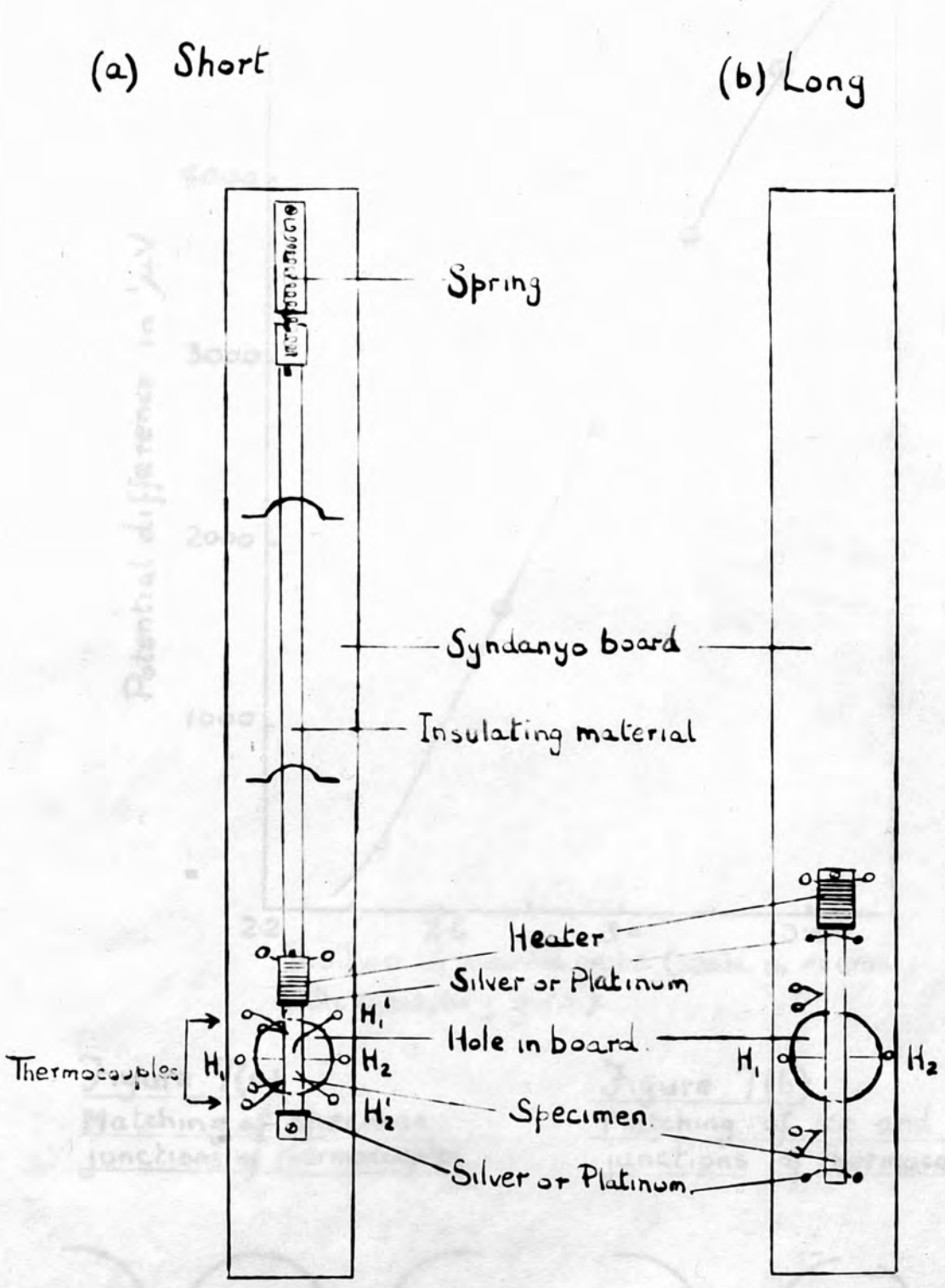

Figure 6. Potential along specimen for constant current (Specimen R 3.21.)

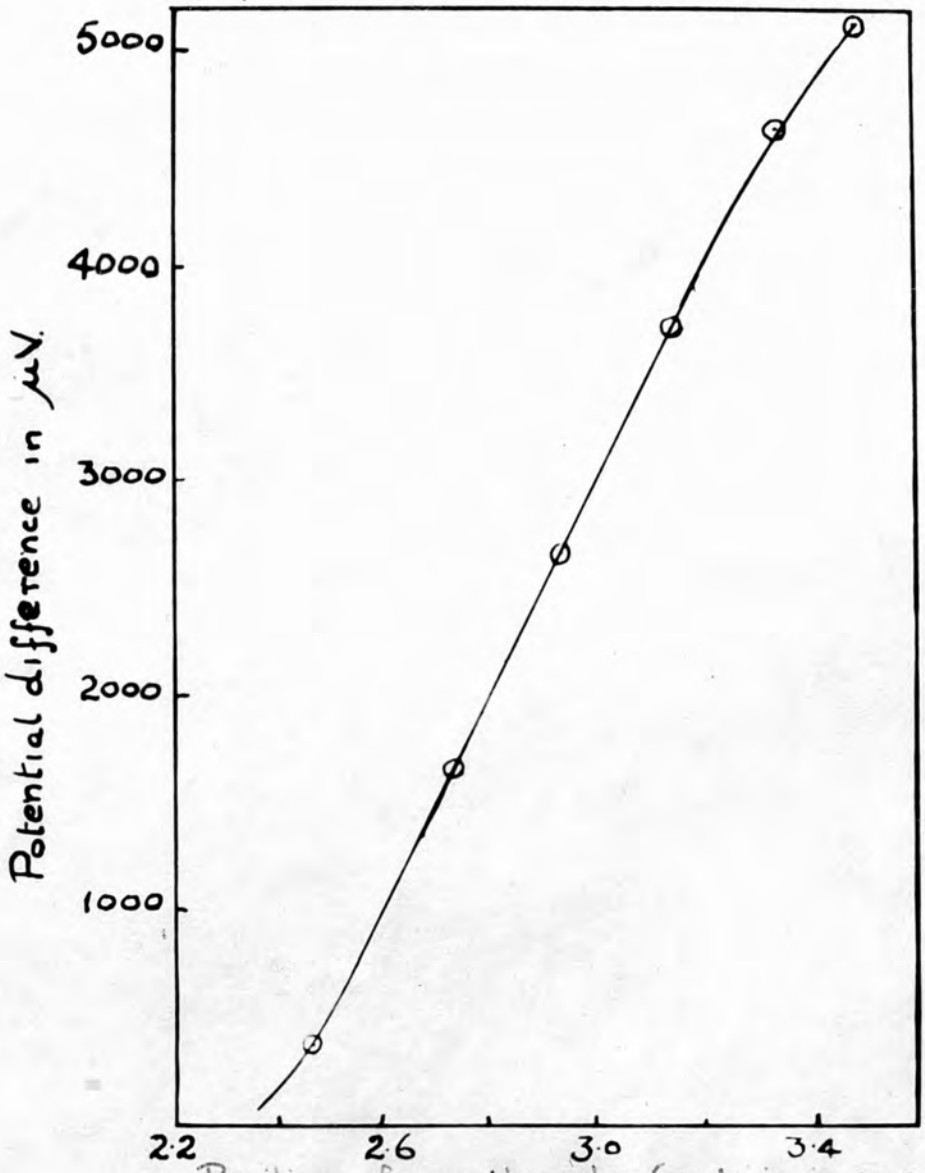

Figure 7(a)
Matching of specimen junctions of thermocouples.

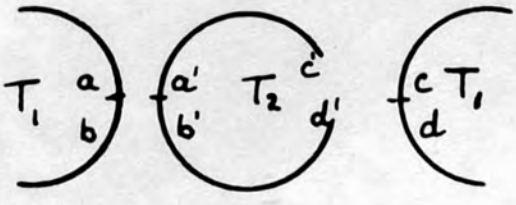

Figure 7(b)
Matching of ice and specimen junctions of thermocouples.

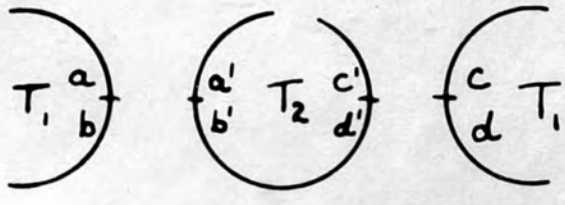

Figure 7(c). Circuit Diagram.

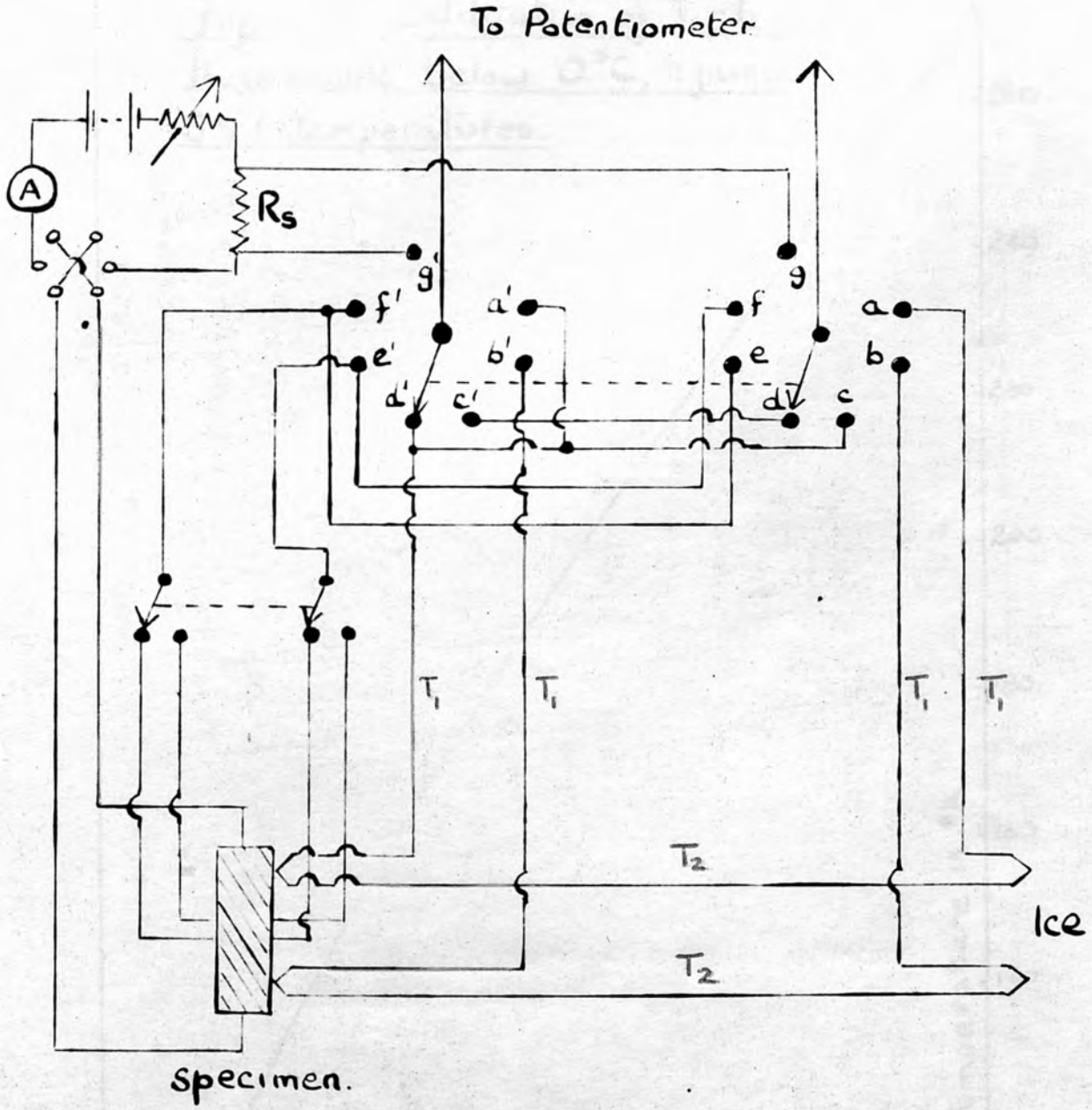

Figure 8. Calibration of $T_1 - T_2$ thermocouple below 0°C, against S.V.P temperatures.

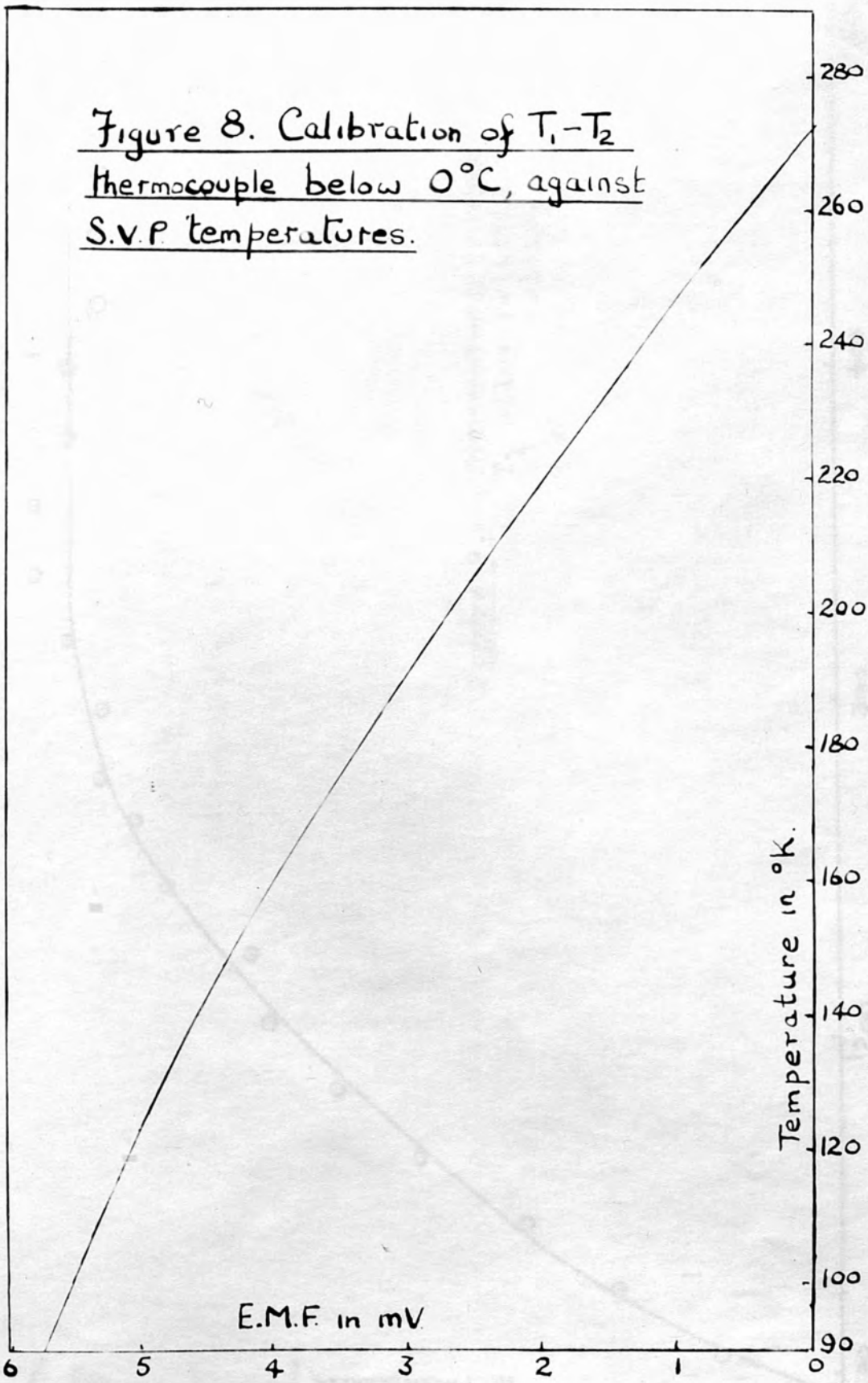

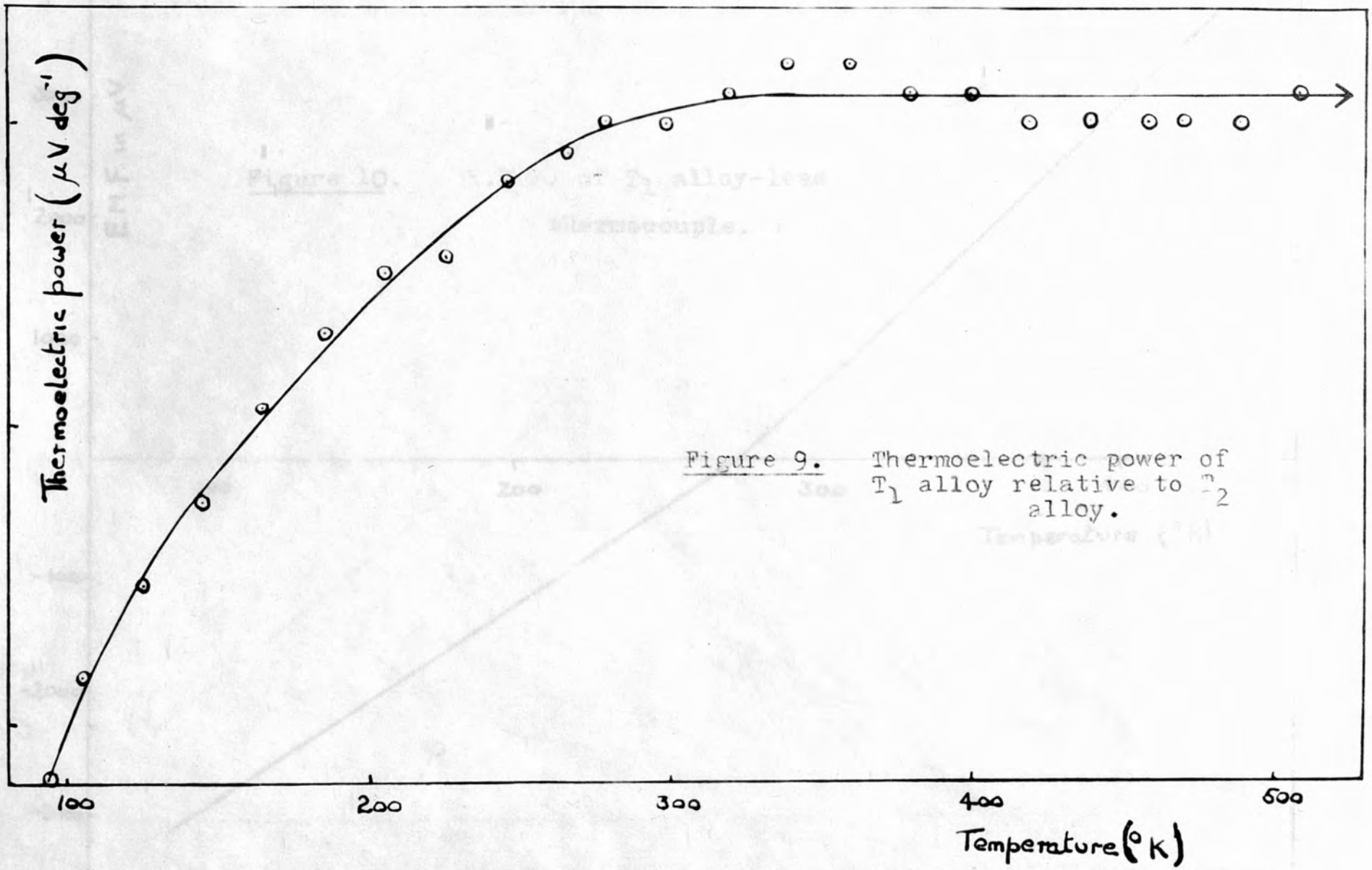

Figure 9. Thermoelectric power of T_1 alloy relative to T_2 alloy.

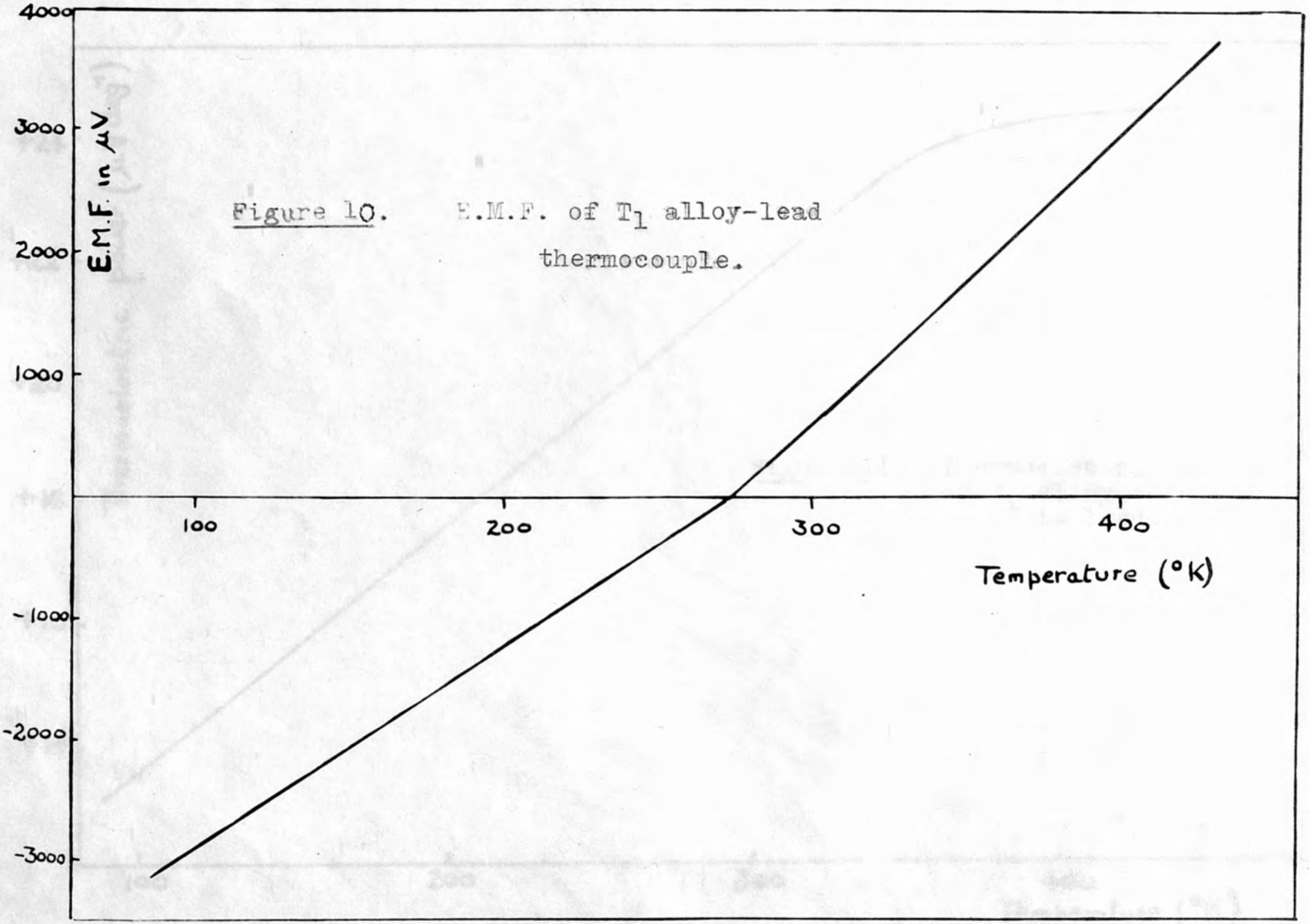

Figure 10. E.M.F. of T_1 alloy-lead thermocouple.

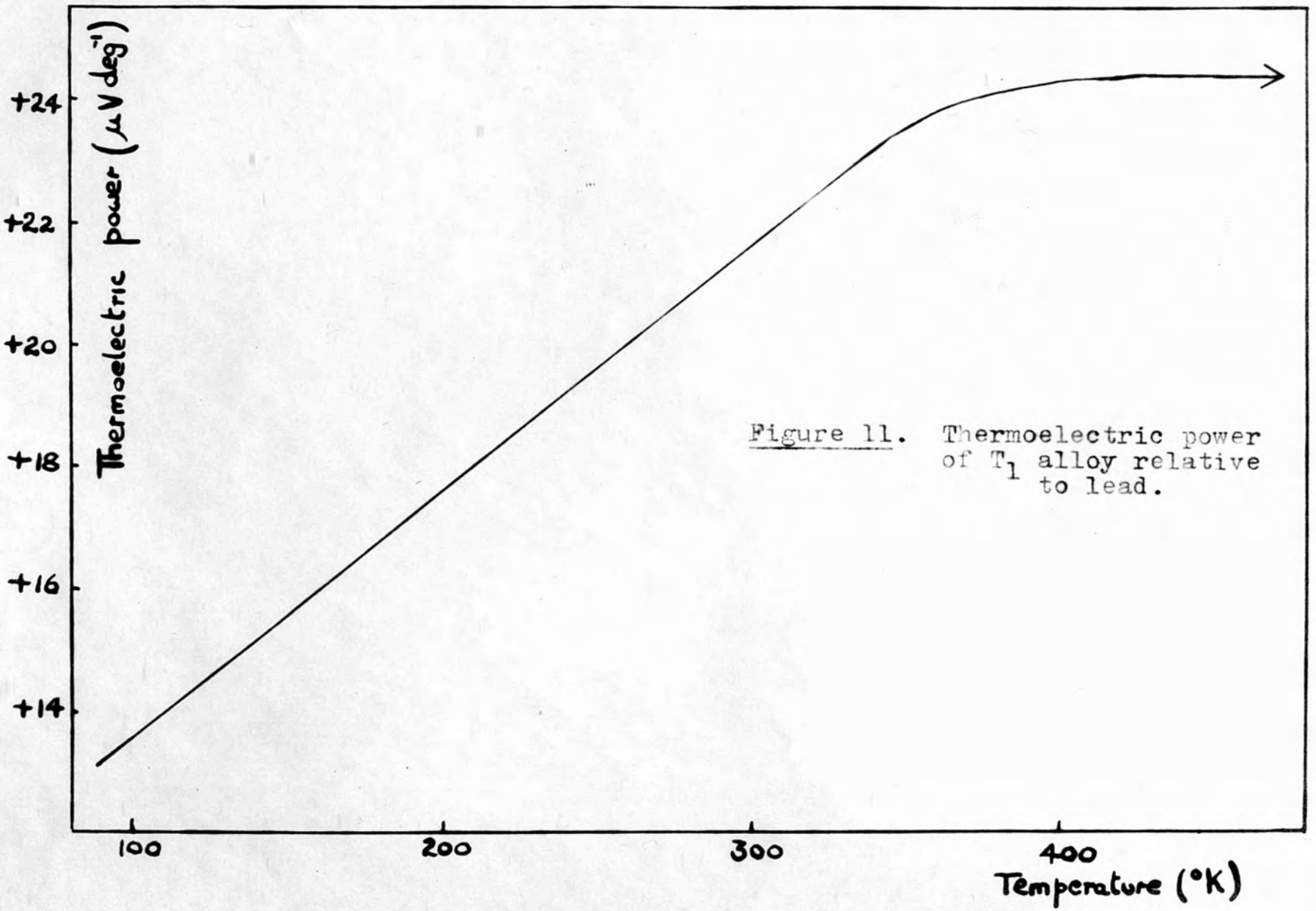

Figure 11. Thermoelectric power of T_1 alloy relative to lead.

Figure 12. Variation of the Hall coefficient of specimen R5 with magnetic field at room temperature.

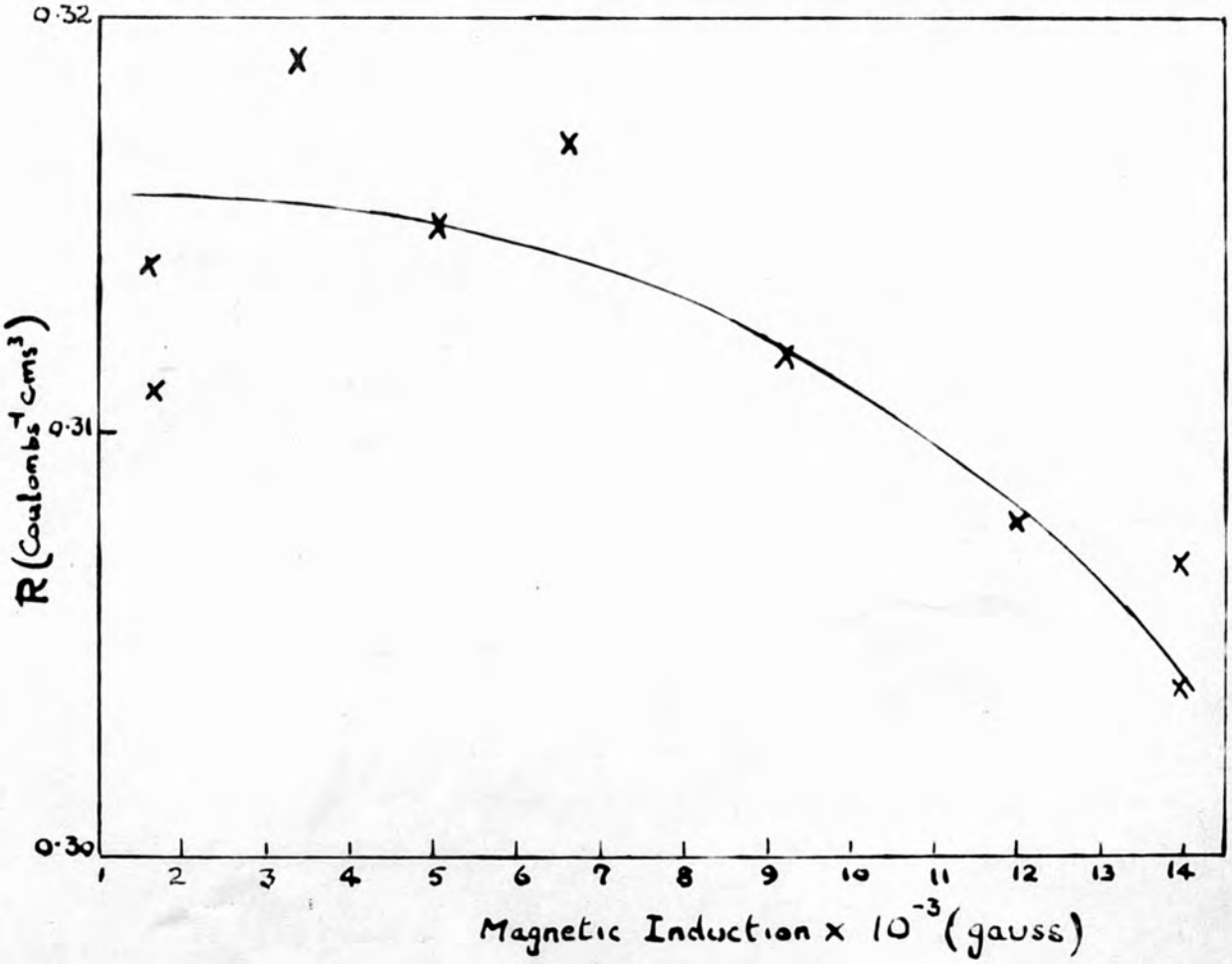

Figure 13. Experimental arrangements.

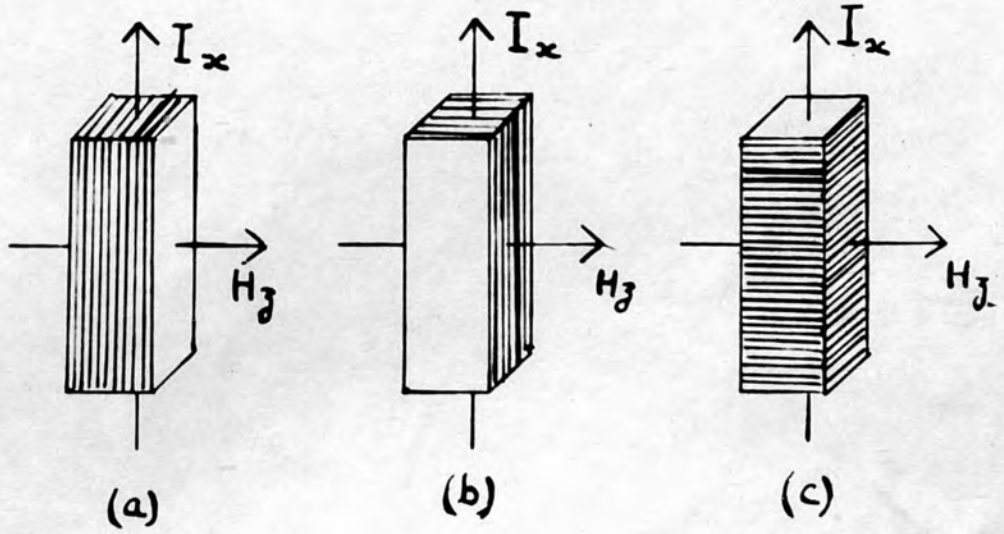

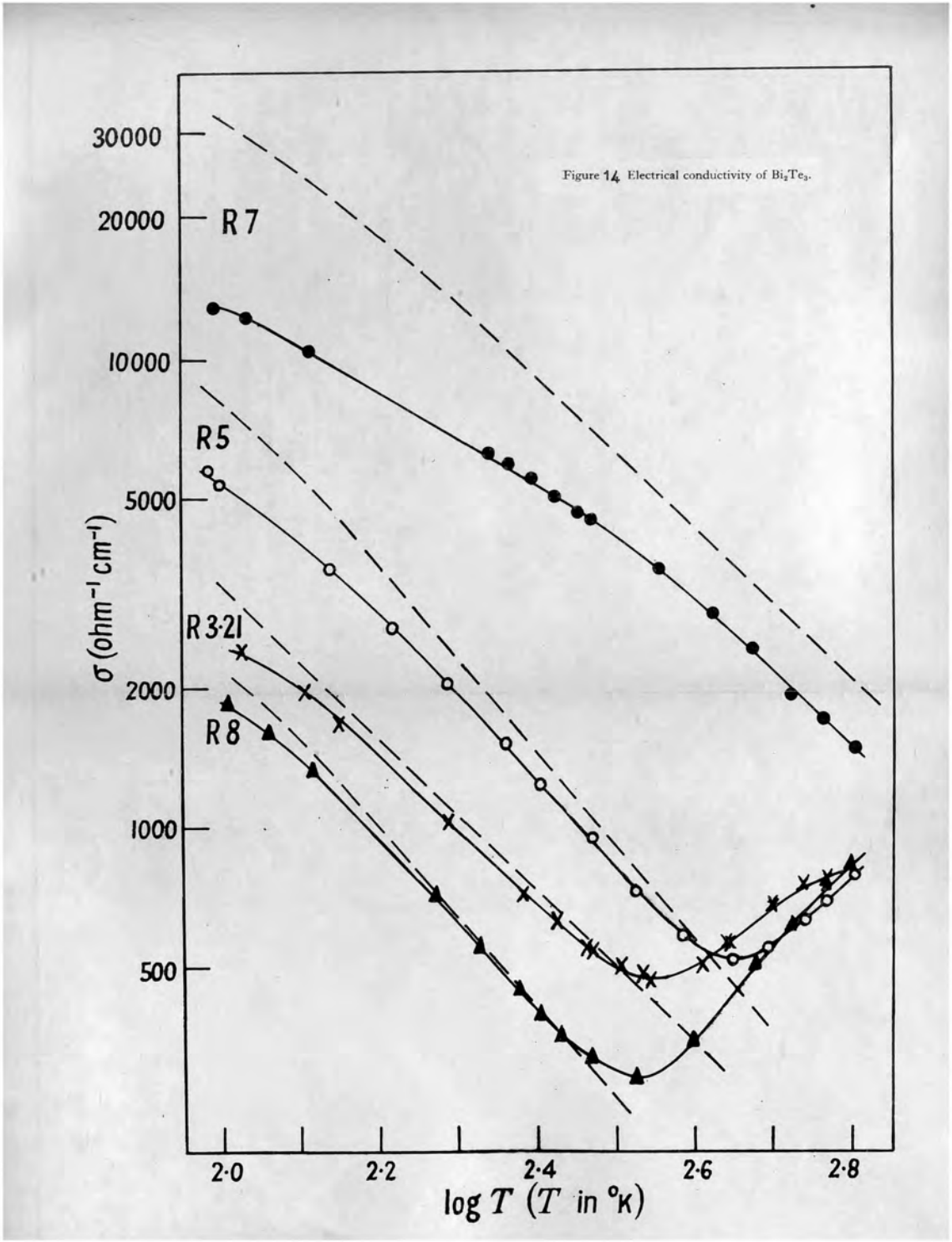

Figure 14 Electrical conductivity of Bi_2Te_3.

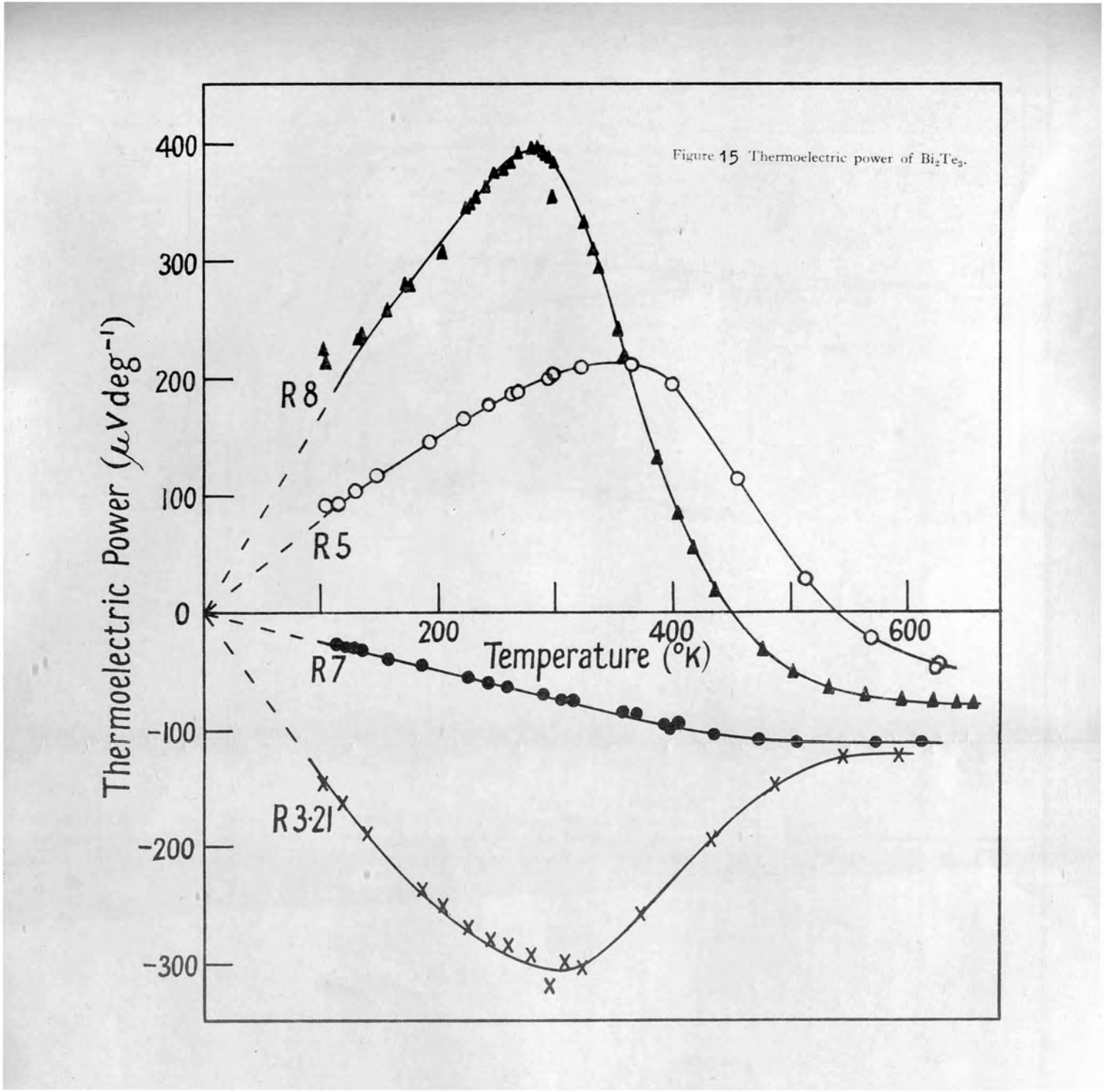

Figure 15 Thermoelectric power of Bi_2Te_3.

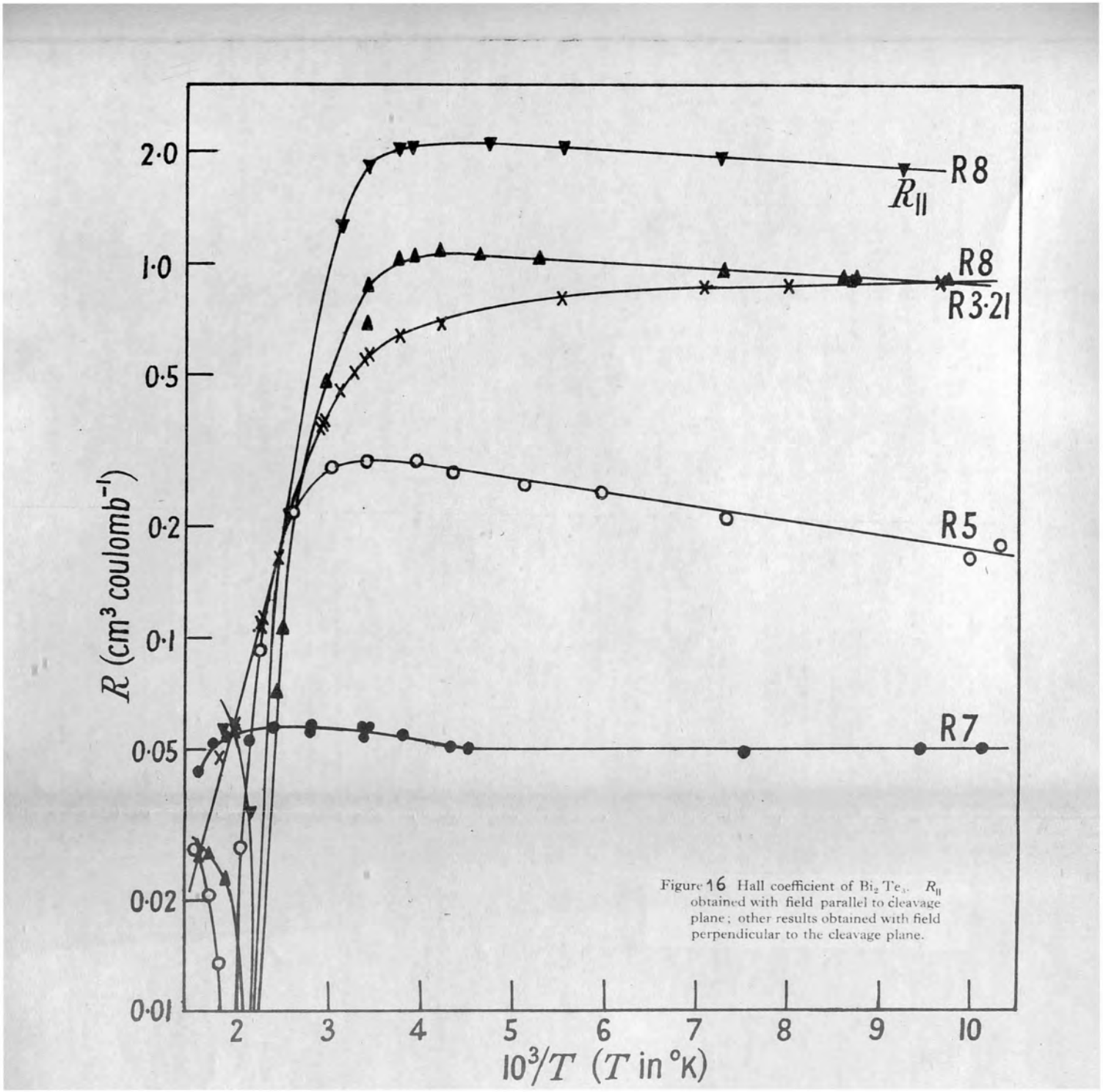

Figure 16 Hall coefficient of Bi_2Te_3. R_{II} obtained with field parallel to cleavage plane; other results obtained with field perpendicular to the cleavage plane.

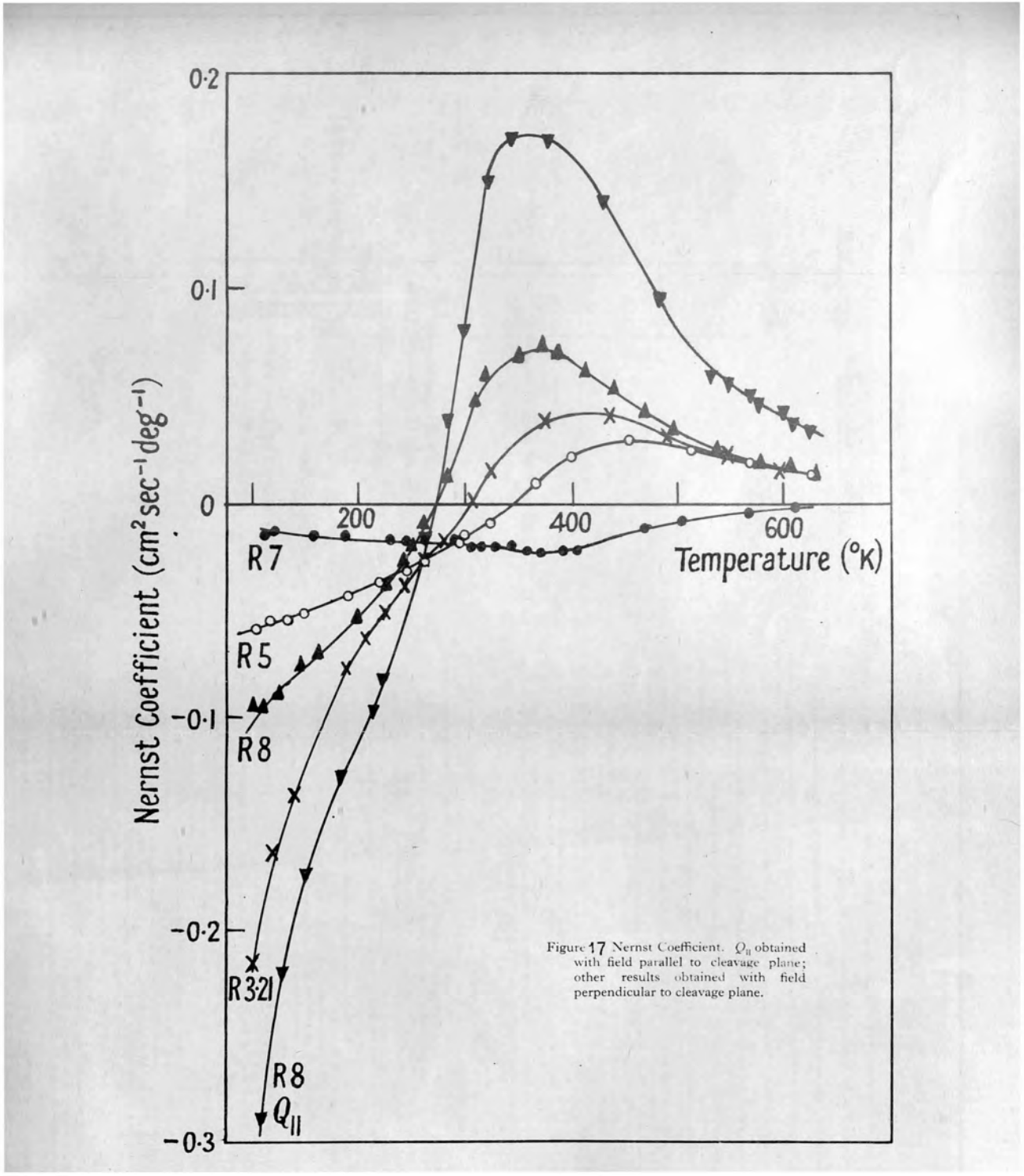

Figure 17 Nernst Coefficient. Q_{11} obtained with field parallel to cleavage plane; other results obtained with field perpendicular to cleavage plane.

Figure 18. Mounting of specimens R5 and R9, for simultaneous measurement of the isothermal and quasi-adiabatic coefficients.

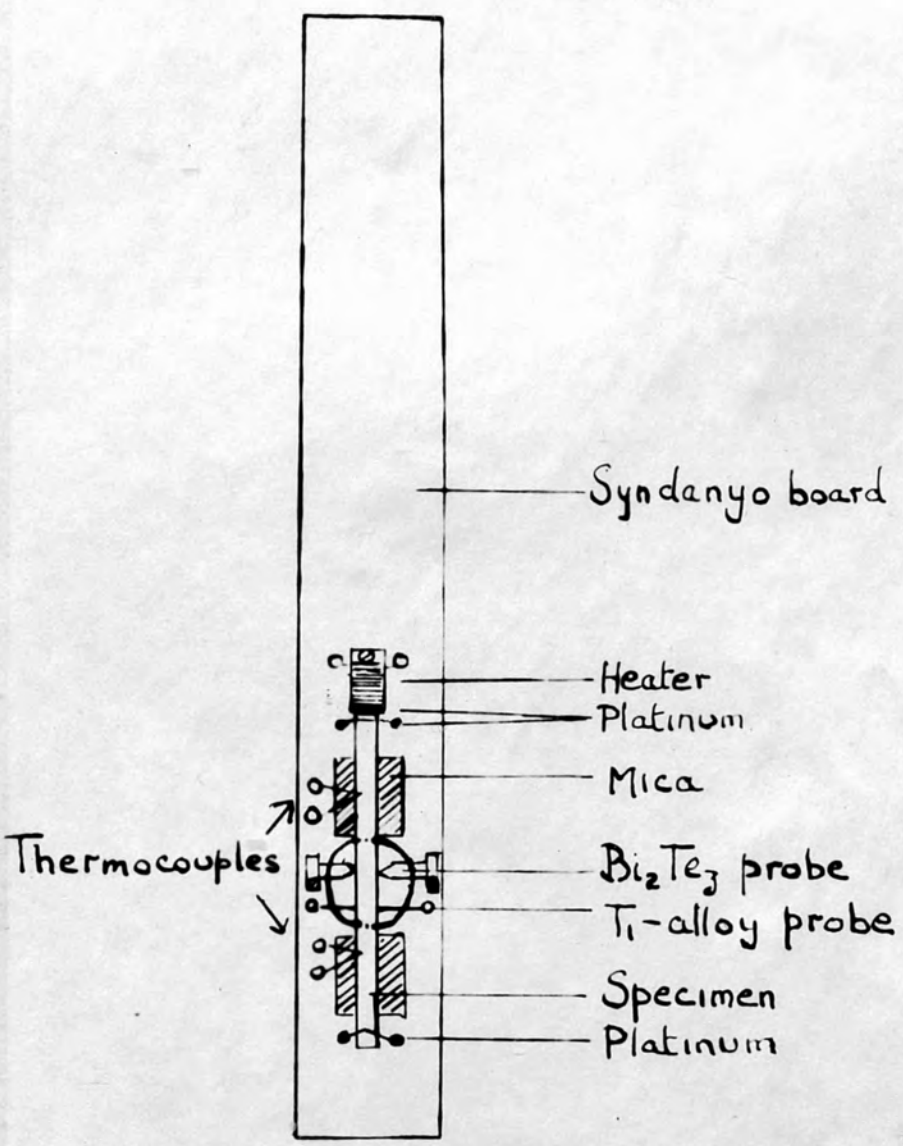

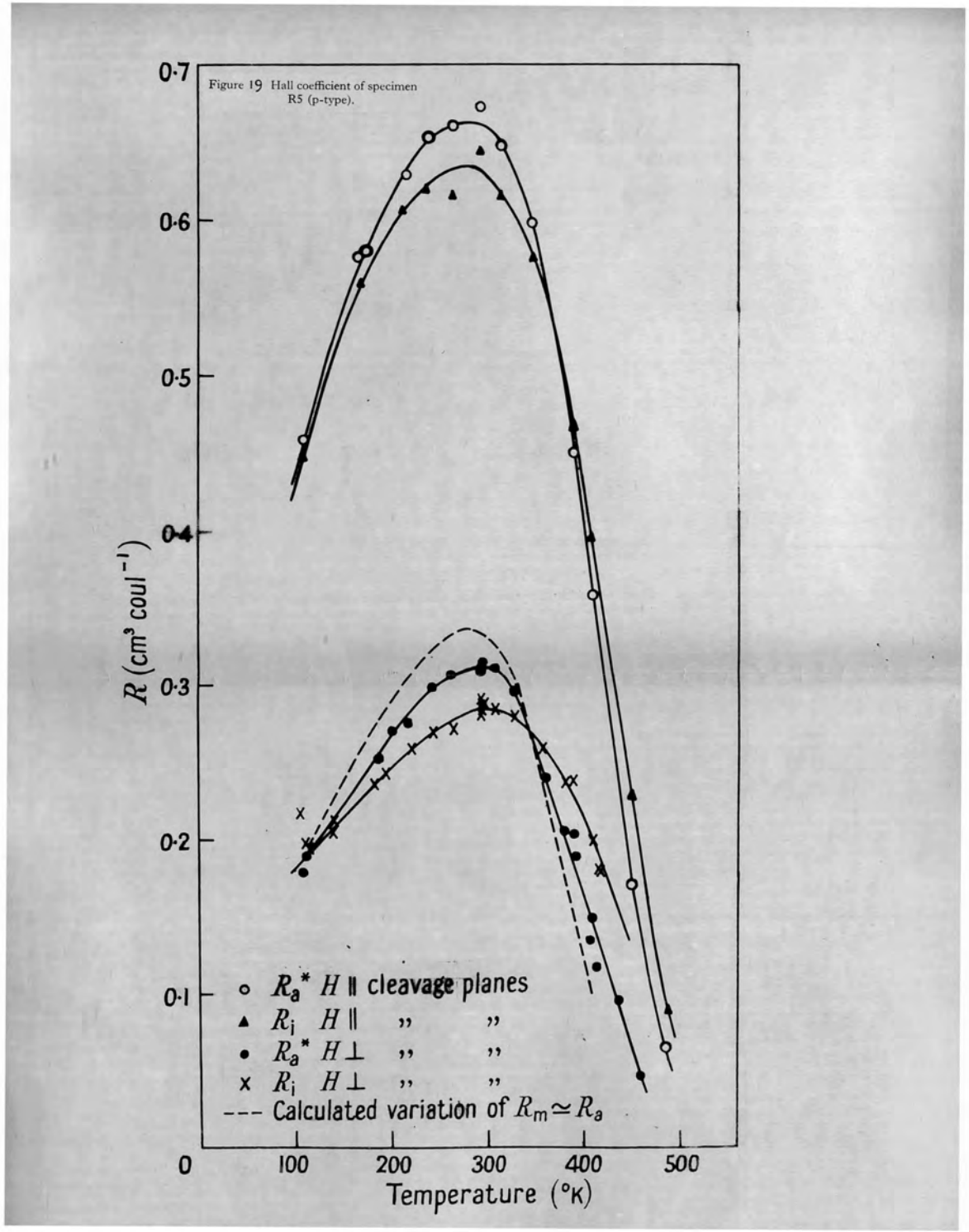

Figure 19 Hall coefficient of specimen R5 (p-type).

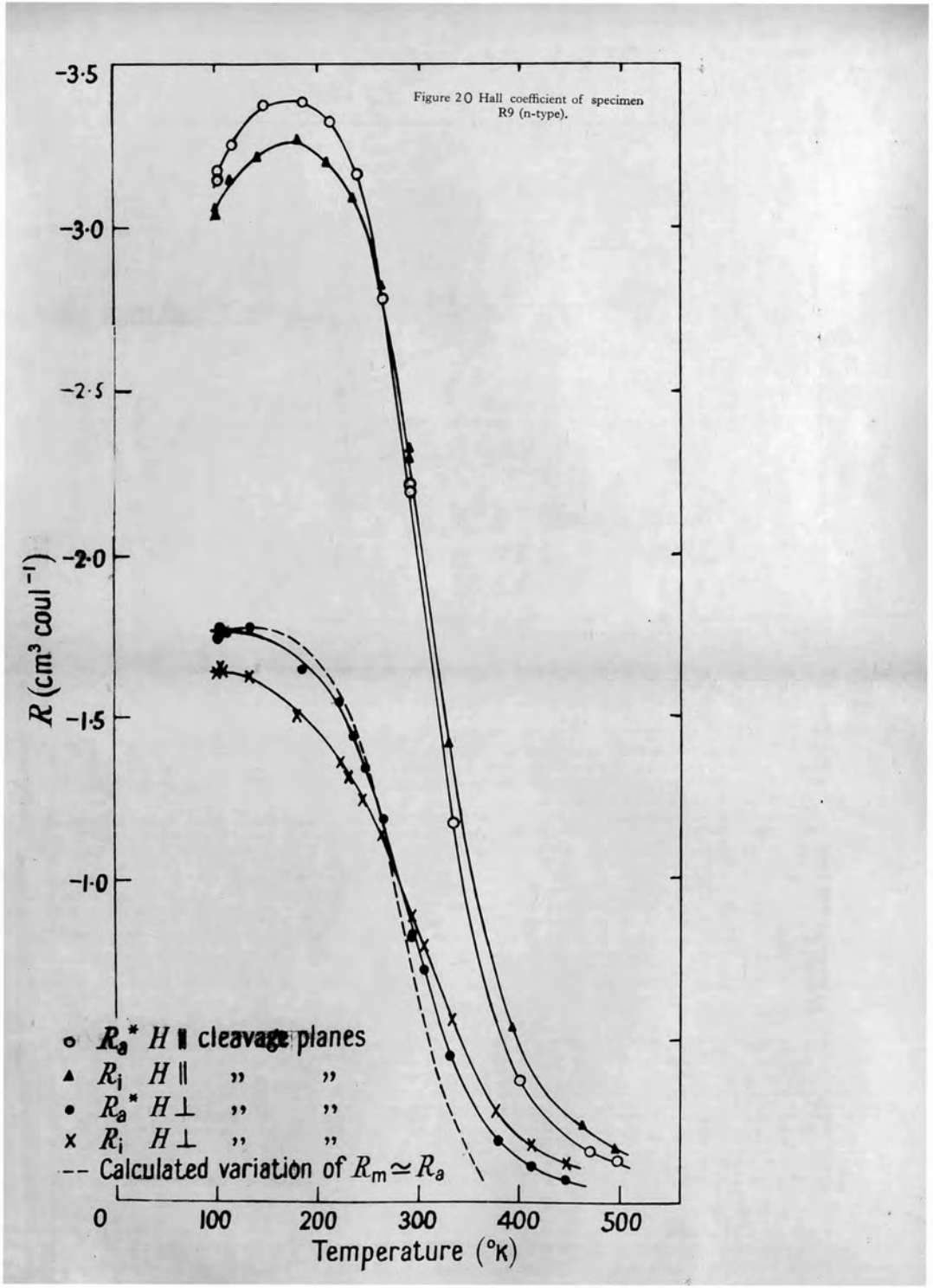

Figure 20 Hall coefficient of specimen R9 (n-type).

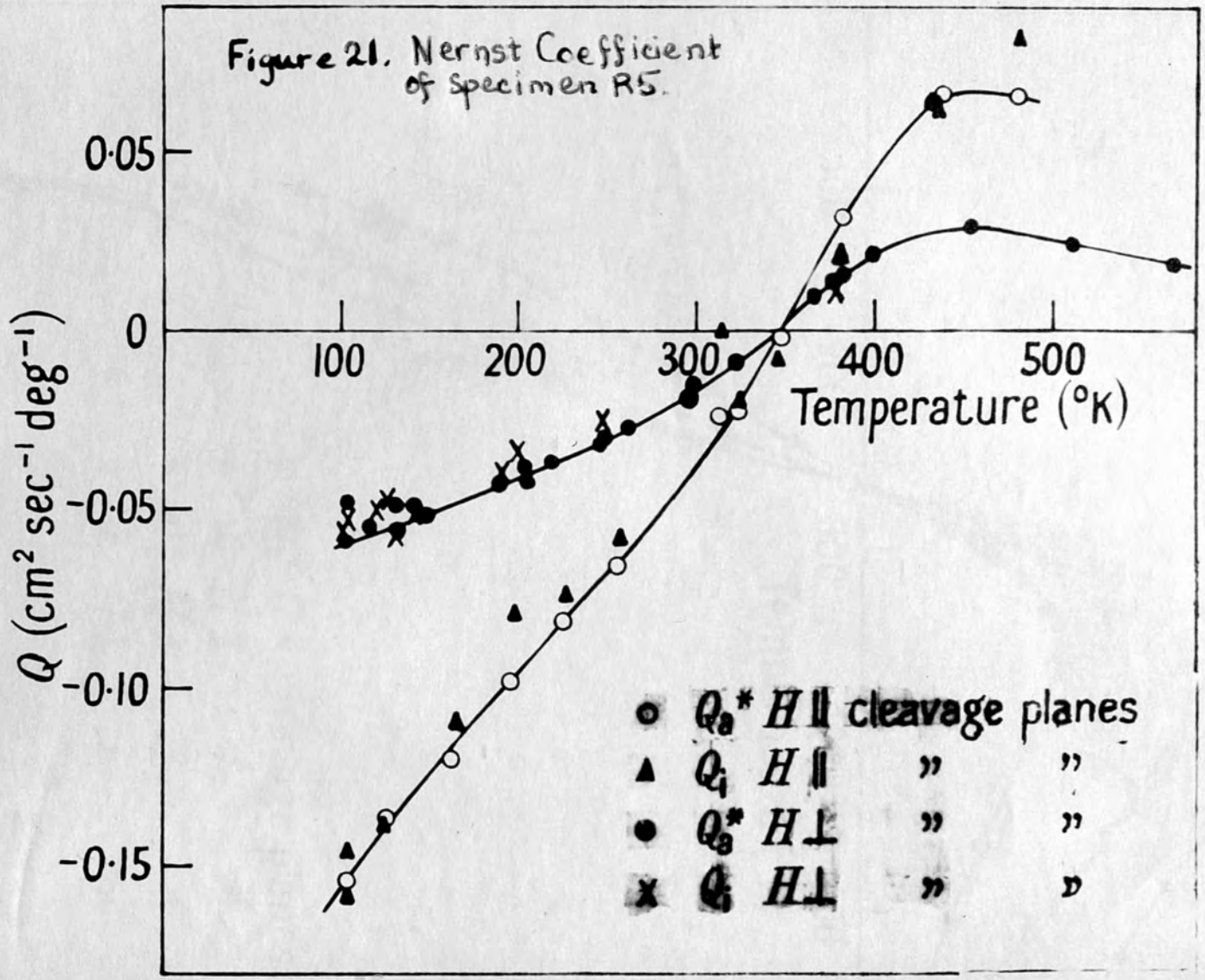
Figure 21. Nernst Coefficient of Specimen R5.
0·05
0
-0·05
-0·10
-0·15
Q (cm² sec⁻¹ deg⁻¹)
100
200
300
400
500
Temperature (°K)
Q₂* H ∥ cleavage planes
Q₁ H ∥ " "
Q₃* H ⊥ " "
Q₄ H ⊥ " "

Figure 22. Nernst Coefficient of specimen R9.

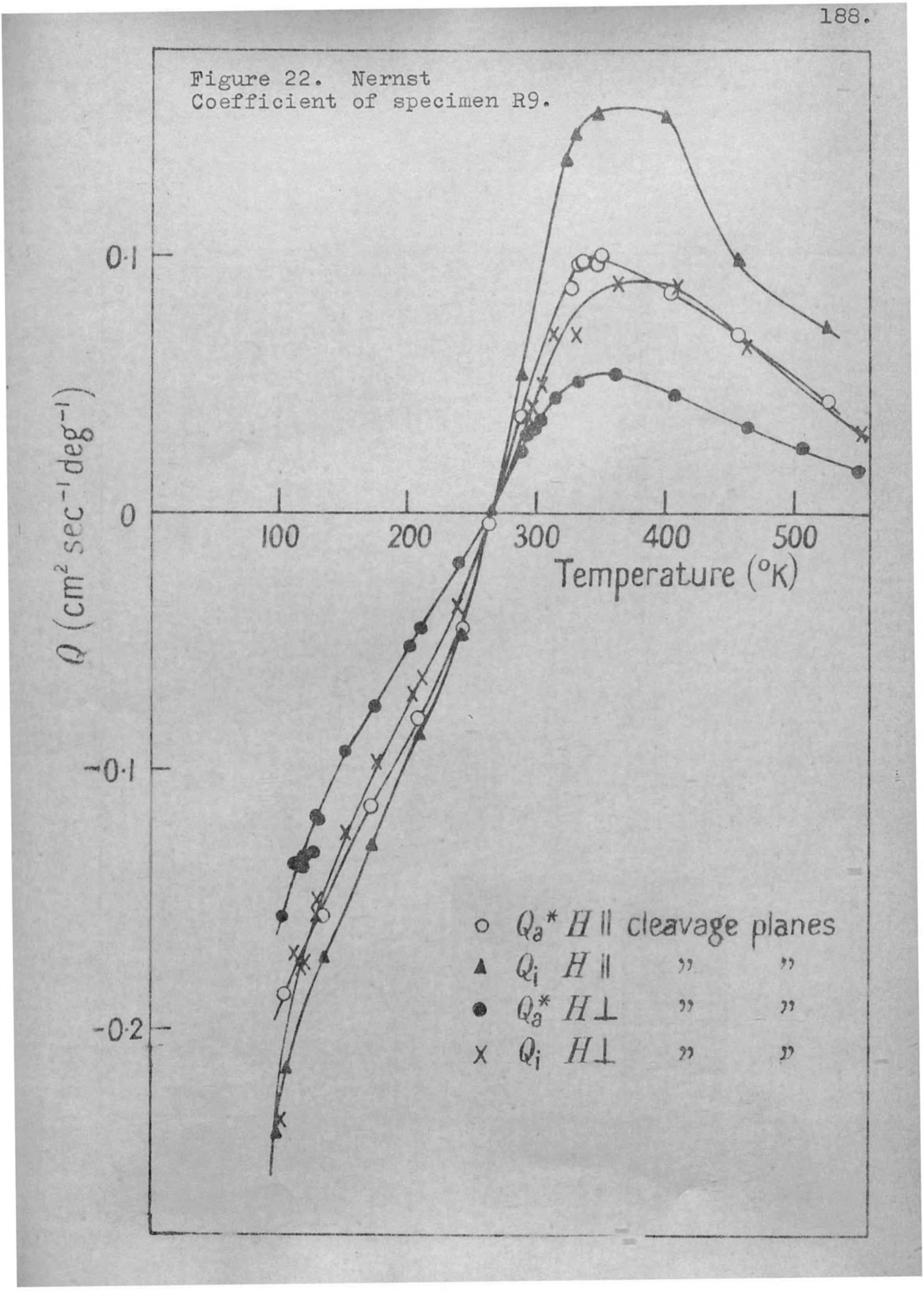

Figure 23. Electrical conductivity of specimen R9.

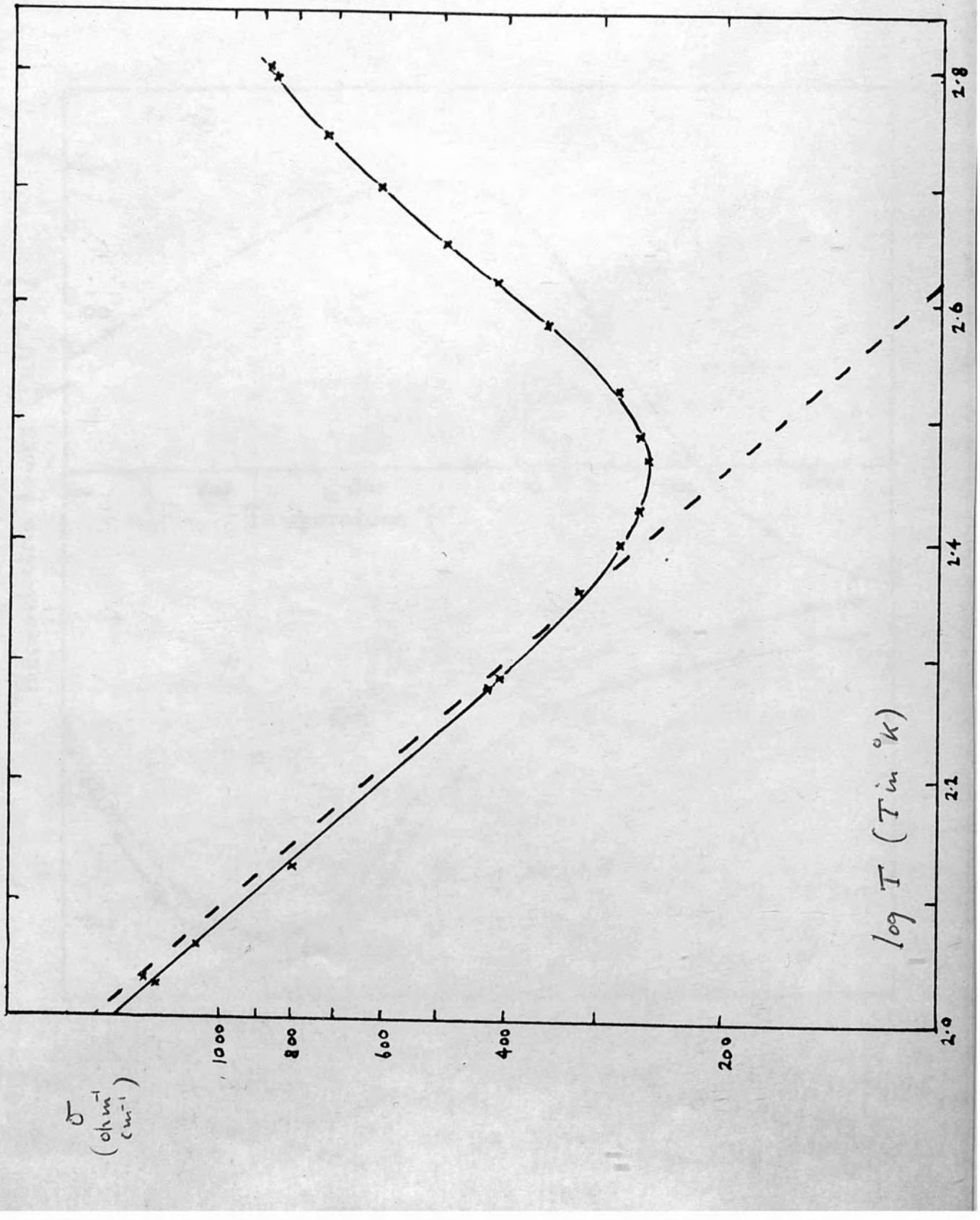

Figure 24. Thermoelectric power of R5 and R9.

o Relative to lead
× Relative to Ti-alloy

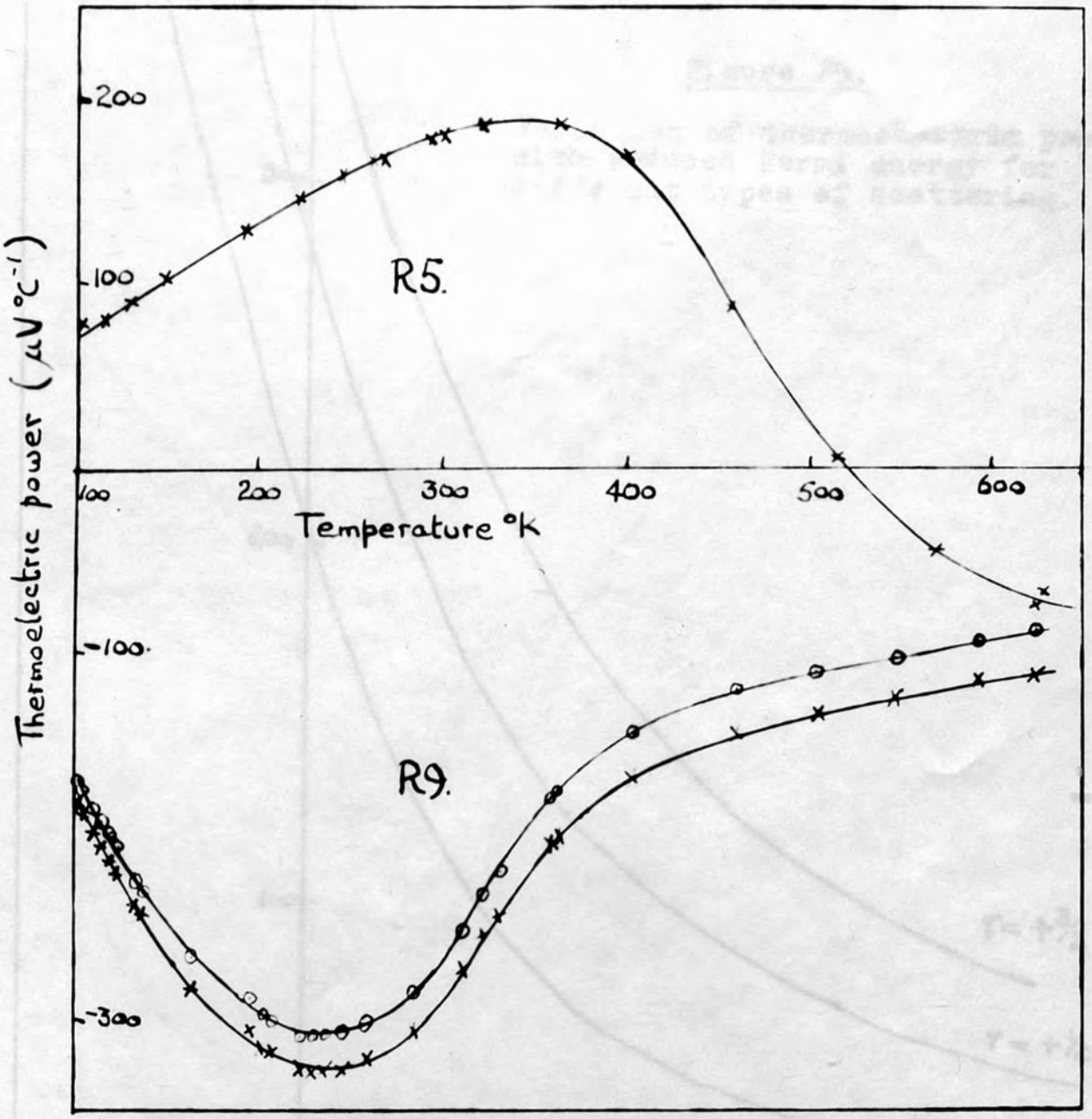

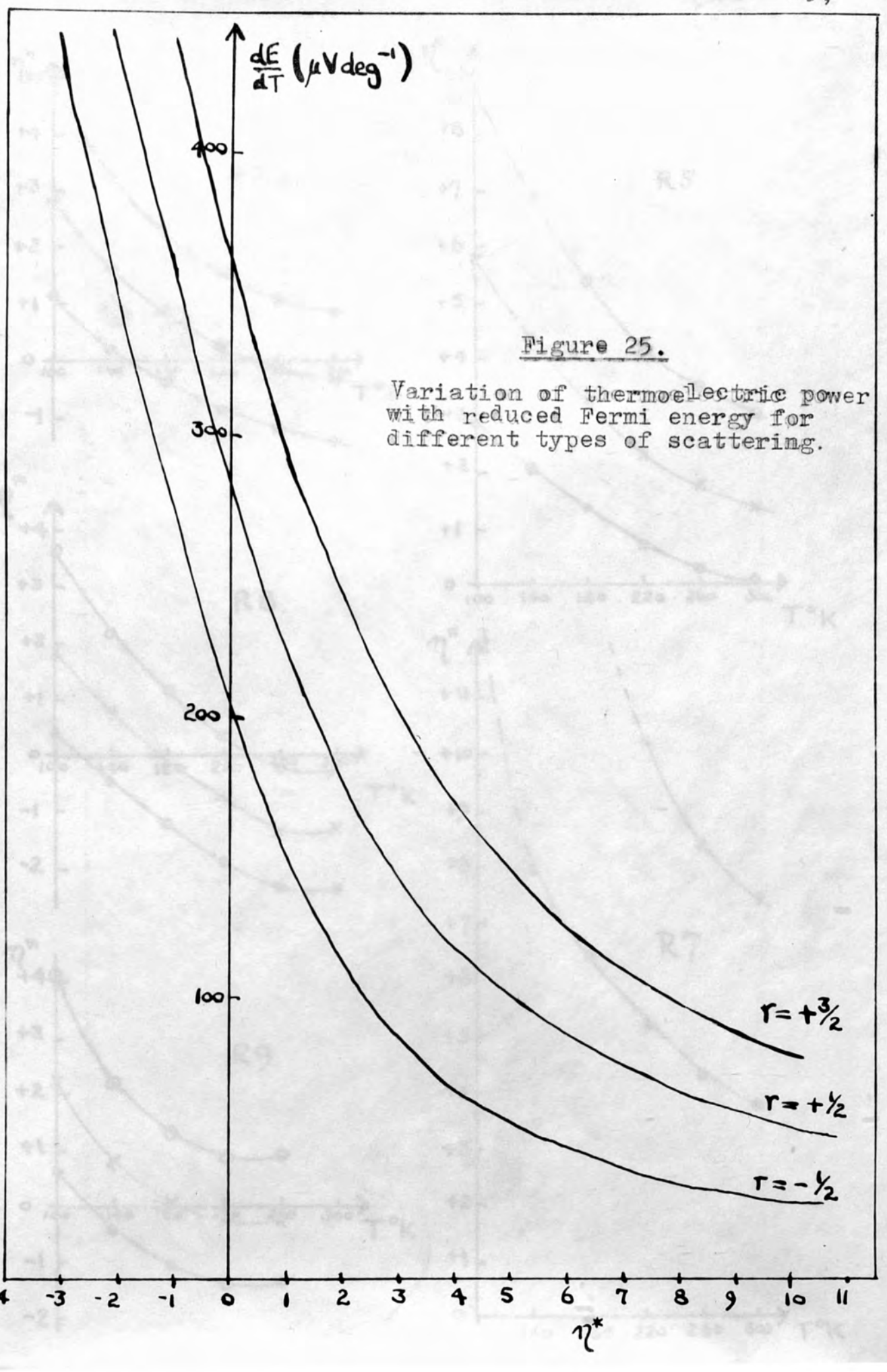

Figure 25.

Variation of thermoelectric power with reduced Fermi energy for different types of scattering.

Figure 26. Variation of η^* with temperature [⊙ r = ± 3/2 × r = + 1/2 • r = − 1/2

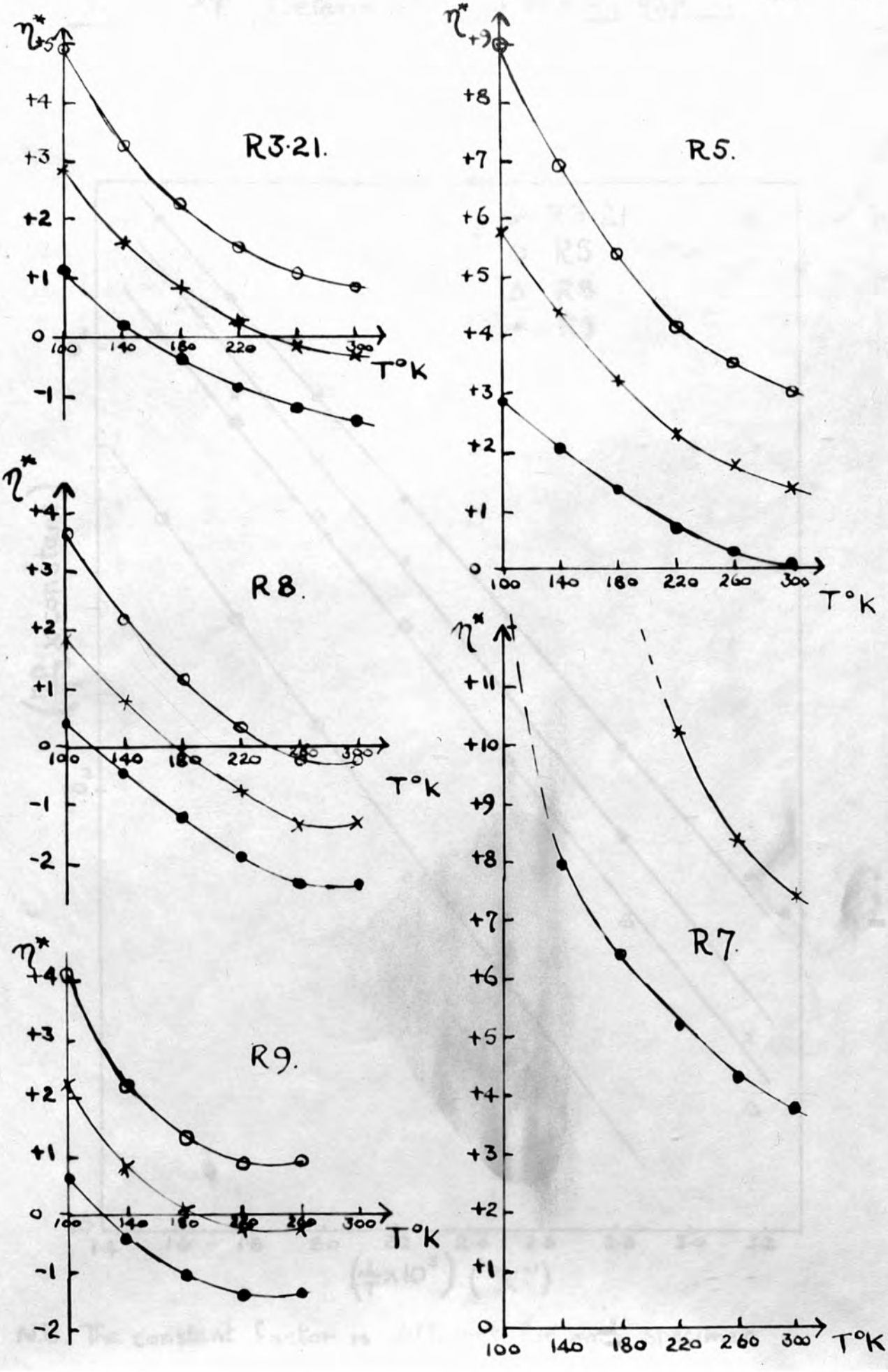

Figure 27. Determination of energy gap at 0°K.

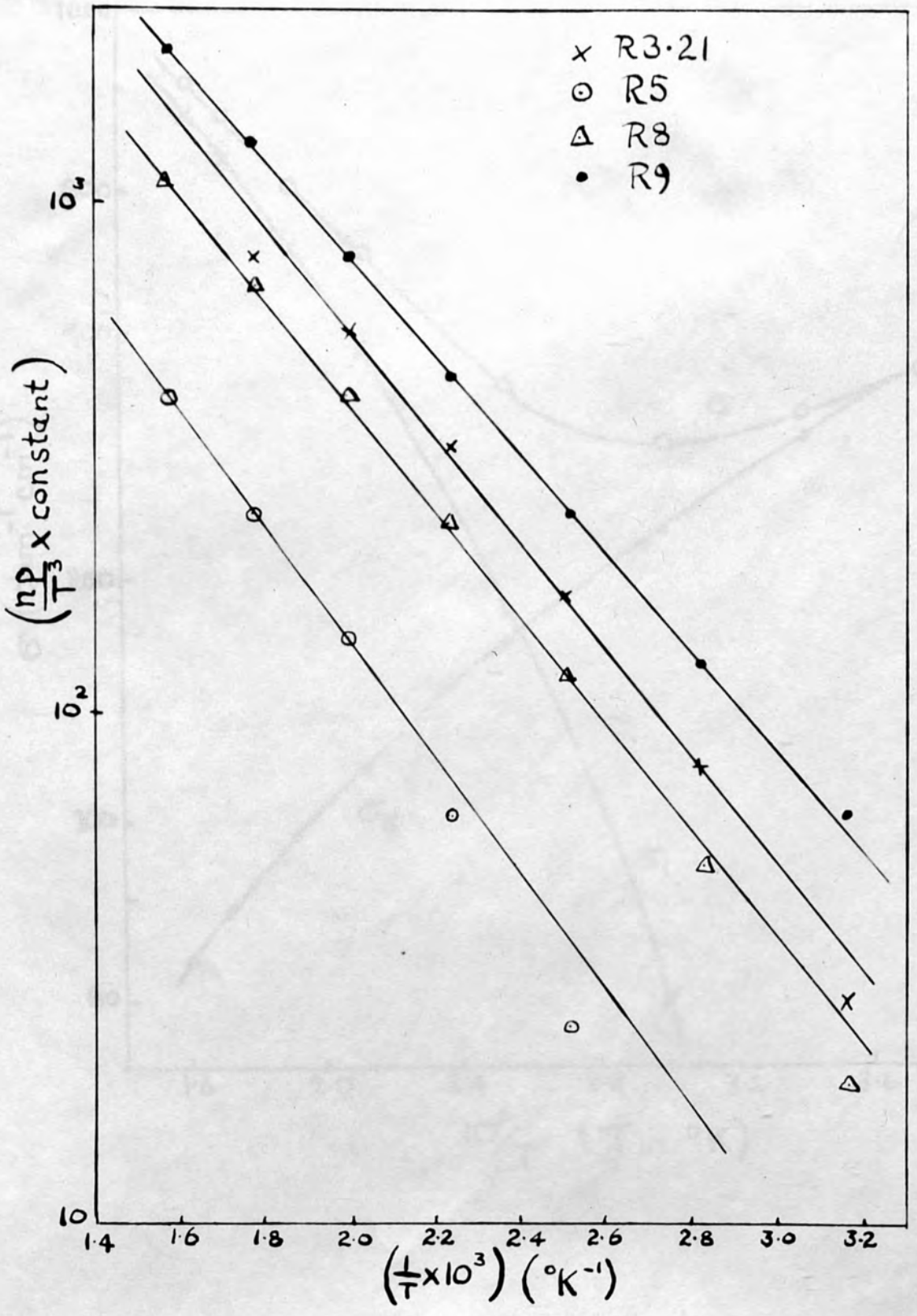

N.B. The constant factor is different for each specimen.

Figure 28 High temperature conductivity of R8

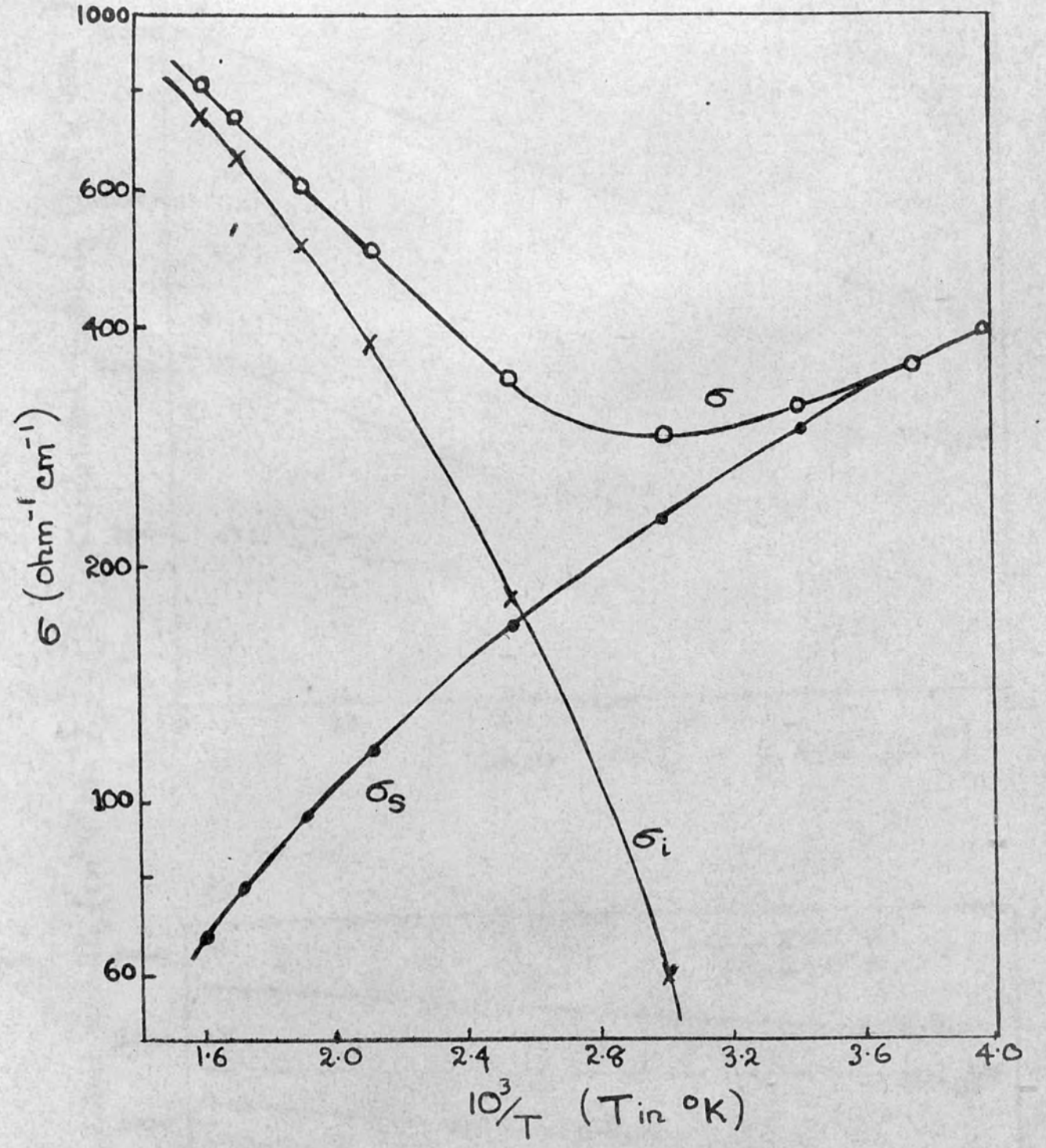

Figure 29. Impurity scattering.

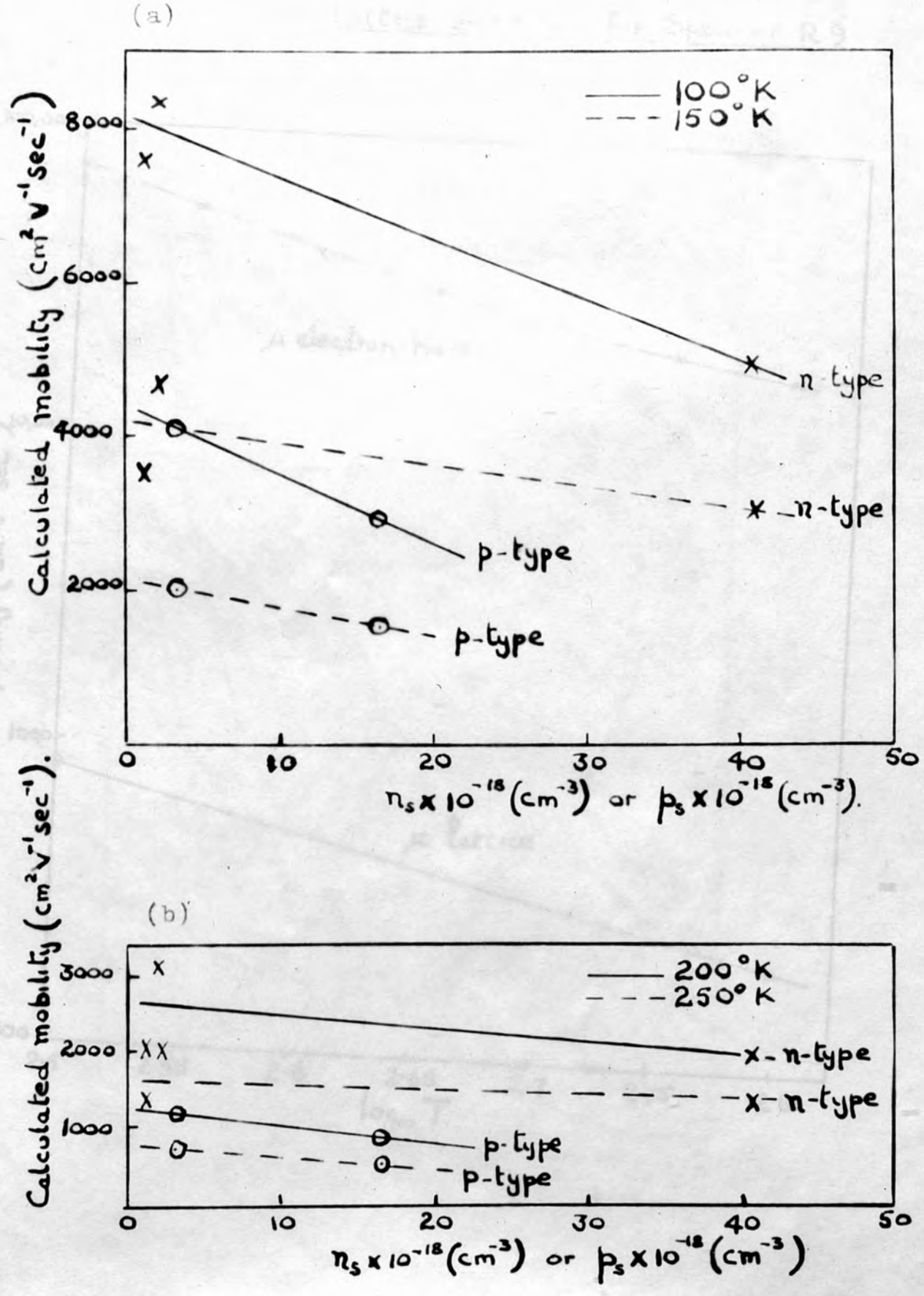

Figure 30. Comparison of the electron - hole and lattice mobilities for Specimen R.9.

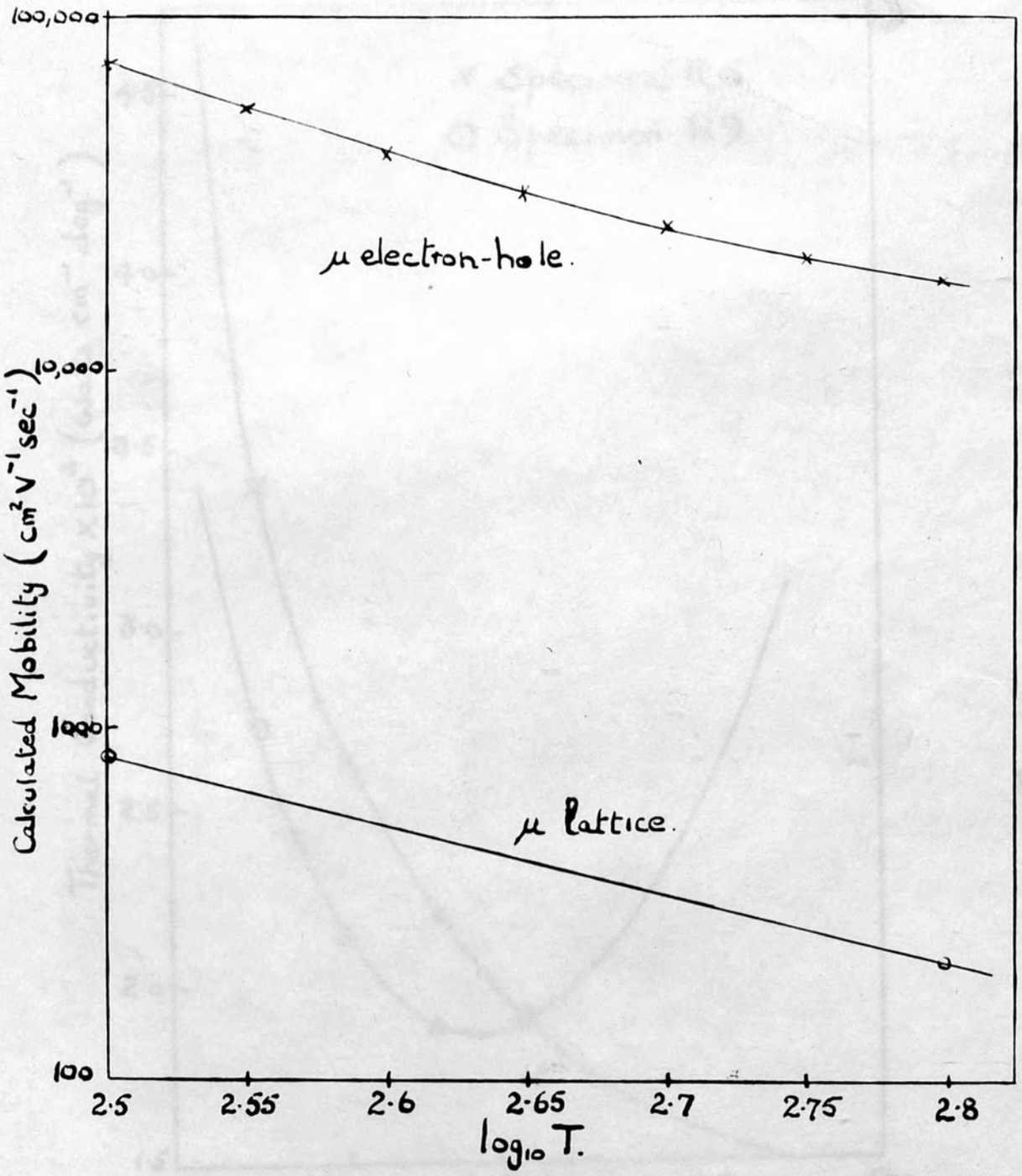

Figure 31. Thermal conductivity, with heat flow along the cleavage planes, for specimens R5 and R9.

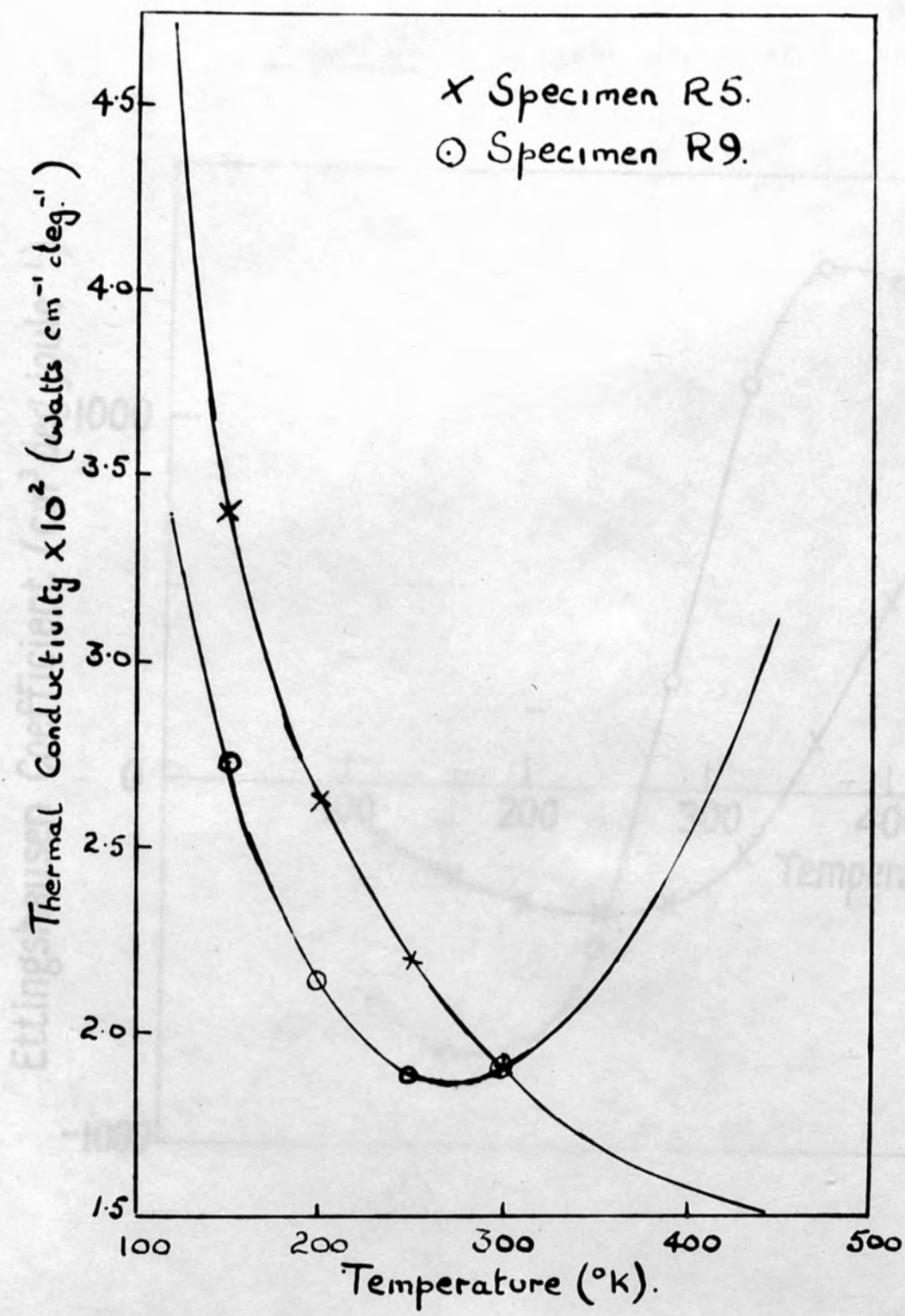

Figure 32. Ettingshausen coefficient of Bi_2Te_3.

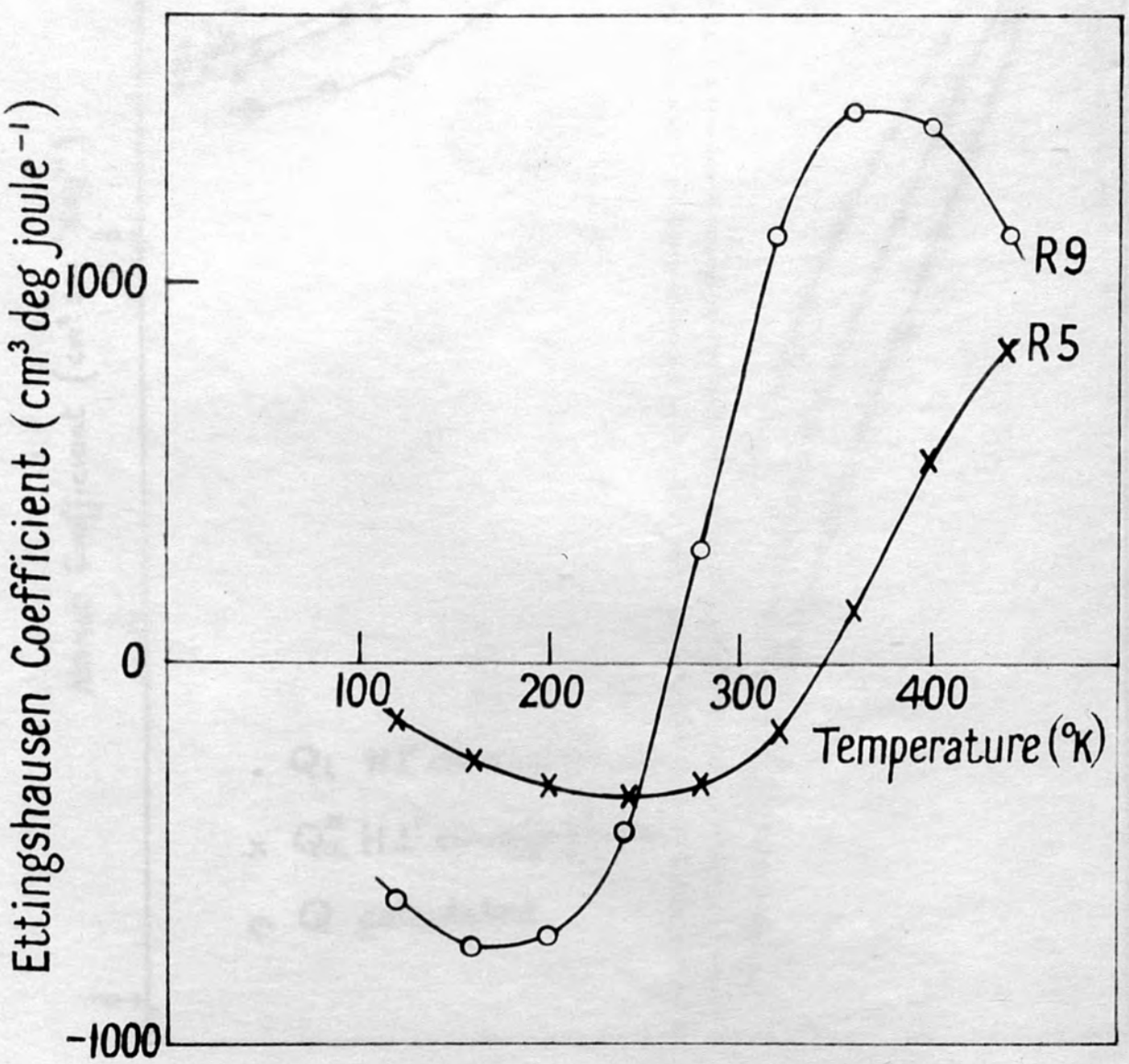

Calculated Nernst Coefficient.

Figure 33. Specimen R5

Figure 34. Specimen R9

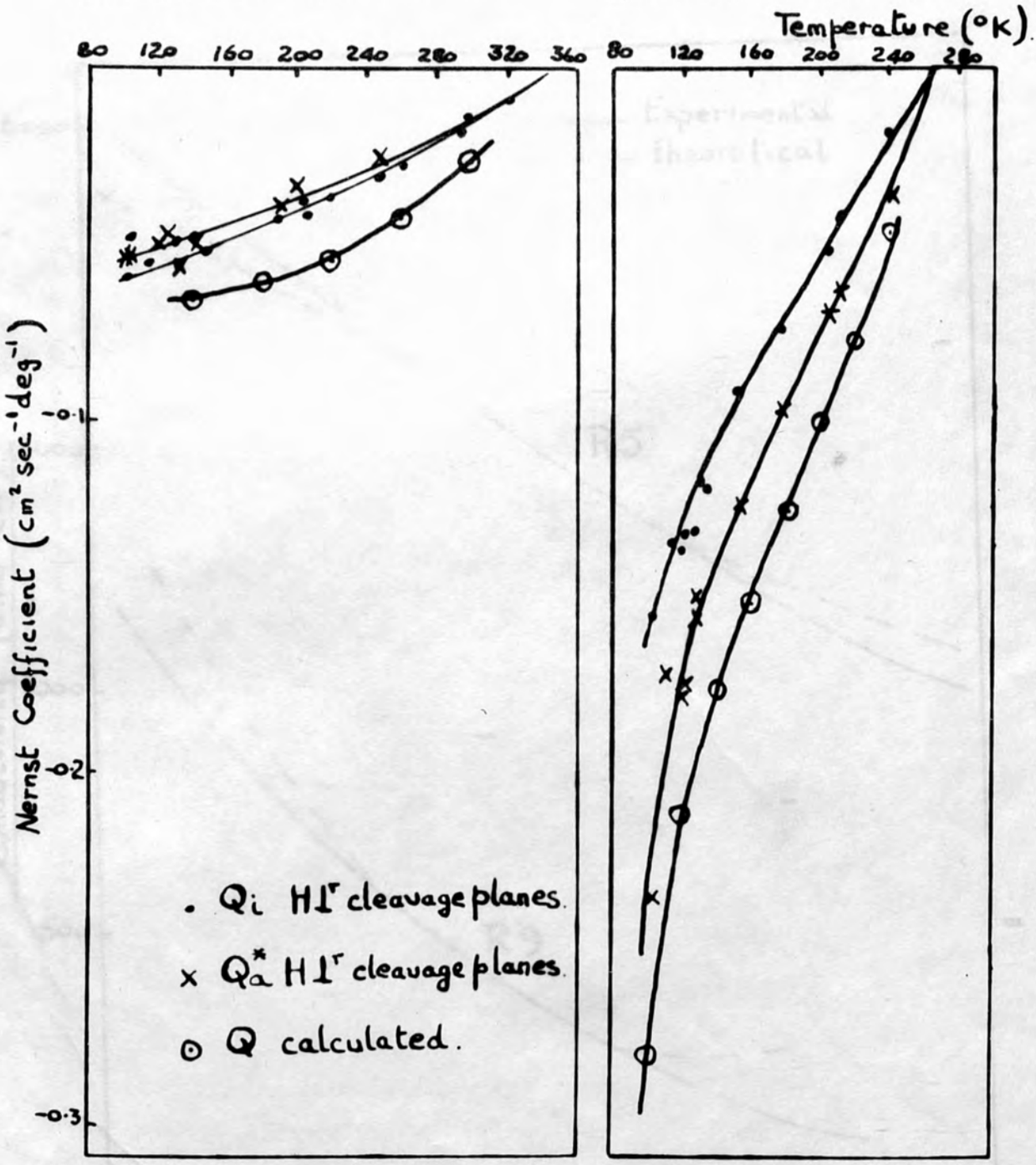

Figure 35 Comparison of experimental and theoretical conductivity.

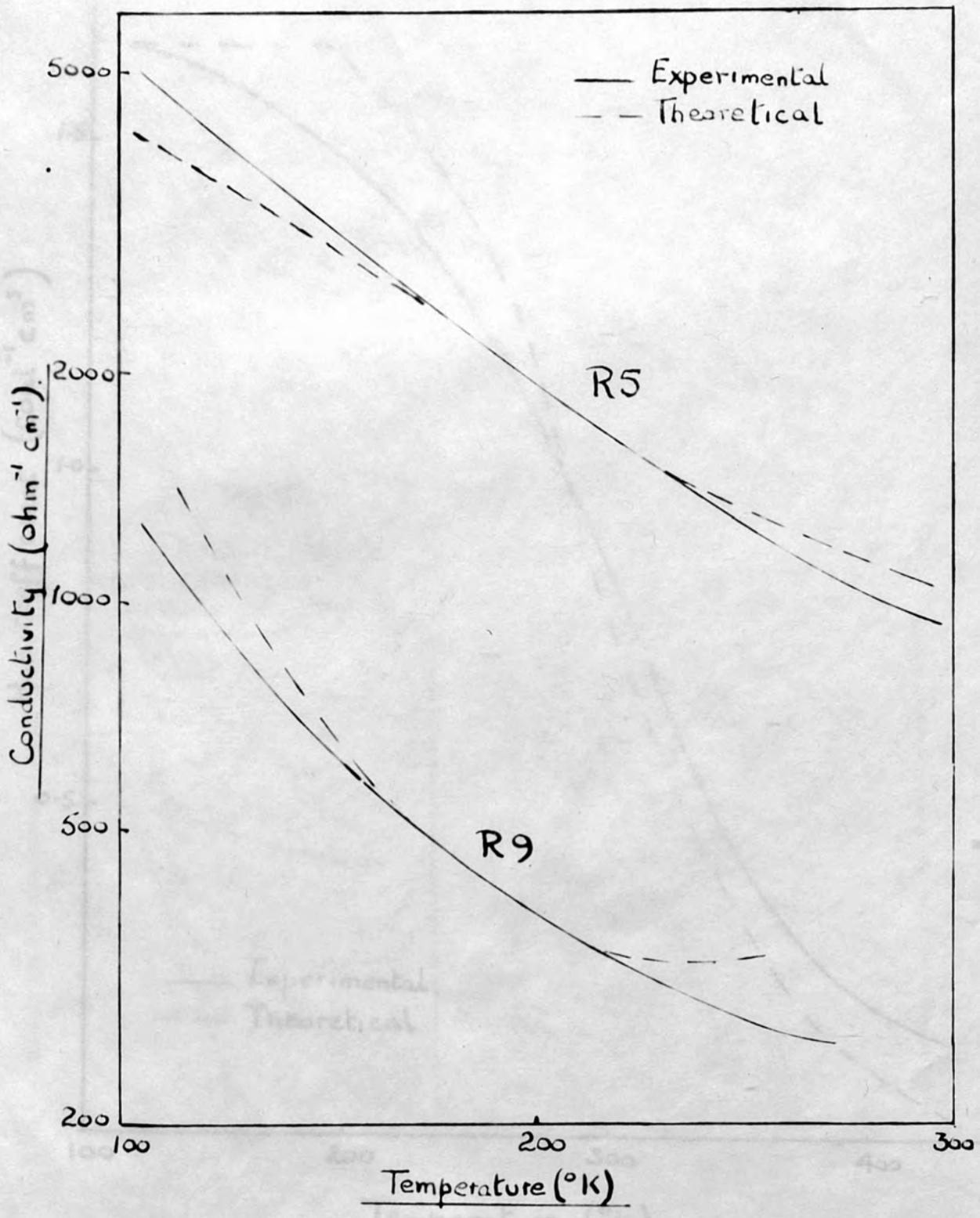

Figure 36 Comparison of experimental and theoretical Hall coefficient (Specimen R 9).

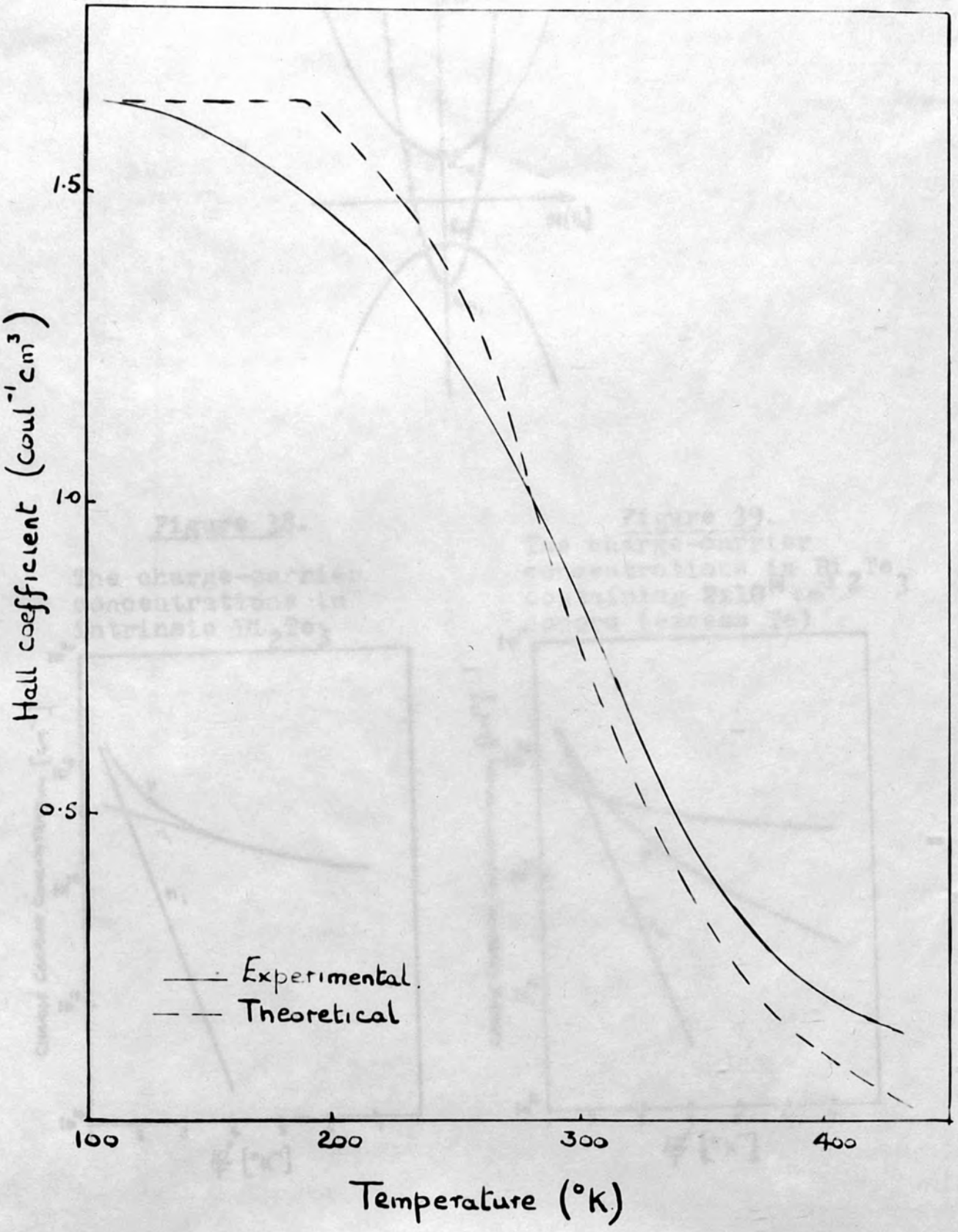

Figure 37.

The three-band model used by Mooser and Pearson to calculate the charge-carrier concentrations in Bi_2Te_3.

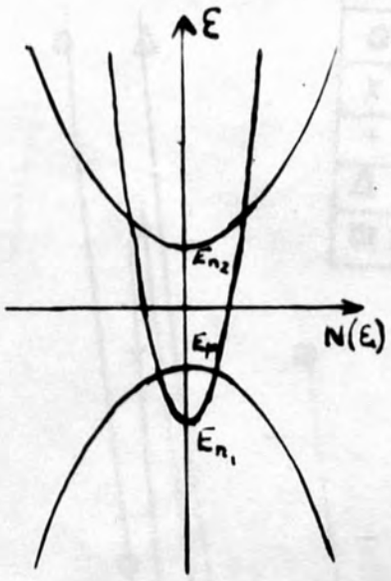

Figure 38.

The charge-carrier concentrations in intrinsic Bi_2Te_3

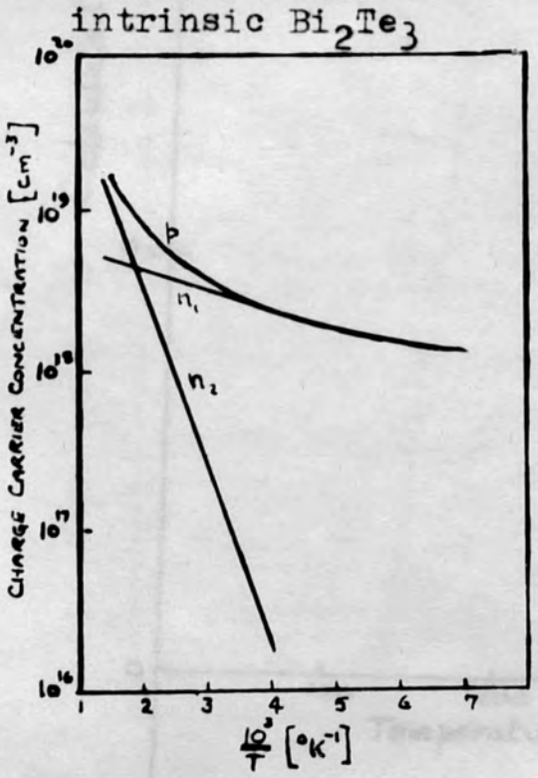

Figure 39.

The charge-carrier concentrations in Bi_2Te_3 containing 2×10^{18} cm^{-3} donors (excess Te)

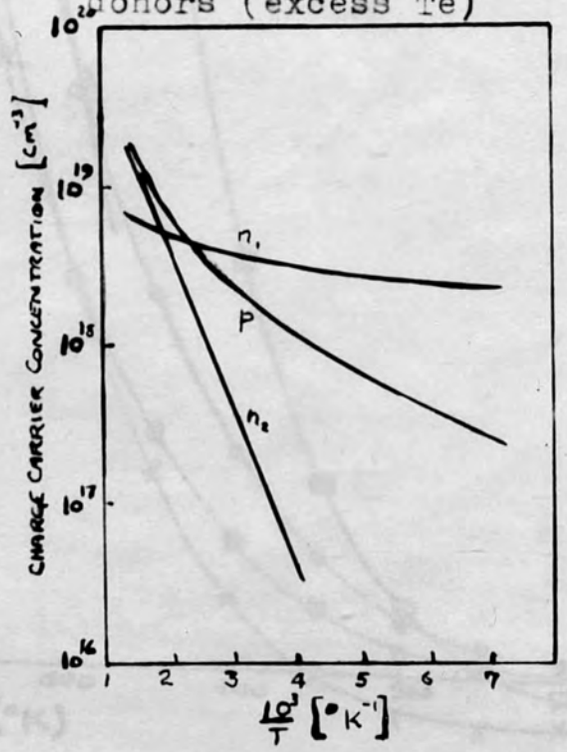

Figure 40. Calculated Hall Coefficient using Model proposed by Mooser and Pearson and concentrations of carriers given by Figure 38.

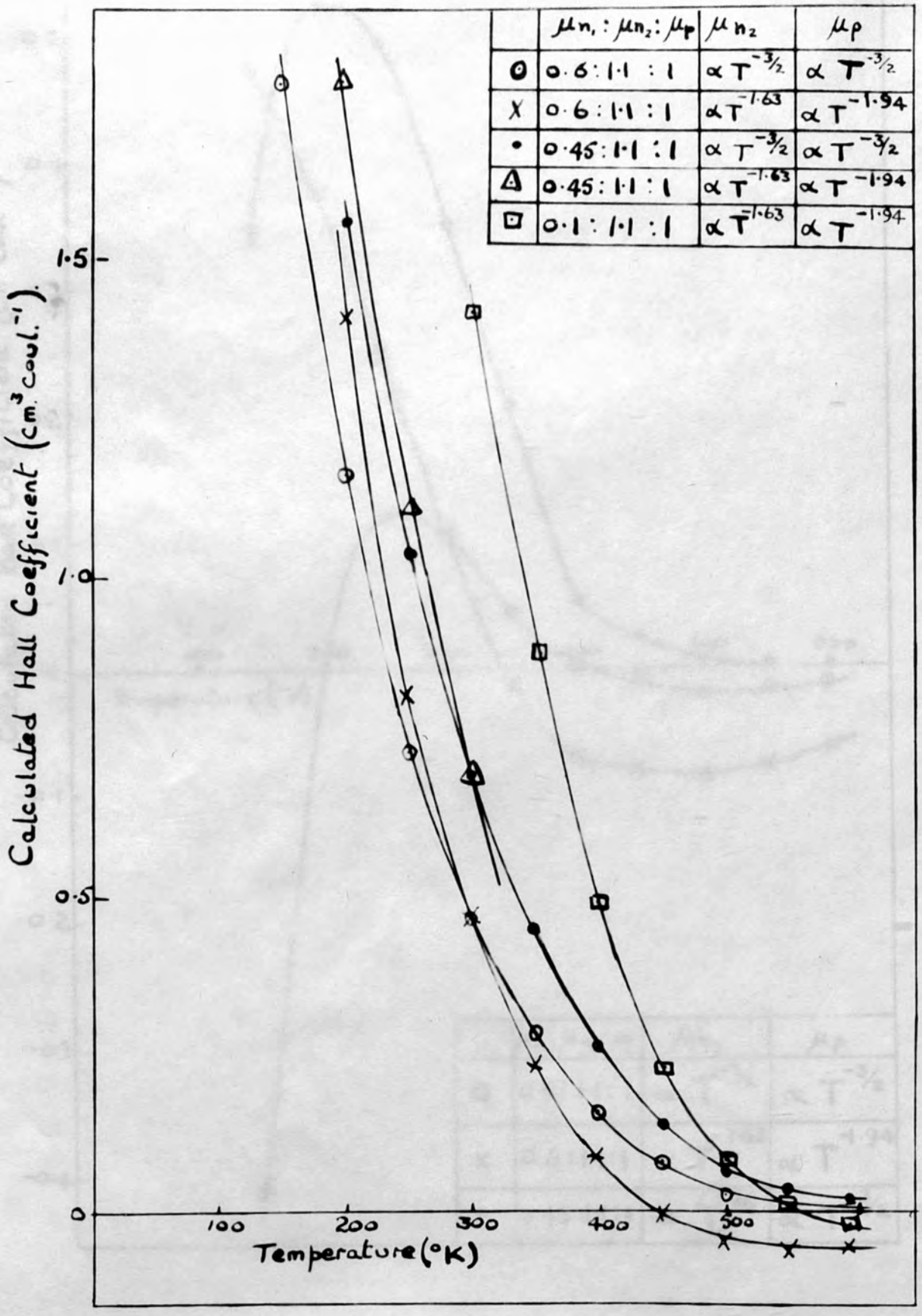

Figure 41. Calculated Hall coefficient using model proposed by Mooser and Pearson and concentrations of carriers given in Figure 39.

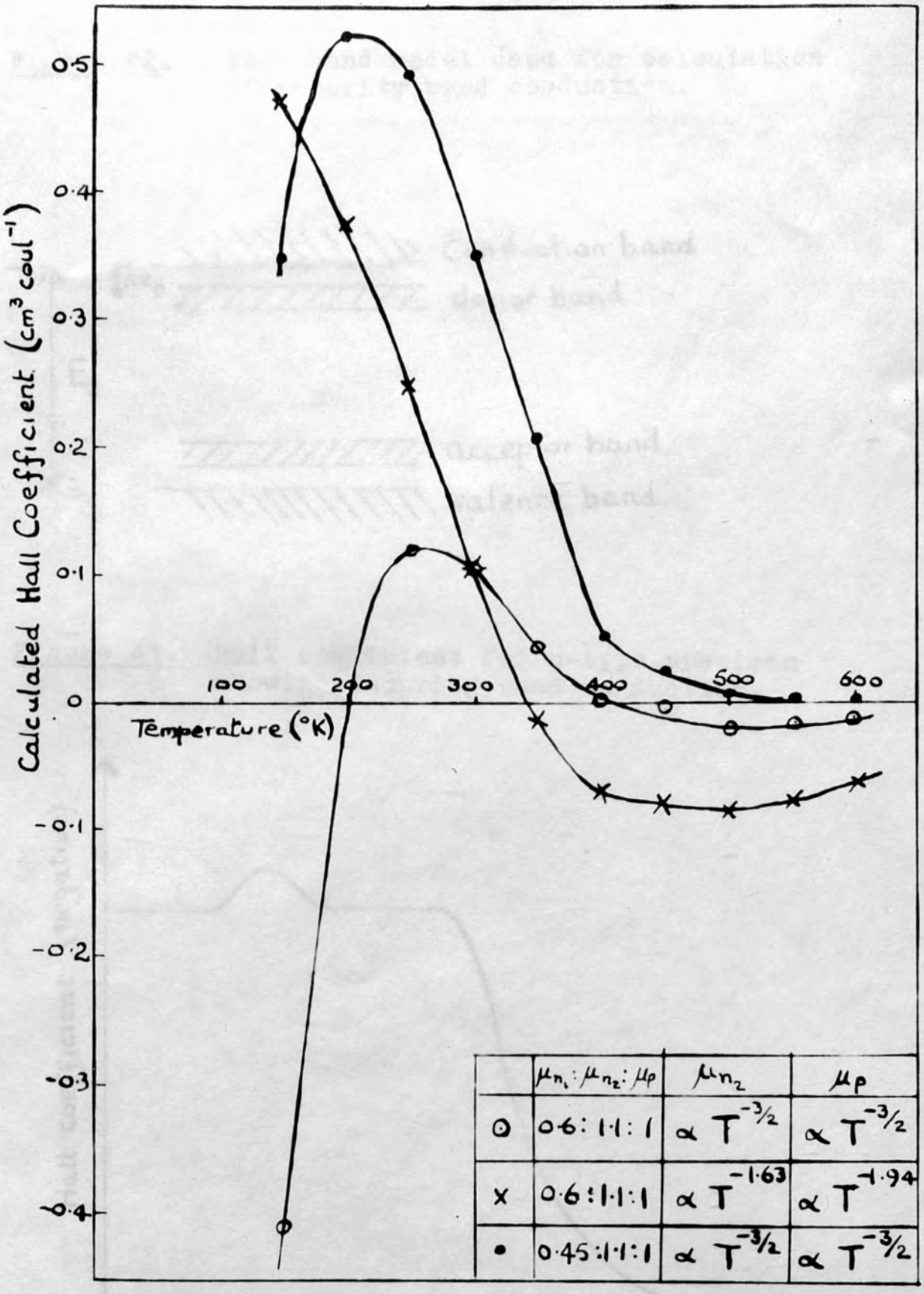

Figure 42. Four band model used for calculation of impurity band conduction.

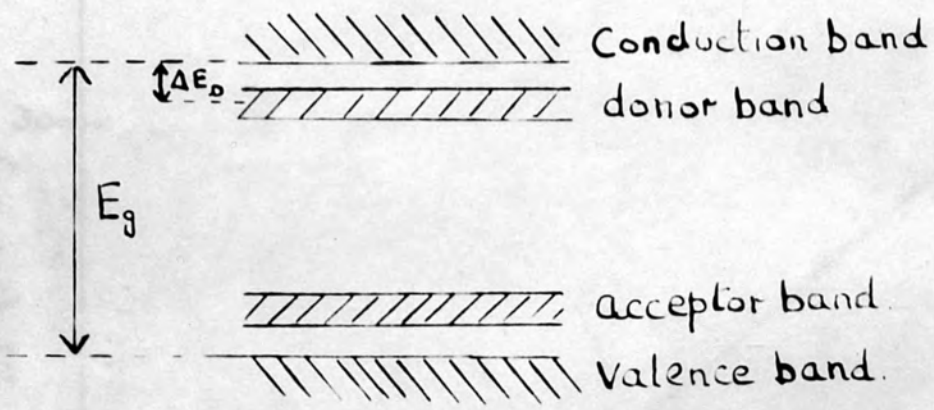

Figure 43. Hall coefficient for n-type specimen showing impurity band conduction.

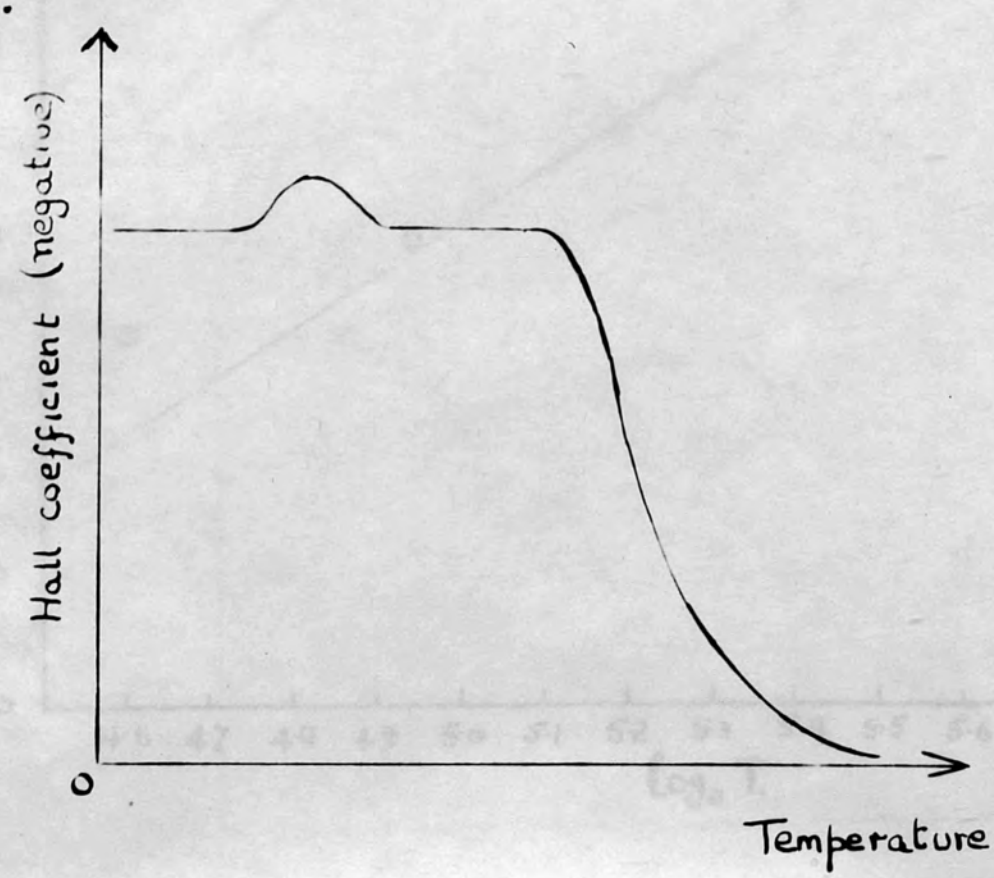

Figure 44. Thermoelectric power as a function of temperature.

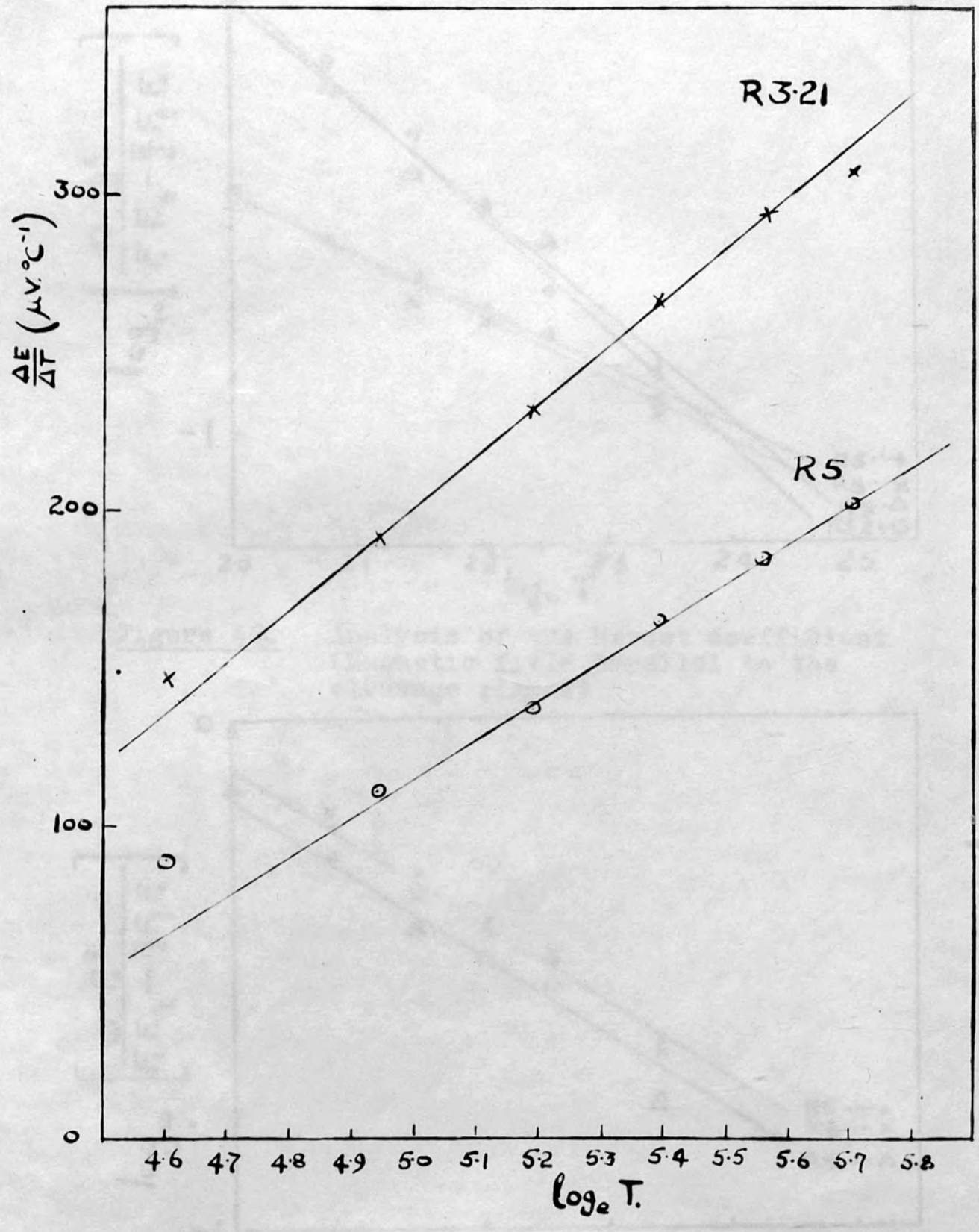

Figure 45. Analysis of the Nernst coefficient in the extrinsic region. (Magnetic field perpendicular to the cleavage planes).

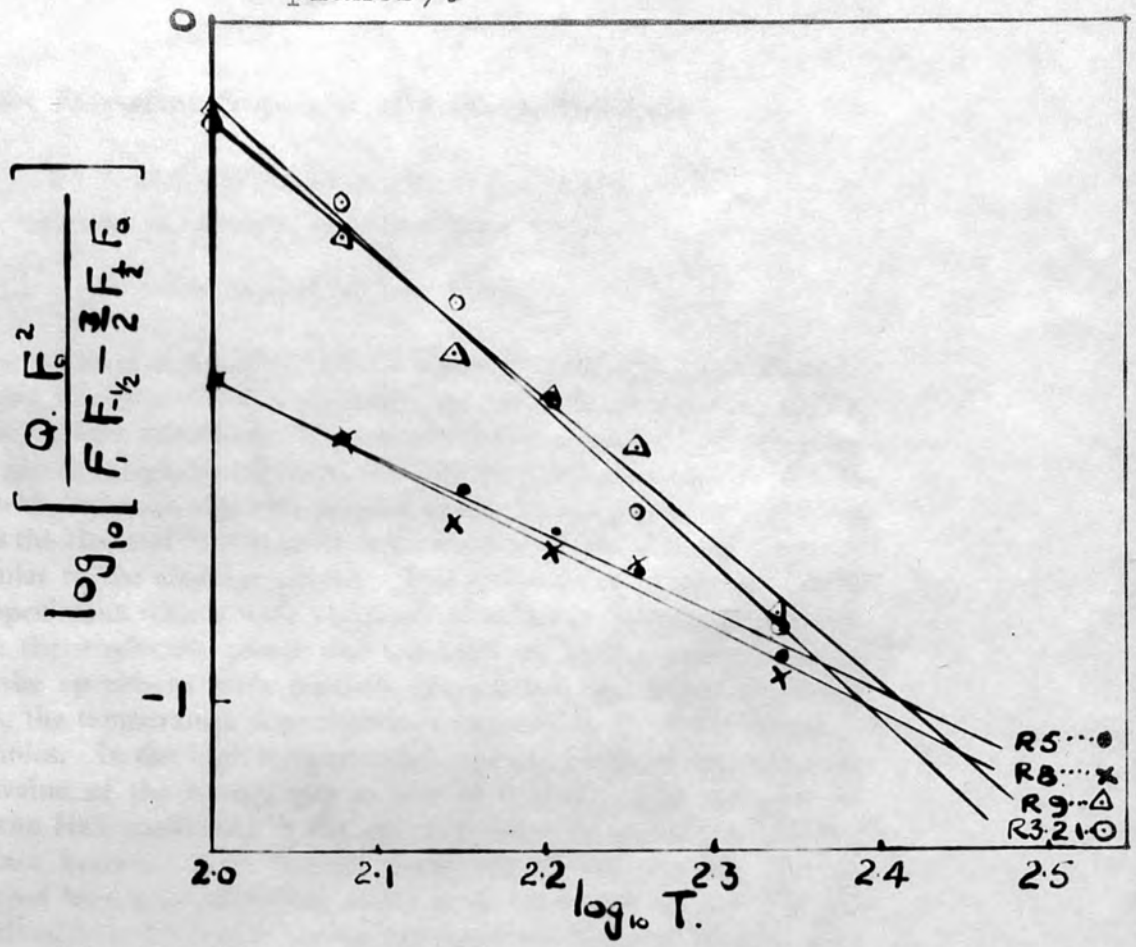

Figure 46. Analysis of the Nernst coefficient (Magnetic field parallel to the cleavage planes)

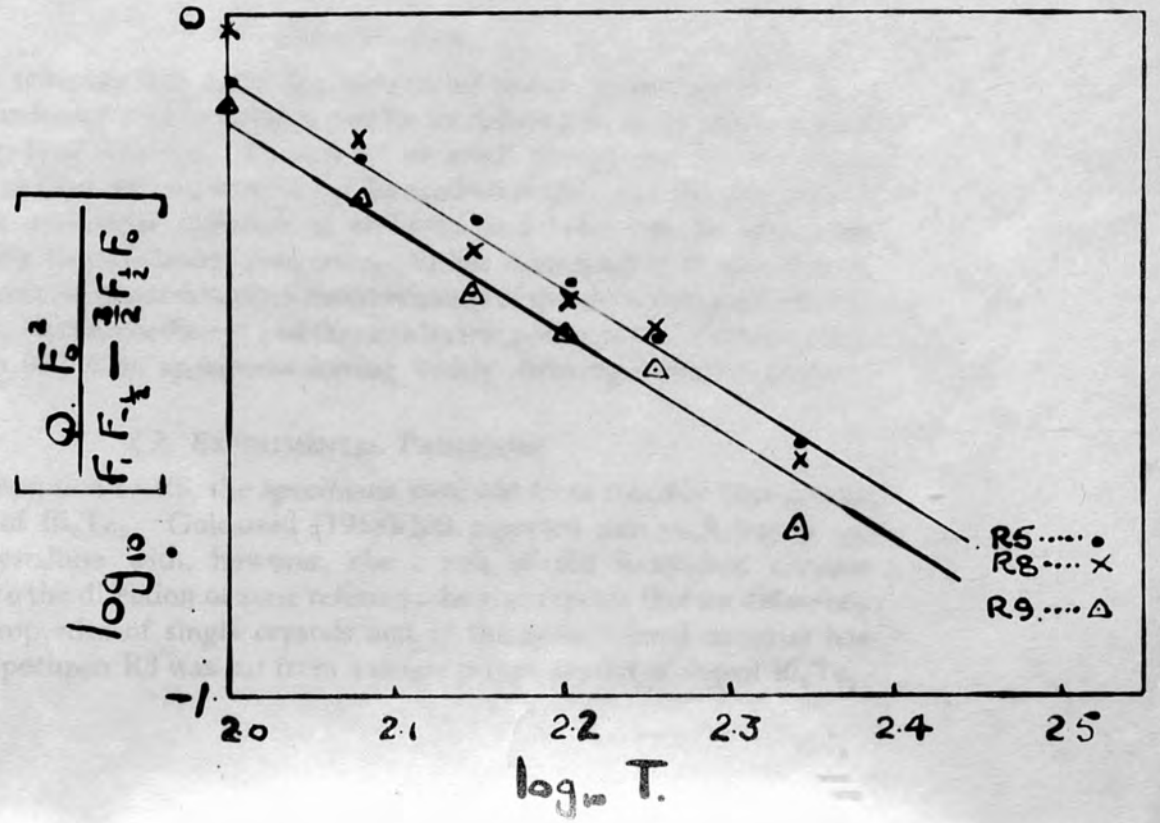

REPRINTED FROM THE
PROCEEDINGS OF THE PHYSICAL SOCIETY, VOL. LXXII, p. 733, 1958

PRINTED IN GREAT BRITAIN

The Electrical Properties of Bismuth Telluride

BY R. MANSFIELD AND W. WILLIAMS
Physics Department, Bedford College, London

MS. received 2nd June 1958

Abstract. Measurements of the electrical conductivity, Hall coefficient, thermoelectric power and Nernst coefficient on specimens cut from zone melted Bi_2Te_3 and on a single crystal are described. The current flow was parallel to the cleavage planes and the galvanomagnetic effects of the single crystal were measured with the magnetic field perpendicular and parallel to the cleavage planes. For the other specimens the Hall and Nernst coefficients were measured with the magnetic field perpendicular to the cleavage planes. The temperature range was 100°K to 600°K and specimens with a wide variation of impurity content were used. Analysis of the thermoelectric power and conductivity in the extrinsic range indicated that the specimens were partially degenerate, and when allowance is made for this, the temperature dependence of mobility is $T^{-1\cdot63}$ for electrons and $T^{-1\cdot91}$ for holes. In the high temperature range the conductivity measurements yield a value of the energy gap at 0°K of 0·21 ev. The temperature dependence of the Hall coefficient in the extrinsic range is anomalous and the explanation is not known. The Nernst coefficient Q exhibits the general behaviour expected for a semiconductor, and it is shown that it obeys a relation which can be derived from Moreau's relation, Q being proportional to $TR\sigma\, d^2E/dT^2$ (thermoelectric power $= dE/dT$, Hall coefficient $= R$, conductivity $= \sigma$).

§ 1. INTRODUCTION

BISMUTH telluride has been the subject of many recent papers. It is a semiconductor and impurities can be introduced so as to produce both n- and p-type material. Because of its small energy gap the transition from extrinsic to intrinsic conduction can be studied readily and the phenomena associated with ambipolar diffusion of electrons and holes can be examined. It has interesting thermoelectric properties and has been used in thermoelectric devices. The present paper describes measurements of the electrical conductivity, Hall coefficient, Nernst coefficient and thermoelectric power over the temperature range 100°K to 600°K on specimens having widely differing impurity content.

§ 2. EXPERIMENTAL PROCEDURE

With the exception of R8, the specimens were cut from suitably doped zone melted ingots of Bi_2Te_3. Goldsmid (1958) has reported that such ingots are usually polycrystalline with, however, the c axis of the individual crystals perpendicular to the direction of zone refining; he also reports that no difference between the properties of single crystals and of the zone refined material has been found. Specimen R8 was cut from a single p-type crystal of doped Bi_2Te_3.

All measurements were made with the current flow parallel to the cleavage plane. Initial experiments were made to investigate the uniformity of the specimens by determining the potential gradient down the length of the specimen with a constant current flowing. Only those results obtained with specimens having a uniform potential gradient or constant conductivity down their length are reported here.

Difficulty was experienced in making good current contacts to the specimens. Because of the high temperature readings soldered contacts were not possible and pressure contacts had to be used. These were spring loaded and the contacts were of silver or platinum. The potential probes were in the form of thermocouples, which were required for the measurement of the thermoelectric power and Nernst coefficient. They were made by silver soldering 40 s.w.g. T_1T_2 alloys. The junctions were made as small as possible and were pressed against the side of the specimen. When the electrical contact so formed was improved by a condenser discharge, a satisfactory probe was produced which was suitable over the whole temperature range studied. A saturated vapour pressure thermometer was used to calibrate the thermocouples below room temperature, and above room temperature the standard calibration was checked and found to be satisfactory. The Hall probes were of T_1 alloy, also spot-welded to the specimen. The magnetic field was usually perpendicular to the cleavage plane, except in the case of R8 for which measurements were made of the galvanomagnetic effects with the field both perpendicular and parallel to the cleavage plane. The magnetic field was determined using the Hall effect of a specimen of InSb which had been calibrated over a range of magnetic fields using a proton resonance method.

The conventional d.c. method was used for the measurement of conductivity and Hall coefficient. The thermoelectric power and Nernst effect were determined by having a small temperature gradient down the specimen produced by a heater placed at one end. The temperature difference between the two thermocouples was determined and the e.m.f. between the T_1 arms of the thermocouples was measured. Hence the thermoelectric power of Bi_2Te_3 relative to T_1 alloy was calculated. This result was then corrected to give the thermoelectric power of Bi_2Te_3 relative to lead, using the previously determined thermoelectric power of T_1 relative to lead. A check was made by repeating some of the readings using the T_2 alloy and correcting in the same manner. The results obtained were independent of the intermediate metal used, and both thermoelectric power and Nernst effect appeared independent of the temperature gradient over the range 5° to 40° per centimetre. The galvanomagnetic effects were determined under approximately adiabatic conditions.

It is difficult to assess the accuracy of the measurements. As is usual when measuring the bulk electrical properties of solids, the accuracy with which one can measure the change of the electrical properties with temperature appears much greater than the measurement of the absolute quantities, which depend on the determination of the dimensions of the specimen, the distance between the probes and the crystalline state of the specimen. However, in the case of Bi_2Te_3, because of the large thermoelectric power, the use of a d.c. method introduces additional errors, the importance of which are difficult to estimate. The influence of the Peltier effect on the conductivity can be reduced by measurements on the centre portion of a long specimen. This was possible for R5 and R8. In each

case the conductivity was determined by measuring the change of potential between the probes on reversing the current as quickly as possible.

Preliminary experiments showed that irreversible effects were produced on heating if copper was in contact with the specimen; such an effect has been reported by Goldsmid (1958). With the contacts used subsequently, the readings of the conductivity, Hall coefficient and Nernst coefficient were reproducible. However, in the case of the thermoelectric power, the value obtained was dependent on the surface conditions. For specimen R8 the room temperature value of the thermoelectric power was reduced by 10%, after heating the specimen to 620°K. After cleaning the surface the original value and variation with temperature could be obtained, although values of the thermoelectric power at room temperature differing by 20% were obtained when the thermocouples were in contact with different parts of the specimen.

§ 3. Results and Discussion

The temperature variation of the various electrical properties are illustrated in figures 1 to 4.

In many respects the results are in agreement with the results obtained with other semiconductors and the properties can be explained in general terms by the usual theory. However, Drabble, Groves and Wolfe (1958) have pointed out that the anisotropic structure of bismuth telluride appreciably affects the derivation from the experimental results of the various parameters such as mobility and concentration of charge carriers. Furthermore, the values of the thermoelectric power indicate that there is a transition from non-degenerate to degenerate statistics over the extrinsic range. Consequently, only a qualitative discussion of the results can be given at this stage.

The temperature dependence of the Hall coefficient is anomalous and for this reason it is more useful to consider the conductivity mobility (Drabble *et al.* 1958) rather than the Hall mobility. Consequently, in figure 1 the conductivity has been plotted on a double logarithmic scale. The shape of the curve indicates that below 300°K the specimens are extrinsic, and if it is assumed that the concentration of charge carriers is constant in this region, then this figure gives the temperature dependence of the conductivity mobility. The n-type specimens R7 and R3·21 have widely differing impurity content, and it is seen that the temperature dependence of mobility is different for these specimens. R7 behaves like a metal with mobility proportional to T^{-1}, whereas R3·21 has the temperature dependence of a semiconductor, $T^{-1\cdot5}$. This difference is what would be expected if there is a transition from degenerate to non-degenerate statistics.

In order to discuss the effect of degeneracy it is necessary to know the Fermi level. This can be calculated directly from the thermoelectric power provided the energy dependence of the relaxation time is a simple power law $\tau \sim \epsilon^r$. The value of r which is most consistent with the observations is that given by scattering of the charge carriers by acoustical modes ($r = -\frac{1}{2}$). It might be considered that for a compound semiconductor scattering by optical modes should be important, however it is likely that the Debye temperature is low for Bi_2Te_3 and consequently the high temperature approximation would be applicable. In this case $r = \frac{1}{2}$ and the temperature variation of mobility would be much less rapid than that observed.

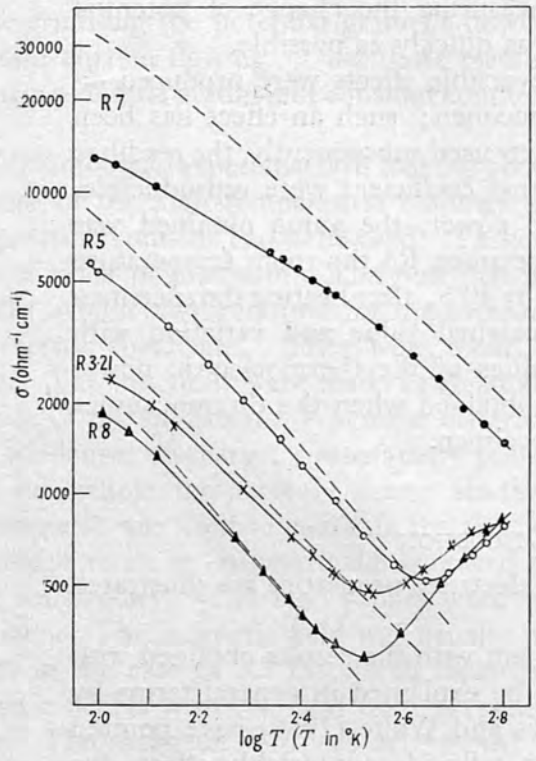

Figure 1. Electrical conductivity of Bi_2Te_3.

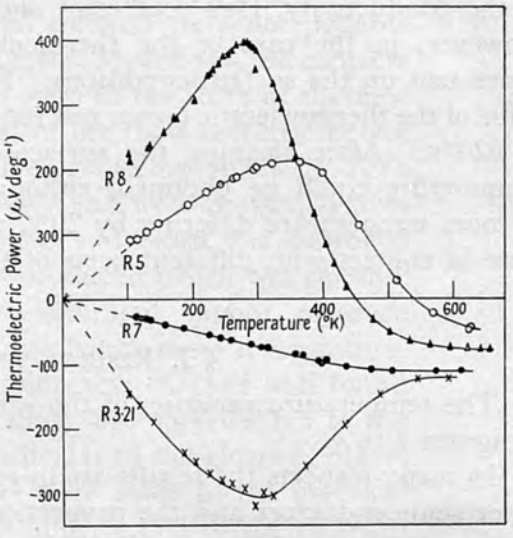

Figure 2. Thermoelectric power of Bi_2Te_3.

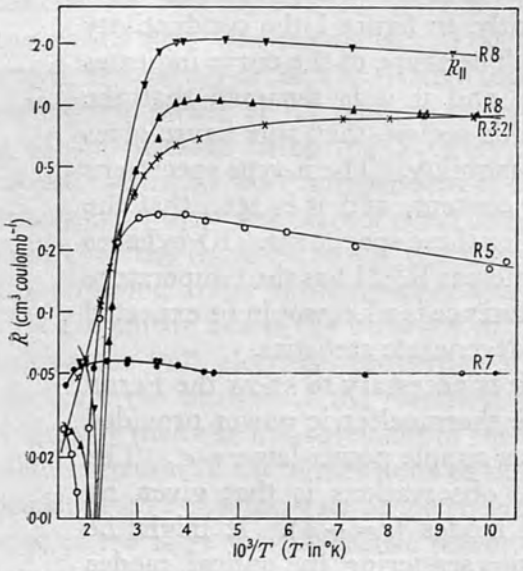

Figure 3. Hall coefficient of Bi_2Te_3. R_{II} obtained with field parallel to cleavage plane; other results obtained with field perpendicular to the cleavage plane.

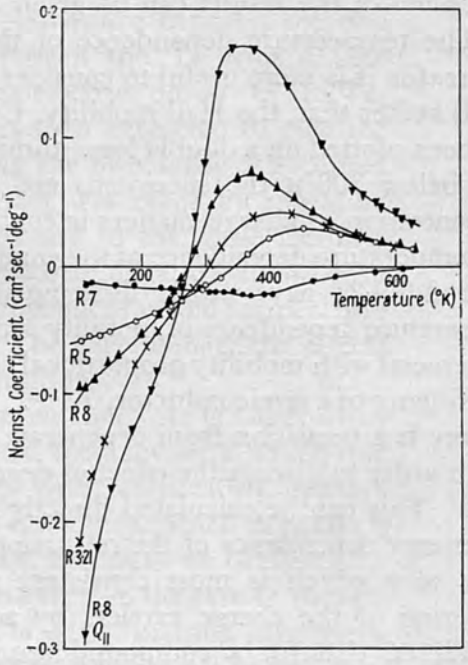

Figure 4. Nernst Coefficient. Q_{II} obtained with field parallel to cleavage plane; other results obtained with field perpendicular to cleavage plane.

Assuming therefore a scattering mechanism giving $r=-\frac{1}{2}$, the reduced Fermi level η^* was determined from the thermoelectric power, using the equation

$$\frac{dE}{dT}=-\frac{\boldsymbol{k}}{\boldsymbol{e}}\left(\frac{2F_1(\eta^*)}{F_0(\eta^*)}-\eta^*\right), \qquad F_m(\eta^*)=\int_0^\infty \frac{\eta^m\,d\eta}{1+\exp(\eta-\eta^*)}$$

and the conductivity σ_0 which would be obtained if there were no degeneracy was calculated from the measured conductivity σ, using the expression

$$\sigma_0=\sigma\frac{2F_{1/2}(\eta^*)}{\sqrt{\pi}F_0(\eta^*)}.$$

The derived curves in figure 1 show the values of σ_0. It is seen that for the two n-type specimens the mobility varies as $T^{-1\cdot63}$. The temperature dependence of the two p-type specimens differs slightly, being $T^{-2\cdot12}$ for R5 and $T^{-1\cdot94}$ for R8. The latter value, obtained on a single crystal, is probably more reliable.

The energy gap between valence and conduction bands can be calculated from the high temperature conductivity measurements, provided that the contribution to the conductivity due to extrinsic carriers is small in this range. Black *et al.* (1957) obtained a value of the energy gap at the absolute zero of temperature $E_G=0\cdot16$ ev from the slope of $\log\sigma$ against $1/T$. Goldsmid (1958), taking into account the departure of the mobility from the expected $T^{-1\cdot5}$ dependence, also obtained a value of 0·16 ev. However, Satterthwaite and Ure (1957) and Shigetomi and Mori (1956) obtained a value of 0·2 ev by calculating np/T^3 from conductivity and Hall coefficient measurements. This method might be criticized because of its dependence on the relation $R=3\pi/8n\boldsymbol{e}$. However, it is possible to obtain the temperature dependence of np/T^3 from the conductivity without using the Hall coefficient as follows. For material which is p-type in the extrinsic range

$$\sigma=n\boldsymbol{e}u_n+p\boldsymbol{e}u_p, \qquad n=p-p_s$$

hence

$$np=(p-p_s)p$$

and

$$\frac{np}{T^3}=\frac{1}{\boldsymbol{e}^2(u_n+u_p)^2T^3}(\sigma-\sigma_s)(\sigma+b\sigma_s)=N_cN_v\exp(-E_G/\boldsymbol{k}T)$$

where $\sigma_s=p_s\boldsymbol{e}u_p$ is the extrapolated extrinsic conductivity, N_c and N_v are the density of states in the conduction and valence bands, and b is the ratio of the mobilities u_n and u_p of electrons and holes. A similar expression is obtained for n-type extrinsic material with $1/b$ substituted for b. Specimen R8, the specimen with the least concentration of extrinsic carriers, was analysed using this equation. It was assumed that u_n was proportional to $T^{-1\cdot63}$ and u_p to $T^{-1\cdot94}$. The ratio of mobilities was considered to be close to unity and was determined by assuming $b=1$ at 380°K. The reason for this assumption is that a sign reversal of the Hall effect is observed in the p-type specimens shown in figure 3, and has also been observed by Shigetomi and Mori (1956), indicating that $b>1$ above 430°K, whereas Satterthwaite and Ure, using n-type specimens with low impurity content, find a reversal in the Hall coefficient, indicating that $b<1$ below 320°K. The value of the energy gap obtained by this method was 0·21 ev. It is probable that the lower value obtained by authors using the $(\log\sigma, 1/T)$ plot was because the condition $\sigma\gg\sigma_s$ was not satisfied. Thus in the case of R8, figure 5 shows the measured conductivity σ at high temperatures. Also shown are the extrapolated

extrinsic conductivity obtained from figure 1 and the calculated intrinsic conductivity σ_i obtained from the equation $\sigma_i = (\sigma - \sigma_s)(\sigma + b\sigma_s)$. It is seen that the graph of the measured conductivity appears linear and this linear portion gives $E_G = 0{\cdot}16$ ev (when $\log \sigma T^{0{\cdot}33}$ is plotted against $1/T$, $E_G = 0{\cdot}19$ ev), in agreement with other authors who used this method. However, in the case of specimen R8, the condition $\sigma \gg \sigma_s$, which is required to estimate the energy from conductivity measurements directly, was not satisfied.

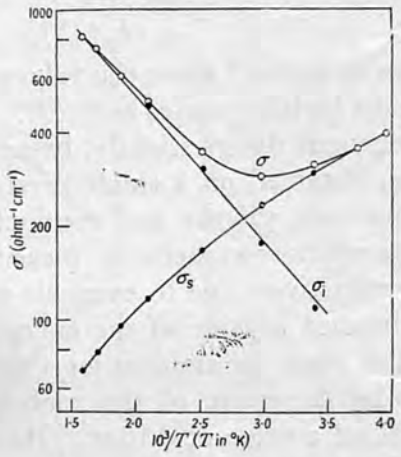

Figure 5. High temperature conductivity of R8 (single crystal).

On the assumption of a constant concentration of carriers in the extrinsic range, the isothermal Hall coefficient should be almost independent of temperature up to 300°K. Figure 3 shows, however, that for the p-type specimens there is a decrease in R and for R3·21 an increase as temperature decreases. There should be a slight change due to the effect of degeneracy which can be calculated using the expression (assuming $r = -\frac{1}{2}$)

$$R = \frac{x}{ne} \ldots, \qquad x = \frac{3}{4} \frac{F_{1/2}(\eta^*) F_{-1/2}(\eta^*)}{\{F_0(\eta^*)\}^2}.$$

The effect is a small decrease in the Hall coefficient, which in the case of R5 is 8% as the temperature changes from 300°K to 100°K and does not explain the observed decrease.

Now the Hall coefficient was measured under conditions which approximate to adiabatic rather than isothermal conditions, and because of the large thermoelectric power it is possible that there will be an appreciable difference between the adiabatic and isothermal coefficients. The difference arises from a transverse temperature gradient due to the Ettingshausen effect which, together with the thermoelectric effect, gives rise to a voltage which is combined with the Hall voltage. On applying the magnetic field the transverse voltage should change as the temperature gradient is established. Experiments to observe such a change were unsuccessful and any effect must have occurred during the interval when the field was established or removed (2 seconds). Because of the simple thermodynamic relation between the Ettingshausen and the Nernst coefficients, $P = QT/K$ where K is the thermal conductivity, when $Q = 0$ the two Hall coefficients R_a and R_i will be identical, and this condition is satisfied at approximately 300°K. At lower temperatures the Ettingshausen effect should be negative and consequently for both n- and p-type material $R_a > R_i$. The anomalous decrease in

the Hall coefficient of p-type material as the temperature is decreased from 300°K to 100°K cannot therefore be explained by this effect. In fact, the anomaly becomes even larger if there is a difference between the two coefficients. Experiments were carried out to test whether this anomaly could be due to a dependence of R on magnetic field. At room temperature, however, the Hall coefficient of R5 was independent of magnetic field up to 14 000 gauss. Finally, Drabble, Groves and Wolfe (1958) have shown that an anisotropic factor has to be introduced into the equation for the Hall coefficient and there is a possibility of a degeneracy or temperature dependence of this factor.

The temperature variation of the Nernst coefficient shown in figure 4 is in rough agreement with theory. In the extrinsic range the Nernst coefficient is negative and increases as the temperature decreases. For a semiconductor in the extrinsic range the Nernst coefficient should be negative if r is negative ($\tau \sim \epsilon^r$) and should be proportional to the mobility. It is found, however, that the Nernst coefficient does not vary so rapidly with the temperature as the mobility, and this is to be expected if the specimens become degenerate.

A comparison of figures 2 and 4 is of interest. For the specimens which show mixed conduction it is found that the temperature for which $Q=0$ coincides with the maximum of the thermoelectric power, and that the temperature for which the Nernst coefficient is a maximum coincides with the point of inflexion of the thermoelectric power. This would suggest a simple relation between Q and d^2E/dT^2. Now Moreau proposed a relation between the Nernst coefficient, Thomson coefficient μ, Hall coefficient and electrical conductivity which is as follows (Bridgman 1924: a negative sign has been introduced because of the different sign convention of the thermoelectric effects):

$$Q_0 = -\mu R\sigma = -T\frac{d^2E}{dT^2}R\sigma$$

since $\mu = T\,d^2E/dT^2$.

In the table are compared the values of Q_0 deduced from the above formula with the experimental values Q_E and shows that over a wide variation of Q_E the ratio Q_E/Q_0 is constant. The actual value of the constant depends on the measurements of the absolute values of the various electrical properties and the cumulative error involved will be large. However, there is an indication that the constant increases with impurity content. This relation is not obeyed in the intrinsic range.

Measurements of R and Q with the magnetic field parallel to the cleavage plane were made on specimen R8 and are shown in figures 3 and 4. The ratio of the Hall coefficient for the two orientations of the field is $2{\cdot}0 \pm 0{\cdot}1$ and is independent of temperature. A similar result is obtained for the Nernst coefficient with the ratio $2{\cdot}4 \pm 0{\cdot}1$. Measurement of the ratio of the electrical conductivity with current flow parallel and perpendicular to the cleavage plane was made on n-type material. The ratio is 3·9. Similar results have been obtained by Drabble *et al.* (1958) for the Hall coefficient and conductivity.

§ 4. Conclusions

The results obtained for the conductivity, Hall coefficient and thermoelectric power confirm those obtained by other authors. The variation of the Hall coefficient with temperature in the extrinsic range is anomalous and the explanation

Specimen	R 3·21			R 5			R 7			R 8		
T (°K)	Q_0	Q_E	Q_E/Q_0	Q_0	Q_E	Q_E/Q_0	Q_0	Q_E	Q_E/Q_0	Q_0	Q_E	Q_E/Q_0
120	−0·281	−0·169	0·60	−0·096	−0·056	0·58	−0·016	−0·014	0·88	−0·228	−0·090	0·39
160	−0·189	−0·110	0·58	−0·070	−0·049	0·70	−0·016	−0·015	0·94	−0·202	−0·071	0·35
240	−0·073	−0·040	0·55	−0·052	−0·033	0·63	−0·017	−0·017	1·00	−0·124	−0·029	0·23
320				−0·017	−0·010	0·59	−0·017	−0·020	1·17	+0·166	+0·055	0·33
400	+0·038	+0·040	1·05	+0·030	+0·021	0·70	−0·016	−0·022	1·37	+0·036	+0·065	1·80
480	+0·015	+0·033	2·2	+0·016	+0·028	1·7	−0·003	−0·010	3·3	0	+0·038	—

is not known. The Nernst coefficient agrees qualitatively with theory and there appears to be an interesting relation between the various electrical properties except at high temperatures.

Further measurements on the isothermal rather than adiabatic effects would be of interest. The use of an a.c. method for measuring the Nernst coefficient would be difficult since a large alternating magnetic field would be required. A simple arrangement would be to use probes of the same material as the specimen.

Acknowledgments

The authors are grateful to the General Electric Company and the Associated Electrical Companies for supplying the specimens of Bi_2Te_3 used in this investigation. This work was aided by a grant from the research fund of the University of London.

References

Black, J., Conwell, E. M., Seigle, L., and Spencer, C. W., 1957, *J. Phys. Chem. Solids*, **2**, 240.

Bridgman, P. W., 1924, *Phys. Rev.*, **24**, 644.

Drabble, J. R., Groves, R. D., and Wolfe, R., 1958, *Proc. Phys. Soc.*, **71**, 430.

Goldsmid, H. J., 1958, *Proc. Phys. Soc.*, **71**, 633.

Satterthwaite, C. B., and Ure, R. W., 1957, *Phys. Rev.*, **108**, 1164.

Shigetomi, S., and Mori, S., 1956, *J. Phys. Soc. Japan*, **11**, 915.

REPRINTED FROM THE
PROCEEDINGS OF THE PHYSICAL SOCIETY, VOL. LXXIII, p. 739, 1959

PRINTED IN GREAT BRITAIN

Some Adiabatic and Isothermal Effects in Bismuth Telluride

BY W. WILLIAMS
Physics Department, Bedford College, London

MS. received 1st *January* 1959

Abstract. Isothermal and quasi-adiabatic Hall and Nernst coefficients were measured on n- and p-type Bi_2Te_3 over a temperature range 100°K to about 450°K. The current flow was parallel to the cleavage planes, and measurements were made with the magnetic field either parallel or perpendicular to the cleavage planes. The difference between the two Hall coefficients follows the expected variation with temperature. However, the Nernst coefficients do not, and the reason is not known. Results obtained with the magnetic field perpendicular to the cleavage planes have been used to calculate the Ettingshausen coefficient.

§ 1. INTRODUCTION

MEASUREMENTS of the Hall and Nernst coefficients in semiconductors are often made under approximately adiabatic conditions, whereas formulae used in the interpretation of the results are usually in terms of the isothermal coefficients. In Bi_2Te_3, because of the large value of the thermoelectric power, this could lead to misinterpretation—if the Hall coefficient is in error due to an Ettingshausen effect, and the Nernst coefficient due to a Righi–Leduc effect. In addition, the electrical conductivity may be in error due to a Peltier effect.

It is known that the Hall coefficient of Bi_2Te_3 is anomalous in the extrinsic region (Mansfield and Williams 1958, to be referred to as MW). The value of the coefficient for p-type material decreases by as much as 50% on decreasing the temperature from 300°K to 90°K, whereas electrical conductivity measurements indicate that the material is extrinsic over this temperature range. This variation of Hall coefficient with temperature is inexplicable in terms of the usual theory of impurity semiconductors.

Under adiabatic conditions any transverse Ettingshausen temperature gradient would, in conjunction with the thermoelectric power, produce a voltage which would be combined with the Hall voltage. This Ettingshausen voltage cannot be separated from the Hall voltage by the normal direct current method of making Hall coefficient measurements. Measurements have therefore been made simultaneously of both adiabatic (or near adiabatic) and isothermal Hall coefficients from 100°K to approximately 450°K for both n- and p-type material.

§ 2. EXPERIMENTAL PROCEDURE AND RESULTS

Previous workers have used various methods, including alternating current methods, to obtain the isothermal Hall coefficient of metals and semiconductors. However, in MW it was suggested that the method of measuring isothermal effects by using probes of the same material as the specimen (Jan 1957) is particularly suited to Bi_2Te_3. Hence the isothermal Hall coefficient R_i was measured

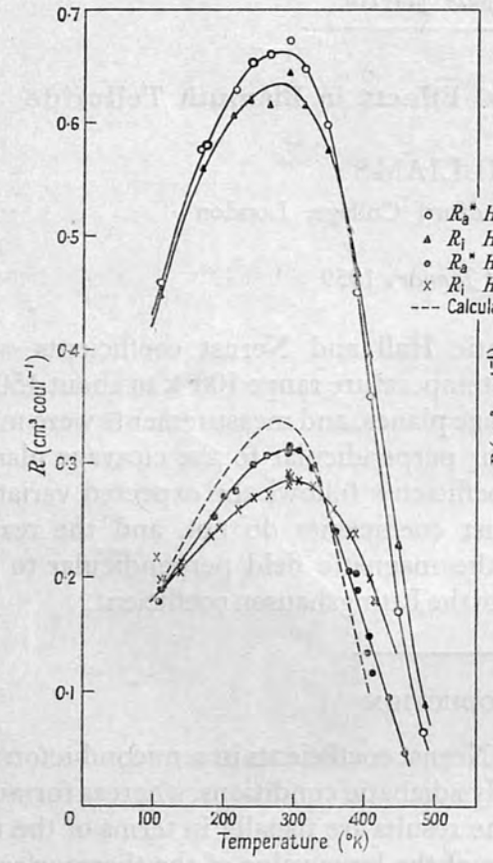

Figure 1. Hall coefficient of specimen R5 (p-type).

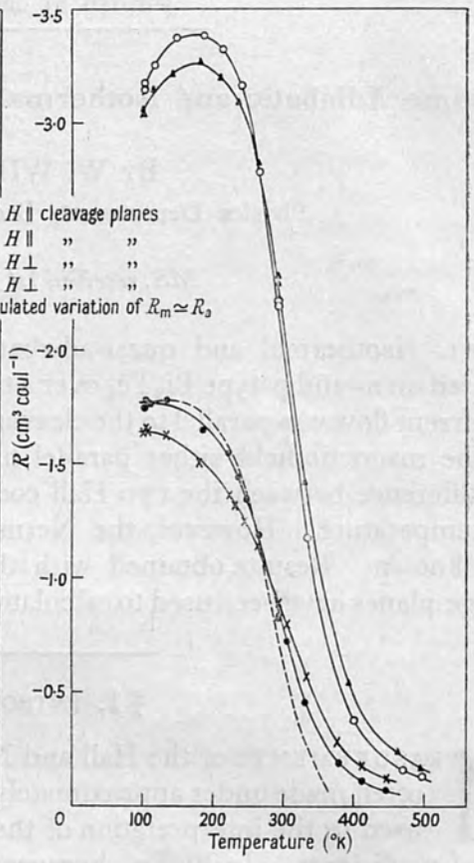

Figure 2. Hall coefficient of specimen R9 (n-type).

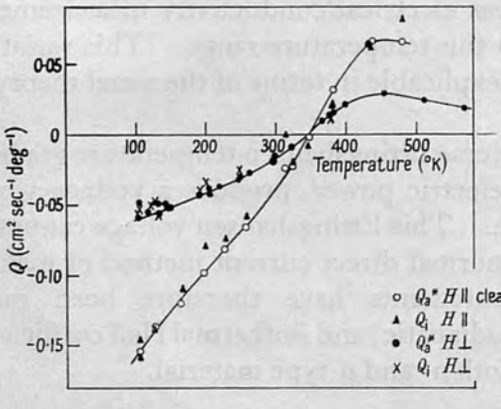

Figure 3. Nernst coefficient of specimen R5.

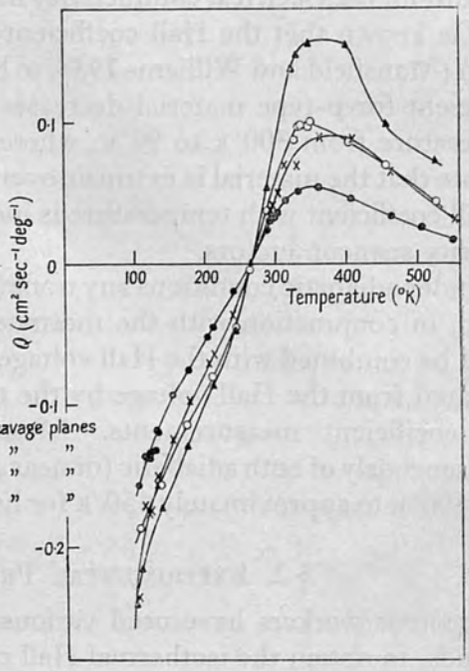

Figure 4. Nernst coefficient of specimen R9.

using probes of Bi_2Te_3 cut from material originally adjacent to the specimen used. A quasi-adiabatic coefficient, R_a*, was measured using probes of T_1 alloy. Measurements were made with the magnetic field both parallel and perpendicular to the cleavage planes. The results obtained are shown in figures 1 and 2. The p-type specimen is the one labelled R5 in MW. Specimen R9 is n-type.

The corresponding values of the isothermal and quasi-adiabatic Nernst coefficients (Q_i and Q_a* respectively) are shown in figures 3 and 4.

Measurements were also made of the electrical conductivity and thermoelectric power of both specimens over the temperature range 100°K to 600°K.

§ 3. Discussion of Results

The sign convention used is that stated by Gerlach (1928) together with a convention for the thermoelectric power which gives this quantity the same sign in the extrinsic region as the charge carriers. Thermoelectric power is positive when conventional current flows from metal to semiconductor at the hot junction.

Using a right-handed system of coordinates in which the primary electric current J or primary thermal current ω is in the x direction and the magnetic field H is applied in the z direction, the transverse galvanomagnetic and thermomagnetic effects respectively are measured in the y direction. The qualification of 'isothermal' and 'adiabatic' then refers to conditions in the y direction. For isothermal conditions $\partial T/\partial y = 0$, and for adiabatic conditions $\omega_y = 0$. Thus :

$$\text{Isothermal Hall coefficient } R_i = \frac{E_y}{H_z J_x} \; ; \; \left[J_y = 0, \; \frac{\partial T}{\partial x} = \frac{\partial T}{\partial y} = 0 \right]$$

$$\text{Adiabatic Hall coefficient } R_a = \frac{E_y}{H_z J_x} \; ; \; \left[J_y = 0, \; \frac{\partial T}{\partial x} = 0, \; \omega_y = 0 \right].$$

The relations between isothermal and adiabatic coefficients (Heurlinger relations) follow directly from the definitions of the various coefficients. With the sign convention used in the present paper, the relation between R_i and R_a is (cf. Chambers 1952):

$$R_a = R_i - \frac{dE}{dT} P \qquad \ldots\ldots (1)$$

where dE/dT is the absolute thermoelectric power of Bi_2Te_3 relevant to heat flow in the y direction and P is the Ettingshausen coefficient. The conditions under which P is defined are necessarily adiabatic and are the same as for R_a.

Taking into account the lattice thermal conductivity when deriving the Bridgman relation,

$$P = \frac{Q_i T}{K_y} \qquad \ldots\ldots (2)$$

where Q_i is the isothermal Nernst coefficient, and K_y is the isothermal thermal conductivity relevant to heat flow in the y direction and in a transverse magnetic field†.

This relation should hold for an isotropic medium over the whole temperature range investigated. Bi_2Te_3 is anisotropic. However, when the magnetic field is

† For a comprehensive account of the definitions of all the possible effects and the relations between them, see Jan (1957).

perpendicular to the cleavage planes, the cleavage planes are in the xy plane and thus the x and y directions in the crystal are equivalent. With primary currents in the x direction and the transverse effects measured in the y direction, the Bridgman relation should apply.

The sign of P is thus always the same as that for Q_i, and R_a should equal R_i at the temperature where $Q_i = 0$. Then from equation (1) $|R_a| > |R_i|$ below, and $|R_a| < |R_i|$ above this temperature for both n- and p-type specimens. It is seen that the general behaviour is as predicted, not only for the case considered, with the magnetic field perpendicular to the cleavage planes, but also when the magnetic field is applied parallel to the cleavage planes.

Under adiabatic conditions, with $\omega_y = 0$, the adiabatic Hall coefficient R_a is not directly measurable. The measured Hall coefficient R_m is given by the relation

$$R_m = R_i - \left(\frac{dE}{dT}\right)_{T_1} P \qquad \ldots\ldots (3)$$

where $(dE/dT)_{T_1}$ is the thermoelectric power of Bi_2Te_3 relative to T_1 alloy, the material of the measuring probes (Jan 1957). However, the thermoelectric power of Bi_2Te_3 is large compared with that of the metal of the measuring probes, so that the value of R_m is approximately equal to R_a.

The measurements of thermoelectric power were made with the heat flow parallel to the cleavage planes. The variation of K_y with temperature was calculated for each specimen from the measured electrical conductivity and data given by Goldsmid (1958) from measurements made on Bi_2Te_3 with the heat flow parallel to the cleavage planes. Thus, for the case when the magnetic field is perpendicular to the cleavage planes, values of P have been calculated from the measured values of Q_i using equation (2). These have been used to calculate $|R_m - R_i|$ from equation (3). Then, using the measured values of R_i, the variation of R_m with temperature has been calculated. This is plotted for both specimens on figures 1 and 2. It is seen that this theory always predicts a larger value for $|R_m - R_i|$ than is, in fact, found experimentally.

In equations (2) and (3), K_y and $(dE/dT)_{T_1}$ are respectively the thermal conductivity and thermoelectric power in a transverse magnetic field. In the calculations values of these quantities were used which had been obtained for zero magnetic field. However, it is known that these quantities are almost independent of magnetic field (Goldsmid 1958, Bowley *et al.* 1958), and this factor would not lead to the observed differences between the measured and calculated values of R_m. There are also other second order effects which can contribute to the measured voltage in the adiabatic case (Fieschi 1955, Jan 1957). Probably the main factor contributing to this difference is the fact that ω_y is not zero and true adiabatic conditions are not obtained. It is, in fact, difficult to know the exact experimental conditions in the y direction. In preliminary experiments no effort was made to reduce the transverse heat flow, and an even smaller value of $|R_m - R_i|$ was observed. While taking the readings shown in figures 1 and 2, an effort was made to reduce this heat flow to a minimum. However, if $\omega_y \neq 0$, the quantity measured would be a quasi-adiabatic Hall coefficient R_a^*, where

$$|R_a^* - R_i| < |R_m - R_i|.$$

Thus, assuming equation (2) to be obeyed in Bi_2Te_3 for this direction of the magnetic field with respect to the cleavage planes, the variation of the Ettingshausen

coefficient with temperature, obtained using this relation, is plotted in figure 5. Sufficient data are not available for interpreting the corresponding results obtained with the magnetic field parallel to the cleavage planes.

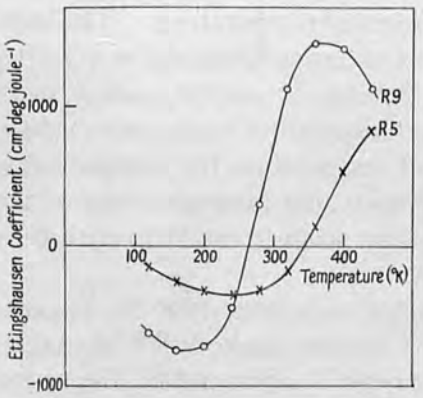

Figure 5. Ettingshausen coefficient of Bi_2Te_3.

An interpretation of the adiabatic and isothermal Nernst coefficients is more complicated. The relation between the two quantities is (cf. Chambers 1952)

$$Q_a = Q_i - \frac{dE}{dT} . S \qquad \ldots\ldots (4)$$

where S is the Righi–Leduc coefficient.

Now there is no simple relation giving the sign of S from some experimentally determined quantity over the whole temperature range. However, according to simple semiconductor theory, S is positive for p-type specimens and negative for n-type specimens in the extrinsic range, only changing sign in p-type specimens ($b > 1$) after Hall and thermoelectric power readings have indicated that the specimens have become intrinsic (Putley 1955). Thus, over the complete temperature range studied, S should be negative for R9 and positive for R5, and from equation (4) below the temperature where $Q_i = 0$, it is predicted that $|Q_a| > |Q_i|$, while above this temperature $|Q_a| < |Q_i|$. As with the adiabatic Hall coefficient, the quantity Q_a is not directly measurable. However, following the same reasoning as for the Hall coefficient, a quasi-adiabatic Nernst coefficient Q_a^* should be obtained such that $|Q_a^* - Q_i|$ is smaller than predicted. No definite results could be obtained for R5 (figure 3). For R9, the results are not as predicted, and S does not appear to behave according to the simple theory.

R9 is a zone-refined specimen of n-type material which was tested for uniformity along its length. A plot of log σ_0 against log T, where σ_0 is the electrical conductivity corrected for degeneracy, gives a temperature dependence of mobility of $T^{-1\cdot91}$ compared with the previous value for electrons of $T^{-1\cdot63}$. A plot of log (np/T^3), obtained from electrical conductivity data as in MW, against $1/T$ gives a value for the energy gap at 0°K of 0·19 ev compared with the previous value of 0·21 ev.

In MW it was shown that, except in the intrinsic region, Be_2Te_3 obeys the Moreau relation

$$Q = -T\frac{d^2E}{dT^2}R\sigma$$

where σ is the electrical conductivity. Use of the isothermal quantities in this relation did not give better agreement in the intrinsic region. The ratio of the coefficients for the two orientations of the magnetic field is of interest. The ratio of the isothermal Hall coefficients is $2{\cdot}2 \pm 0{\cdot}1$ for R5 and $2{\cdot}3 \pm 0{\cdot}2$ for R9, both quantities being independent of temperature. The ratio of the Nernst coefficients for R5 is also independent of temperature and is $2{\cdot}3 \pm 0{\cdot}1$. For R9 the ratio of the isothermal Nernst coefficients is approximately unity at 100°K. The ratio increases with increasing temperature for negative values of the Nernst coefficient, becoming independent of temperature for positive values of the coefficient with a value of $1{\cdot}7 \pm 0{\cdot}1$. It is seen that measurements of the Nernst coefficient of R9 in the extrinsic range do not seem to conform with those on the other specimens studied here and in MW.

Readings of the electrical conductivity of Bi_2Te_3 are subject to a possible error due to Peltier heating. This was checked on R5 by taking readings simultaneously of the conductivity using both T_1 alloy and Bi_2Te_3 probes. R5 is a long specimen (7 cm) so that for small currents both quantities should be the same. Readings were taken for different values of the current J_x at room temperature and at 110°K. Over the range of currents normally used, no evidence could be found of an error in σ due to the Peltier effect. However, such an error would depend on the size of the specimen and is much more likely to be appreciable for small specimens.

§ 4. Conclusions

A simple method has been used to obtain the isothermal Hall and Nernst coefficients in Bi_2Te_3 and it is found that the value of these coefficients can differ appreciably from the quasi-adiabatic coefficients often measured. Measurement of the isothermal Nernst coefficient provides a simple method of obtaining the Ettingshausen coefficient. The extrinsic Hall coefficient in p-type material is known to be anomalous, but although this anomaly is decreased by measuring the isothermal coefficient, it is not removed.

Acknowledgments

The author wishes to thank Dr. R. Mansfield for helpful discussions and advice, and the General Electric Company for supplying the specimens of Bi_2Te_3.

This work was aided by a grant from the research fund of the University of London.

References

Bowley, A. E., Delves, R., and Goldsmid, H. J., 1958, *Proc. Phys. Soc.*, **72,** 401.
Chambers, R. G., 1952, *Proc. Phys. Soc.* A, **65,** 903.
Fieschi, R., 1955, *Nuovo Cim. Suppl. Ser.* 10, **1,** 1.
Gerlach, W., 1928, *Handb. d. Phys.*, **13,** 228 (Berlin: Springer).
Goldsmid, H. J., 1958, *Proc. Phys. Soc.*, **72,** 17.
Jan, J. P., 1957, *Solid State Physics*, Vol. 5 (New York: Academic Press), p. 1.
Mansfield, R., and Williams, W., 1958, *Proc. Phys. Soc.*, **72,** 733.
Putley, E. H., 1955, *Proc. Phys. Soc.* B, **68,** 35.